



City Research Online

City, University of London Institutional Repository

Citation: Ram, V. (1986). The Automatic Recording of Relative and Tremor Movements of the Eyes. (Unpublished Doctoral thesis, The City University)

This is the accepted version of the paper.

This version of the publication may differ from the final published version.

Permanent repository link: <https://openaccess.city.ac.uk/id/eprint/35655/>

Link to published version:

Copyright: City Research Online aims to make research outputs of City, University of London available to a wider audience. Copyright and Moral Rights remain with the author(s) and/or copyright holders. URLs from City Research Online may be freely distributed and linked to.

Reuse: Copies of full items can be used for personal research or study, educational, or not-for-profit purposes without prior permission or charge. Provided that the authors, title and full bibliographic details are credited, a hyperlink and/or URL is given for the original metadata page and the content is not changed in any way.

585

THE AUTOMATIC RECORDING OF
RELATIVE AND TREMOR MOVEMENTS
OF THE EYES

BY VAFA RAM

A THESIS SUBMITTED FOR THE AWARD OF THE DEGREE OF
DOCTOR OF PHILOSOPHY
DEPARTMENT OF ELECTRICAL & ELECTRONIC ENGINEERING

SCHOOL OF ELECTRICAL ENGINEERING AND APPLIED PHYSICS
THE CITY UNIVERSITY
LONDON

OCTOBER 1986

1. ☐ **Yes** 2. ☐ **No** 3. ☐ **Don't know**

[REDACTED]

TABLE OF CONTENTS

Chapter 1 Physiology of the Eye

1.4.9 The Limbus..... 19

PART I RELATIVE EYE MOVEMENTS

Chapter 2 Relative Movement of the two Eyes

2.1	A Survey of Previous Methods and Instruments.....	22
2.1.1	Introduction.....	22
2.1.2	Direct Observation.....	22
2.1.2.a	Duction.....	23
2.1.2.b	Version.....	23
2.1.3	Mackenzie Method.....	23
2.1.4	Bielschowsky's or Head Tilt Test.....	24
2.1.5	Photographic Methods.....	25
2.1.6	Maddox Rod.....	26
2.1.7	Electromyography.....	27
2.1.8	Cover Test.....	27
2.1.9	Red Glass Test.....	29
2.1.10	Hess-Lancaster Test (Red-Green Test)....	31
2.1.11	L.E.D. Screen Methods.....	40
2.1.12	Miscellaneous Methods.....	40
2.1.13	Conclusions.....	42
2.2	Initial Design Considerations.....	43
2.3	Introduction to the Automated System.....	46

Chapter 3 Hardware Design (Blank Monitor)

3.1	Introduction.....	51
3.2	Joy-Stick System.....	52
3.3	Light Pen System.....	58
3.3.1	Digital Methods.....	59
3.3.2	Analogue Methods.....	60
3.4	Adopted Design.....	61
3.4.I	T.V. Sync. Generator.....	65
3.4.II	Integrator.....	67
3.4.III	Raster Mixer.....	73
3.4.IV	Sample and Hold.....	75
3.4.V	Timer (Delay).....	78
3.4.VI	Light Pen.....	80
3.4.VII	Smoothing Filter.....	85
3.4.VIII	3-Pole Low-Pass Filter.....	89
3.4.IX	S-R Flip-Flop and Differentiator.....	90
3.5	Summary.....	92

Chapter 4 Hardware Design (Chart Monitor)

4.1	Introduction.....	94
4.2	Bank Memory.....	94
4.3	Video Display Generators.....	95

4.4	Cushion Effect.....	95
4.5	Microprocessor (The Use of Software).....	96
4.6	Adopted Design (The Use of Hardware).....	96
4.6.I	Horizontal Coordinate Generator.....	98
4.6.I.a	Clock.....	98
4.6.I.b	Clock Divider.....	100
4.6.I.c	X-Coordinate Memory.....	101
4.6.I.d	Digital Comparator.....	102
4.6.I.e	Monostable.....	104
4.6.II	Vertical Coordinate Generator.....	105
4.6.III	Window Inhibit.....	106
4.6.IV	Keyboard Control.....	110
4.6.V	Mixer.....	113
4.7	Summary.....	113

PART II EYE TREMOR MOVEMENTS

Chapter 5 Tremor Movement of the Eye

5.1	A Survey of the Previous Methods and Instruments..	116
5.1.1	Introduction.....	116
5.1.2	Direct Observation.....	117
5.1.3	Mechanical Transducers.....	117
5.1.4	After-Image Methods.....	119
5.1.5	Sound Methods.....	119
5.1.6	The Counting Method.....	120
5.1.7	Direct Photography.....	120
5.1.8	Corneal Reflections.....	121
5.1.9	Reflections from Attachments to the Eye..	124
5.1.10	Double Purkinje Image Method.....	125
5.1.11	Contact Lens Method.....	128
5.1.11.a	Optical Contact Lens.....	129
5.1.11.b	Electromagnetic Contact Lens.....	130
5.1.12	Electro-Oculography (EOG).....	133
5.1.13	Impedance Oculogram.....	135
5.1.14	Photoelectric Methods.....	136
5.1.14.a	Scanning Systems.....	138
5.1.14.b	Feedback Methods.....	140
5.1.14.c	Differential Reflection Methods....	140
5.1.15	T.V. Methods.....	143
5.1.16	Summaries and Conclusions.....	147
5.2	Initial Design Considerations.....	150
5.3	Introduction to the Automated System.....	152

Chapter 6 Hardware Design

6.1	Introduction.....	156
6.2	Data Allow Generator.....	156

6.3	Design Concepts.....	159
6.3.1	Digital Methods.....	160
6.3.2	Filtering Methods.....	160
6.3.3	Analogue Methods.....	162
6.4	Adopted Design.....	168
6.4.I	Mixer.....	171
6.4.II	Data Allow Extractor.....	172
6.4.III	Analogue Switch.....	173
6.4.IV	Limbus Pulse Generator.....	174
6.4.V	Integrator.....	178
6.4.VI	Sample and Hold.....	179
6.4.VII	3-Pole Low-Pass Filter.....	181
6.5	Summary.....	181

Chapter 7 System Construction, Testing and Application

7.1	Introduction.....	184
7.2	Construction of the Circuits and the Test Desk....	184
7.3	Power Supply Unit.....	187
7.4	50-OHM Line Drivers.....	189
7.5	Relative Movement Measurements.....	205
7.5.1	Case Studies.....	191
7.6	Tremor Measurements.....	205
7.6.1	T.V. Method using Artificial Model Eye..	205
7.6.2	Patient's Eyes Tests.....	217
7.6.2.a	Photoelectric Test.....	217
7.6.2.b	T.V. Method Test.....	217
7.6.3	Case Studies.....	219

Chapter 8 Discussion and Conclusions

8.1	Relative Eye Movement.....	248
8.1.1	Observations arising from Case Studies..	248
8.1.2	Further Points for Discussion.....	248
8.1.3	Comparisons of the Automated System and Previous Methods.....	250
8.2	Eye Tremor Movement.....	255
8.2.1	Observations arising from Case Studies..	255
8.2.2	Further Points for Discussion.....	257
8.2.3	Comparisons of the T.V. System and Previous Methods.....	258
8.3	Conclusions.....	267

Chapter 9 Suggestions for Further Work.....270

Appendices

I	Hess Chart.....	275
II	T.V. Systems.....	277
III	Light Pen.....	279
IV	Integrators.....	284
V	Op-Amp Integrator & Ramp Non-Linearity.....	287
VI	Voltage Summation of an Op-Amp.....	292
VII	Clock Operation.....	296
VIII	Memories Contents.....	299
IX	T.V. Camera Modification.....	302
X	Delay Calculations in Televisions.....	316
XI	3-Pole Active Filters.....	320
XII	Copies of Printed Circuit Boards.....	323
XIII	Professional Comments on the Final Designs.....	326
XIV	Comments on an Automated System.....	331

<u>References</u>	333
-------------------------	-----

ACKNOWLEDGMENTS

I am indebted to [REDACTED], without whose initial inspiration and spiritual support I would not have begun and completed my research.

I would also like to render my deepest gratitude to my supervisor Mr. Roger Chapman, of the Department of Electrical and Electronic Engineering, and also to [REDACTED] of the Department of Civil Engineering, for their continuous encouragement during this study and tremendous assistance in the preparation of this thesis. I also wish to thank my external examiner [REDACTED] for wading through a thesis which is not exactly the paradigm of perspicacity.

I am also grateful to the Ministry of Health and Social Security, for providing the funds to conduct the research and to the London Refraction Hospital, the Moorfield Eye Hospital, the London Hospital, Link Electronics Limited and Jackson Electronics Limited, for providing either patients or useful information.

Finally, I thank [REDACTED] for typing (and typing), and [REDACTED] for proof-reading and help in syntactical style. Also my thanks to [REDACTED] for their technical assistance.

ABSTRACT

There is a need for both accurate and practical methods to measure human ocular movements. Hitherto, little progress has been achieved in terms of producing suitable and technologically advanced equipment for use in ophthalmic departments of hospitals, and to facilitate research into ocular disorders.

Two types of ocular motility are considered in this thesis. Relative Eye Movements, which are the discrepancy in conjugate eye movements, and Tremor Eye Movements, especially the condition known as nystagmus.

The present study describes the design, development and use of an improved system to measure eye movements, utilising advances in video technology but based on conventional ophthalmic concepts. The incorporation of this technology has automated and substantially improved the Hess Chart Test which measures relative eye movements, and also provided a semi-automated and more accurate means of measuring the frequency and amplitude of nystagmus movements.

The efficiency of the equipment has been evaluated by direct testing of normal individuals and patients suffering from various ocular disorders.

The conclusions of the study suggest that this new automated system is more efficient than the currently employed conventional methods, which may be vulnerable to human error by both patient and ophthalmologist.

Furthermore, the tests are simple, flexible and fast to conduct, requiring relatively little calibration or setting up time. They can be performed on patients with little experience, and without causing them any discomfort or anxiety since there are no attachments to the eyes.

The almost unique ability of the system to video record eye movements permits subsequent and, if necessary, repeated analyses of the tests to improve diagnosis. Furthermore, because the tests are conducted in 'real time', subsequent steps of the test procedure can be determined during the examination.

Although the initial capital cost of the equipment, is of the same order as some of the previous methods, the running costs are extremely low, because of the reduced manpower required. Furthermore, the accommodation of the entire experiment on a mobile desk, drastically reduces the amount of space occupied.

The series of simultaneously obtained data during these tests provide invaluable measurements of the various parameters of optical disorders which argues well for better diagnosis and treatment.

These results may have important implications in providing a better understanding in the field of eye movements and may contribute positively to the development of better techniques in the diagnosis and therapy of these important ocular conditions.

DEFINITIONS

Abduction: The rotation, temporally, of an eye away from the mid-line, the diverging of the eyes away from the each other.

Adduction: The rotation of an eye towards the mid-line (nasally).
Converging of the eyes towards each other.

Cell: A cell is equivalent to the duration of one clock cycle on the T.V. screen (250ns duration).

Cornea: The transparent anterior portion of the eye.

corneal Reflex: Light reflection in the cornea.

C.R.T.: Cathode Ray Tube.

Data Allow: A pulse of a duration of 10us which can be placed over any T.V. lines. Video information is allowed during this period and suppressed for the rest of the field.

Diopter: A unit of measurement of the power of a lens, the reciprocal of the focal distances in metres.

Fixation: The process, condition, or act of directing the eye towards the object of regard, causing, in a normal eye, the image of the object to be centred on the fovea.

Fovea: A small depression where the image is formed.

Fundus: The base of the internal surface of a hollow organ, the part opposite the aperture.

I_{IH}: Input high current.

Insertion: The insertion of a muscle refers to where the muscle is attached to the particular organ that it actuates.

I_{OH}: Output high current

Iris: A circular pigmented membrane perforated to form the pupil.

Left-Beating Nystagmus: The fast phases of the eye movements are to the left.

Limbus Pulse: A pulse the leading edge of which is the leading edge of the Data Allow, and its trailing edge is at the Limbus of the eye.

Nystagmus: An involuntary, rapid to-and-fro oscillatory movement of the eyeball which may be horizontal, vertical, rotatory, or mixed.

Orbit of the Eye: One of the cavities in the skull which contains an eye ball.

Origin: The origin of a muscle is where the muscle begins.

Over-Action: Is an indication that there may be some paresis in a syneric muscle in the other eye.

Pendular Nystagmus: Equal velocities in opposite directions.

Primary Position: The position of the eye when looking straight ahead at zero degree level (looking at the centre 'square dot' in the Hess Chart).

Raster: A predetermined pattern of scanning lines that provides substantially uniform coverage of an area.

Right-Beating Nystagmus: The fast phases of the eye movements are to the right.

Rotational Nystagmus: Rotation of the eye globe.

S & H: Sample and Hold.

Sclera: The white outer tunic of the eye ball.

Square Dots: The square dots are generated on the T.V. screen and have the same coordinates as the intersections of the lines of longitude and latitude of an imaginary sphere centred at the eye.

Trochlea: A ring-like structure attached to the trochlear fossa through which passes the tendon of the superior oblique muscle.

V_{CC}: Supply rail.

Vestibular Nystagmus: Slow-quick jerk.

V_{OH}: Output high voltage.

Under-Action: Is an indication of a paretic tendency in an extraocular muscle.

INTRODUCTION

The characteristics of central and peripheral disorders of ocular motility constitute valuable diagnostic signs for both clinicians and researchers. Such ocular motilities and their associated disorders have, in this study, been considered under the two general categories of either 'relative' or 'tremor' eye movements.

Relative eye movements, except for vergence, can be defined as the discrepancy in conjugate eye movements, and are discussed in the first part of this thesis.

In general, the two eyes move together and in synchrony to produce two parallel sets of visual information. Although small discrepancies in conjugate eye movements exist in everyone, these may become extreme in some individuals, such as those suffering from multiple sclerosis, and result in visual disorders. Whether such disorders are due to one or more eye muscle imbalances or to other factors, the distorted visual information requires compensation by the superposition capabilities of the brain.

The accurate evaluation of these discrepancies, or relative eye movements, thus becomes an invaluable part of both ophthalmological and neurological investigations. Such measurements may also localise and even determine the cause of the disorder, thus facilitating its diagnosis.

The need for an accurate method of measuring relative eye movements has long been realised, and numerous different systems have been proposed over the last century. Many of these methods have attempted to be accurate, precise and fast to conduct. In

practice, however, most of their attributes have been compromised, resulting in systems that are less than ideal. The most noteworthy method is the Hess Chart test, which was devised in 1908 and which is found to have the greatest potential for development since it possesses a certain degree of accuracy and versatility.

The aim of the first part of this thesis has therefore been to extend and develop the accuracy of the Hess Chart, whilst still incorporating many of the more advantageous attributes of the other methods. This has been achieved by the use of video technology, which has not only automated the Hess Chart test but has also increased its accuracy to an extent where further research into this area is now possible.

This automation has required the design and development of a system that incorporates a pattern generator, T.V. monitors, an X-Y recorder and a light pen.

Tremor eye movements, which are discussed in the second part of this thesis, may be the result of particular nervous disorders and include movements such as saccadic, pursuit and nystagmus.

Measurements of such movements are useful to several different types of specialists. For example, they provide a permanent objective record for ophthalmologists to diagnose oculomotor disorders and to detect nystagmus, unusual fixation movements and vergence difficulties. Measurements of association and dissociation, and also of amplitude, frequency, duration and direction of the tremors are important for otolaryngologists in determining the state of the semi-circular canals of the inner ear. The study of saccadic and pursuit movements during fixation

assists diagnosis by neurologists, whilst the characteristic eye movements may also be used by ^aanesthetists to determine the state of ^aanesthesia of the patient.

The need for an accurate method of measuring such tremor movements has been realised for over a century, but little progress has been made in providing a system which accurately measures these movements and, at the same time, incorporates many of the attributes required by both the ophthalmologist and patient. Although there are several reported methods of measuring such tremor movements (for example Benghi, 1968; Young, 1975; Thomas, 1977 and Davies, 1978), further modifications and refinements are required to increase their accuracy, sensitivity, versatility and also speed and simplicity of use.

Of the various forms of tremor movement, nystagmus is probably one of the most prominent and best-documented. It is also the main type of tremor considered in this thesis. Nystagmus involves a to-and-fro oscillation of the eyes, and occurs in about 0.1 per cent of the population (Nystagmus Action Group, 1986).

The several different approaches used to resolve the problems associated with nystagmus recording, can be classified under three main measuring techniques. Mechanical methods include physical attachments to the eyes, or the use of pressure sensing devices. Optical methods include photography and light reflections, whilst electrical methods include techniques such as electro-oculography.

More recent techniques of measuring eye tremor movements involve scanning and T.V. methods, which identify specific

features of the eye such as the pupil, limbus or the corneal reflex.

Extracting information from these features must be performed without the interference of the eye-lids or the eye-lashes. Both scanning and T.V. methods have the disadvantages of system noise, shading and non-uniform illumination, making automatic measurements generally difficult.

The second part of this thesis has therefore been concerned with the design and development of a new semi-automated system to detect and record eye tremors on an X-Y plotter with signal processing circuits, and T.V. monitors and cameras.

The equipment whose design and construction is described in the following Chapters, is for the simultaneous and automatic measurement of relative and tremor eye movements. The devised system has taken full advantage of the available video technology to improve on the old classical methods of detecting ocular movements. The system has been designed to be accurate, sensitive, reliable and also simple to operate. At the same time, however, the production and running costs have been minimised since the system is envisaged for use in ophthalmic departments of hospitals. Hence, more commercially available equipments have been used and modifications have been kept to bare minimum.

The accuracy and effectiveness of the system has been tested on a number of patients from the London Refraction Hospital. The results from these studies are used to evaluate the working system and to discuss the implications on further research and development of the equipment. Modifications to enable the incorporation of additional components, such as micro-processors

for enhanced monitoring and analysis, are also considered.

It is envisaged that the cost-effectiveness of this system will allow a more widespread study of ocular disorders, hence permitting more precise diagnosis and at the same time enabling a greater degree of ophthalmological and neurological research.

1.1 Introduction

animal species is made evident by the fact that the majority of the more advanced species have well-developed, complex visual organs.

The two eyes in man, for example, are essential for him to comprehend and conceive the complexity of the outside physical world, and to exploit it to his best advantage.

The eyes are one of the few organs with which a whole range of quantitative and qualitative information is provided to the brain, for example, distance, size, shape, colour and composition. In addition, information such as depth, is available due to the reception of two sets of parallel visual data by the eyes. Another advantageous feature of the man's two eyes is that they can move in all directions, together and in unison.

In order to be able to conduct research and to develop instruments for the accurate measurement of eye movement, a good understanding of the physiology of the human eye and its associated muscles is first required. The following sections briefly describe the characteristics of the eye which are relevant to this study, and which can be used for measuring ocular motility.

CHAPTER 1

PHYSIOLOGY OF THE EYE

1.1 Introduction

The necessity of eyes to the survival and advancement of animal species is made evident by the fact that the majority of the more advanced species have well-developed, complex visual organs.

The two eyes in man, for example, are essential for him to comprehend and conceive the complexity of the outside physical world, and to exploit it to his best advantage.

The eyes are one of the few organs with which a whole range of quantitative and qualitative information is provided to the brain, for example, distance, size, shape, colour and composition. In addition, information such as depth, is available due to the reception of two sets of parallel visual data by the eyes. Another advantageous feature of the man's two eyes is that they can move in all directions, together and in unison.

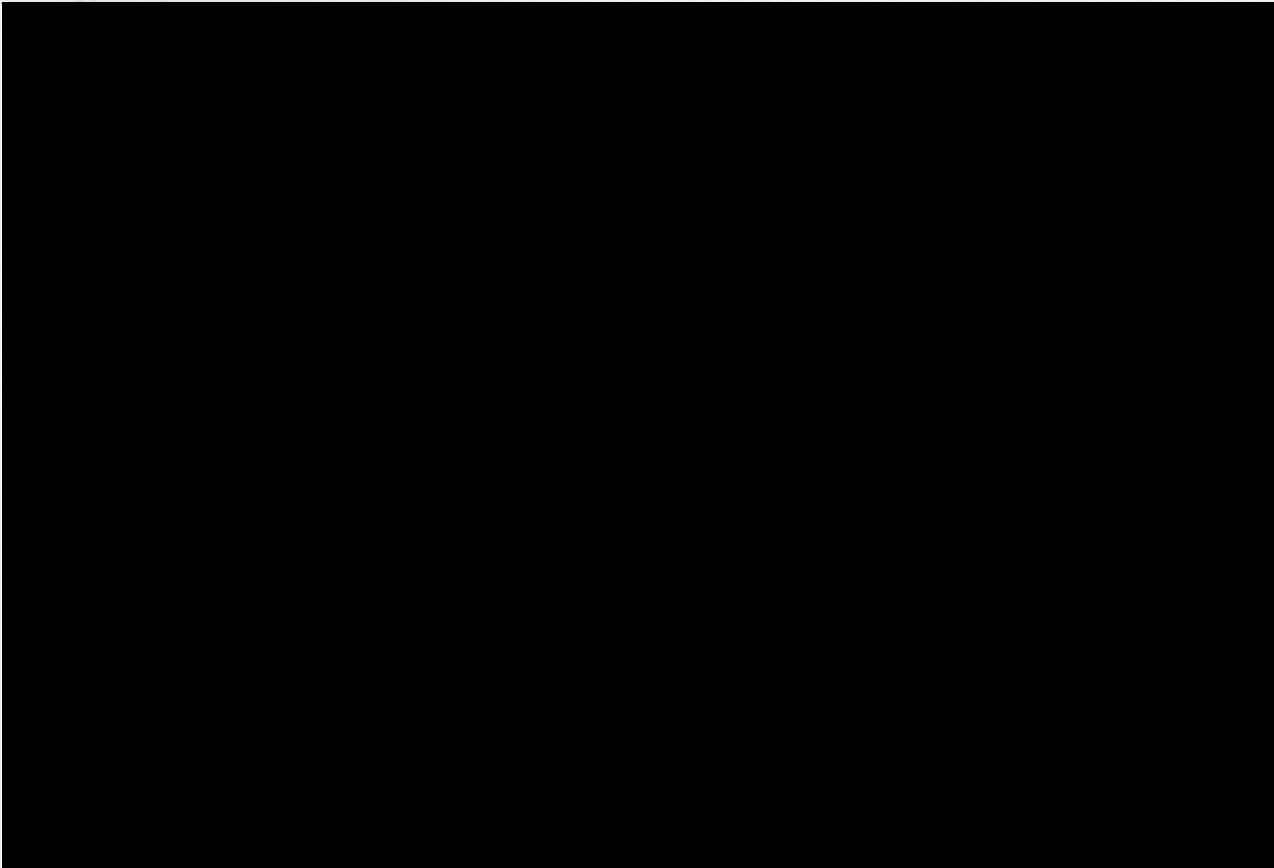
In order to be able to conduct research and to develop instruments for the accurate measurement of eye movement, a good understanding of the physiology of the human eye and its associated muscles is first required. The following sections briefly describe the characteristics of the eye which are relevant to this study, and which can be used for measuring ocular motility

1.2 Physiology of the Eye

The correct functioning of the eyes is dependent upon optical, mechanical and neurological processes. Some of the features of the eyes which are relevant to the development of instruments for ocular eye measurements in this thesis are noted below:

1.2.1 Optical Sections:

Fig. 1.1 illustrates some of the optical components of the eye globe.



Axial Length	24.0mm
Anterior Radius of Cornea	7.8mm
Thickness of Cornea	0.5 to 0.8mm
Thickness of Sclera	0.3 to 1.0mm
Width of Cornea	10.6 to 11.6mm

Fig. 1.1 Section of the Left Eye

The Retina, which forms part of the inner globe, consists of

light-sensitive receptors called 'rods' and 'cones', which constitute a fine network of nerve-fibres. The spherical Sclera, makes up about 60 percent of the globe and is a white, relatively tough protective tissue. The transparent Cornea, is elliptical in shape, forms the front part of the globe and has a good optical quality. The Conjunctiva are a continuation of the eye-lids, and cover the anterior part of the sclera. The transitional region between the sclera and the cornea is called the Limbus and has a width of about 1mm. The Anterior and Posterior Chambers contain intra-ocular fluid which has a refractive index of 1.33. The Iris is a diaphragm with a variable opening called the Pupil. The diameter of the pupil, which is controlled by the Ciliary Muscles, varies with light intensity so that at high illuminations the pupil area is only 3mm^2 but expands to about 45mm^2 at low illuminations.

1.2.2 Mechanical Section (Eye Muscles):

Eye movements are brought about by the action of six eye muscles, each responsible for the movement in a particular direction. The six consist of four recti and two obliques as follows:

The Internal Rectus (Medial Rectus): This muscle is attached to the eye globe at its equator, and is inserted 6mm behind the limbus. It is the largest and strongest muscle, with a length of 41mm and an insertion of 10mm.

The External Rectus (Lateral Rectus): This lays between the orbital fat and the bony wall of the orbit encircling the equator, and is inserted 7mm from the limbus. It has a length of 41mm and is the second strongest muscle.

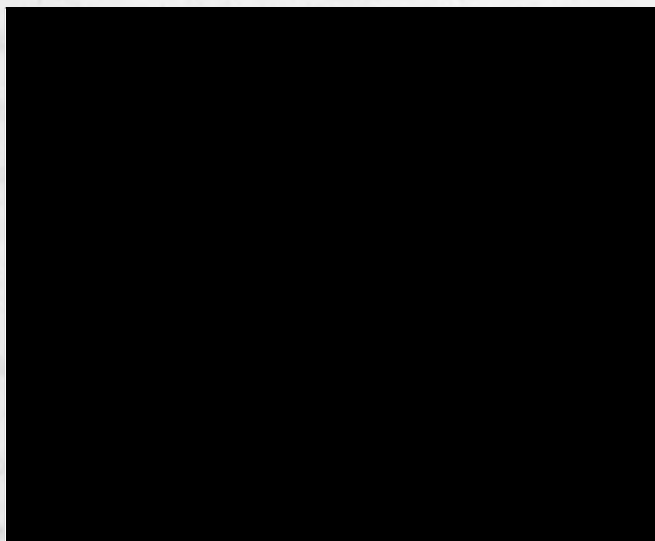


Fig. 1.2 Eye Muscles

The Superior Rectus: This muscle crosses over the long diameter of the orbit, and circles the equator of the globe. It also has a length of 41mm and is inserted 7.6mm above and behind the limbus.

The Inferior Rectus: This lays in the lower part of the orbit, and is inserted into the sclera 6.5mm from the limbus. A few of the strands of this muscle control movement of the lower eye-lid.

The Superior Oblique: The size of this muscle is reduced as it approaches the trochlea, but broadens out into a wider band as it passes backward from the trochlea forming an angle of 50 degrees with itself. It is inserted in the sclera, behind the equator, and also in the external quadrant of the globe. The muscle, which lays obliquely on the globe, has a length of 18.5mm, and an insertion width of 16.5mm.

The Inferior Oblique: This muscle stretches outward and upward, and is in contact with the lower surface of the inferior

rectus muscle. It then rotates upward and backward, so that it inserts into the sclera behind the equator and in the outer and lower quadrant of this part of the eye. The insertion measures from 7 to 9.5mm and is opposite to the insertion of the superior oblique.

1.2.3 Muscle Movements:

The action of each individual muscle is dependent upon its origin, the centre of its rotation and its insertion. These six ocular muscles can be divided into three pairs. Each antagonistic pair of muscles acts independently to rotate the eye on a particular axis, which always passes through the centre of rotation.

1.2.3.a Action of Internal and External Rectus:

Fig. 1.3 illustrates the action of the internal and external rectus in the right eye viewed from above. Here, 'O' represents the origin of the muscles, 'I' the insertion and 'R' the centre of rotation. These muscles rotate the eye around a vertical axis VV' which passes through the centre of rotation. The action of the external rectus produces abduction whilst the internal rectus produces adduction. In this instance no elevation or depression of the eye globe takes place.

1.2.3.b Action of Superior and Inferior Rectus:

The action of the superior and inferior rectus is shown in Fig. 1.4. The insertions are oblique and make an angle of 30 degrees with the vertical axis. The muscles rotate the eye around

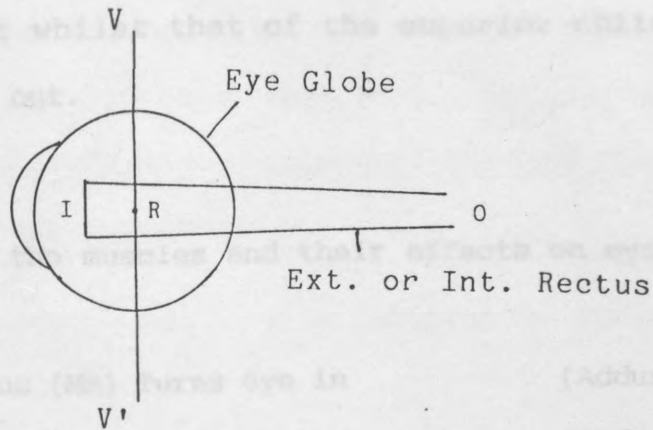


Fig. 1.3 Action of Internal and External Rectus

the axis AA' which is parallel to the insertion 'I', whilst the superior rectus elevates and rotates the eye, the inferior rectus depresses it and rotates it.

1.2.3.c Action of Superior and Inferior Oblique Muscles:

The axis of eye rotation effected by the oblique muscles is shown in Fig. 1.5. The insertion is on the posterior side of the equator so that the contraction of the oblique muscle causes the cornea to rotate upward. The axis of this rotation is parallel to the insertion 'I' and makes an angle of 40 degrees with the

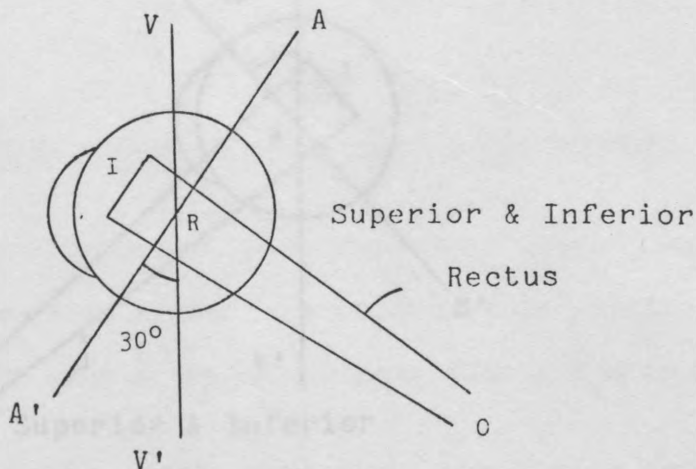


Fig. 1.4 Action of Superior and Inferior Rectus

vertical axis. The action of the inferior oblique is to rotate the eye up and out whilst that of the superior oblique is to rotate it down and out.

1.2.3.d A Summary:

A summary of the muscles and their effects on eye movement is as follows:

Internal Rectus (MR)	Turns eye in	(Adductor)
External " (LR)	" " out	(Abductor)
Superior " (SR)	" " up & in	(Elevator)
Inferior " (IR)	" " down & in	(Depressor)
Superior Oblique(SO)	" " down & out	(Depressor)
Inferior " (IO)	" " up & out	(Elevator)

It is clear therefore that no individual muscle can rotate the globe on the vertical axis or move the eye directly up or down and that at least two muscles are required to perform such an action (Swann, 1931).

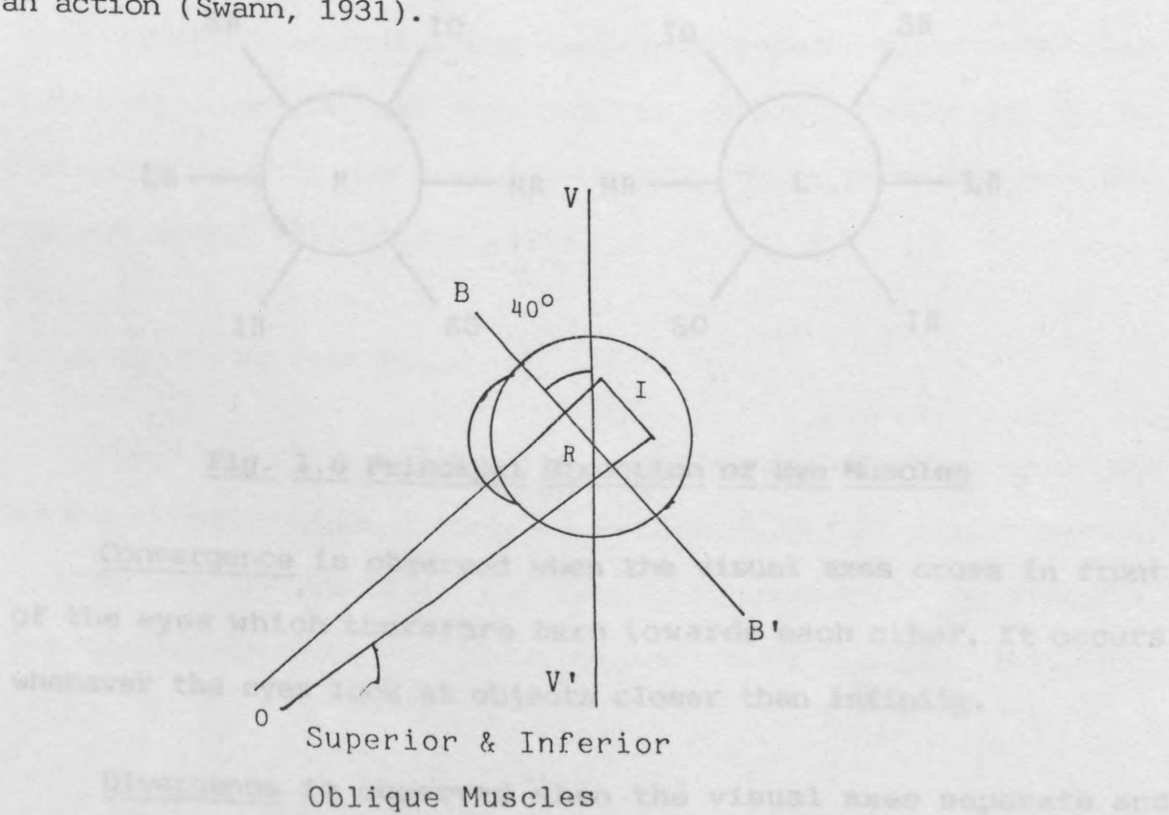


Fig. 1.5 Action of Superior and Inferior Oblique Muscles

Fig. 1.6 summarises the principal direction of action of each pair of antagonistic muscles. The power of the eye muscles is estimated to be 500-fold that required for normal eye movements. Hence, a precise comparison of the two eyes is vital to demonstrate slight sicknesses.

The movement of the two eyes in relation to one another can be categorised as follows:

Versions are movements of the two eyes together and in the same directions.

Vergences are disjointive movements and occur when the two eyes move in opposite directions. These can be either convergent or divergent:

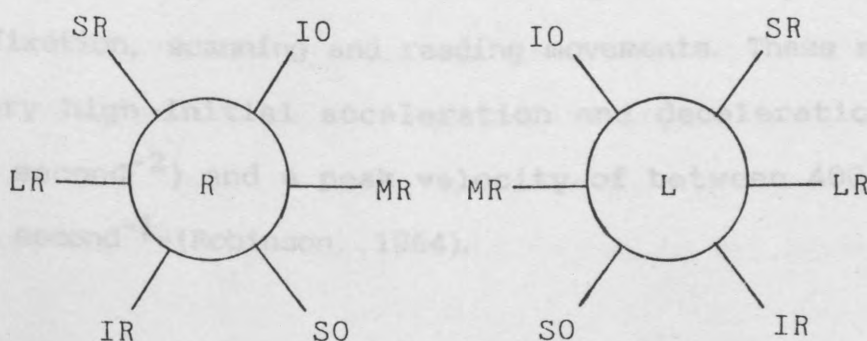


Fig. 1.6 Principal Direction of Eye Muscles

Convergence is observed when the visual axes cross in front of the eyes which therefore turn towards each other. It occurs whenever the eyes look at objects closer than infinity.

Divergence is observed when the visual axes separate and turn outward. A normal subject is capable of only a few degrees

of divergence beyond the straight position.

The other types of movement which occur during tremor eye movements are explained in the following section.

1.3 Different Types of Eye Movement

To be able to research and develop instruments to accurately monitor eye movements, a full understanding of the different types of movement and methods of measurement must be obtained. Some of the known eye movements, which are relevant to this study, are described below.

1.3.1 Saccadic Eye Movements:

These are the rapid and standard conjugate movements of everyday life which are the results of the voluntary changes of fixation from one point to another. They include the 'jump and reset' fixation, scanning and reading movements. These movements have very high initial acceleration and deceleration ($40000 \text{ degrees second}^{-2}$) and a peak velocity of between 400 and 600 $\text{degrees second}^{-1}$ (Robinson, 1964).

1.3.2 Smooth Pursuit Movements:

These are again conjugate eye movements which closely follow moving objects within a range of between 1 and 30 $\text{degree second}^{-1}$.

They are not voluntary and usually require a moving stimulus. The acceleration and velocity appear to be limited (Robinson, 1965).

1.3.3 Smooth Compensatory Movements:

These closely follow the apparent movement of a fixation point resulting from compensation for the active or passive movements of the body or the head.

1.3.4 Nystagmus Movements:

These are characteristic saw-tooth pattern (to-and-fro) eye movements and are made up of a slow shift whilst the eyes fixate, and a fast return saccadic jump for re-fixation.

There is a 0.2 second time duration between the fast returns which result in a typical frequency of usually not more than about 5Hz.

A particular form of nystagmus, called 'gaze nystagmus', is associated with a number of neurological disorders. The amplitude of these movements can be large enough for direct observation or can be small, requiring recording instruments. In this study an attempt is made to record gaze nystagmus with an horizontal amplitude of not less 0.5 degree in all directions of gaze.

Nystagmus, as described above, could be either 'asymmetric' containing a slow phase and a fast phase, or 'pendular' showing small high-frequency oscillations of about 4 to 10Hz.

1.3.5 Torsional Movements:

Such movements occur when either the head or body rotates about the eye axis. This produces rotation of the eye-ball about

the line of gaze of up to 10 degrees.

1.3.6 Vergent Eye Movements:

These are movements of the two eyes in opposite directions so as to fuse images at different distances and maintain adequate binocular fixation. These movements are much slower and smoother than conjugate eye movements, with a maximum velocity of about 10 degrees second⁻¹ and a range of nearly 15 degrees.

1.3.7 Miniature Eye Movements:

These are very small movements which occur at all times. They are also referred to as 'fixation movements' since they are present even though the eye-ball is supposedly stationary. Their amplitude is always less than 1 degree during fixation.

For the detection of any of the above eye movements, a point of reference on the eye is required. The following section describes some of the criteria for identifying this reference point.

1.4 Physical Characteristics of the Eye which are used in the

Measurements

Different components or land-marks of the eye may be used to monitor its movement. The more widely used eye characteristics are described below:

1.4.1 The Retina:

The retina, which moves with the eye-ball, facilitates the

visual position sensing and hence provides a subjective assessment of the eye movements. The After Image technique was one of the earliest quantitative methods, which used the retina, for measuring the velocity of the eye during saccadic and pursuit eye movements.

1.4.2 Cornea-Retinal Potential:

Between the cornea and the retina there usually exists a potential difference of up to 1mV, which is widely used as the basis of an applied clinical eye movement technique or Electro-Oculography (E.O.G.) (Young, 1975).

1.4.3 Electrical Impedance:

An impedance can be measured between two electrodes placed at the outer canthi of the two eyes. This impedance may vary with the eye position, and is due either to the non-homogeneous or to the anisotropic nature of electrical characteristics of the eye-ball tissues. Therefore changes in position of the eye tissues alter the resistivity of the path between the two electrodes which can be a measure of the eye movement (Geddes, 1965).

1.4.4 The Corneal Bulge:

The cornea has a smaller radius of curvature than the eye-ball, yet its centre is close to the optical axis. This characteristic is used in a number of important methods for measuring eye movements. The corneal bulge, which can be felt through the eye-lid of a closed eye, can be detected by a pressure transducer placed over the eye-lid, and can therefore be used to monitor eye movements.

1.4.5 Corneal Reflections:

The corneal bulge is only a 25 degree spherical section of a sphere. As reflections of a light source from the cornea, or any convex surface, form a virtual image behind the surface, such images can be photographed or recorded. The position of this corneal reflex is a function of eye position. Rotation of the eye-ball produces translational and rotational movements of the cornea, which is used in Corneal Reflection Systems for measuring eye movements.

1.4.6 Reflections from other layer of the eye - Purkinje Image:

Beside the corneal reflection, light is also reflected from each surface of the eye where there is a change in refractive index. Corneal reflections together with reflections from the posterior surface of the cornea and the anterior and posterior surfaces of the lens produce four Purkinje Images (Fig. 5.1). After the first corneal reflection the next brightest Purkinje image is the fourth reflection from the posterior of the lens. As the eye-ball moves, the relative displacement between the first and fourth images is used to measure the orientation of the eye in space, independent of its relation to head position.

1.4.7 The Pupil:

The reflectance of the pupil and the iris are different and under controlled lighting conditions, the pupil appears to be much darker than the iris. This is because the majority of incident light on the pupil is trapped in the eye-ball so that no

reflection is received from it. However, by shining collimated light along the optical axis of the eye, most of the incident light may be reflected back so that the pupil appears considerably brighter than the iris. In either case, the pupil can be optically distinguished from the surrounding iris. This distinction can be further sharpened by the use of infrared light which is nearly entirely absorbed by the retina.

1.4.8 Other Land-marks:

Scleral blood vessels, folds of the iris and the retinal vessels could all be used for imaging and tracking especially when using a travelling microscope. Furthermore, artificial land-marks, such as a globule of mercury placed on the eye could also be used (Barlow, 1952). Other examples include the use of chalk and egg membrane or a small piece of metal embedded in the sclera. The latter method may be especially useful for magnetically tracking the eye.

1.4.9 The Limbus:

The iris is always distinct from the sclera and is normally visible. These features form the basis of the standard visual assessment of the angle of gaze. The position of the limbus can be measured relative to the head by the T.V. method of eye tracking. The ratio of reflected white light between the bright sclera and the dark iris could be measured by using photodiodes and phototransistors and form the basis for photoelectric measurements.

1.5 Conclusions

A pre-requisite to the development of instruments for the accurate and successful measurement of relative and tremor eye movements is, an appreciation of the functioning of the eye and its component parts.

The measurement of relative eye movements must be to identify anomalies in any of the six eye muscles. This entails a test which requires the eye to move in all directions so as to bring all six muscles into action. Furthermore, knowledge of the different types of relative eye movements will help to distinguish the correct movement and to analyse the results.

Apart from the different eye movements, the physical characteristics of the eye must also be understood so as to provide the necessary tools to measure tremor movements of the eye. From the previous sections the limbus detection was an attractive proposition, because of its high contrast and its size.

PART I

RELATIVE EYE MOVEMENTS

In the following Chapters of Part I, the more conventional methods of measuring relative eye movements are critically discussed, and the requirements of an automated system with improved characteristics described. The design and construction of the hardware for the automated system is also presented.

CHAPTER 2

2.1 A Survey of Previous Methods and Instruments

2.1.1 Introduction:

Any effective test is required to be accurate, precise and fast. Many of the methods described below, such as the cover test, the red/green test and the head-tilt test, are qualitative in nature and provide information which may, in conjunction with other neurological investigations, localise and establish the cause of the disorder. However, the more quantitative methods, such as measurement in the various directions of gaze, the prism cover test and the Hess screen test, will also allow the progress of the disorder to be established.

Furthermore, many of the tests are only subjective, and measure the deviation for distant fixation. Others may be used for near and distant fixation, but only in the primary position. If measurements in all nine cardinal fields are required, then different tests are necessary, but this may change the fusion entirely.

The methods reviewed below are for the detection, and also the measurement of ocular muscles imbalances such as heterophoria, strabismus and ocular paralysis.

2.1.2 Direct Observation Method:

This is one of the earliest and quickest methods devised to evaluate eye movements. Either one eye, as in the duction test,

or both eyes, as in the version test, are studied.

2.1.2.a Duction:

Whilst one eye was covered, the other was fixed on a sharp-pointed object which was moved to the various gaze positions. Any departure from this fixation was therefore indicative of ocular eye paralysis. This method was later up-dated by monitoring the reflection of a moving light source from the cornea. Any displacement of this reflection, relative to the pupil, similarly demonstrated poor fixation. Because of the eye-lids, findings of the duction test were more difficult to evaluate in the vertical direction than in the horizontal direction (Hugonnier, 1969). Although this was a very fast and relatively effective test, it was crude and did not produce permanent records.

2.1.2.b Version:

In this method, both eyes were kept open and the head was kept motionless. The patient fixated on a moving light source in the nine directions of gaze. The corneal reflection was centred on the dominant eye. However, if at any point, the reflection was not centred on the deviating eye, this was indicative that certain ocular muscle imbalances existed (Fig. 2.1) (Hirschberg, 1881; Hugonnier, 1969).

2.1.3 The Mackenzie Method:

Mackenzie, in 1833, suggested that diplopia could be identified by the loss of power in the eye muscles when the patient follows the movement of a finger from side to side and upward and downward (Sloan, 1951).

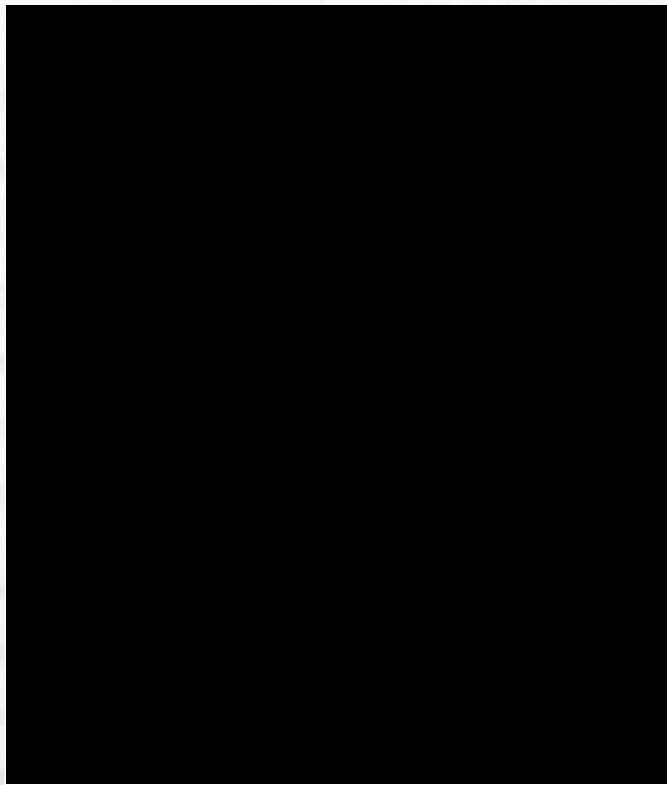


Fig. 2.1 Hirschberg Test. Taken from Von Noorden (1967)

2.1.4 Bielschowsky's (or Head Tilt) Test:

When the eyes are at the primary position, tilting the head towards a shoulder may result in differences in eye level, indicative of the presence of ocular muscle imbalance. This is a simple test used to confirm a paralysis of the superior oblique, and is performed by the patient tilting his head towards the shoulder where he has paralysis, while keeping his head erect and his eyes in the primary position. If the superior oblique muscle is paralysed, with the head in this position, the eye makes a very distinct movement of elevation, and diplopia is at its maximum. By tilting the head to the other side, diplopia may be weak or absent, with therefore no change in eye levels.

Many patients with super oblique paralysis, habitually carry their head tilted to one shoulder. With his head tilted towards the opposite shoulder, the patient would experience a very large vertical deviation in his eye.

The testing of eyes with the head tilted successively towards one shoulder and then the other, was initially introduced by Hofmann and Bielschowsky in 1900 and then widely developed by Bielschowsky (1938) and is now commonly referred to as the Head Tilt Test. This useful test gives constructive findings and can be readily used in the examination of young children who as yet can not respond to subjective tests.

Later, Bielschowsky (1938) performed the test by positioning a light in the centre of a tangent scale at a distance of 2.5 meters from the patient's eyes but on the same level and in the median plane of his head. A dark red glass plate, which was dark enough to block all images except the red image of the light behind it, was first put in front of one eye, then the other eye. Instead of moving the light source, fixated by the patient, the practitioner turned the patient's head so that he had to move his eyes in the opposite direction in order to maintain fixation. This rotation of the head induced various ocular movements giving the practitioner the advantage of being able to control the position of the head and hence the eyes of the patient. The patient could therefore see the position of the red light, relative to the tangent scale, and could indicate the number on the scale which gave a measure of the deviation of his eyes.

2.1.5 Photographic Methods:

In these methods, photographs are taken of the eyes in the primary position and also in each of the directions of gaze where the imbalance is the most pronounced. Such methods produce sets of permanent records for the examination of ocular imbalances and are also ideal for teaching purposes and presentations

(Hugonnier, 1969). head was moved to nine cardinal positions.

2.1.6 Maddox Rod:

Maddox (1898) described the use of a tangent scale and a glass rod to measure relative eye movements. A cross was constructed which contained a central light, and markings of arc degrees of eye movement at a distance of 5 meters. With the patient seated in front of the cross, readings were taken with the head at nine different positions. By rotating the head in this way, rather than the cross, eye movement was stimulated. A maddox rod was then held before one eye in such a way that it could not be focused. The patient was then able to indicate where the streak of the Maddox rod passed through the scale, thus giving horizontal and vertical measurements of deviation (Fig. 2.2). This method was later modified by the use of prisms, which corrected the displacement, and gave a measure of the relative imbalance of the eyes (Solomons, 1978).

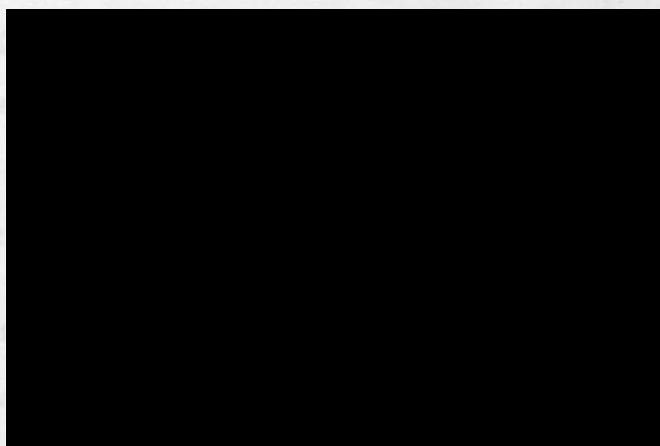


Fig. 2.2 Maddox Rod Test. Modified from Von Noorden (1967)

Two other similar methods are also described here. Duane (1896) used a reversible screen which was black on the patient's side and white facing the practitioner. A red glass plate was placed in front of the right eye and the light source, rather

than the patient's head, was moved to nine cardinal positions. Different images were located on the screen with pins, thus indicating the displacement in degrees. Diplopia was then evaluated on the white side of the screen, and subsequently a reduced diagnosis chart was produced.

Later Stevens (1906) presented his tropometer, designed to measure various rotations of the eye. This instrument consisted of a telescope with either a 45 degree prism or a mirror at its objective end so as to reflect light perpendicularly. Stevens claimed that the tropometer offered a perfect means of measuring the rotation ability of an affected muscle.

2.1.7 Electromyography:

This rather cumbersome method, which was first introduced by Bjork (1952), required the patient to lie flat on an electrically isolated material and to have electrode needles inserted into his muscles. The discharge, due to the contraction of a group of muscle fibres, produced a signal which was transmitted to an amplifier and then to a C.R.O. as well as to a loud-speaker.

2.1.8 Cover Test:

This is a relatively fast method which can be used to monitor eye movements in all directions. Although it allows many facts about the status of a patient's neuro-muscular condition to be established, the results, as in the version and duction tests, cannot easily be plotted graphically so that permanent records are not usually obtained (Von Nooden, 1985).

In this method the patient was asked to fixate on a small

distant light source with one eye covered. If imbalances were present, the covered eye would first deviate, but would then move back to resume fixation when it was uncovered. The other eye, however, maintained fixation and made no movement. This deviation, and its direction of movements, determined the type of muscle imbalances that existed (Duane, 1896).

To be able to document the results, prisms could be introduced so as to quantitate the deviation in arc degrees. This was done by firstly estimating the amount of deviation and then placing a prism, with a strength less than that of the estimate, in the appropriate direction in front of the eye so as to reduce the deviation. The prism strength was then increased until there was zero movement. Although this modification provided permanent records, it extended the duration of the test (Hugonnier, 1969).

White (1944) suggested the following pre-requisites for a successful cover test.

1. Sufficient light so that small movements can be observed.
2. The cover of the eye must not attract attention to its position (The cover must not be focused).
3. The cover should not be moved more rapidly than the eye can take up fixation.

The cover test may not reveal small deviations but, in general, this limitation should not undermine its value of simplicity. It also lacked accuracy since the results were dependent on the observer's ability to judge the extent of deviation (Borish, 1970).

Investigations of diplopia are based on two different groups of experiments or tests, depending on the principles they apply.

These two groups, which are the red glass test and the Hess-Lancaster test, are described in the two following sections.

2.1.9 The Red Glass Test:

In this method, a single object was presented to both eyes when one was covered by a red filter (Fig. 2.3). The red glass had to be dark enough to allow the patient to only see the red image of the object. The distance between the red and the

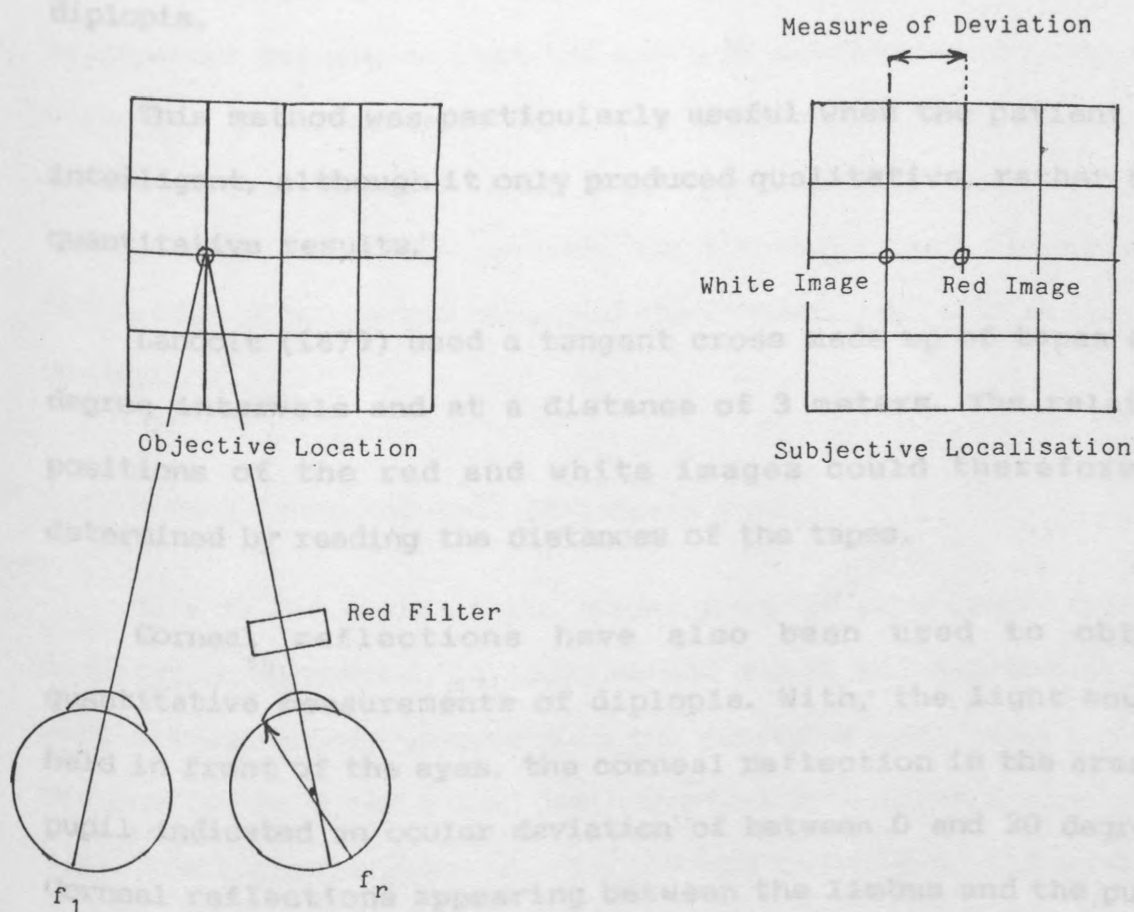


Fig. 2.3 Principle of the Red Glass Test

ordinary images was a measure of the deviation (Von Noorden, 1985).

Hirschberg (1881), one of the first to suggest and employ

this method, used a candle flame as the object and asked the patient to indicate the positions of the two subjective images of the flame (c.f. Fig. 2.1). This test was carried out in front of a wall painted with square divisions, each representing 5 degrees deviation of the eye from the primary position. Previously, Carter (1876) had suggested the use of coloured glass filters and an elongated fixation testing object. Later, many other researchers, such as Ziegler (1893), Duane (1896), Maddox (1898), Jackson (1900), Nettleship (1900), Tiffany (1902) and Stevens (1906), also used a candle and a red filter to investigate diplopia.

This method was particularly useful when the patient was intelligent, although it only produced qualitative, rather than quantitative results.

Landolt (1879) used a tangent cross made up of tapes at 5 degree intervals and at a distance of 3 meters. The relative positions of the red and white images could therefore be determined by reading the distances of the tapes.

Corneal reflections have also been used to obtain quantitative measurements of diplopia. With, the light source held in front of the eyes, the corneal reflection in the area of pupil indicated an ocular deviation of between 0 and 20 degrees. Corneal reflections appearing between the limbus and the pupil border indicated a deviation of 20 to 45 degrees, whilst broad and distorted corneal reflections on the sclera were representative of deviations greater than 45 degrees (Jones, 1970). A draw-back of these methods, however, was that they were only of use on patients with large degrees of squints, since small deviations could not be detected by using a single coloured

filter (Sloane, 1951).

Sloane also described a method, which he found valuable for everyday use. It consisted of a transparent piece of plastic board with a light-weight handle. At its centre was placed a bulb with a Maddox cross, indicating tangents up to ± 24 degrees horizontal and ± 12 degrees vertical. The observer stood directly behind a screen, held at a distance of 0.5m, so that he was able to observe the patients' eye movements. The patient, with his head fixed, and one of his eyes covered by a red filter, was asked to point at the position of the red light over the transparent screen, so that the angle of deviation could be read directly. The same procedure was then repeated at different angles of gaze. Krusius (1908) used a similar glass screen, which was divided into small squares, for the above test. He employed two luminous bulbs and observed the corneal reflection for any deviations.

2.1.10 Hess-Lancaster Test (Red-Green Test):

This is the basis of the second group of experiments used to investigate diplopia. In this method a red and a green object were simultaneously presented to the patient's eyes, when one eye was covered by a red filter and the other by a green filter (Fig. 2.4). The apparent positions of the two objects to the patient was a measure of the ocular deviation of his eyes (Von Noorden, 1985).

Hering (1899) was one of the first to use this method. He placed a red filter before the right eye and a green filter before the left, and then moved the red and green targets, seen monocularly with each eye, until they appeared superimposed. He

used faint red and green lights as his targets so that the red target was invisible through the green filter and vice versa.

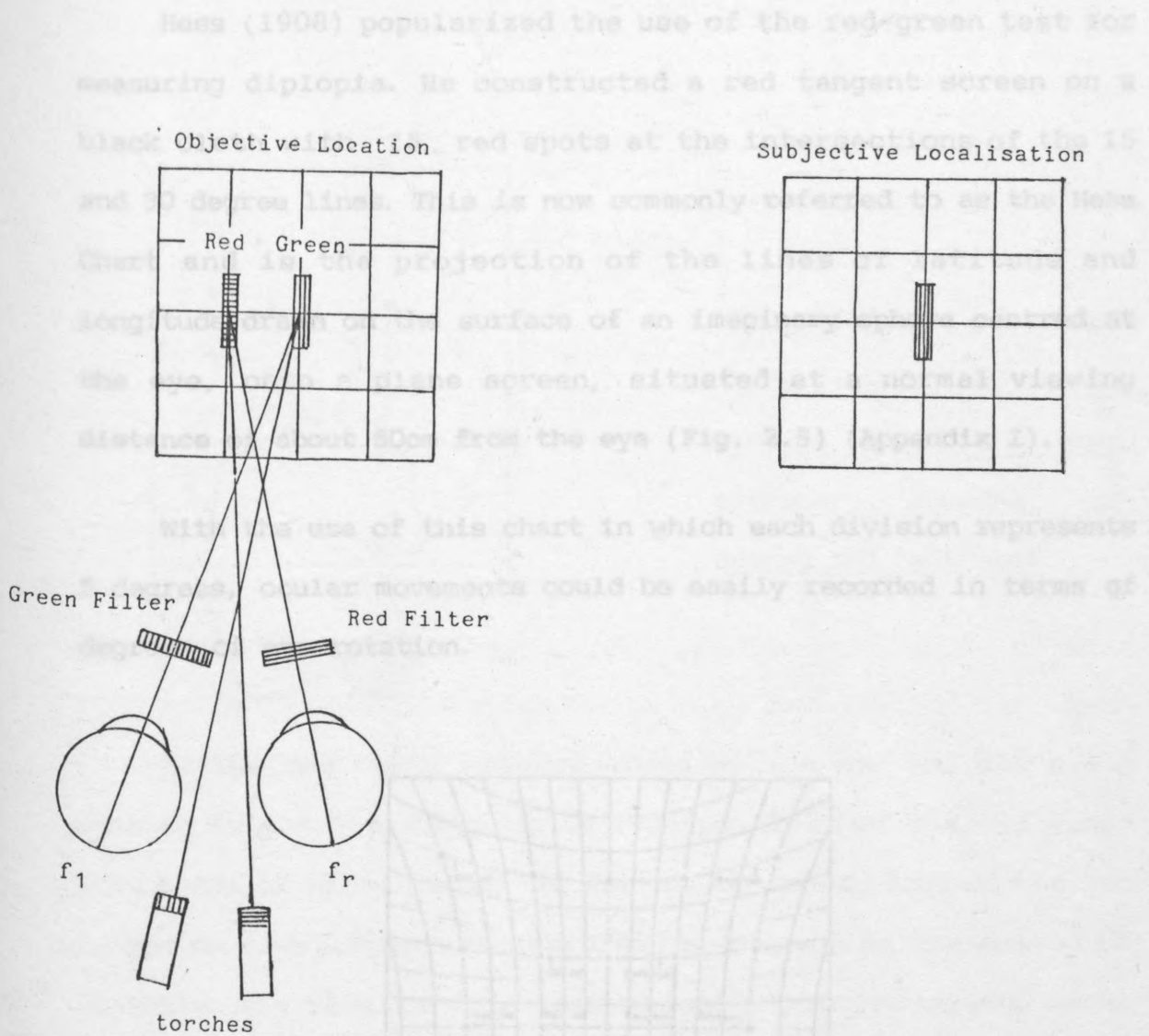


Fig. 2.4 Principle of the Red-Green Test

Williams (1901) constructed a cross with red lights and green numbers on its arms. His patient was asked to wear a pair of complementary red-green goggles and to sit in front of the cross at a distance of 20 feet. Williams was then able to switch "on" the vertical red lights and read the horizontal deviation on the horizontal green numbers and also vice versa, by switching the red lights "off" on the vertical arm and "on" on the horizontal arm. Unfortunately, he only performed the test in the primary position and made no mention of the various positions of

gaze.

Hess (1908) popularized the use of the red-green test for measuring diplopia. He constructed a red tangent screen on a black cloth with 25 red spots at the intersections of the 15 and 30 degree lines. This is now commonly referred to as the Hess Chart and is the projection of the lines of latitude and longitude drawn on the surface of an imaginary sphere centred at the eye, onto a plane screen, situated at a normal viewing distance of about 50cm from the eye (Fig. 2.5) (Appendix I).

With the use of this chart in which each division represents 5 degrees, ocular movements could be easily recorded in terms of degrees of eye rotation.

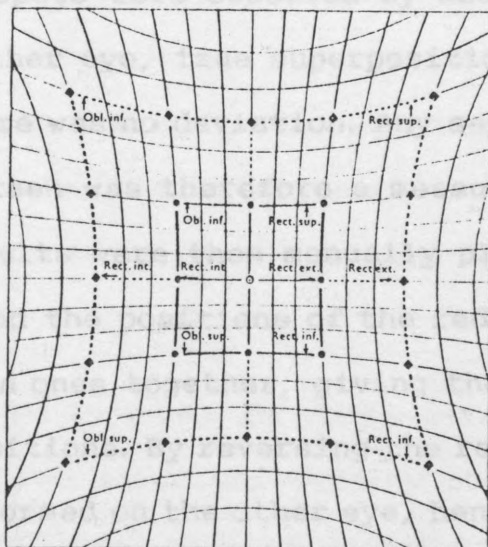


Fig. 2.5 Hess Tangent Screen

The patient, sitting about 0.5 metre away from the screen and wearing a pair of complementary red-green goggles, was asked to point at each of the spots with a green pointer. Thus the eye looking through the red filter could only observe the red spots and the lines of the tangent screen whilst the other eye, looking

through the green filter, could only observe the green pointer on the end of his stick (Fig. 2.6)

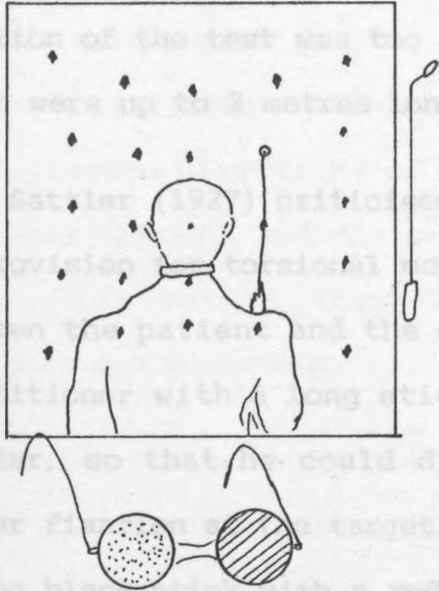


Fig. 2.6 One of Hess's early methods of screen test with red and green glasses, showing the screen and indicator

As the red spots were observed by one eye and the green pointer by the other eye, true superposition of the two would only occur if there was no deviation. Any separation of the two images on the screen was therefore a measure of the extent of diplopia. The results were then manually plotted onto a small chart which joined the positions of the red spots together and those of the green ones together, giving the deviations in the nine cardinal positions. By reversing the red and green filters the test was performed on the other eye, hence producing a plot for each eye.

Although this was a quick and easy method giving permanent records, the obstruction by the use of goggles posed problems for the angles of deviation greater than 20 degrees. Furthermore, colour-blind patients and aging of the colours of the filters could cause fusional stimulus.

Ohms (1906) constructed a complicated piece of apparatus with movable green and red arrows on the vertical and horizontal arms respectively. As the red arrow was also able to rotate, it could be superimposed on the green arrow, and thus give a measure of the torsional deviations. It was considered, however, that the duration of the test was too long and the movements of the arms, which were up to 2 metres long, were too troublesome and clumsy.

Sattler (1927) criticised Hess's method because of the lack of provision for torsional movements and the use of 50cm distance between the patient and the chart. He, therefore, provided the practitioner with a long stick at the end of which was a green pointer, so that he could direct the patient's attention for proper fixation at the target. The patient was also provided with a long black stick with a red pointer, so that he could indicate the position of his fixation. Sattler commented that, for a pronounced paresis, a 20 degree field was sufficient to identify the imbalanced muscle, whilst a larger field was necessary with weak paresis. However, his method was generally thought to be difficult to conduct since the screen was a green chart painted on a wall.

Lancaster (1939) replaced the sticks with torches and used a white screen. The red torch was used by the examiner and the green torch by the patient. To investigate muscle imbalances in each eye the filters placed in front of the eyes or, the torches, could be interchanged. The deviation of the eyes was determined from the extent of relative deviation between the red and green lights. These results were entered onto a small chart on which an image of the screen was reproduced. The test had the advantage of providing the examiner with a greater degree of flexibility to examine a particular field of fixation. Its disadvantages were,

however, the need for a dark room, a steady hand for the projection of the light and the manual recording of results.

A modification to the Lancaster method was made by Anderson (1947), who used torches to produce horizontal lines rather than dots. He projected a red horizontal line in the middle of the chart and asked the patient to project a green line over it. For the different directions of gaze, the projection of the entire chart was changed, but the red line was always projected at its centre. This method, therefore, facilitated the recording of torsional eye movements.

Burian (1941) used the effect of polarisation to measure the extent of deviation. Here, the tangent screen was projected in horizontal polarized light whilst a dot was projected in vertical polarized light. The deviation was measured by placing polarized glasses in front of the eyes of the patient, and then reversing the glasses, so that the chart for the other eye could be plotted. This method has, however, been criticised for the amount of equipment involved and the time required to set up the apparatus.

Lees (1949) modified the Hess screen test by eliminating the problem of colour-separation. This problem arose because of the difficulties in manufacturing true complementary coloured goggles, pointer and screen. Furthermore, aging may have effected the colour stability of the materials. Therefore, for example, the red pattern of the chart may have been faintly visible through the green filter, or the green pointer through the red filter. Hence, the dissociation obtained, may only have been relative, with the results of large errors in the test. Even if the colours were made truly complementary, errors may still have

occurred if the eclipse of the red screen, which took place as the pointer was moved across it, was noticed by the observer. The monocular localisation of the pointer would have caused fusional stimuli and distorted the true angle of deviation. Lees, who developed his method at the Manchester Royal Eye Hospital, noticed that with the Hess method, because of the low level of contrast, many patients also had difficulties in recognising the chart pattern or the pointer. Colour-blindness also contributed to this problem.

Lees then constructed his system around a mirror with two reflecting surfaces which could be placed in front of either eye. The mirror was situated exactly half-way between two identically printed Hess tangent screens at right angles to each other. Each screen could be illuminated from the back for the pattern to appear or disappear as required during the test. The patient was seated in such a way that he could observe one screen directly and the other via the mirror, so that the two Hess charts appeared exactly superimposed. In order to avoid fusional stimuli, the deviation was plotted as one of the screens was made to disappear, leaving only a blank surface.

As illustrated in Fig. 2.7, the patient was seated close to the mirror and facing the screen A. Whilst this screen was observed with one eye, screen B was observed, through the mirror, by the other eye. Screen A was blanked whilst screen B was illuminated to show the Hess chart. The practitioner then indicated a particular point on screen B and asked the patient to indicate, on screen A, the position of the point. By momentarily illuminating screen A, the practitioner was able to identify the position of the patients' pointer and manually record it onto a

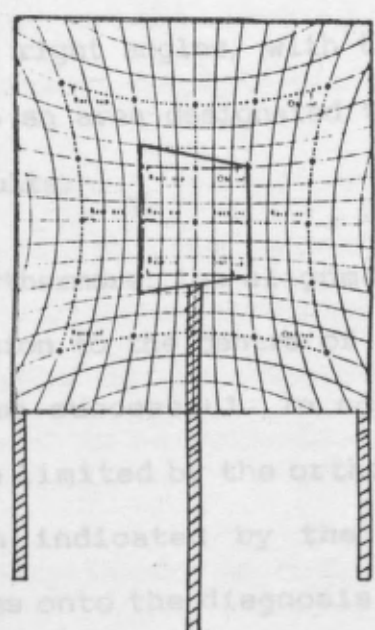
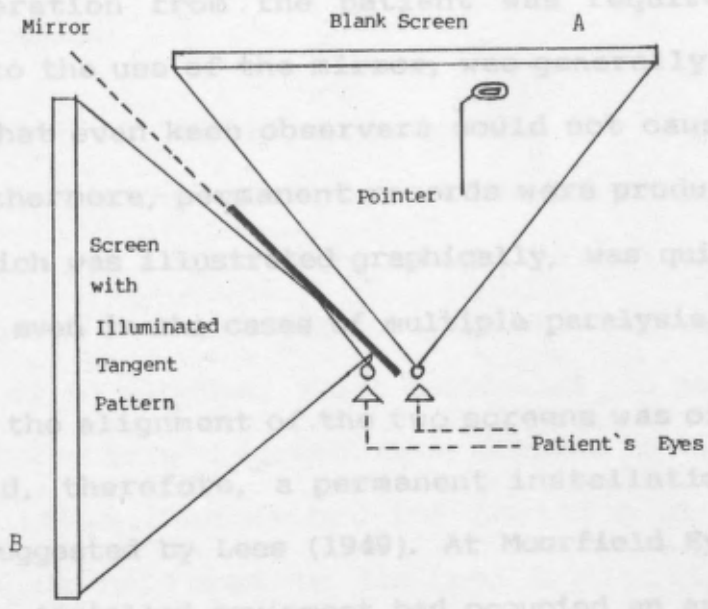
small printed Hess chart. The examiner could then place his pointer at various positions of gaze on the screen and transfer his findings onto the Hess chart, as with the red-green test.

This method was more accurate than the Hess test and gave away the test result and had accuracy error as low as 10%.

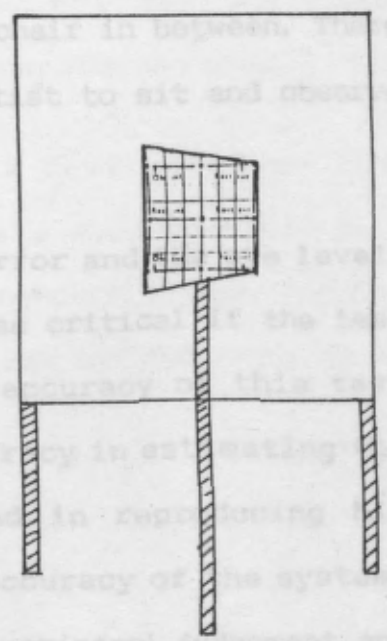
Amongst its other advantages were that minimum cooperation from the patient was required and the patient was unaware of the test. The test was also very easy to perform and the results were produced and the deviation, which was usually graphically, was quick and easy to interpret, even in cases of multiple paralysis.

However, the alignment of the screens was of paramount importance and, therefore, a permanent installation could be required as suggested by Lees (1949). At Moorfield Eye Hospital, London, the installed equipment had occupied an area of about 10 ft².

The two screens were permanently mounted on two adjoining walls at right angles to each other. The patient's eyes were positioned at the vertex of the two screens.



Two Charts Superimposed



One screen is Blanked for Performance of the test

Fig 2.7 Lay Out of Lees Screens

small printed Hess chart. The examiner could then place his pointer at various positions of gaze on the screen and transfer his findings onto the small chart, as with the red-green test.

This method was more accurate than the Hess test and gave more rapid results. Amongst its other advantages were that minimum cooperation from the patient was required and the patient, due to the use of the mirror, was generally unaware of the test so that even keen observers could not cause fusional stimulus. Furthermore, permanent records were produced and the deviation, which was illustrated graphically, was quick and easy to interpret, even in the cases of multiple paralysis.

However, the alignment of the two screens was of paramount importance and, therefore, a permanent installation could be required as suggested by Lees (1949). At Moorfield Eye Hospital, in London, the installed equipment had occupied an area of about 4m^2 . The two screens were permanently mounted on two adjoining walls at right angles, with the patient's chair in between. There was also an area designated to the orthoptist to sit and observe the results.

Furthermore, the alignment of the mirror and the eye level, in relation to the centre of the chart, was critical if the test was to be successful. In addition, the accuracy of this test could be limited by the orthoptists' accuracy in estimating the position indicated by the patient, and in reproducing his estimates onto the diagnosis chart. The accuracy of the system, therefore, was clearly dependent on the examiners' judgement and experience. However, such experience could be detrimental to the accurate estimation of the position indicated by the patient. Quite frequently, orthoptists look for a previously defined trend

in relative eye movements and interpret the position of the patient's pointer according to their expectations. As a result, they use the diagnosis Hess chart to look for trends and not for numerical results. Finally, the manufacturing cost was proved to be more than the Hess test.

2.1.11 L.E.D. Screen:

Rouse (1980) attempted to automate the Hess test by replacing the Lees screen with nine red light emitting diodes mounted on a board, referred to as the target screen. The patient, who wore a pair of red-green goggles, was able to adjust a marking arm of an autoplots, which controlled the projection of a green dot on the target screen. Once aligned by the patient, the autoplots could then record the position of the green projected dot in relation to the red L.E.D., lit by the practitioner via a control panel. This method was a marked improvement on the Hess-Lancaster test, but had the same shortcomings of complete dissociation between the two eyes.

Furthermore, the patients' view was restricted by the goggles and the room had to be "completely dark to avoid any fusional movements stimulated by visible contours" (Rouse, 1980). The alignment of the autoplots with the screen and its paper were also thought to be cumbersome.

2.1.12 Miscellaneous Methods:

Kestenbaum (1946) described a quick but rather crude method of measuring diplopia without the use of goggles. A candle and a pencil were held before the patients' eyes in such a way that the patient observed two images of the candle and two images of the

pencil. The pencil was then moved until one of its images was superimposed on the image of the candle, and so the actual distance between the candle and the pencil was a measure of diplopia (Fig. 2.8).

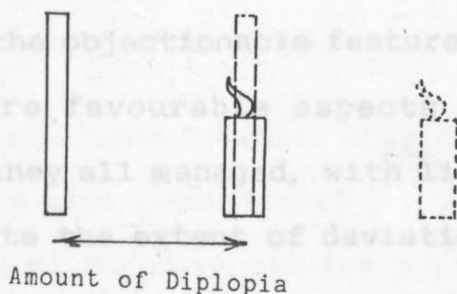


Fig. 2.8 Double Image Method

Investigation into ultrasonic scan systems had indicated that these did not offer accurate methods of measuring eye movements (Fuller, 1977).

The A-scan system of measuring eye movements was beneficial in terms of speed, but did not produce a correct measure of eye movement. This was because the system could only be applied from the side of the eye, i.e. in the same plane as the eye's surface, and could only measure lateral, rather than rotational, eye movements. The B-scan system almost catered for this problem, but then the speed of the measurement was limited by the speed of the mechanical scan of the ultrasonic transducer. The C-scan system, which gave a raster T.V. picture of the eye, was yet more limited in speed due to the increased mechanical scanning required. Hence, it could take in the order of seconds to produce a full image of the eye. Furthermore, the method required too many attachments to the eye, including a water bath as the medium to match and transfer the transducer frequency to that of the eye tissues (Restori, 1985).

2.1.13 Conclusions:

Over the last century many different methods of diplopia-field tests have been produced. The methods described above, all achieved their basic objectives of determining and measuring diplopia. Whilst the objectionable features of the tests were tolerated, the more favourable aspects were extended and exploited so that they all managed, with little difficulty, to analyse and evaluate the extent of deviation in the eyes.

The testing distance varied from 50cm to 6 metres. Whilst 50cm was criticised for stimulating accommodation, and thus influencing the angle of deviation, 6 metres was also criticised for being too far for accurately observing the eye.

Tangents of the arc degrees scale was a more favourable measure and was utilized by most of the studies. This gave larger divisions for squares further away from the zero point for primary position.

Most of the tests moved the target rather than the patients' head, although Lancaster (1939) stated that, for wider excursions, the head could be turned. Movement of the chart, however, was found to be even more precise and easier to measure than movement of the head.

In order to limit a given field to the action of a single muscle, many were tempted to test the eye beyond 15 degrees deflection, hence requiring an increase in the size of the tangent screen. Ohms (1906) and Scattler (1927) used screens suitable to accommodate eye deflections of up to ± 50 degrees. However, given the practical size of the examination room, the

use of head movements is a more realistic method of measuring large ocular deflections.

As more investigations were directed towards the recording of relative eye movements, the benefits of eyes' dissociation for the patient, became more evident. However, this dissociation of the eyes involved far more expensive pieces of equipment.

Whilst some of the tests revealed only the separation of the double images, others also demonstrated the influence of torsion. Since the evaluation of diplopia was far more important than the evaluation of torsion, former tests had survived and were more routinely used.

In general, the cover test and the use of prisms produced accurate results, although the handling and placing of the large number of strong prisms, was found to be difficult. The corneal reflex method was not very accurate, but was quick and easy to perform.

Overall, the Hess-Lancaster and the Lees screen test, which incorporated many of the best features of the other tests reviewed above, including the production of a good record of data, were considered to be the most favourable of the methods. However, it should be noted here, that different methods were suitable for different circumstances, and the knowledge of the principles involved in their theories and operations could only bring a better understanding.

2.2 Initial Design Consideration

After a full survey of the available methods and instruments, it was apparent that the design of a system with all

the advantages and objectives of existing systems without their associated disadvantages was a very difficult task. In this section, it^{is} intended to outline most of the considerations used in the previous methods, so to produce the design specification of a new automated system. These design considerations are as follows:

1. It was clear from the previous sections that systems which were based on the dissociation of the eyes for measuring diplopia, had more merit than the alternatives. Lee (1949) achieved this by presenting two separate screens, one to each eye, hence providing complete dissociation of the two eyes. This was hence to be adopted for the new automated system.

2. The distance between the patient's eye and the test screen had been a matter of much controversy. Although criticised for the stimulation of accommodation, many had used 50cm as a comfortable distance. Sloane (1951), who had many years of clinical experience, states:

"In the matter of diagnosis of an ocular paresis, I have found no disadvantage in using the test at a 0.5m distance as compared with the 2-metre distance that I had been using with the double-image type of test for the past 11 years".

A distance of about 50cm, therefore, was chosen as a comfortable distance for fixation.

3. The extent of permitted eye rotation must also be considered. Most methods utilized ranges from 0 to 20 degrees. In this study, however, a range of up to 20 degrees vertically and even 30 degrees horizontally was used to provide an adequate and sensitive method for accurate measurement. This would also

facilitate the identification of the action of each eye muscle separately (c.f. section 1.2.3.d).

4. Early systems used equi-distant division charts to record the degree of eye rotation. Later Hess, for the first time, used the projection of the lines of latitude and longitude drawn on the surface of an imaginary sphere centred at the eye, onto a plane "tangent" screen. This is considered to be a more favourable charting method as it produces a more representative measure of eye rotation.

5. The ease with which the test was performed was also of interest to both patients and orthoptists. The simplicity of the test would reduce both the patient's anxiety and fatigue and hence considerably improve the results.

6. One way of successfully introducing an automated system into a hospital as a standard test was to reduce the duration of the test. This could be achieved by making provisions for a preliminary test, which would initially test for only nine cardinal eye positions and then, if necessary, extend the number of measurements.

7. Relieving the orthoptist from involvement in the test during operation, would greatly increase the popularity of the test in hospitals. The results of the measurements could automatically be recorded without any supervision.

8. Provision should be made for the orthoptist to limit the test to specific fields of diplopia without proceeding with the entire test.

9. The space occupied by the equipment was another feature of interest to hospitals. Although, a confined system would be

beneficial to hospital departments which housed an increasing amount of electronic equipment, principles involved in performing the test should not be sacrificed by reducing equipment size.

10. Whilst relative eye movements are being recorded, it would be advantageous if the system could also allow the detection of other eyes disorders.

Other considerations, which were to be included in the design, will be discussed later as their importance and application become apparent.

2.3 Introduction to the Automated System

The aim of this part of the study was to automate the red-green method of measuring relative eye movements, as accurately, cheaply and occupying the least space as possible.

This automated system was to be achieved by the use of video technology which replaced the bulky Lees screens with T.V. monitors, and automated the recording process of the test by using the special characteristics of a T.V. screen in conjunction with a light pen (Section 3.3).

The automated system was to be designed to relieve the orthoptist, reduce the possibility of human error and, hence, to increase the accuracy of the test. For example, in the Lees screen test, which is highly dependent on human judgement (section 2.1.10), inaccuracies can be introduced by the orthoptist pre-judging or estimating either the position pointed by the patient, or plotting his estimates onto a small printed chart. With the proposed system, however, these errors could be eradicated because the positions pointed to by the patient on the

T.V. screen are automatically plotted without the orthoptist's intervention.

The reliability of the results was to be increased by replacing the 50cm long pointer with a joystick or light pen. In the latter case, the T.V. screen was to be placed only 50cm away from the patient who could more accurately control the light pen's movement.

In previous methods an orthoptist was required to set up the equipment at the start of the test, attend throughout its duration and finally, check the results and switch off the equipment. Automation, however, would considerably reduce the running cost of the test since only one orthoptist could record both relative and tremor eye movements simultaneously.

Although the final designs were not intended for mass production, the initial cost of the equipment was to be kept as low as possible. Thus every ophthalmic department of a hospital could purchase the equipment.

In section 2.1 it has been shown that the space required for the Lees screen test is approximately four square meters. The proposed apparatus was to be designed to take up no more space than a normal sized desk. The design was to incorporate wheels for the apparatus, giving greater mobility and relieving the need for a fixed designated area.

As previously stated, the two Lees screens were to be replaced by two T.V. monitors and the pointer by a moving square (target) or a light pen. Fig.2.9 shows the T.V. set-up for such a test to be undertaken without the presence of an orthoptist. The patient was to be seated in front of Monitor A and Monitor B, his

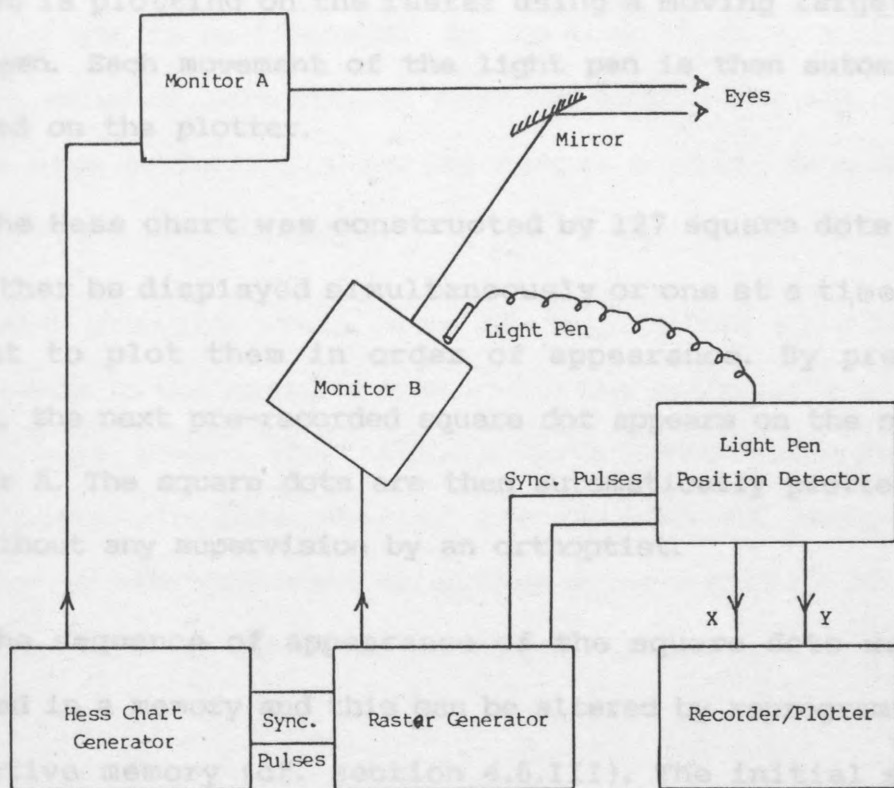


Fig.2.9 The Replacement of the Classical Hess Chart Test
By a T.V. System.

right eye observing Monitor A (the chart monitor) and his left eye observing Monitor B (the blank monitor) with the aid of a mirror, thus achieving complete dissociation of binocular vision. The left eye observes a light pen held in his hand ready to be used on the blank monitor. The patient's brain synthesizes the two observations as if Monitor A and Monitor B were superimposed on each other. The patient thus see one charted screen with the light pen over it.

For clarification, the whole process can be seen from two

Hess chart for observation by the patient. In the next two different perspectives; the patient's perspective outlined above, and an observer's perspective.

The observer sees that the patient points the light pen at the monitor which displays a raster, as if the patient is not seeing the Hess chart. An X-Y plotter responds to what the patient is plotting on the raster using a moving target or his light pen. Each movement of the light pen is then automatically recorded on the plotter.

The Hess chart was constructed by 127 square dots*. These can either be displayed simultaneously or one at a time for the patient to plot them in order of appearance. By pressing a switch, the next pre-recorded square dot appears on the screen of Monitor A. The square dots are then automatically plotted one by one without any supervision by an orthoptist.

The sequence of appearance of the square dots was to be recorded in a memory and this can be altered by reprogramming the respective memory (cf. section 4.6.III). The initial sequence recorded in the EPROM was to be the same as that used at present. The 15 degrees deflection of the eye is covered from the primary position and then expanded to 30 degrees if necessary.

The total system for recording the relative movement of the eye can be divided into two parts, one an analogue section which deals with the recording of the chart by the patient and the other, a digital section which deals with the construction of the

* The square dots are generated on the T.V. screen and have the same coordinates as the intersections of the lines of longitude and latitude of the imaginary sphere mentioned in section 1.2.10

Hess chart for observation by the patient. In the next two chapters the above two sections (Monitors 'B' & 'A') are examined respectively under the heading:

HARDWARE DESIGN - BLANK MONITOR

1. Blank Monitor -This was to be the same as the blank screen in the Lees system, where previously the patient placed his pointer and now places his light pen. On this monitor a raster of medium intensity was to be displayed. In the case of using a light pen a minimum value of intensity is required to activate the light pen. In the case of having a moving target a black screen with a bright target is sufficient.

2. Chart Monitor -This was to display the Hess Chart and corresponds to the chart screen where the orthoptist placed his pointer and where the square dots were made to appear sequentially. In this chapter the options of using digital circuits, a microprocessor or simply using a picture of the Hess chart on cardboard are to be discussed.

HARDWARE DESIGN - BLANK MONITOR3.1 Introduction

As explained previously, in the Lees screen test a blank screen is used for the patient to show the orthoptist where he is superimposing the Hess chart. The orthoptist then manually records the position on a diagnosis chart.


In order to automate this process a system has been devised to sense the positions where the patient is pointing. Either a sensitive screen or a sensitive pointer is required.

A television screen is constructed by a moving electron beam scanning the face of the cathode ray tube. This scanning is time dependent and therefore the electron beam at a specific position on the screen corresponds to a specified instant of time. Hence, the position of the electron beam at a given instant can be referred to as the time lapsed from the start of the T.V. field to that given instant.

This characteristic of the television system can be used to replace the Lees Blank screen. The T.V. screen can either be used as a sensitive screen, for example, in conjunction with a joystick or, an emitting (radiating) screen used in conjunction with a sensitive pointer such as a light pen.

In the next two sections both of the above possibilities are explored.

3.2 Joy Stick System

A blank monitor was set up and together with the circuit in Fig.3.1 an attempt was made to produce a cross-shape  which is movable across the total screen area of the monitor using a joy-stick. This enables the patient to position the cross where he sees the illuminated square dot.

To produce a cross, timers were driven by the line and the field drive waveforms to give the required size and thickness of the cross. In Fig. 3.1 the line and the field drive waveforms from a T.V. sync. generator chip were taken to four timers T_1 , T_3 , T_5 , and T_7 and the outputs of each of these were taken respectively to four other timers T_2 , T_4 , T_6 and T_8 to produce the lengths and thicknesses of the horizontal and vertical lines of the cross.

T_1 and T_5 - Variable by the joy-stick between 0 and 64 us (length of the T.V. line, cf. Appendix II) to determine the horizontal position of the cross-shape.

T_3 and T_7 - Variable by the joy-stick between 0 and 20 ms (length of the T.V. field) to determine the vertical position of the cross- shape.

T_2 = 0.3us - thickness of the vertical bar of the cross-shape.

T_4 = 624us - length of the vertical bar of the cross-shape.

T_6 = 1.5us - length of the horizontal bar of the cross-shape.

T_8 = 93.6us - thickness of the horizontal bar of the cross-shape.

The combination of these timers did not produce a cross-

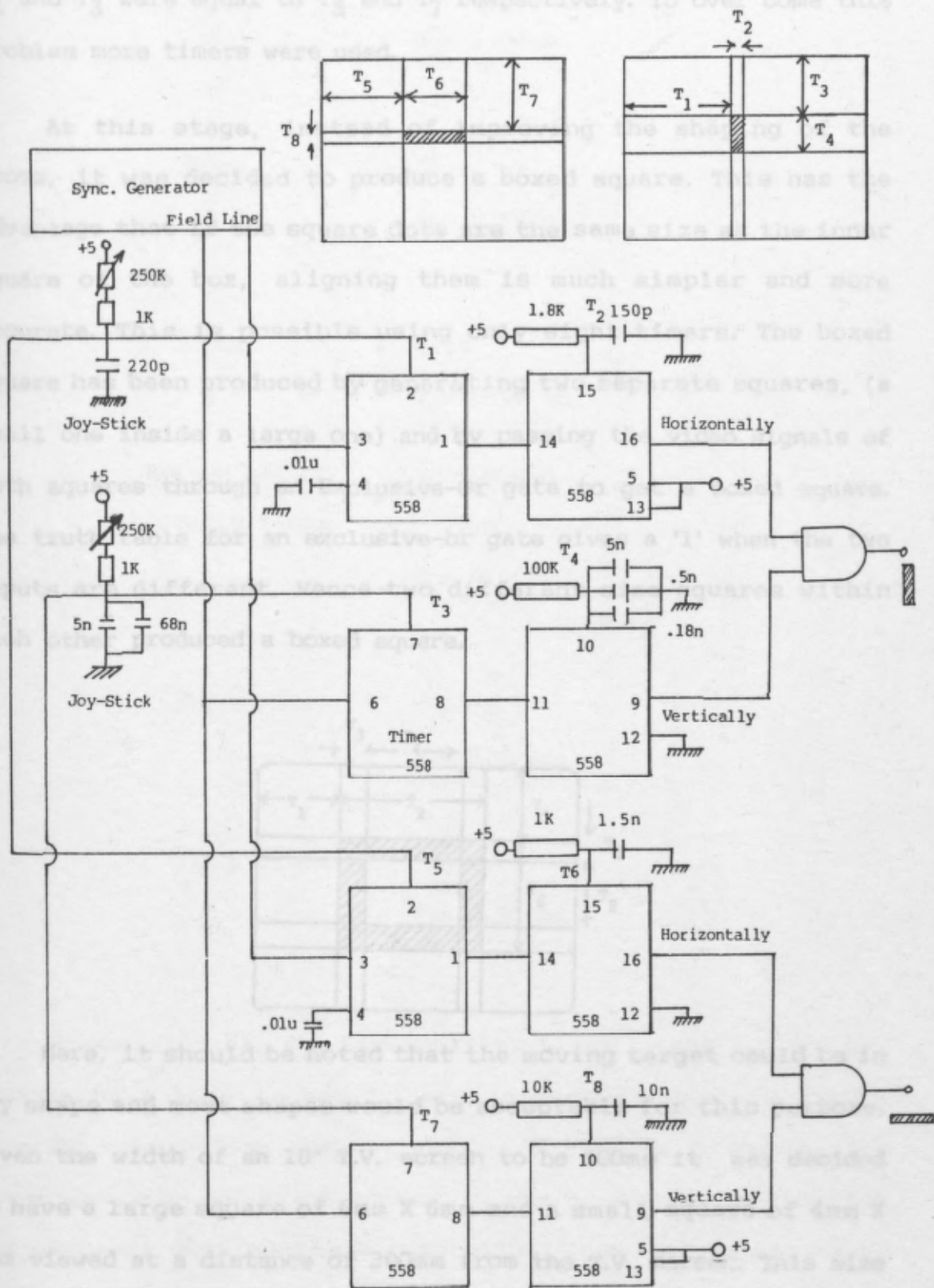


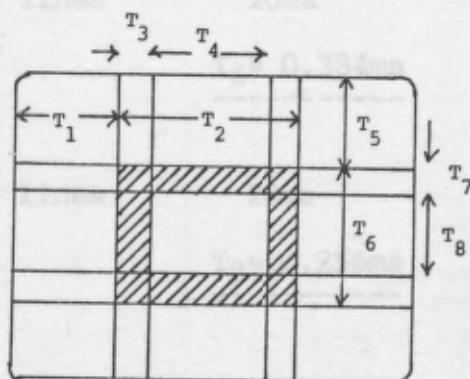


Fig. 3.1 First Design For The Moving Target

shape  but resulted in an inverted L-shape  because T_1 and T_3 were equal to T_5 and T_7 respectively. To overcome this problem more timers were used.

At this stage, instead of improving the shaping of the cross, it was decided to produce a boxed square. This has the advantage that if the square dots are the same size as the inner square of the box, aligning them is much simpler and more accurate. This is possible using only eight timers. The boxed square has been produced by generating two separate squares, (a small one inside a large one) and by passing the video signals of both squares through an Exclusive-Or gate to get a boxed square. The truth table for an exclusive-or gate gives a '1' when the two inputs are different. Hence two different size squares within each other produced a boxed square.



Here, it should be noted that the moving target could be in any shape and most shapes would be acceptable for this purpose. Given the width of an 18" T.V. screen to be 300mm it was decided to have a large square of 6mm X 6mm and a small square of 4mm X 4mm viewed at a distance of 300mm from the T.V. screen. This size boxed square was found to be quite visible.

Screen WidthLine Length

300mm

52us

6

 $T_2 = 1.04\mu s$

300mm

52us

1

 $T_3 = 0.17\mu s$

300mm

52us

4

 $T_4 = 0.69 \mu s$
-----Screen HeightLine Length

312.5 lines

20ms

1

 $T_7 = 0.064ms$

312.5 lines

20ms

6

 $T_6 = 0.384ms$

312.5 lines

20ms

4

 $T_8 = 0.256ms$

By chaining all the timers after timer T_1 and T_5 , the two squares have been locked to each other and hence a single joystick controlling both T_1 and T_5 is capable of moving the boxed square on the blank screen. T_1 and T_5 are the horizontal and vertical displacements respectively. T_1 can be any value between 0 and 52us and T_5 between 0 and 20ms.

The circuit in Fig. 3.2 produces the boxed square described above. The joy-stick has been tested and the boxed square is

large enough to be seen clearly and accurately positioned over the square dots in the chart. The disadvantage lies in the movement of the boxed square; - the inability of the operator's hand to control sensitively the joy-stick in moving the boxed square. This is not very practical for use by elderly patients who find positioning the target by the joy-stick extremely sensitive. This is usually because of tremor in their hands. The best commercially available joy-stick potentiometer does not give a linear and smooth sweep of the target across the screen. Moreover, the movement of the square has been full of jitters unless expensive multi-turn potentiometers are used which nevertheless cannot be employed in a joy-stick assembly (maximum sweep angle ± 25 degrees).

Most of the joy-sticks used in video games have been designed simply to close a switch which in turn enables internal counters to run. These counters then move the target across the screen. As long as the joy-stick is activated the counters cause the target to sweep the screen. This type of joy-stick has proved to be unsatisfactory because an optimum speed for the counters has not been found, since the movement had to be slow enough for no over-shooting to occur in positioning the target. However, this slow speed results in an undesirable increase in the duration of the test.

Alternatively, the joy-stick can have two switches in each of the four directions. The first switch for slow motions and the second for faster sweeps. However, this has been found to be very labourious for elderly patients. The system can, however, be equipped with such a joy-stick for use by younger and trained patients.

Another solution that has been considered is to use two separate ten turn potentiometers; one for horizontal movements and the other for vertical movements. This is complicated for an untrained patient and does not help in presenting a simple apparatus. However, the accuracy of this last method is one of the best and the procedure simple enough for use by patients between 10 and 25 years old. The use of ten turn potentiometers, as opposed to 'ordinary ones', has been necessary since the latter produced the same problems of jitter and excessive sensitivity.

A simple and cheap method has been found which uses the patient to point at the blank screen of the T.V. with a pen. Their hand can thus rest against the screen of the monitor and stop any hand tremor. This method has an advantage in that it indicates the normal practice of pointing at things to draw attention to them. The above reasons caused the use of a light pen to be considered.

Some of the points raised here may seem trivial. However, the procedure of the test relies on the cooperation of the patient, and thus careful consideration must be given to these points.

3.3 LIGHT PEN SYSTEM

The use of a light pen together with an X-Y plotter has been included as a replacement for an orthoptist to record the results of the test. This pen has been used to sense the position at which the patient points, and to instruct the X-Y plotter to record the position on a diagnosis chart. Thus the photodiode of

the light pen detects the light emitted from the phosphor of the T.V. screen, illuminated as a result of the electron beam from the C.R.O. gun hitting the surface of the T.V. This produces a short pulse in the light pen. Due to the scanning properties of the T.V. screen, this pulse is repeated every 20ms (every field) and has been regarded as the position of the light pen relative to the raster of the blank screen - its distance from the start of the field as the y-coordinate and its distance from the start of the line as the x-coordinate of the pen for the X-Y plotter. These distances, however, can be measured either by digital or analogue methods.

3.3.1. Digital Methods:

The circuit in Fig. 3.3 shown below is a simple example for a possible digital method. This includes a binary counter which counts the number of lines from the beginning of the field sync. up to the pulse generated by the light pen. This count enables the vertical distance of the light pen from the top of the T.V. screen to be measured. By converting this digital value to an analogue voltage (by means of a D to A convertor) it is possible to get the x-y plotter to show this vertical position. The horizontal position can also be determined using a similar binary counter driven by a crystal with a frequency of 11.5MHz. This value is determined by the smallest horizontal movement of the light pen recognised by the plotter. For example, if this smallest horizontal movement is 0.5mm on a 300mm width T.V. screen, then the period of the highest frequency is:

$$\frac{(52\mu\text{s} \times 0.5\text{mm})}{300\text{mm}} = 86.7\text{ns} \text{ giving a frequency of } 11.5\text{MHz}.$$

This requires a 10 bit counter and a 10 bit D to A convertor. However the least significant bit is ignored to stop the pen of the plotter jittering between two adjacent bytes and hence the actual recognisable horizontal movement is reduced to 1mm. (Fig. 3.3).

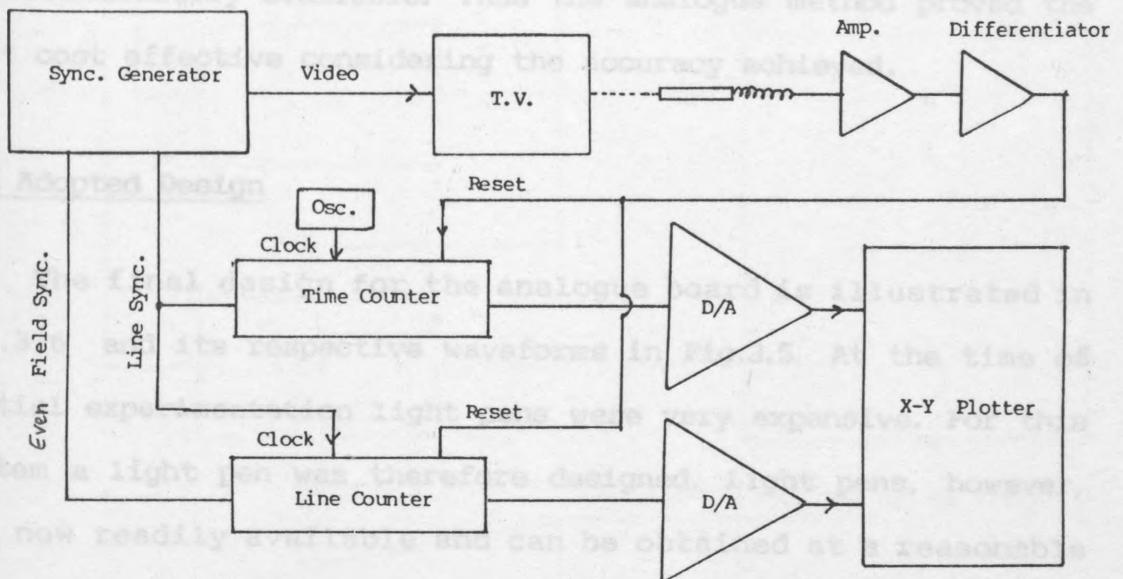


Fig. 3.3: Digital System for the Light Pen

3.3.2. Analogue Methods:

The circuit in Fig. 3.4 is another possible design to determine the X and Y coordinates of the light pen using analogue signal processing.

In this method the Sample and Hold amplifiers register the coordinates by the aid of ramps which are generated by the line and field drive waveforms and the pulse out of the light pen. This pulse causes the Sample and Hold amplifiers to hold the value of the ramp for the duration of a T.V. field until the next pulse sent by the light pen.

The analogue method was tested and proved to be very

satisfactory. The use of a simple Sample and Hold was found adequate to give very accurate results which is a distinct advantage considering the points raised in section 3.4.IV. Analogue was thus chosen as the most desirable method.

The chosen Sample and Hold amplifier is an inexpensive one and commercially available. Thus the analogue method proved the most cost effective considering the accuracy achieved.

3.4 Adopted Design

The final design for the analogue board is illustrated in Fig.3.6 and its respective waveforms in Fig.3.5. At the time of initial experimentation light pens were very expensive. For this system a light pen was therefore designed. Light pens, however, are now readily available and can be obtained at a reasonable price. Nevertheless, reliable and efficient light pens are still difficult to acquire. The designed light pen produces a positive short pulse when its photodiode is struck by the photons from the face of the T.V. screen. A detailed discussion is given in sections 3.4.VI and 3.4.IX.

For the photodiode to detect the photons, a raster of adequate intensity was constructed using the Mixed Video Blanking and Mixed Video Sync. waveforms, obtained from the T.V. waveform generator, in a simple voltage adder. However, this mixer could not have been constructed using only passive components since the low input impedance of the monitor would have loaded the mixer, hence the use of an op-amp. was necessary.

To measure the position of the light pen on the raster, the

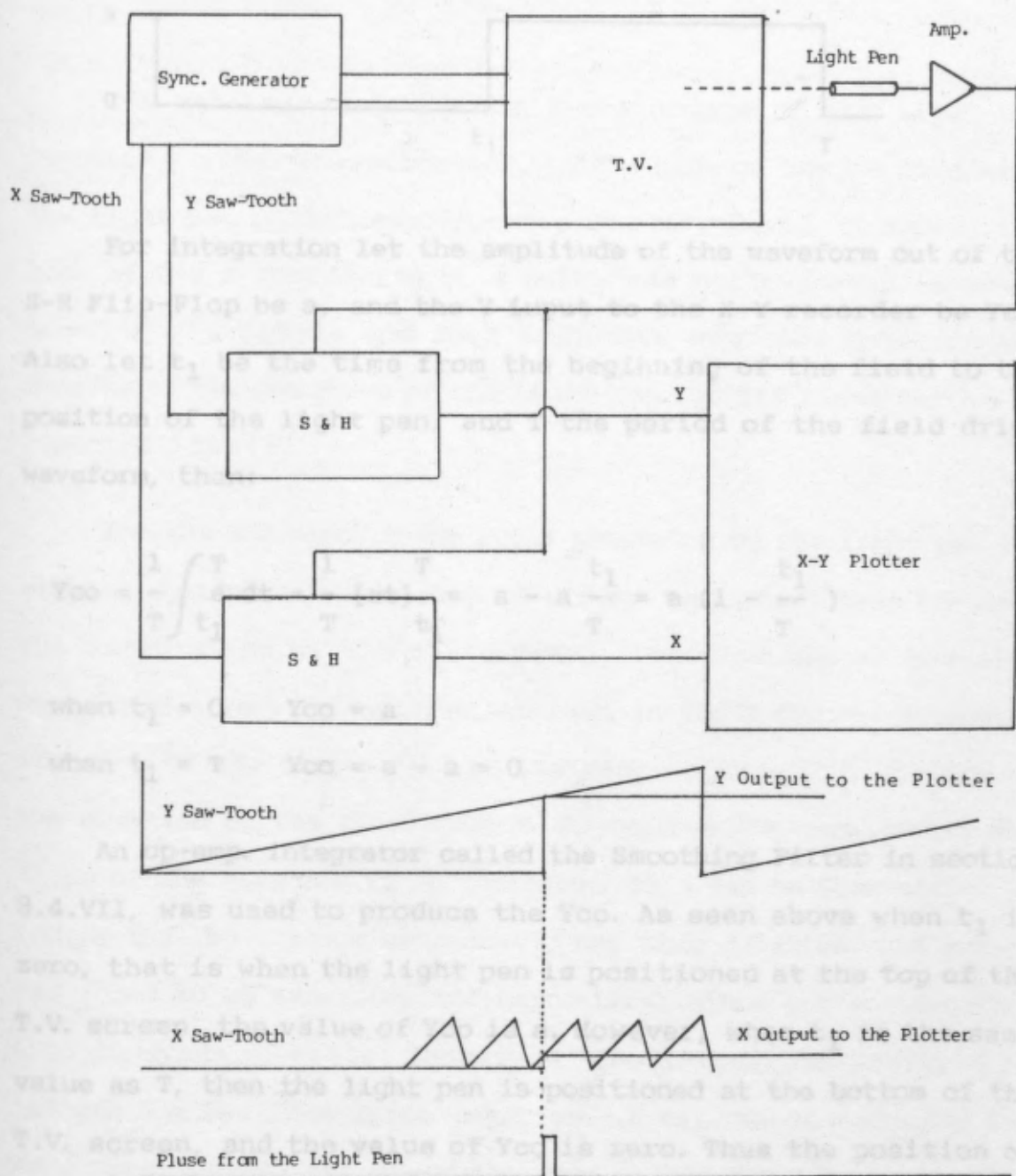
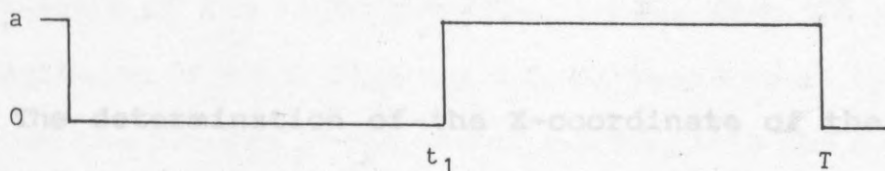


Fig 3.4: Analogue System for the Light Pen

field drive was used to determine the y-coordinate of the light pen by integrating the area under the curve generated by the S-R Flip-Flop (Fig. 3.6). This waveform was similar to a square waveform with its negative going edge being the start of the field and its positive going edge being the position of the light pen.



For integration let the amplitude of the waveform out of the S-R Flip-Flop be a , and the Y input to the X-Y recorder be Y_{co} . Also let t_1 be the time from the beginning of the field to the position of the light pen, and T the period of the field drive waveform, then:

$$Y_{co} = \frac{1}{T} \int_0^T a \, dt = \frac{1}{T} [at]_0^{t_1} = a - a \frac{t_1}{T} = a \left(1 - \frac{t_1}{T}\right)$$

when $t_1 = 0$ $Y_{co} = a$

when $t_1 = T$ $Y_{co} = a - a = 0$

An op-amp. integrator called the Smoothing Filter in section 3.4.VII, was used to produce the Y_{co} . As seen above when t_1 is zero, that is when the light pen is positioned at the top of the T.V. screen, the value of Y_{co} is a . However, when t_1 is the same value as T , then the light pen is positioned at the bottom of the T.V. screen, and the value of Y_{co} is zero. Thus the position of the light pen at any other point on the screen gives a fraction of the value of a . These values were interpreted by the X-Y recorder and hence the Y-coordinate of the pen of the recorder was found.

Due to the above integration the output of the Smoothing Filter was found to be a ramp of small amplitude sitting on a d.c. voltage (non-ideal integrator). To smooth this even further and hence eradicate the vibration on the plotter, a 3-pole low pass filter with 20Hz roll-off frequency (section 3.4.VIII) was

used.

The determination of the X-coordinate of the light pen required further investigation. In the case of the y-coordinate the light pen pulse was occurring in every field, though in the case of the x-coordinate this pulse was not repeated in every line. Thus a Sample and Hold technique was used enabling the storage of the position of the light pen for 312 lines before it repeated itself.

For the S&H circuit the pulse generated by the light pen was sampled against a linear ramp. The ramp could have been taken as the integration of the field drive, but this use of the ramp would give a very insensitive movement in the X-direction because the slope of the ramp would be its peak voltage (3V) divided by the duration of the field (20ms). To improve the sensitivity the slope of the ramp had to be increased. This can be done either by increasing the voltage or reducing the time duration. The former was found to be expensive and impractical since the voltage runs into hundreds of volts. Therefore, the latter was achieved by integrating the line drive (section 3.4.IX), hence reducing the ramp duration 312 times and increasing the slope of the linear ramp.

This ramp was sampled by a pulse generated at the position of the light pen. The light pen pulse had to be differentiated and delayed for one T.V. line (64us timer) as described in sections 3.4.IV and 3.4.V. The S&H circuit thus sampled the ramp at the position of the light pen for a duration of one line and held the sampled value for 20ms until the next field.

This produced a d.c. voltage with its value representing the

X-coordinate of the light pen (Fig. 3.5.H). When the pen was at the beginning of a T.V. line the d.c. voltage was at its minimum and when the pen was at the end of the T.V. line the d.c. voltage was at its maximum.

A noise of 64us duration was present in this d.c. output due to the sampling period of the S&H circuit. This noise was smoothed with a Smoothing Filter as described in section 3.2.VII.

The circuits of the block diagram (Fig.3.6) are described in detail in the next nine sections.

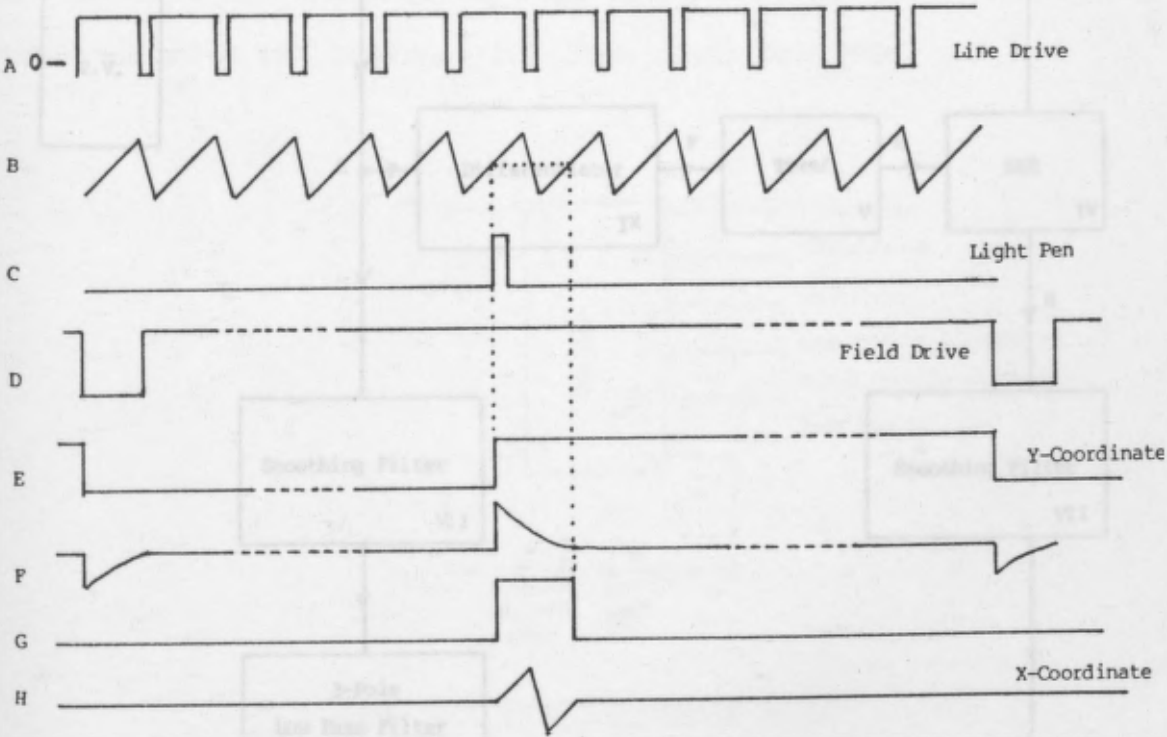
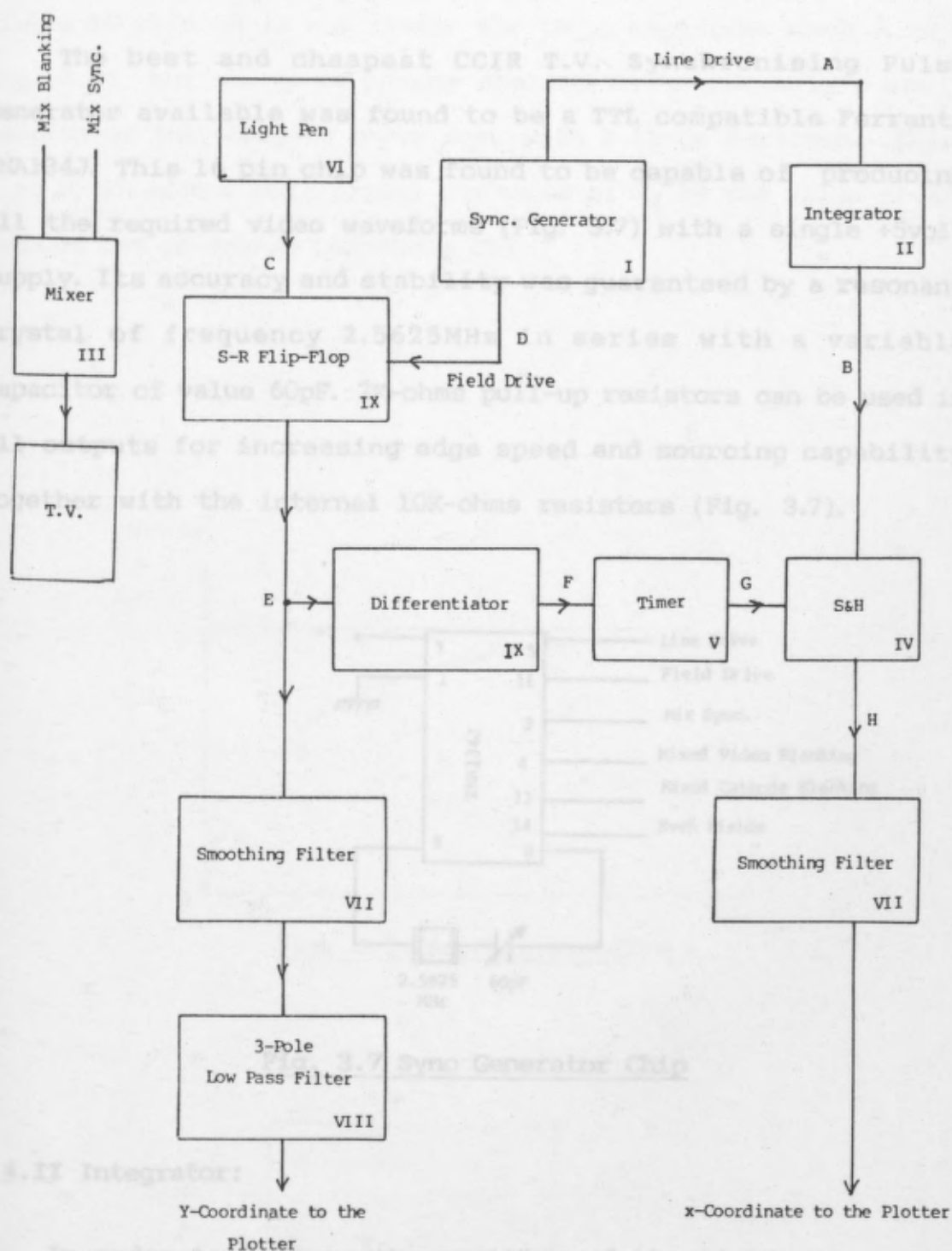


Fig. 3.5 Waveforms for the Block Diagram in Fig.3.6.

3.4.I Sync. Generator:

The light pen system has to synchronise with an accurate and stable incoming field and line drive waveforms. For this purpose a T.V. sync. pulse generator was placed at the heart of the

system. Available T.V. sync. generators, at the time of initial experimentation, were often either made in American NTSC system or did not produce the sync. in accordance with CCIR standards.



A, B, C, D, E, F, G, H Waveform Codes

I, II, III, IV, V, VI, VII, VIII, IX Section Numbers

Fig. 3.6 Block Diagram of the Light Pen Circuits

system. Available T.V. sync. generators, at the time of initial experimentation, were often either made in American NTSC system or did not produce the syncs. in accordance with CCIR standards.

The best and cheapest CCIR T.V. Synchronising Pulse Generator available was found to be a TTL compatible Ferranti ZNA134J. This 16 pin chip was found to be capable of producing all the required video waveforms (Fig. 3.7) with a single +5volt supply. Its accuracy and stability was guaranteed by a resonant crystal of frequency 2.5625MHz in series with a variable capacitor of value 60pF. 2K-ohms pull-up resistors can be used in all outputs for increasing edge speed and sourcing capability together with the internal 10K-ohms resistors (Fig. 3.7).

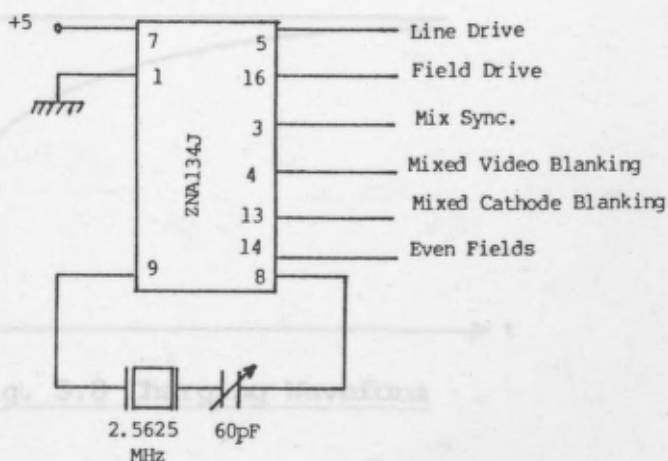


Fig. 3.7 Sync Generator Chip

3.4.II Integrator:

In order to measure the position of the light pen on the T.V. screen, it was necessary to generate a linear ramp of 64uS duration for feeding the Sample and Hold circuit. Ramp generation using digital methods was investigated and the simplest method was found to be the direct integration of the line drive

From Fig. 3.8 waveform. A simple RC network is sufficient for ordinary integration but to get the best linearity over the ramp it was decided to use an a.c. op-amp integrator (Clayton, 1979). A simple RC network is not linear for large amplitude (Part A to C Fig. 3.8), but using an op-amp enables us to use only a small section of the charging curve even with a large amplitude. (Part A to B, in effect multiplying the value of V_A by the value of the gain of the op-amp A) (Appendix IV).

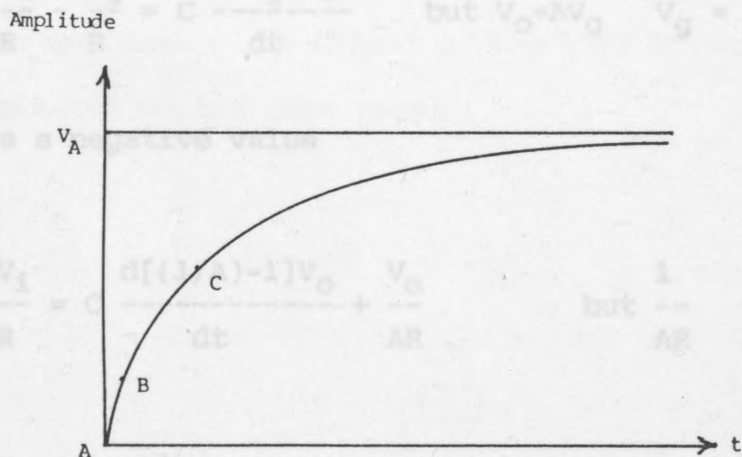


Fig. 3.8 Charging Waveform

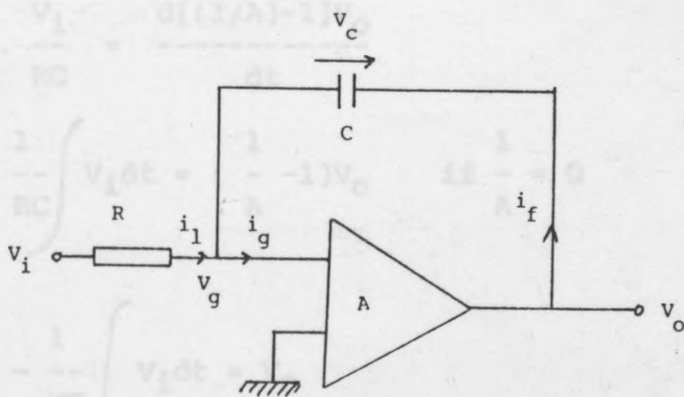


Fig. 3.9 op-amp Integrator

From Fig. 3.9

$$i_1 + i_f = i_g \dots\dots\dots (1)$$

$$V_c = \frac{1}{C} \int i_f dt$$

$$i_f = C \frac{dv_c}{dt}$$

equation (1) becomes :

$$\frac{V_i - V_g}{R} + C \frac{d(V_o - V_g)}{dt} = i_g \quad \text{but } i_g = 0$$

$$\therefore \frac{V_i}{R} - \frac{V_g}{R} = C \frac{d(V_g - V_o)}{dt} \quad \text{but } V_o = AV_g \quad V_g = \frac{V_o}{A}$$

Where A is a negative value

$$\therefore \frac{V_i}{R} = C \frac{d[(1/A) - 1]V_o}{dt} + \frac{V_o}{AR} \quad \text{but } \frac{1}{AR} \text{ is small}$$

$$\therefore \frac{V_o}{AR} = 0$$

$$\therefore \frac{V_i}{RC} = \frac{d[(1/A) - 1]V_o}{dt}$$

$$\therefore \frac{1}{RC} \int V_i dt = \left(\frac{1}{A} - 1 \right) V_o \quad \text{if } \frac{1}{A} = 0$$

$$\therefore - \frac{1}{RC} \int V_i dt = V_o$$

Many different op-amps were tested, specifically a 741,

CA3029 and finally a CA3140. The latter was chosen due to its wide bandwidth and its ability to function without external phase compensation.

Using the integrator as in Fig 3.9 would soon cause the op-amp to drift into saturation due to amplifier bias current and offset voltage. To prevent this, the d.c. feed back loop was closed by a large value resistor (R_f) in parallel with the capacitor C. This provides a d.c. path through R_f and hence disables the op-amp to act as a d.c. integrator. A similar effect could also have been achieved by using an F.E.T. transistor to switch on during each flyback to discharge the capacitor, thus resetting the circuit to zero. The final circuit diagram for the integrator follows. (The effect of the 10uF capacitor and diode D are explained on the next page).

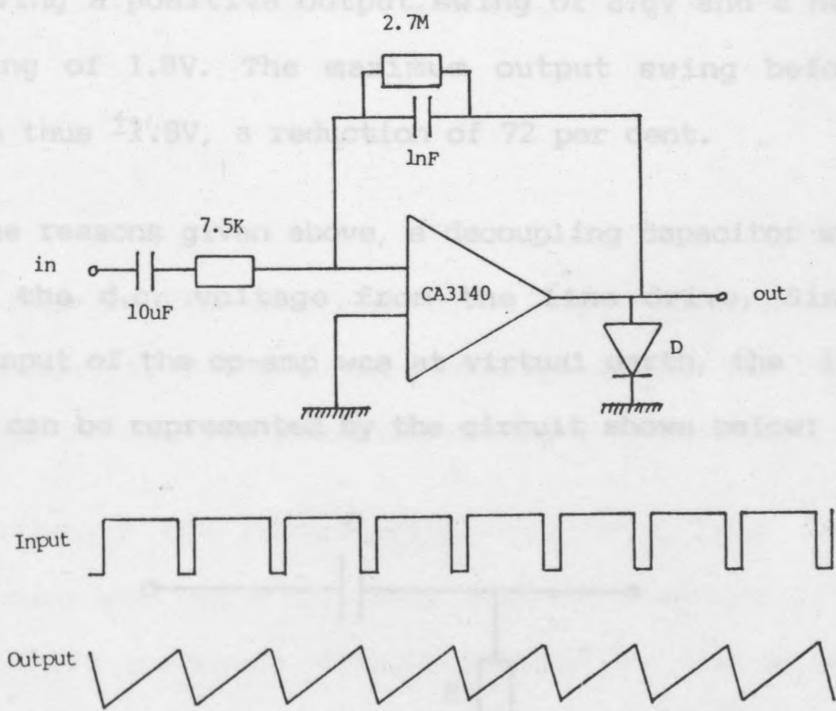


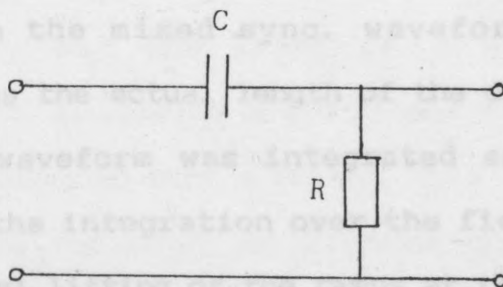
Fig 3.10 Integrator Section and its Input and Output Waveforms

It is important that the ramp generated by this circuit should be linear and stable, for if the ramp is not linear the X-coordinate of the moving pen of the X-Y plotter is also not linear. If the ramps are not stable and jitters are present then the same jitter appears in the X-Y plotter. To generate a linear and stable ramp the following four precautions were taken:

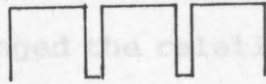
1) An integrating capacitor with high leakage current causes the dV_C/dt to lose constancy, since i_C drifts due to leakage. This was overcome by using a 1nF polystyrene capacitor.

2) The input to the integrator had to be free of any d.c. voltage since this limits the maximum amount of the output swing. If a d.c. voltage is present at the input of the op-amp the output also carries a d.c. voltage depending on the value of R_f/R_1 . The supply voltage to the op-amp was $\pm 5V$ so the total peak to peak swing was 10V. If a +10mV d.c. is present at the inverting input, $-10 \times 10^{-3} \times R_f/R_1 = -3.6V$ appears on the output, giving a positive output swing of 8.6V and a negative output swing of 1.8V. The maximum output swing before any clipping is thus $\pm 1.8V$, a reduction of 72 per cent.

For the reasons given above, a decoupling capacitor was used to remove the d.c. voltage from the line drive. Since the inverting input of the op-amp was at virtual earth, the input to the Integrator can be represented by the circuit shown below:



This is a differentiator and if the value of the capacitor is not high enough, relative to the 7.5 K-ohms resistor, it tends to differentiate the square input and therefore does not produce a linear ramp. If the input is the following square waveform:



and decoupling capacitor is not high enough then the output would look like this:



It was found that in order to produce a linear ramp by the integrator the aiming voltage for the charging period of the capacitor had to remain constant.

If the charging equation of the capacitor is

$$v = V (1 - e^{-t/CR}) \text{ where } V = \text{aiming voltage}$$

$$\therefore \frac{dv}{dt} = \frac{V}{CR} e^{-t/CR}$$

Therefore the rate of change of voltage with time (the ramp) is proportional to V, the aiming voltage. Hence the line drive waveform had to have its flattened portions exactly horizontal.

3) Although the mixed sync. waveform from the sync. generator chip was the actual length of the displayed T.V. lines, the line drive waveform was integrated as the mixed sync. waveform caused the integration over the field sync. period to introduce a gradual lifting of the ramps at the end of the field,

which resulted in a vertical shift of the ramp and thus gave different X-coordinates for the plotter's pen's various Y-coordinates while the X-coordinate of the light pen remained unchanged.

4) Hum in the system either on the power supply or on the line drive itself changed the relative position of the ramps to each other. A diode D was used to clamp the output to the earth and thus each ramp was held in a fixed position relative to each other. Thus the plotter's pen did not drift due to hum when the light pen was stationary. It was also ensured that when the movement of the light pen was completely vertical the X-coordinate of the plotter remained the same.

The linearity of the ramps was checked using a Marconi oscilloscope type TF1331A. This oscilloscope has the facility of a calibrated X and Y shift and hence enables the systematic measurement of the slope of the ramp and thus a check of its linearity. This linearity was later confirmed by plotting the Hess Chart using the signal produced to display the chart itself (section 4.6) rather than by plotting the chart using the light pen signal. The percentage of the non-linearity introduced by the op-amp is calculated in Appendix V.

3.4.III Raster Mixer:

The purpose of this circuit was to produce a noise free and stable raster so that the light pen's position could be determined from it. Initially a check was made to measure the delay caused by producing such a raster. This delay together with the delay caused by the light pen circuits creates a discrepancy

between the coordinates of the light pen and the pen of the plotter. The delay in producing the raster was found to be a function of (1) the electronic circuits of the monitor, (2) the time taken for the electrons to travel from the cathode to the screen in the T.V. Cathode Ray Tube, (3) the time taken for the phosphor on the screen to glow. Delay calculations are found in Appendix X.

As demonstrated, in Appendix X, of the three delays the latter one was the largest and therefore the longest delay was approximately a few u-seconds. This delay did not have any effect on the Y-coordinate but it shifted the X-coordinate by a few u-seconds. Since it was always constant it could be ignored. However, in section 3.4.V the effect of this delay is completely absorbed in a 64uS artificially generated delay. The question of the delay having been satisfied, the raster was constructed.

In Fig. 3.11 a resistor matrix was used to superimpose the Mixed Video Blanking waveform from pin 4 of the pulse generator on the Mixed Sync. from pin 3, to give a waveform with the correct amount of blanking together with equalising pulses (Appendix VI).

An op-amp, CA3029, was then used to act as a buffer stage with a set gain of 1.43.

$$\text{The Gain} = 1 + \frac{R_f}{R_1} = 1 + \frac{4.3}{10} = 1.43$$

47pF capacitors and 1K-ohms resistors were used for phase compensation.

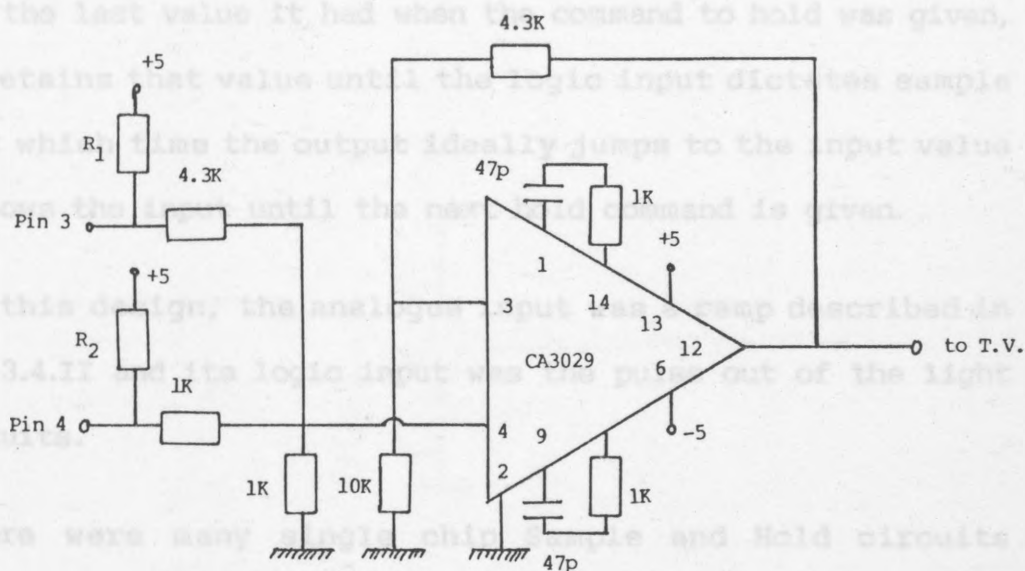


Fig. 3.11 Raster Mix Circuit

Since the output of the sync. generator was too high for the op-amp, a 1K-ohms resistor was connected between pin 4 of the op-amp and earth to reduce the input signal. R_1 and R_2 were the 2K-ohms pull-up resistors needed for the sync. generator. This produced a noise free and stable raster with optimum brightness for the eye and the light pen. It was found that if the raster was too bright, the eyes were stressed causing inaccurate results. Meanwhile, the raster had to have enough intensity for the light pen to pick up adequate signal in order to produce a stable pulse output, hence a balanced intensity was desirable.

3.4.IV Sample and Hold:

The principle application for Sample and Hold amplifiers is to maintain the value of an analogue input constant during the Hold period and precisely follow its analogue input during the Sample period. These two periods are known as the two modes of

S&H amplifiers. In the sample mode, the output follows the input. When the mode switches to hold, the output of the S&H ideally retains the last value it had when the command to hold was given, and it retains that value until the logic input dictates sample mode, at which time the output ideally jumps to the input value and follows the input until the next hold command is given.

In this design, the analogue input was a ramp described in section 3.4.II and its logic input was the pulse out of the light pen circuits.

There were many single chip Sample and Hold circuits available. It was found that the hold time was much longer than the sample time thus it was decided to use LF398 which is a very cheap single chip Sample and Hold amplifier. The circuit is shown in Fig. 3.12.

As a low cost S&H circuit was used all its limitations were examined to ensure satisfactory operation under required testing conditions. These are described below:

Fig. 3.12 Sample and Hold circuit and its Waveform

Aperture time: The value of the aperture time is not critical since the response of the patient in recording the coordinates of the light pen on the plotter is much longer than the aperture time. Also at constant room temperature the aperture time remains constant. Thus this consideration can be ignored as the recorded chart is shifted by a constant amount.

Acquisition Time: The acquisition time of the Sample and Hold did not affect its function for two reasons. The first was that during the recording of its coordinates the light pen was stationary on the T.V. screen hence the value of the output of

the Sample and Hold remained constant. Second was that the width of the logic input to the S&H was much longer than the acquisition time (next section).

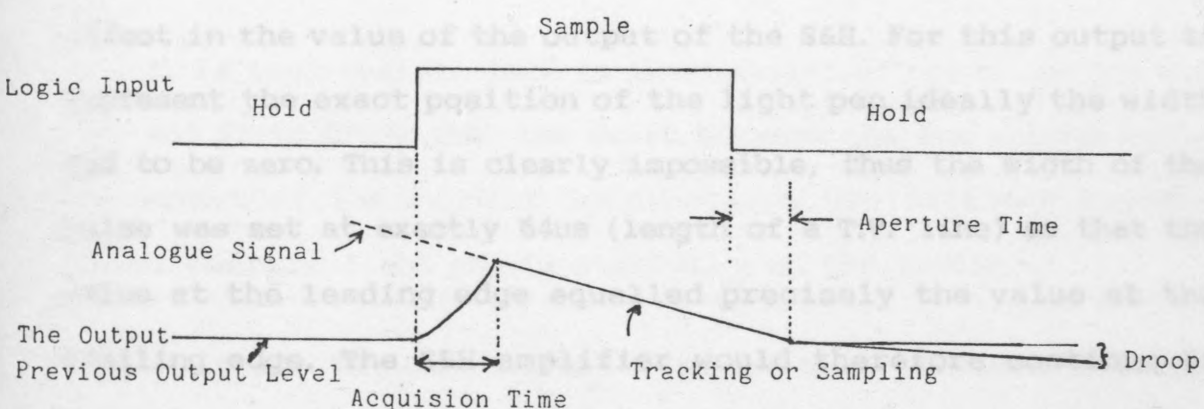
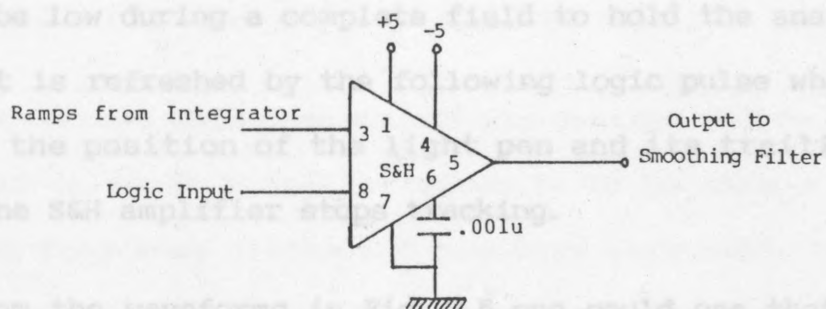


Fig. 3.12 Sample and Hold circuit and its Waveforms

Droop Voltage: The output droop rate with a 0.001uF capacitor was $3 \times 10^{-2} \text{ Vs}^{-1}$, hence for 20ms (duration of a T.V. field, or the hold period) the droop voltage was 0.6mV. If the total output swing of the S&H amplifier was 3V and the width of the T.V. screen 300mm then the equivalent horizontal displacement of the light pen was 0.06mm which is negligible.

In total, the S&H functioned most satisfactorily and helped in producing both a very stable and sensitive signal representing the X-coordinates for the position of the light pen.

3.4.V Timer (Delay):

The Sample and Hold amplifier tracks its analogue input when its logic input is high and holds the last value of the analogue input when the logic input becomes low. Therefore the logic input has to be low during a complete field to hold the analogue value until it is refreshed by the following logic pulse whose leading edge is the position of the light pen and its trailing edge is where the S&H amplifier stops tracking.

From the waveforms in Fig. 3.5 one could see that the width of the pulse connected to the logic input had a considerable effect in the value of the output of the S&H. For this output to represent the exact position of the light pen ideally the width had to be zero. This is clearly impossible, thus the width of the pulse was set at exactly 64 μ s (length of a T.V. line) so that the value at the leading edge equalled precisely the value at the trailing edge. The S&H amplifier would therefore continue to track the input until the exact position on the next line was reached. This was made possible since the ramp generated for the analogue input was the integration of the T.V. line itself (Fig. 3.10)

The precise horizontal position of the light pen was thus established although the noise at the output of the S&H was increased. However, this increase does not pose any serious difficulty as the smoothing filter is well capable of suppressing this noise.

This delay of 64 μ s can be achieved by a timer or monostable. The delay time = CR where C and R are the timing components of

the timer. If C and R each have an average tolerance of 10% then the delay time has a tolerance of 20 per cent.

The delay time is anything between 50us & 80us. With these figures the Sample and Hold has a totally wrong value and sometimes even represents the value of the flyback portion of the ramp.

To overcome this problem, it was decided to try to measure this 64uS delay by a digital circuit. To do this a number of different frequency clocks and counters were used. The digital method was not very successful, however, due to the following reasons:

1. If the crystal clock is independent of the clock for the line and field drive then the drift between the two clocks makes the output of the counter jump between two adjacent logical states when the light pen is stationary on the raster.

2. If the crystal clock is the same as the clock for the line and field drive then when the light pen is moving smoothly over the raster, the output of the counters moves in steps and if the light pen stopped between two adjacent logical states then the output starts to vibrate between the two states.

3. Finally, if the clock is generated from the beginning of the light pen signal, then one can count a delay of 64us digitally. This however, involves designing a separate and non-crystal clock. The use of a timer was therefore reconsidered. An adjustable timing component was used and this was set at 64uS with adjusts on board (A.O.B.) facility to compensate for the tolerance of the components.

3.13.

was 250ms which meant:

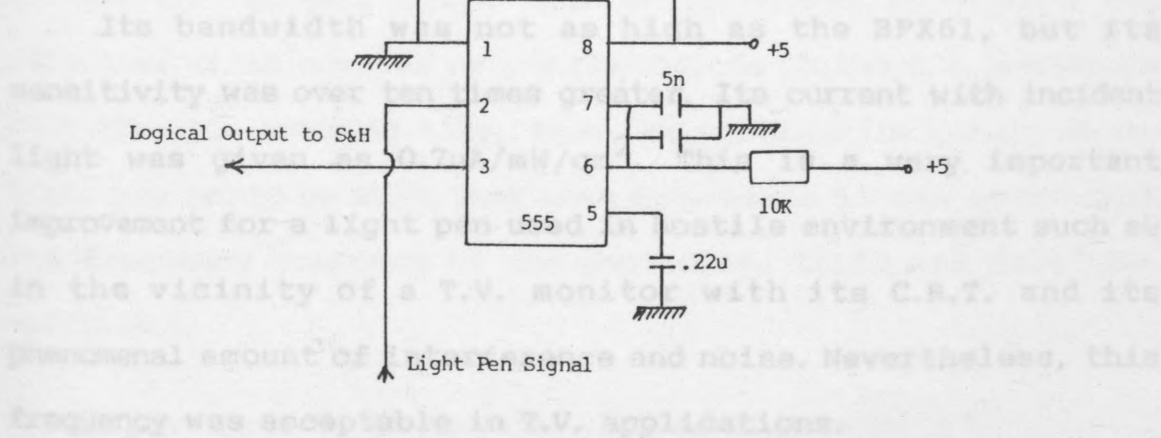


Fig. 3.13 Timer Delay of 64us

3.4.VI Light pen: (Appendix III)

There are many good light pens available on the market especially light pens designed for T.V. application such as T.V. games. However, the cost of these light mics are so high that it was decided to design a light pen suitable for this research project.

Many different photodiodes and phototransistors were tested. BPX61 is a typical fast photodiode with a rise time of 50ns.

Since $B \times Tr = 0.35$ Where B = Bandwidth

$$Tr = \text{Rise time} = 5 \times 10^{-9}$$

$$\text{Then } B = 0.35/Tr = 0.35/(5 \times 10^{-9})$$

$$\therefore B = 7\text{MHz}$$

This was quite adequate for use in the light pen but its current with incident light was only $0.06\mu\text{A}/\text{mW}/\text{cm}^2$. The IPL33 photodiode was not as fast as the BPX61 since its rise time (Tr) was 250ns which meant:

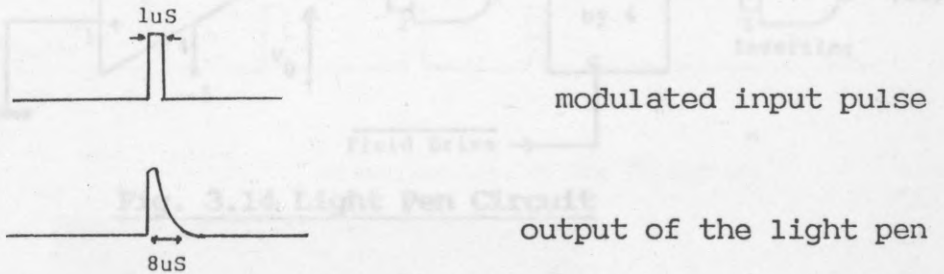
$$B = 0.35/Tr = 0.35/(250 \times 10^{-9})$$

$$\therefore B = 1.4\text{MHz}$$

Its bandwidth was not as high as the BPX61, but its sensitivity was over ten times greater. Its current with incident light was given as $0.7\mu\text{A}/\text{mW}/\text{cm}^2$. This is a very important improvement for a light pen used in hostile environment such as in the vicinity of a T.V. monitor with its C.R.T. and its phenomenal amount of interference and noise. Nevertheless, this frequency was acceptable in T.V. applications.

For this diode, as a result of the fall in the bandwidth, the frequency response was checked by disconnecting the x and y deflectors of the C.R.T. in an ordinary T.V., so that the beam of the gun was only projected onto the centre of the T.V. screen. The gun was then modulated with very short duration pulses at a

frequency of not more than 50Hz so that the average beam intensity was very low, in order not to burn the phosphor of the T.V. screen. By placing the photodiode in front of the illuminated dot one can observe the output of the pen and compare it with the input pulse.



Provided that the op-amp used in conjunction with the photodiode has a wide bandwidth response, the 8μs width of the output of the light pen is due to the after-glow of the phosphor of the T.V. screen. Given that under normal conditions the effective width covered by the photodiode on the T.V. screen is less than 1μs scanning time, then the width of the output of the light pen would be even less than 8μs. Hence it was shown that the frequency response of the photodiode IPL33 was more than sufficient.

Other types of photodiodes such as light-activated switches were tested but their frequency response and sensitivity to visible light did not prove to be adequate.

The circuit for the light pen is shown in Fig. 3.14.

The amplifier used was an F.E.T. input op-amp with a unity gain bandwidth of 20MHz. Ordinary op-amps such as a 741 and a CA3029 have low input impedance, hence the reverse current through the photodiode would be lost, while an F.E.T. input op-

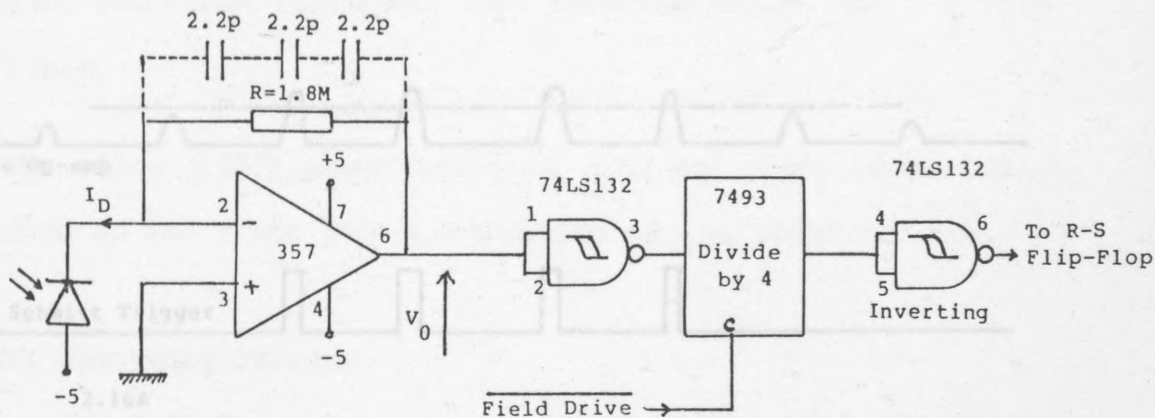


Fig. 3.14 Light Pen Circuit

amp 357 with its 10^{12} ohms input resistance and 10pA input offset current would pick up the small reverse current of the IPL33 photodiode ($V_O = I_D R$, $R = 1.8\text{M Ohms}$, $I_D = 0.7\mu\text{A/mW/cm}^2$ when the negative input of the op-amp was at virtual earth).

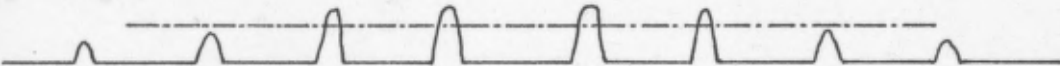
Some comparators were also tested but none of these, including a LM311 with input offset current of only 6nA, gave a result as good as the 357 J.F.E.T. op-amp with its high input impedance.

The diode and its F.E.T. input op-amp were housed in a heavily earthed box with a tube channelling the light so that the screen of the T.V. did not interfere with the functioning of the light pen circuits. The output of the op-amp was then passed through a Schmitt trigger gate to clean the edges of the pulses and to square them by reducing the rise and fall times, as shown in Fig. 3.15a*. The reason for the presence of so many pulses at

* The hysteresis property of the Schmitt trigger was particularly helpful in producing stable and effective pulses representing the position of the light pen over the monitor screen.

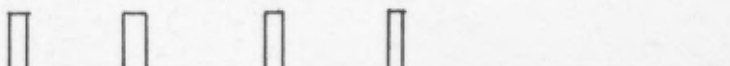
pulses and to recognise the 5th pulse as the actual position of the light pen. This pulse was then inverted before the S-R flip-flop stage.

Output of the Op-amp



Three 2.2pF capacitors were used for phase compensation depending on the shape and construction of the light pen box.

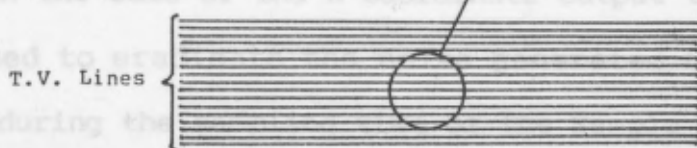
Output of Schmitt Trigger



3.4.VII Smoothing Filters:

2.16a

Effective Area of the Photodiode



2.16b

Fig. 3.15 a. Light Pen Waveforms

b. Effective Area of the Photodiode Relative to T.V. Lines.

was to integrate the square waveform generated by the S-R flip-flop to give as straight a line as possible, or alternatively, to average the area under the curve. This gave a saw-tooth waveform of a very small amplitude (further smoothing and explanation in the next section) with a large d.c. offset. The amount of the d.c. depended on the area under the curve and was representative of the Y-coordinate.

the output of the photodiode is that the effective area of the photodiode covers many lines on the T.V. screen, shown in Fig. 3.15b. The top and bottom lines, covered by the photodiode, produces very weak and unstable pulses for two reasons. The first is that the pulses were only picked up for a short period and the second is that being at the corner of the effective area the light intensity was considerably less. Hence the amplitude of these pulses was found to be less than those at the centre of the photodiode. After observing the waveform, it was realised that the first few pulses were unstable because the angle of the light pen held against the T.V. screen was not always constant and that the actual place of measurement of the position of the light pen was the centre of the effective area of the photodiode. Therefore it has been proved (cf. Appendix VI) that for an integrator by passing the output of the Schmitt trigger gate through a divide by four counter it was possible to ignore the first four

pulses and to recognise the 5th pulse as the actual position of the light pen. This pulse was then inverted before the S-R flip-flop stage.

The three 2.2pF capacitors were used for phase compensation depending on the shape and construction of the light pen box.

3.4.VII Smoothing Filters:

In the case of the X-coordinate output the smoothing filter was used to eradicate the noise generated (with a duration of 64us) during the sampling time of the Sample and Hold I.C. In the absence of the smoothing filter, large jitters would appear on the plotter, every 20ms, in the direction of the X-axis.

In the case of the Y-coordinate output, the smoothing filter was to integrate the square waveform generated by the S-R flip-flop to give as straight a line as possible, or alternatively, to average the area under the curve. This gave a saw-tooth waveform of a very small amplitude (Further smoothing and explanation in the next section) with a large d.c. offset. The amount of the d.c. depended on the area under the curve and was representative of the Y-coordinate.

The circuits of both filters are shown in Fig. 3.16. An optimum value of R and C in Fig. 3.16 was chosen so that no jitters appeared on the plotter, whilst shortening the response time of the pen of the X-Y recorder, relative to the movement of the light pen.

It has been proved (cf. Appendix V) that for an integrator;

$$\frac{V_O}{V_i}(s) = - \frac{R_f}{R_i} \frac{1}{sCR_f + 1}$$

$$\therefore \frac{V_O}{V_i}(j\omega) = - \frac{R_f}{R_i} \frac{1}{1 + j\omega CR_f}$$

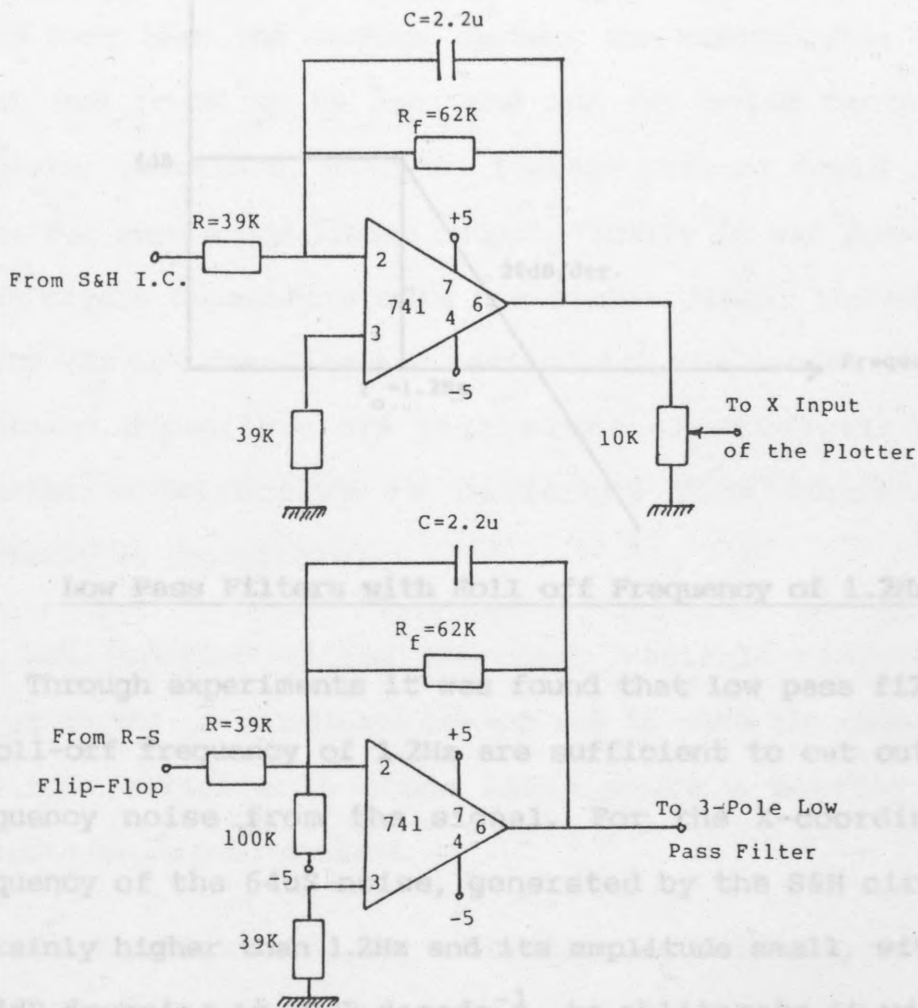


Fig. 3.16 Smoothing Filters

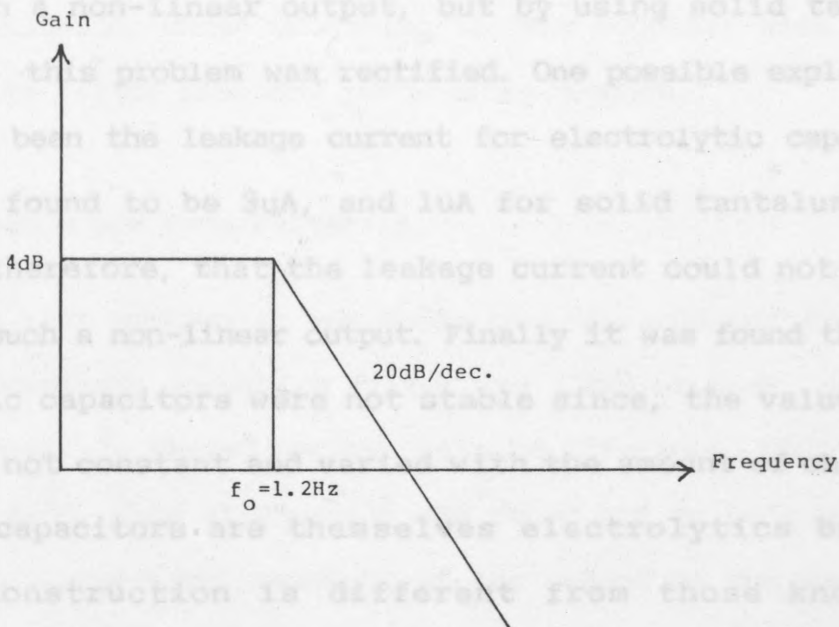
Therefore at the pole $\omega_0 CR_f = 1$

$$\therefore \omega_0 = \frac{1}{CR_f} \quad \therefore f_0 = \frac{1}{2\pi CR_f}$$

when $C = 2.2 \times 10^{-6} \text{ F}$

and $R_f = 62 \times 10^3 \text{ Ohms}$

$f_o = 1.2 \text{ Hz}$.



Low Pass Filters with Roll off Frequency of 1.2Hz.

Through experiments it was found that low pass filters with a roll-off frequency of 1.2Hz are sufficient to cut out any high frequency noise from the signal. For the X-coordinate, the frequency of the 64uS noise, generated by the S&H circuit, was certainly higher than 1.2Hz and its amplitude small, with respect to 4dB dropping at 20dB decade^{-1} , to obliterate it without any difficulties. However, for the Y-coordinate, the frequency was not as high and its amplitude as small as the X-coordinate and this, although attenuating much of the a.c. voltage, still transferred some of the higher frequency components to the output (For more information c.f. section 3.4.VIII).

By observation it was also found that the roll-off frequency of 1.2Hz was high enough not to produce a slow response time of

the plotter's pen to the movement of the light pen. This was worth considering for the use of the instruments, by trained or fast and confident patients.

Initially electrolytic capacitors were used and this resulted in a non-linear output, but by using solid tantalum capacitors, this problem was rectified. One possible explanation could have been the leakage current for electrolytic capacitors which was found to be $3\mu\text{A}$, and $1\mu\text{A}$ for solid tantalum. This suggests, therefore, that the leakage current could not be the cause for such a non-linear output. Finally it was found that the electrolytic capacitors were not stable since, the value of C , ($q=VC$) was not constant and varied with the amount of charge q . (Tantalum capacitors are themselves electrolytics but the internal construction is different from those known as electrolytic capacitors).

The function of the 10K-ohms variable resistor at the output of the x-coordinate op-amp was to make the output voltage amplitude variable in those cases where a plotter lacked a variable amplitude control.

The output of the R-S flip-flop was either 0 or 5V. If the light pen was at the top section of the T.V. screen then the output of the R-S flip-flop was a short duration pulse and thus the area under the curve was small giving a minimum d.c. output from the smoothing circuit. If the light pen was at the bottom section of the T.V. screen then the output of the R-S flip-flop was a long duration pulse and the area under the curve was large giving a maximum d.c. output from the smoothing circuit. This caused the smoothing circuit to saturate. To overcome this

problem the R-S flip-flop's output was shifted so that it could change between a negative value, -2V, for example, and a positive value of $(-2 + 5) + 3V$. The purpose of a 100K-ohms resistor at the inverting input of the Y-coordinate op-amp was to shift the output of the S-R flip-flop negatively.

In conclusion, these smoothing filters together with the 3-pole low pass filter provided jitter-free outputs.

3.4.VIII 3-Pole Low Pass Filter:

In the last section it was shown that the roll-off frequency of the Y-coordinate smoothing filter was 1.2Hz at +4dB, dropping at 20dB decade⁻¹. Therefore the gain at 12Hz was -16dB and at 120Hz was -36dB. This attenuation was found not to be enough and resulted in a saw-tooth waveform at the output of the smoothing circuit. Its frequency was 50Hz, hence by placing a low pass filter with a roll-off frequency of 20Hz, it was possible to produce a clean enough d.c. signal to the plotter for Y deflections.

As, in section 6.4.VII an active 3-pole low pass filter was already designed and used, the same circuit was adopted here (Appendix XI). The circuit is shown in Fig. 3.17.

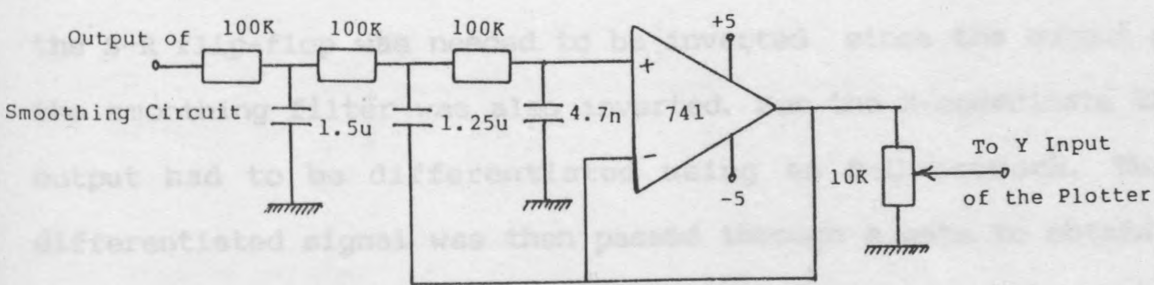


Fig. 3.17 3-Pole Low Pass Active Filter

of a pulse.

The design was based on a Chebyshev filter type with 1dB ripple and rapid (60dB decade^{-1}) cut off with minimum number of components, using capacitors, resistors and an op-amp. This had a roll-off frequency of 20Hz and 100K-Ohms resistance level for a compromise constrained by the amplifier input current offset and drift on the one hand, and the desire for small capacitor values on the other.

The variable resistor at the output of the filter was to vary the voltage amplitude as in the previous section to cater for those plotters with no variable amplitude control.

3.4.IX S-R Flip-Flop and Differentiator:

As explained in section 3.4.VIII, the purpose of this circuit was to generate an output of zero Volts from the beginning of the field to the position of the light pen, and 5 Volts from the position of the pen to the end of the field waveform.

Thus the S-R flip-flop would be set by the light pen signal and reset by the field drive waveform. The circuit is shown in Fig.3.18.

For use in the y-coordinate smoothing filter the output of the S-R flip-flop was needed to be inverted since the output of the smoothing filter was also inverted. For the X-coordinate the output had to be differentiated using an R-C network. This differentiated signal was then passed through a gate to obtain a proper negative going square pulse suitable for the timer circuits. The timer was only triggered by the negative going edge

of a pulse.

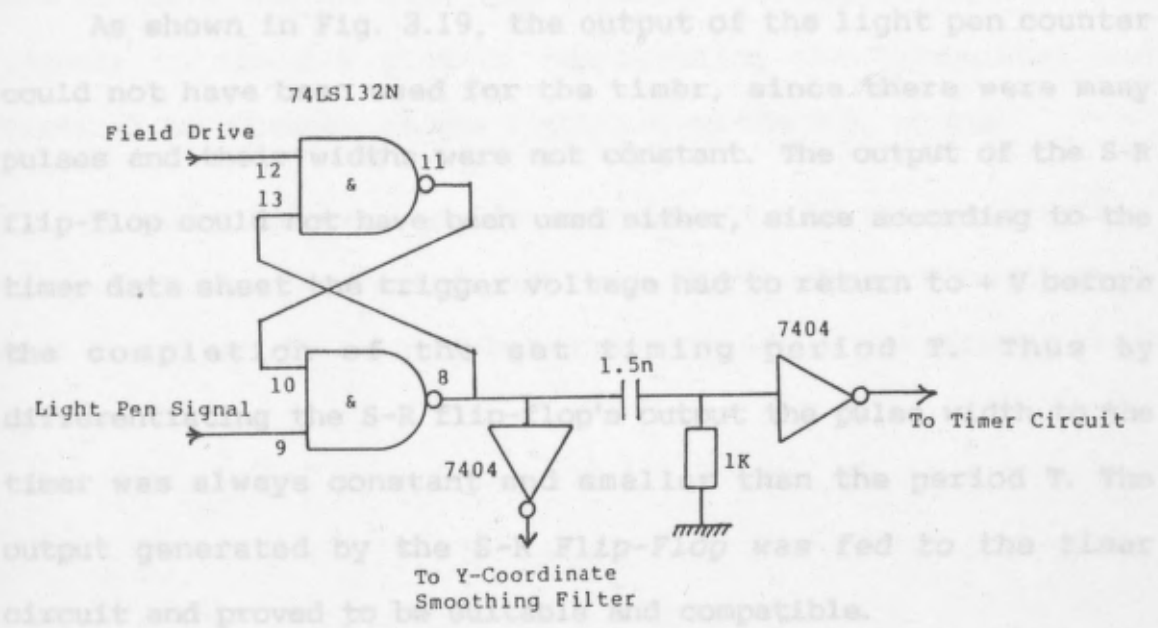
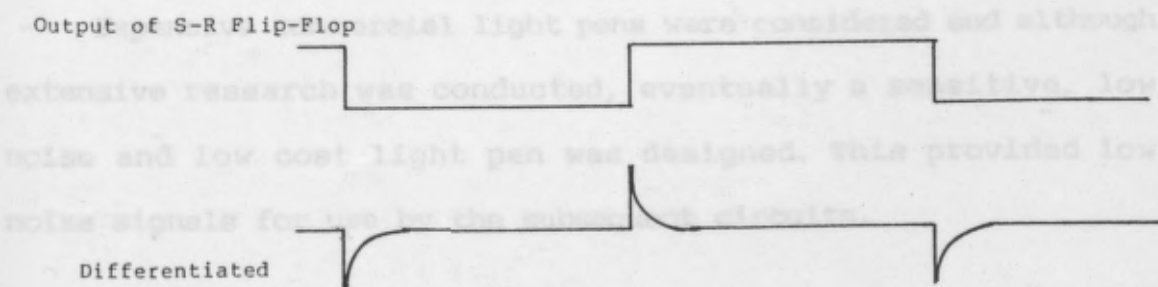
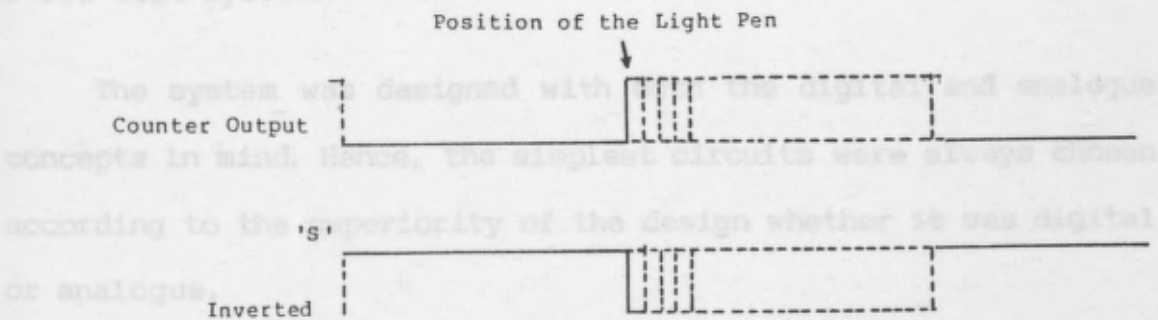


Fig. 3.18 S-R Flip-Flop

3.3 Summary

The monitors and the X-Y plotter used in this section were kept free from modifications because the cost of the system was a low cost system.



The Sync. Generator proved to be very useful and produced very accurate waveforms. The waveforms were used in both in this and subsequent chapters.

Fig. 3.19 S-R Flip-Flop Waveforms

The inputs to the system consisted of the power supply +5V

As shown in Fig. 3.19, the output of the light pen counter could not have been used for the timer, since there were many pulses and their widths were not constant. The output of the S-R flip-flop could not have been used either, since according to the timer data sheet the trigger voltage had to return to + V before the completion of the set timing period T. Thus by differentiating the S-R flip-flop's output the pulse width to the timer was always constant and smaller than the period T. The output generated by the S-R Flip-Flop was fed to the timer circuit and proved to be suitable and compatible.

3.5 Summary

The monitors and the X-Y plotter used in this section were kept free from any modifications hence ensuring the production of a low cost system.

The system was designed with both the digital and analogue concepts in mind. Hence, the simplest circuits were always chosen according to the superiority of the design whether it was digital or analogue.

Expensive commercial light pens were considered and although extensive research was conducted, eventually a sensitive, low noise and low cost light pen was designed. This provided low noise signals for use by the subsequent circuits.

The Sync. Generator proved to be very useful and produced very accurate waveforms which were used throughout the circuits both in this and subsequent chapters.

The inputs to the system consisted of the power supply +5

and -5 Volts and the light pen signals. Its outputs were two d.c. signals to the X-Y plotter representing the horizontal and vertical coordinates of the light pen on the T.V. screen.

It must, however, be mentioned that due to the complexities attributed to television interlace, the designed circuits were only driven by the even field output (Pin 14) of the SNAL34J chip in Fig. 3.7.

(Chapter 3) and, his other eye, through a mirror, would be imaging the Hess chart. This chart was to be displayed over a second T.V. screen, so that either the whole or part of the chart would be exposed to view.

The Hess chart, as stated previously, is the projection, onto a plane screen situated at a normal viewing distance from the eye, of the lines of latitude and longitude drawn on the surface of an imaginary sphere centred at the eye. The chart printed onto the T.V. screen was to be designed in such a way to generate small bright squares at the intersections of these latitude and longitude lines.

The positioning of these square dots must be very accurate (c.f. Appendix 1) and their brightness tightly controlled for good superposition of the chart onto the black screen. For generation of such a display, a few different methods were considered which are outlined as follows:

4.2 Bank Memory

One of the ways of producing the Hess chart on the T.V. was to have a bank of memories storing the total area of the T.V. screen. In this way the complete chart was to be generated in

CHAPTER 4

HARDWARE DESIGN (CHART MONITOR)

4.1 Introduction

As has already been discussed, one eye of the patient would be directly observing a blank monitor together with its light pen (Chapter 3) and, his other eye, through a mirror, would be imaging the Hess chart. This chart was to be displayed over a second T.V. screen, so that either the whole or part of the chart would be exposed to view.

The Hess chart, as stated previously, is the projection, onto a plane screen situated at a normal viewing distance from the eye, of the lines of latitude and longitude drawn on the surface of an imaginary sphere centred at the eye. The chart printed onto the T.V. screen was to be designed in such a way to generate small bright squares at the intersections of these latitude and longitude lines.

The positioning of these square dots must be very accurate (c.f. Appendix I) and their brightness tightly controlled for good superposition of the chart onto the blank screen. For generation of such a display, a few different methods were considered which are outlined as follows:

4.2 Bank Memory

One of the ways of producing the Hess chart on the T.V. was to have a bank of memories storing the total area of the T.V. screen. In this way the complete chart was to be memorised in

ROMs; which could be simply addressed by a counter. This method, although not very complex, was found to be expensive and therefore not viable in this project.

4.3 Video Display Generators

Using a V.D.G. in conjunction with a microprocessor was found to be a very advantageous method. However, at the time of designing this circuit all V.D.G. I.C.'s available were NTSC (U.S.) system and not compatible with PAL television (such as A.M.I. S68047 or Motorola MC6847Y). Also the maximum resolution on Graphic 7 (A.M.I., 1978) was 256 display elements in columns and 192 display elements in rows, whereas the required resolution was 400 display elements in columns and 315 display elements in rows. The best way of producing the Hess chart in future would be by using a high resolution V.D.G. in conjunction with a microprocessor, so that control would be easily obtained over every individual square dot. This could also provide a suffix in alphanumerics identifying each square dot.

4.4 Cushion Effect

The Hess chart is a symmetrical square chart with its corners pulled outwards and the centre of its four sides pushed inwards (Fig. 2.5). This shape is also the effect of the T.V. screen, when the correcting magnetic bars on the Cathode Ray Tube are missing (cushion effect). If only one line of the Hess chart was to be stored in a memory and repeated to construct a Hess Chart in a perfect square format then one would be able to produce the chart on the T.V. screen by removing the correcting magnetic bars and adjusting the coils of the C.R.T. to give the

chart.

This is a very long and tiring process and not practical on every single T.V. used for this purpose. There is also some doubt about the accuracy of the chart produced by this method.

4.5 Microprocessor (The Use of Software)

A microprocessor could be used to calculate the coordinates of the chart and draw it on the T.V. whilst the beam is scanning the screen. This needs a very fast microprocessor and a lot of software design.

4.6 Adopted Design (The use of Hardware)

In effect the method adopted here for the production of such a chart was, more or less, the same method as would be used in a microprocessor hardware design. The design has the advantage of higher speed and the obliteration of unnecessary sections of hardware found in a microprocessor system. The final design for the digital board is illustrated in Fig. 4.1.

The field drive and the line drive waveforms were fed into two counters - one counting the number of lines and the other, the number of cells on each line. The outputs of the counters were compared with the outputs of two EPROM memories filled with the coordinates of the Hess Chart. If the outputs of the comparators - one for vertical coordinates and the other for horizontal coordinates- were high then the respective point on the T.V. screen would be lit up. Also each pulse output from the comparator would cause the location of the memories to jump to the next coordinate.

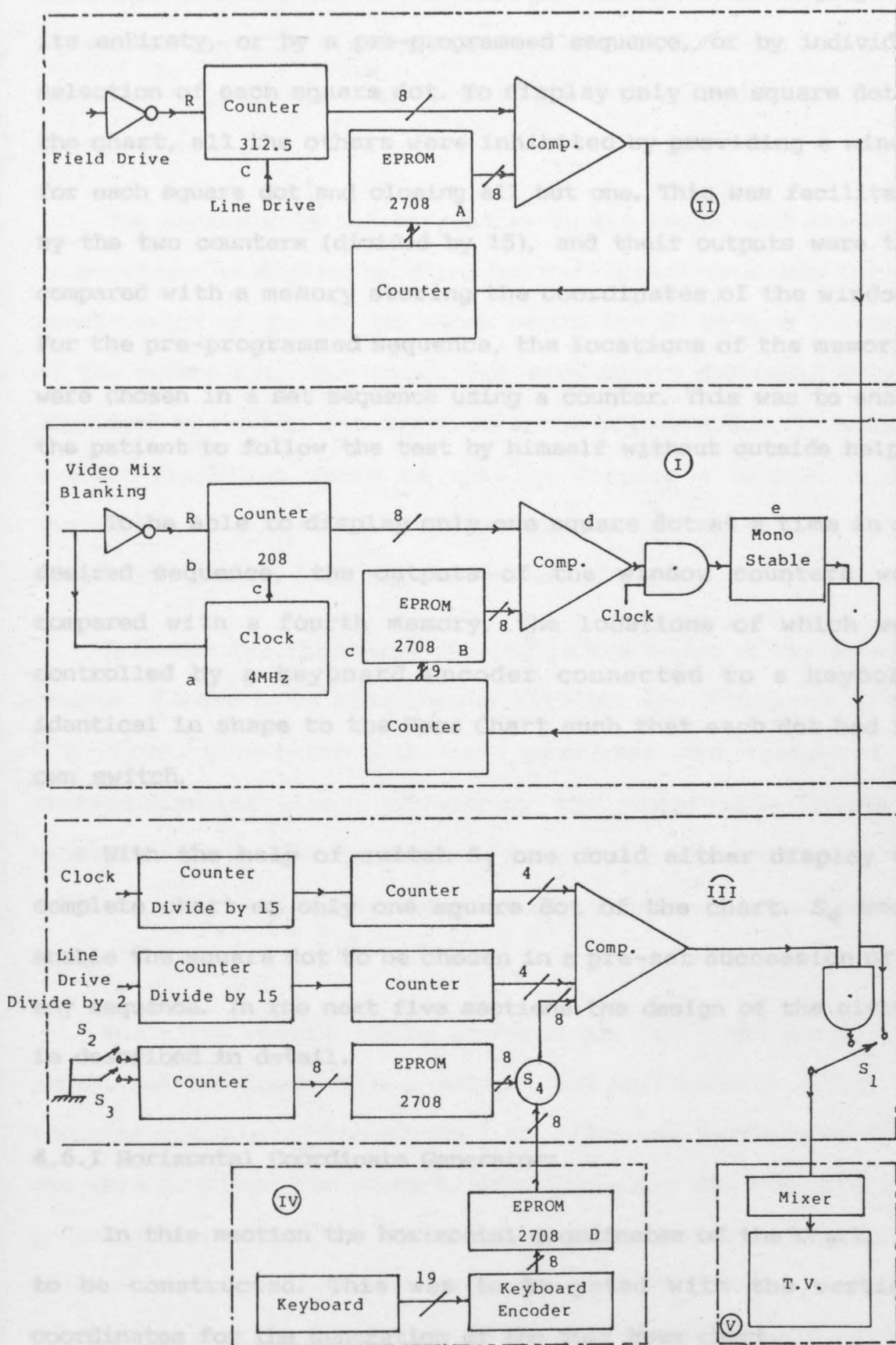


Fig. 4.1 Block Diagram of the Chart Generator

Provisions were made for the chart either to be displayed in its entirety, or by a pre-programmed sequence, or by individual selection of each square dot. To display only one square dot on the chart, all the others were inhibited by providing a window for each square dot and closing all but one. This was facilitated by the two counters (divided by 15), and their outputs were then compared with a memory storing the coordinates of the windows. For the pre-programmed sequence, the locations of the memories were chosen in a set sequence using a counter. This was to enable the patient to follow the test by himself without outside help.

To be able to display only one square dot at a time in any desired sequence, the outputs of the window counters were compared with a fourth memory, the locations of which were controlled by a keyboard encoder connected to a keyboard identical in shape to the Hess Chart such that each dot had its own switch.

With the help of switch S_1 one could either display the complete chart or only one square dot of the chart. S_4 would enable the square dot to be chosen in a pre-set succession or in any sequence. In the next five sections the design of the circuit is described in detail.

4.6.I Horizontal Coordinate Generator:

In this section the horizontal coordinates of the chart, are to be constructed. This was to be gated with the vertical coordinates for the generation of the full Hess chart.

a) **Clock:** The frequency of the clock, which was the heart of

the entire system, was determined by the required horizontal resolution of the chart produced on the T.V. For good chart recognition on a 20" T.V. screen, viewed from 30cms, a 4mm width for each square dot on the chart was considered to be appropriate.

The square dots are arrayed in an arc shape, and the chart is constructed digitally. Thus for sufficient accuracy for the construction of the arc the clock period had to be half the width of the square dot. This meant that each square dot could only be displayed by half of its width from its adjacent dot. Thus using a 4MHz clock one would be able to display a matrix with a resolution of 208 cells of 250ns duration.* These cells were about 2mm wide on a 400mm wide screen (20" T.V.).

Although the clock was sitting in the heart of the system, however, it had to be synchronous with the waveforms out of the T.V. sync. generator I.C. This prompted the design of an enabled/disabled clock, driven by the mixed video blanking waveform of the sync. generator. The circuit for the 4MHz clock is in Fig. 4.2. and the explanation of its operation is found in Appendix VII.

The mixed video blanking waveform was fed to the clock, thus inhibiting the clock during vertical and horizontal blanking and ensuring synchronisation of the two. A 2K-ohms variable resistor was used to adjust the clock to 4MHz frequency. The two inverting gates at the output of the clock acted as buffers to produce

* A T.V. line is 64uS, but 12uS of it is blanked, hence only 52uS was displayed on the screen:

$$\therefore (52 \times 10^{-6}) / (250 \times 10^{-9}) = 208 \text{ cells.}$$

clean edged pulses.

For the reason given in section 'e' the clock pulses required a small Mark Space ratio. Therefore some of the components of the clock had to be changed to the ones shown in Fig. 4.3.

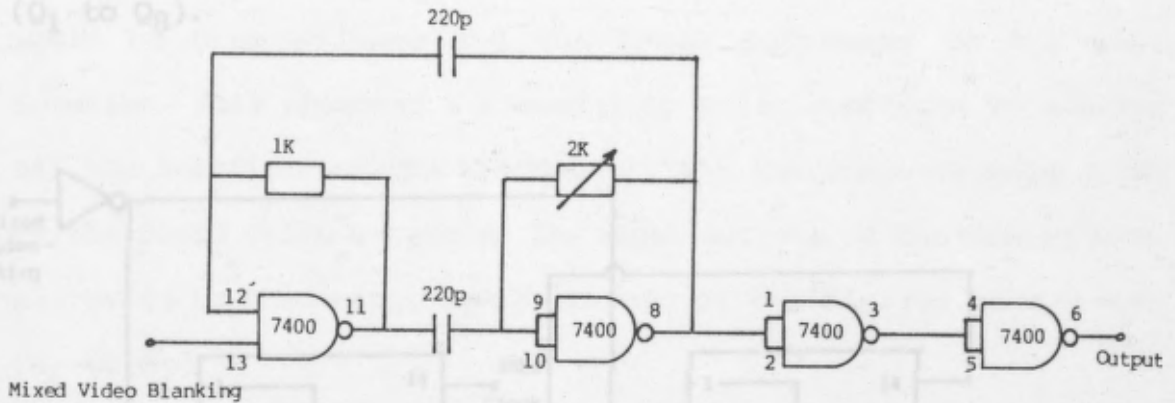


Fig. 4.2 4MHz Clock Circuit

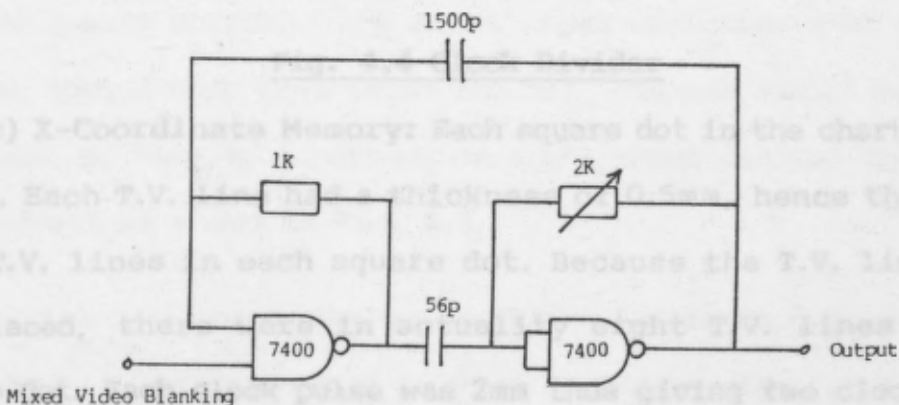


Fig. 4.3 Final Design for the Clock

b) **Clock Divider:** With a frequency of 4MHz and a screen of 400mm, there were 208 cells to produce across the screen using counters. To be able to count up to 208 cells an eight bit counter was required. At first the eight bit binary counter CD4040B were considered, but this had a propagation delay of 200

to 400ns which was far greater than the clock pulse period. Hence two SN7493 4-bit binary counters were used in cascade. These had a propagation delay of only 13ns. The circuit is shown in Fig.4.4. Both counters were inhibited during vertical and horizontal blankings. (The clock also was inhibited during this period). The eight outputs were all taken to digital comparators (Q_1 to Q_8).

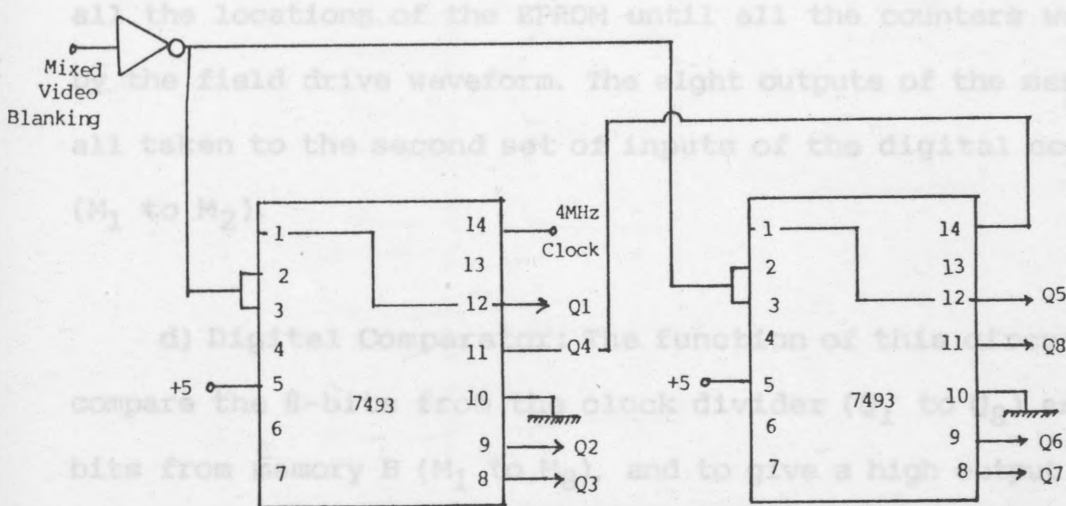


Fig. 4.4 Clock Divider

c) X-Coordinate Memory: Each square dot in the chart was 4mm x 4mm. Each T.V. line had a thickness of 0.5mm, hence there were four T.V. lines in each square dot. Because the T.V. lines were interlaced, there were in actuality eight T.V. lines in each square dot. Each clock pulse was 2mm thus giving two clock pulses per square. However, using a monostable to obtain the full width of the square dot, one would be able to use one clock pulse per square dot, hence each square dot in the chart needed four locations in the x-coordinate memory B. The use of a monostable together with interlacing characteristic of the T.V. system helped to reduce the amount of memory required.

There were 127 square dots to produce, therefore a total of 508 locations required in memory B , using EPROM 2708. The data had to be in hexadecimal format (a requirement of EPROM 2708) and the content of the memory is shown in Appendix VIII. The circuit is shown in Fig.4.1. A counter was used to address the memory with its clock input connected to the output of the digital comparator, hence, with each comparator output pulse, the counter would be clocked once and the EPROM addressed to the next location. This produced a closed loop which continued to address all the locations of the EPROM until all the counters were reset by the field drive waveform. The eight outputs of the memory were all taken to the second set of inputs of the digital comparator (M_1 to M_2).

d) **Digital Comparator:** The function of this circuit was to compare the 8-bits from the clock divider (Q_1 to Q_8) and the 8-bits from memory B (M_1 to M_8), and to give a high output whenever the two inputs corresponded. A two input exclusive -NOR is such a digital comparator (see table below), and one would be able to use eight of them to construct an eight input digital comparator. The circuit is shown in Fig. 4.5.

As the two input exclusive-NOR 74266 is an open collector TTL gate, it, with correct pull up resistor, may be paralleled with each other to perform the Wired-AND function. (Texas Instruments, 1978).

$$R_L(\text{max}) = \frac{V_{CC} - V_{OH}}{n \times I_{OH} + N \times I_{IH}}$$

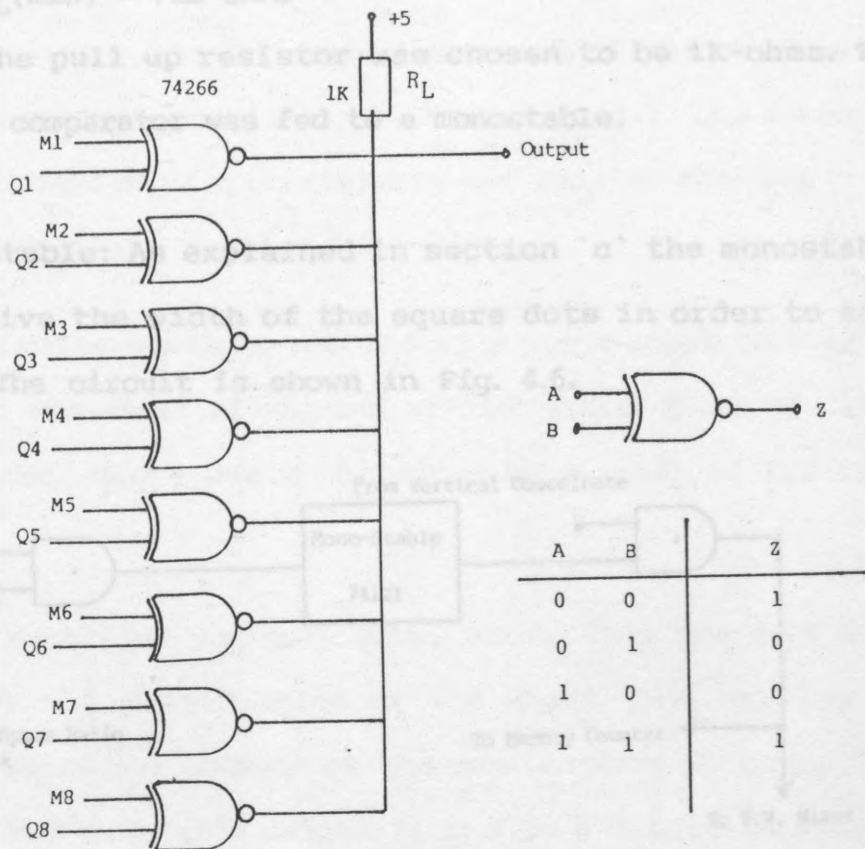


Fig. 4.5 Digital Comparator/Exclusive-NOR

$n = 8$ Ecx-NOR

$N = 1$ TTL at output

$I_{OH} = 250\mu A$

$I_{IH} = 40\mu A$

$V_{CC} = + 5\text{volt}$

$V_{OH} \text{ min} = 2.4\text{volt}$

$R_L(\text{max}) = 1.2\text{K-ohms}$

$$R_L(\text{min}) = \frac{V_{CC} - V_{OL\text{max}}}{I_{OL} - N \times I_{IL}}$$

$V_{OL} = 0.4\text{volt}$

$$I_{OL} = 8\text{mA}$$

$$I_{IL} = 1.6\text{mA}$$

$$\therefore R_L(\text{min}) = 720 \text{ ohms}$$

\therefore The pull up resistor was chosen to be 1K-ohms. The output of the comparator was fed to a monostable.

e) Monostable: As explained in section 'c' the monostable was used to give the width of the square dots in order to save memory size. The circuit is shown in Fig. 4.6.

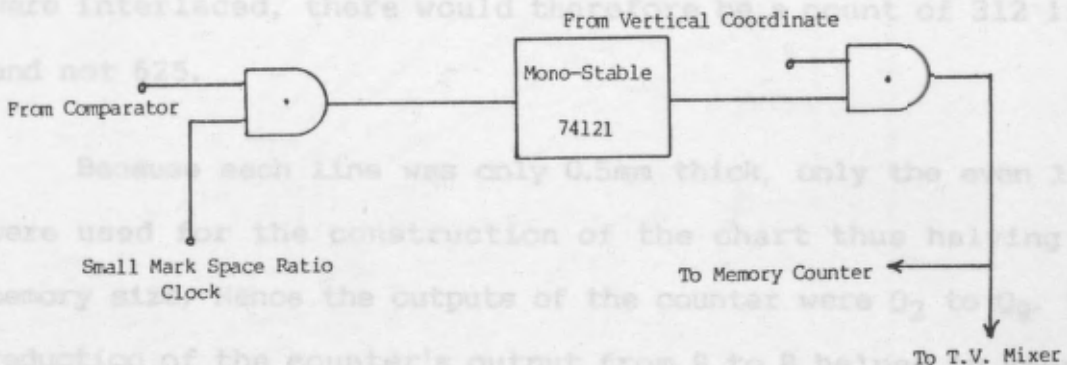


Fig. 4.6 Monostable

The timing value of the monostable was made variable so that the size of the square dots could be adjusted to suit different eyesights.

It was imperative to produce a linear chart, but different outputs of the counter had different delays (Asynchronous Counters) and this had to be synchronised with the incoming clock pulses. Therefore to overcome this problem the output of the comparator was gated with short clock pulses (small mark space ratio). In this way the spaces between output pulses were equal and the presence of the monostable ensured that the pulses for the display were long enough to be recognised by the memory B

counter.

4.6.II Vertical Coordinate Generator:

In this section the vertical coordinates of the chart are to be constructed. The circuit is shown in Fig. 4.7. and as can be seen the basic design is approximately the same as the one in the Horizontal coordinate section 4.6.I.

The line drive waveform was fed as a clock input to a 12 bit counter which was reset at the end of each field. Since the lines were interlaced, there would therefore be a count of 312 lines and not 625.

Because each line was only 0.5mm thick, only the even lines were used for the construction of the chart thus halving the memory size. Hence the outputs of the counter were Q_2 to Q_9 . This reduction of the counter's output from 9 to 8 helped in keeping the number of the inputs to the digital comparator to the standard of 8 and hence using only one 2708 EPROM for memory A.

The chart had 127 square dots, but many of them shared the same lines. Therefore the total number of locations in the memory A was found to be only 69. The content of the memory is found in Appendix VIII.

The construction of the digital comparator and its calculation for R_L , and the EPROM A and its counter is the same as that in the Horizontal coordinate section 4.6.I. The output of this section was gated with the horizontal coordinate generator (Fig. 4.6) for input to the T.V. mixer circuit.

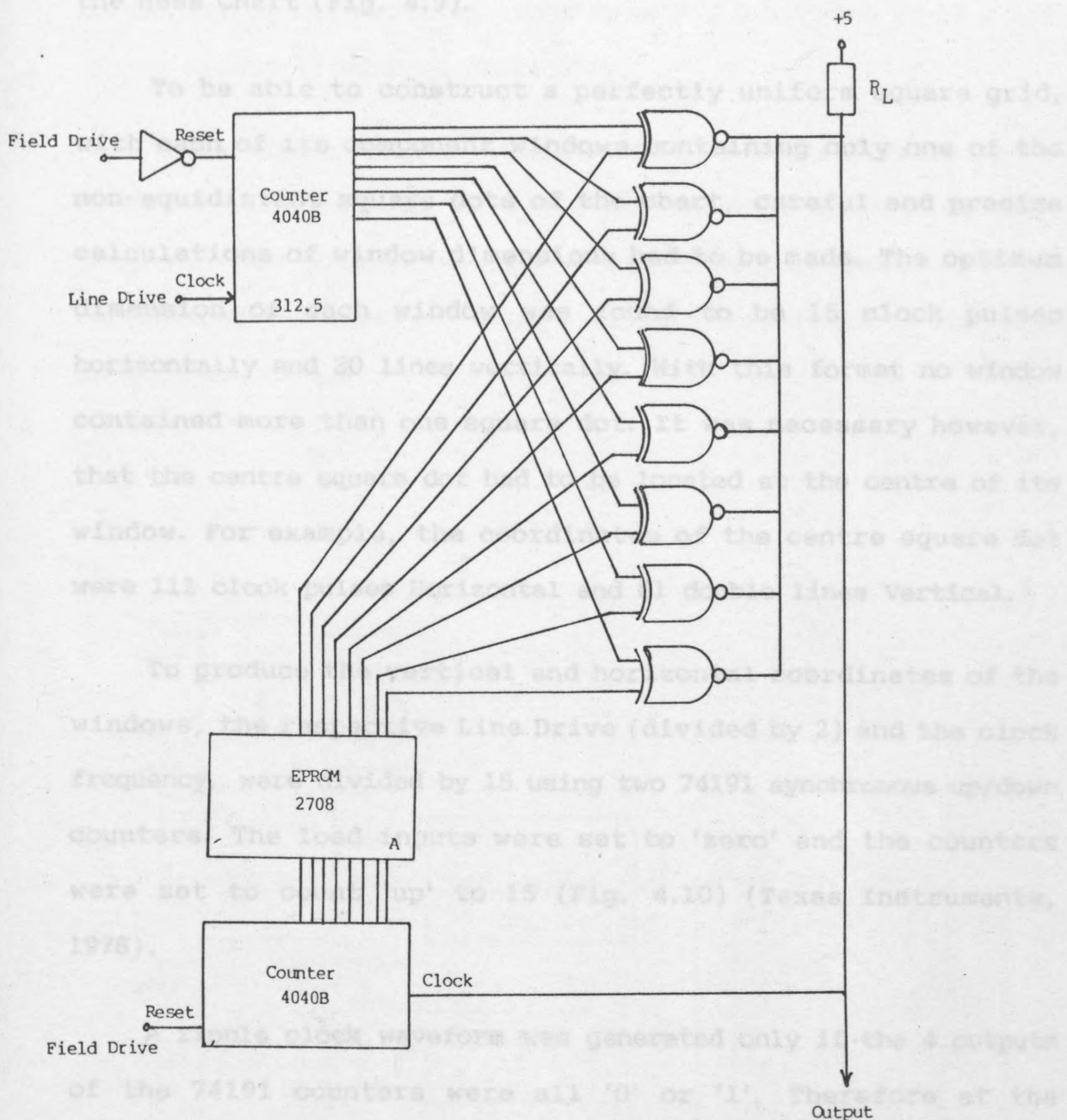


Fig. 4.7 Vertical Coordinate Generator

4.6.III Window Inhibited:

As explained previously, it was often necessary to display, at any one time, only one square dot of the chart. The circuit, illustrated in Fig. 4.8, was designed to achieve this by blanking the whole of the picture except for a particular window which allowed only one square dot of the chart to be displayed. For

example, opening window number 87, displayed the centre dot of the Hess Chart (Fig. 4.9).

To be able to construct a perfectly uniform square grid, with each of its component windows containing only one of the non-equidistant square dots of the chart, careful and precise calculations of window dimensions had to be made. The optimum dimension of each window was found to be 15 clock pulses horizontally and 30 lines vertically. With this format no window contained more than one square dot. It was necessary however, that the centre square dot had to be located at the centre of its window. For example, the coordinates of the centre square dot were 111 clock pulses Horizontal and 81 double lines Vertical.

To produce the vertical and horizontal coordinates of the windows, the respective Line Drive (divided by 2) and the clock frequency, were divided by 15 using two 74191 synchronous up/down counters. The load inputs were set to 'zero' and the counters were set to count 'up' to 15 (Fig. 4.10) (Texas Instruments, 1978).

A ripple clock waveform was generated only if the 4 outputs of the 74191 counters were all '0' or '1'. Therefore at the beginning of the Line Drive waveforms or the Field Drive waveforms there was no ripple clock waveform available since the outputs were holding to the last state of the count. To ascertain that the outputs of the counters at the end of the count cycle were always 'low', the counters were loaded to 0000 and counted up to 1111. The loading waveform was generated by the output of an 'exclusive-OR' with inputs of the ripple clock and the line/field reset waveforms (Fig. 4.8).

The 208 clock count divided by 15 was 14^* windows horizontally. The vertical lines were 312.5 divided by (2×15) , giving almost 11 windows vertically.

To be able to make a matrix of 13 by 11, the outputs of the divide-by-15 counters were fed to two 7493 binary counters (Fig. 4.8). The outputs of these counters were compared with the contents of the memory C using a digital comparator as explained in section 4.6.I.d.

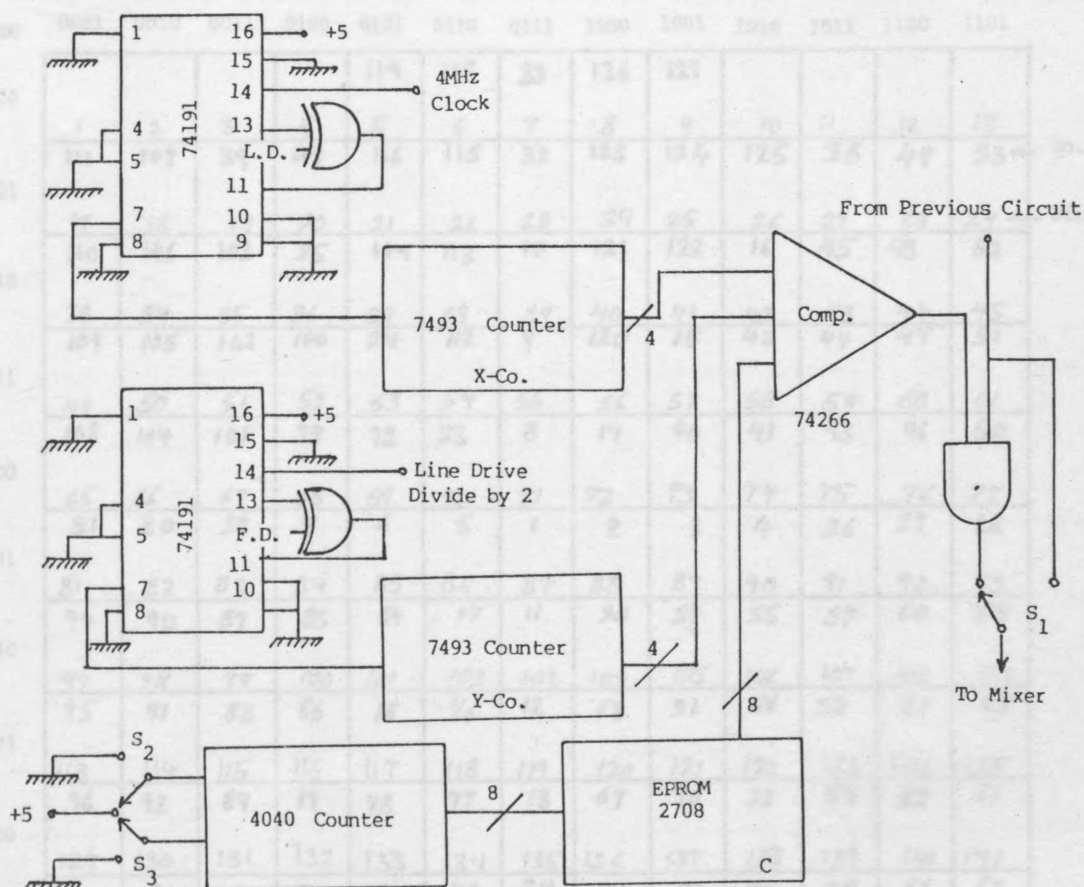


Fig. 4.8 Window Inhibit Circuit

* Since the first column of windows are not used there are only 13 windows horizontally.

The content of memory C was used (Appendix VIII) so that the patient, using a simple switch clocking a counter, addressing EPROM C, could follow a set sequence for drawing the chart point by point. The sequence, which is an extension of the classical test, is shown in Fig. 4.9.

Switch S₂ would clock the counter until the sequence was completed and any more clocking would have no effect unless the counter was reset by pressing switch S₃. The format of the sequence could be changed by rewriting the content of memory C.

Both S₂ and S₃ are antibounce switches.

	0000	0001	0010	0011	0100	0101	0110	0111	1000	1001	1010	1011	1100	1101	
0000					119	118	33	126	127						
	1	2	3	4	5	6	7	8	9	10	11	12	13		No. of Sequence
0001	111	107	39	117	116	115	32	123	124	125	36	49	53		
	17	18	19	20	21	22	28	24	25	26	27	28	29		Binary Number
0010	110	106	103	25	114	113	10	121	122	16	45	48	52		
	33	34	35	36	37	38	39	40	41	42	43	44	45		
0011	109	105	102	100	24	112	9	120	15	42	44	47	51		
	49	50	51	52	53	54	55	56	57	58	59	60	61		
0100	108	104	101	99	98	23	8	14	40	41	43	46	50		
	65	66	67	68	69	70	71	72	73	74	75	76	77		
0101	31	30	29	7	6	5	1	2	3	4	26	27	28		
	81	82	83	84	85	86	87	88	89	90	91	92	93		
0110	94	90	87	85	84	17	11	20	54	55	57	60	64		
	97	98	99	100	101	102	103	104	105	106	107	108	109		
0111	95	91	88	86	18	76	12	68	21	56	58	61	65		
	113	114	115	116	117	118	119	120	121	122	123	124	125		
1000	96	92	89	19	78	77	13	69	70	22	59	62	66		
	129	130	131	132	133	134	135	136	137	138	139	140	141		
1001	77	93	37	81	80	79	34	71	72	73	38	63	67		
	145	146	147	148	149	150	151	152	153	154	155	156	157		
1010					83	82	35	74	75						
	161	162	163	164	165	166	167	168	169	170	171	172	173		

Fig. 4.9 Table for Memory C and Window Number

The output of the comparator was gated with the waveforms generated in sections 4.6.I and 4.6.II so as to produce only one square dot of the Hess Chart on the T.V. screen. Switch S_1 enabled the operator to either display the complete chart or only one square dot (Fig. 4.8).

4.6.IV Keyboard Control:

During the Hess screen test it was frequently necessary to display the square dots of the chart regardless of the sequence stored in memory C, specially to repeat parts of the test where during the automatic test the results were found to be ambiguous

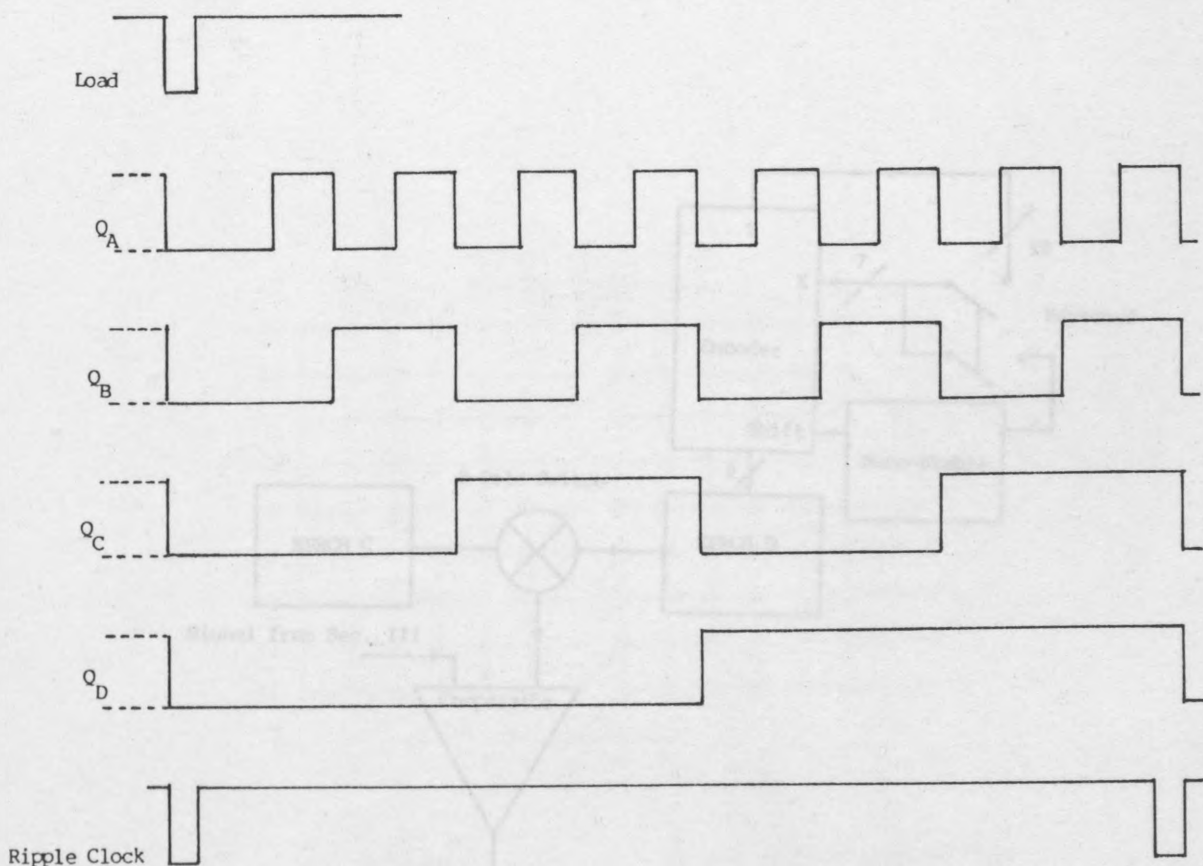


Fig. 4.10 waveforms for 74191 Counter

or, for some patients, only a specific area of the vision needed to be tested. For this purpose a keyboard encoder was used to be able to display any dot by just pressing its respective push button on a keyboard. (The keyboard consisted of 127 push button switches placed on a board isomorphic to the Hess Chart itself).

The encoder used could only handle a matrix of 10×9 , whereas the window matrix was 13×11 . Therefore, if X and Y are the two matrix outputs/inputs of the keyboard encoder, it was also required to use the shift facilities of the encoder, such that 64 of the push button switches connected the X outputs to the Y inputs of the encoder with the remaining 63 switches connecting the X outputs to the Y and the shift inputs. In this way the X output was supplying the Y, and shifting the encoder for the next set of switches (Fig. 4.12). However, the X outputs

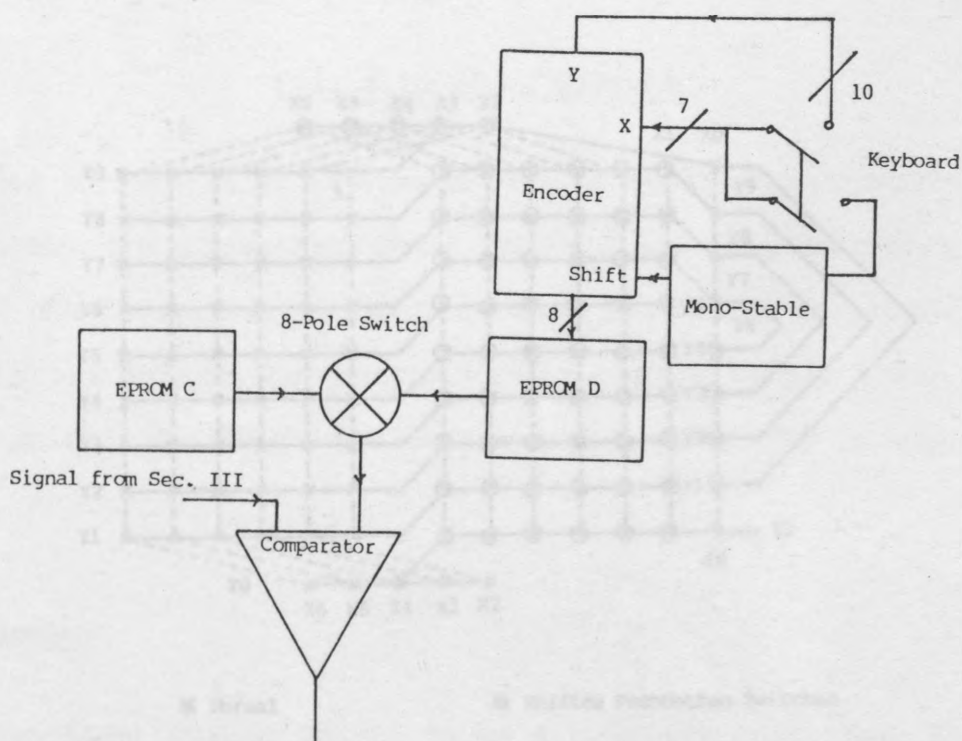


Fig. 4.11 Block Diagram for the Keyboard Encoder

were narrow pulses and the shift input needed to be high at the time of the pressing of the push button. For this reason a monostable 74121 was used at the input of the shift to make sure that the pulse to the shift input was long enough to be recognised.(Fig. 4.11).

This encoder in conjunction with an EPROM could produce the same data required for the digital comparator in section 6.4.III. Thus by an 8 pole switch, one was able to either display the chart in a preset or pre-programmed sequence, or to choose any part of the chart by simply pressing the appropriate push button (Fig. 4.11). The content of this EPROM (Memory D) is shown in Appendix VIII.

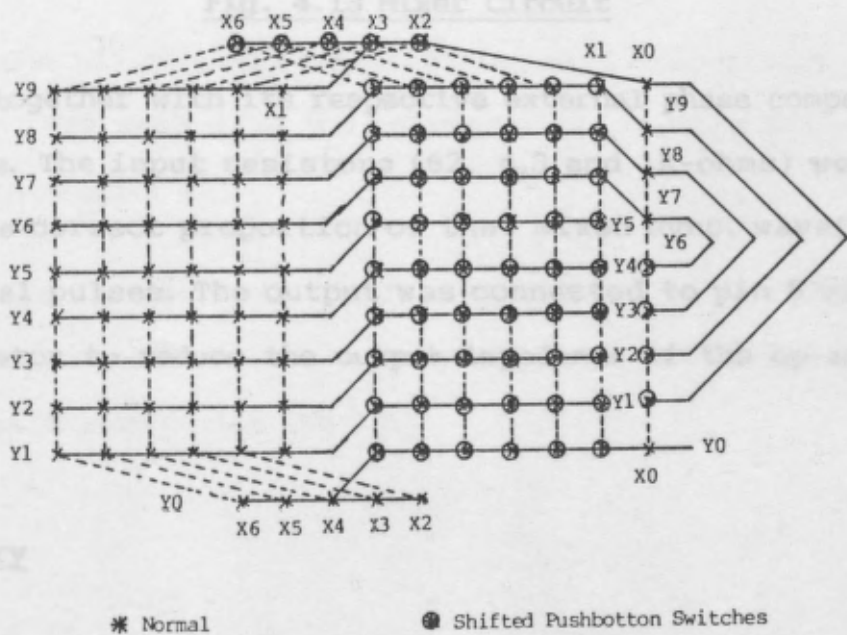


Fig. 4.12. Layout of keyboard's matrix wiring

4.6.V T.V. Mixer:

The outputs of all four sections, after going through some combinational logic, are added to a video waveform through a mixer. The mixer circuit is shown in Fig. 4.13. A CA3029 op-amp

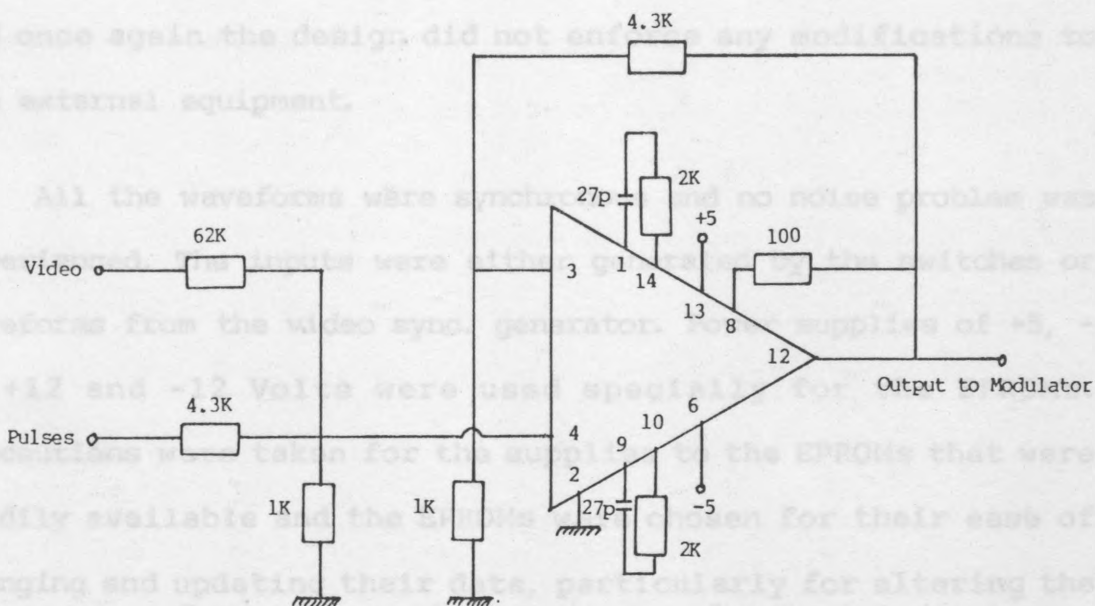


Fig. 4.13 Mixer Circuit

was used together with its respective external phase compensation components. The input resistors (62, 4.3 and 1K-ohms) were used to mix the correct proportion of the mixed sync. waveform and the digital pulses. The output was connected to pin 8 via a 100 ohms resistor to reduce the output impedance of the op-amp (RCA, 1970).

4.7 Summary

The final system proved to be a complete substitute for the Lees' (1949) screen test and offered many more advantages and new

scope for further research in the analysis of the relative movements of the eyes by ophthalmologists.

This section was designed using digital methods and the constructed Hess chart proved to be very accurate and practical. The picture of the generated chart was crystal clear with good intensity and sharpness.

A T.V. monitor was the only commercial equipment required and once again the design did not enforce any modifications to the external equipment.

All the waveforms were synchronous and no noise problem was experienced. The inputs were either generated by the switches or waveforms from the video sync. generator. Power supplies of +5, -5, +12 and -12 Volts were used specially for the EPROMs. Precautions were taken for the supplies to the EPROMs that were readily available and the EPROMs were chosen for their ease of changing and updating their data, particularly for altering the sequence of the automatic test stored in the memory C.

Although all the four memories required very little memory size, four 2708 were used for convenience. Further discussions are made in chapter 8.

Note In section 4.6.I.c each square dot consists of 8 lines, however, as the circuits are driven by even fields, only four lines of each square dot are lit.

PART II

CHAPTER 5

EYE TREMOR MOVEMENTS

5.1 A Survey of the Previous Methods and Instruments

5.1 In the following Chapters of part II, the previous systems of measuring eye tremor movements are discussed and, as a result, the attributes of an effective, semi-automated system chosen. The design and construction of the hardware for the T.V. system is therefore presented.

- a. To be of appropriate resolution, linearity and dynamic range.
- b. To have a flexible level of sensitivity for different applications.
- c. To be stable over time.
- d. Not to interfere with the patient's normal vision.
- e. It should, however, be relatively insensitive to lateral head movements and hence eliminate the need for rigid head fixation.
- f. It should simultaneously measure horizontal, vertical and torsional movements.
- g. It should be insensitive to ambient light, eye blinking and electrical interference.
- h. It should be easy to operate and not be cumbersome for the patient who is without prior experience or extraordinary motivation.

However, as in any research, ideal methods only become practical when some of its standards are compromised and trade-

CHAPTER 5

5.1 A Survey of the Previous Methods and Instruments

5.1.1 Introduction:

A prerequisite to the design and development of a new semi-automated tremor detection system is the determination of the attributes and specifications required. The following characteristics should be borne in mind when the more conventional methods are reviewed.

- a. To be of appropriate resolution, linearity and dynamic range.
- b. To have a flexible level of sensitivity for different applications.
- c. To be stable over time.
- d. Not to interfere with the patient's normal vision.
- e. It should, however, be relatively insensitive to lateral head movements and hence eliminate the need for rigid head fixation.
- f. It should simultaneously measure horizontal, vertical and torsional movements.
- g. It should be insensitive to ambient light, eye blinking and electrical interference.
- h. It should be easy to operate and not be cumbersome for the patient who is without prior experience or extraordinary motivation.

However, as in any research, ideal methods only become practical when some of its standards are compromised and trade-

offs and optimisations are accepted to be a natural path towards realisation.

5.1.2 Direct Observation:

This was the first technique used to monitor human eye movements and simply involves the observation of a subject's eye without the use of any optical aids. Apparently, with a little practice, eye movements can be detected to an accuracy of 1 degree (Yarbus, 1967). This method is still used today as a preliminary clinical examination for establishing the presence or absence of nystagmus.

More accurate measurements of tonic eye movements are possible, provided a travelling microscope is used. This allows the measurement of torsional movements which are difficult to measure by any other method (Merton, 1956).

Although it is a very simple and inexpensive method, it lacks quantitative data and permanent records are usually not kept.

5.1.3 Mechanical Transducers:

Mechanical transducers are old methods, which are now only of historical interest, and operate by interfering with normal eye movements. Raehlmann (1878) was the first to propose that eye movements could be monitored by firmly attaching some solid object to the surface of the eye or to the eye muscles. Many different modifications of this method have been subsequently used. For example, De La Barre (1898) used a plaster-of-Paris contact lens to which was attached a bristle which then

transcribed the eye movements onto a smoked drum. Other methods, included the use of a small concave mirror on the contact lens which by reflecting a strong ray of light onto a photographic plate could accurately reproduce and magnify all the eye movements. Although many disadvantages were associated with this latter method, the most notable was the speed with which the spot of light moved across the sensitive plate.

Other mechanical methods that were used included the resting of a glass rod on the upper eye-lid and which, by attaching to a mechanical lever system, could magnify the movements (Ohm, 1928). A silicon strain-gauge, taped to the upper eye-lid, was also used by Faraday (1969) to measure periods of eye movements during sleep.

A more sophisticated mechanical method was by monitoring the change in capacitance, through the change in frequency of an oscillator, between a small fixed probe positioned near the eye and the eye globe, as the eye ball rotated (Bengi & Thomas 1968). Here, the small probe acted as the fixed plate of a variable capacitor and the eye ball as the earthed moving plate. Bengi & Thomas also suggested a method of communicating rotational movements of the eye, through a piece of soft rubber, to a piezoelectric cantilever strain-gauge. However, these two methods are not very accurate and tend to be uncomfortable for the subject. Further difficulties arise in the latter method since the probe cannot be sterilised, electrical isolation in the vicinity of lacrimal secretions is difficult and also the brittle piezoelectric crystal could break and cause danger to the sclera.

Sandeman (1968) designed a device to measure small

positional changes in the eye of a crab. One end of a light-weight wand was attached to the crab's eye, whilst its other end was placed between two metal ball sensors. Any eye movements therefore altered the potential between the two sensors which were connected to differential inputs of a balanced amplifier. With this simple equipment fairly large movements of the eye, with an accuracy of 0.01 degrees of rotation over 25 degrees, could be measured.

Thomas (1977) used a piezoelectric strain-gauge transducer for measuring the pressure generated by the corneal bulge behind the eye-lid. The advantage of such a method is its 200Hz bandwidth.

5.1.4 After-image Methods:

An early quantitative technique for the determination of the duration of fixation and the velocity of eye movements was through the use of after-images. The number of after-images in a given region was indicative of the duration of fixation whilst the number and spacing of after-images, during a particular eye movement, was used to estimate the velocity of that movement. The basic principle is to flash two successive images of duration, not less than the tremor movement of the eye onto the patient's retina and then asking him to alter an adjustable vernier until it becomes equivalent to the gap between the after-images. This gap is then a measure of the movement of the eye during the successive flashing images (Barlow, 1952).

5.1.5 Sound Methods:

This is one of the simplest methods of monitoring eye

movements recorded in the literature. Ewald Hering (1879) by listening to the muscles of the eye, during its movements, was able to distinguish between two types of movements for fixation, the first was a steady background noise which corresponded to eye tremor and drift and the other was that of dull clicks which corresponded to microsaccades.

Another method utilizing sound is based on ultrasound waves which are generated in air by a piezoelectric transducer, and which are reflected by most materials. The reflected energy is combined with the source energy so that the phase of the reflected energy is altered and a predictable electrical response is produced. Such a response has formed the basis of a non-contacting method for measuring small eye movements (Haines, 1977). Surprisingly, better results were obtained when the eyes were closed since the surface of the eye was found to be a poor reflector of ultrasound waves.

5.1.6 The Counting Method:

The patient is asked to view a uniformly repeated pattern and then to count the number of lines in the pattern. The pattern is then reduced until it assumes a shimmering appearance and the individual elements are no longer identifiable. The angle subtended by the gap between elements is a measure of the amount of tremor movement in the eye.

5.1.7 Direct Photography:

This is mainly done by attaching some bright foreign object to the eye and then photographing the eye during movement (Dodge,

1901 & Judd, 1905). This is an accurate method but it requires the head position to be rigidly fixed and it also consumes a vast quantity of film.

5.1.8 Corneal Reflections:

The corneal reflection principle can be considered as a special case of direct photography recording using the corneal highlights. Incident beams of light are reflected off the front of the cornea and, therefore, produce a highlight on the corneal surface. Since the corneal bulge is of a smaller radius than that of the eye ball, the corneal reflex moves in the same direction as that of the eye, relative to the head. For small angles, the apparent displacement of this reflex will be considerably less than half the displacement of the eye itself and will move in the opposite direction. Its linear range is limited to about 12 degrees and head movements, especially lateral ones, need to be restricted since they can introduce significantly more error than the other methods. The sensitivity of this method is, therefore, half of that which uses the limbus as a detectable feature of the eye. In this latter method, incident light reflected from the convex surface of the cornea form diverging light beams which are imaged through a concave lens onto a film plate or onto moving film for continuous recording.

In early recordings, a temporally located light (on the peripheral field) reflected highlights onto the cornea which were photographed by a camera, as a time trace, on moving film. Simultaneous recordings of vertical and horizontal movements were achieved by splitting the corneal reflex by the use of prisms into two beams; one for each of the recordings (Buswell, 1935).

An accuracy of ± 0.5 degree was achieved by strict head fixation using either a chin rest or a head rest.

This method had two main advantages. The first was that the contrast between the cornea and the highlight was sufficiently high enough to allow easy detection, especially when a T.V. camera was used instead of film. The other advantage was that both vertical and horizontal movements could be easily recorded. Because of these advantages Mackworth and Mackworth (1958) investigated this method for determining the way in which the eye moves over natural visual scenes. They also used a head-mounted light source and corneal reflex cameras. The video output from one T.V. camera, viewing the corneal image, was then mixed with the output of the second camera, viewing the scene which the subject was observing. The total resultant image was that of a bright spot, which followed the movements of the subject's eye, superimposed on a picture of the scene.

Marchant (1967) also used the same method but instead of simply monitoring the corneal reflection highlights, he tracked the centre of the pupil using image-disector tubes and followed the optical landmarks through photoelectric scanning. Eye movement was recorded by measuring the distance between the centre of the pupil and the corneal reflex highlight. However, because of the exposed cornea and its non-spherical nature at the limbus, all corneal-reflection methods are limited to about ± 12 degrees rotation of the eye. Furthermore, as for the methods of direct photography, these methods suffer from sensitivity to lateral head movements. Errors of 1 degree eye rotation could result from a lateral head displacement of 0.1mm.

Although this method of movement recording, was initially

prohibitive because of the amount and cost of film used, these problems were later overcome by the use of T.V. cameras. Furthermore, because the weight and moment of inertia of the helmet and camera were found to be troublesome for free head movements, the camera was mounted separately and the visual information carried via a fibre optics cable.

As mentioned previously, the eye excursions are limited to ± 2 degrees vertically or horizontally, whilst the reflex range is ultimately limited by the size of the cornea and its partial disappearance behind the lids. In addition to the inaccuracies resulting from head movements, other factors, such as variation in corneal shape, the thickness of lachrymal fluid, corneal astigmatism and the production of other reflections by eye-glasses, limit the accuracy to 1-1.5 degrees (Hall, 1972).

Finally, Corby in 1976 used a pupil centre - corneal reflex centre distance method together with a real time, on-line mini-computer to track eye motions.

Corneal reflections are also used to find the point of regard. This method is used to measure the subject's angle of gaze with respect to a light source. It is based on the fact that the corneal reflex of a subject, looking directly at the light, will appear at the centre of the pupil when observed from a position at, or very near the light source (Young, 1975).

Merchant & Morrisette (1974) used a single light source to produce a corneal reflex on the pupil which was always in line with the centre of corneal curvature. The apparent displacement of corneal reflection, from the centre of the eye, was thus equivalent to the apparent displacement of the centre of corneal

curvature from the centre of the eye, which was of course a function of eye rotation.

Salapatek (1966) and later Haith (1969) used multiple light sources, for use with infants. The T.V. picture of the eye contained the corneal reflex of some or all of the six infrared sources that were used, so that the position of gaze could be determined with the aid of T.V. cameras and video recorders.

The advantages of this method are that the head is free from attachment, so that large head movements are permissible and that infrared light is used instead of visible light.

However, the disadvantages of the system are that it is expensive, bulky and complicated to use and also relatively slow (since it is limited to the speed of T.V. systems, ie. 50 samples per second), and of low accuracy.

5.1.9 Reflections from Attachments to the Eye:

In the corneal reflection method, any head movements were found to reduce its sensitivity, because of the curvature of the cornea. Therefore, if the cornea was replaced by a flat mirror, the measurements would become essentially insensitive to small head movements. In practice, a contact lens mounted with a small flat mirror was used (Orschansky, 1898) which permitted eye movements, about all three axes, to be recorded. The use of ordinary scleral-fitting contact lenses unfortunately allow appreciable slip even when the subject is trying to hold his eye steady (Barlow, 1963). Yarbus (1967) designed Yarbus-type lenses which although they were held to the eye by suction, still gave

large errors with large eye movements. Ratliff and Riggs (1950) demonstrated that their lenses did not slip during either fixation or large movements even though the moment of inertia was deliberately increased by attaching a 20 gram mass to the lens. They also indicated some of the critical variations in the fitting and manufacturing of contact lenses. Some probable causes of slippage are also discussed by Byford (1962). In all, most practitioners would probably agree that contact lenses are unsuitable for the accurate measurement of eye movements (Carpenter, 1977).

One major problem as discussed in the contact lens section (section 11) is the contamination of the mirror surface by lachrymal fluid and grease. To avoid this problem, Boyce (1968) mounted the optical mirror on a stalk so that it was remote from the surface of the contact lens. His results suggested the optimum design for the mirror mount.

As an extension to this section, Riva (1979) utilized the Doppler effect produced by moving particles, to measure eye movements. As laser light, scattered by a moving particle, is shifted in frequency by an amount proportional to the particle's velocity, the speed of eye rotation can be similarly determined, so that the distance travelled by the eye can be calculated. The method can be hazardous as 90 per cent of the light is absorbed by the cornea (Feuk, 1971). A further disadvantage is that the moving blood corpuscles in the cornea may also produce doppler effects and confound the results.

5.1.10 Double Purkinje Image Method:

A further extension to the corneal reflection method of

measuring eye movements, is the double Purkinje image method. This has the advantage of greater sensitivity and also of offering a more accurate record.

The front surface of the cornea is not the only optical surface which reflects incident light; secondary, reflected images are also formed by the back of the cornea and by both surfaces of the lens (Fig. 5.1).

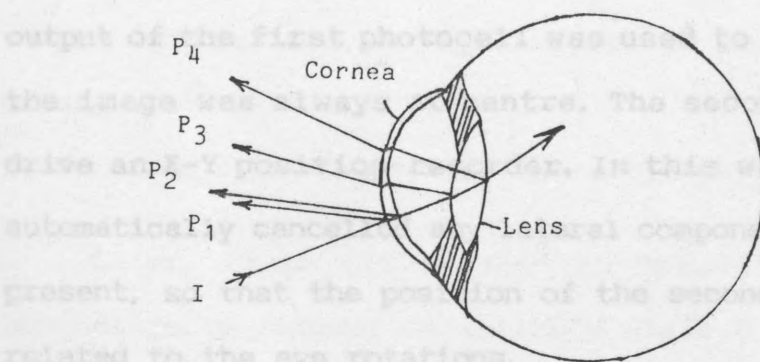


Fig. 5.1 Incident Light on the Eye

As light passes through the eye, reflections occur from different surfaces within the inner eye. The reflection from the front of the cornea is known as the corneal reflection or, the first Purkinje image (P1). A second image (P2) is reflected from the rear surface of the cornea, and the third image (P3) from the front surface of the lens. These two images are not used, however, since P2 is very dim and P3 is formed in a plane far from the others. A fourth image, P4, is reflected from the rear surface of the lens. This is also a dim image but as it is formed by a concave surface, it is real and not virtual.

Cornsweet and Crane (1973) used images P1 and P4 to devise an eye tracker. Like the relationship between the corneal

reflection and the pupil centre, described previously, under the condition of eye displacement, the two mentioned reflections would move together and, under the condition of eye rotation they would move differentially. Although this had the advantage of allowing the eye tracker to be free of introducing errors due to lateral head movements, eye rotation recording did not allow any head rotations.

In this method a light source produced two Purkinje images, each of which was focused on a four-quadrant photocell yielding signals proportional to the position of the off-centre image. The output of the first photocell was used to move a mirror so that the image was always at centre. The second output was used to drive an X-Y position-recorder. In this way the movable mirror automatically cancelled any lateral component which may have been present, so that the position of the second output was directly related to the eye rotations.

The instrument had numerous advantages. It was operated in the infrared region, so that it did not interfere with normal vision and did not require attachments to the eye. Furthermore, it had a sensitivity of about 1min. of arc and operated over a two-dimensional visual field of between 10 and 20 degrees in diameter.

However, the method suffered from the following disadvantages:

- a) Difficulties of calibration, the complexity of use, and the high costs.
- b) Interference from the 3rd Purkinje image was difficult to overcome since its image often fell onto the 1st and 4th photocells. It therefore required pivoted mirrors, driven in

altitude and azimuth, by two separate servomotors. Hence, it required mechanical components which reduced its compactness, ease of operation and high standard of calibration.

c) Although lateral head movements do not affect the measurements, most head movements are rotational and therefore require the use of a bite-board.

d) As the field of view is limited to the pupil diameter, a low light condition is necessary. But a high infrared illumination is required in order to bring the fourth Purkinje image above the noise level.

e) The optics need to be fairly close to the eye and these of course obstruct the view.

f) Problems are encountered when subjects wear glasses.

5.1.11.1 Optical Contact Lens

Later, Crane (1978) used an optometer to keep the eye automatically focused on infinity while a double Purkinje-image eye-tracker recorded the horizontal and vertical movements of the eye.

5.1.11 Contact Lens Method:

One way of recording eye movements is by placing a part of an optical reflection method. For example, the change in the an optical or electromagnetic path in, or on, a contact lens which is tightly attached to the eye.

Common contact lenses, used for cosmetic or correction purposes, float on a film of tear over the cornea and therefore do not follow eye movements well. Lenses which consist of two spherical sections to fit over both the corneal bulge and part of the sclera, could remove some of the obstacles, providing that the lens avoids contact with the sensitive limbus. Fender (1964)

discussed different methods of stabilising contact lenses, for example, by developing a negative pressure between the contact lens and the eye by filling the cavity with a 2 per cent sodium bicarbonate solution which by osmosis moves out through the tissue. Yarus (1967) used a valve on an exit hole through which a small amount of fluid was allowed to escape after applying the lens.

The suction of air from the cavity has also been investigated, but the rate of irrigation by the cornea limited the time of its effectiveness. Generally the contact lens methods can be divided into two sections, one is optical, and the other is electromagnetic.

5.1.11.1 Optical Contact Lens:

This is the most common use of the contact lens method where one or more plane mirrors, which are attached to the lens, reflect light onto a moving, or stationary, photographic plate, a photocell or a four quadrant photocell.

The use of plane mirrors has several advantages over the corneal reflection method. For example, the change in the reflection angle is twice that of the rotation of the eye as opposed to only 1.3 in the corneal reflex method.

Futhermore, it does not suffer from the imperfections of the cornea, which may affect the readings, and also, as for the 1st and 4th Purkinje images, the angle of reflection depends only on eye rotation and not on linear displacement (Ratliff & Riggs 1950). Matin (1964) embedded mirrors directly on the lens, at nearly every angle, so as to reflect infrared beams.

However, as this technique suffers from changes in mirror properties, due to tear film, the mirrors or lights must be mounted on stalks. Byford (1962) positioned a light source on one side of an optical edge, so that a shadow of the edge was produced on a suitably placed screen. Movements of the source at right angles to the edge, and parallel to it, caused the shadow to move in a corresponding manner. Compared to the present techniques available for recording eye movements, the above method has no apparent advantage, whilst it has several disadvantages, for example, the weight of the miniature lamp attached to the stalk; the weight of the attachment itself and the associated blinking problem; and the vibration of the stalk.

However, most of these optical contact lens methods have become out-dated mostly because of their general inaccuracies, whether they employ a stalk or not. In addition, mirrors embedded on a contact lens can be contaminated by tear fluids or grease whilst mirrors mounted on a stalk can interfere with eye blinking. There is also considerable danger in fitting the contact lens with negative pressure, and also the possibility of deforming the cornea.

5.1.11.II Electromagnetic Contact Lens:

Robinson (1963) introduced the concept of the electromagnetic contact lens. He used a search coil, embedded in a contact lens, through which an alternating voltage was induced by a uniform alternating magnetic field. Its amplitude was thus proportional to the sine of the angle between the plane of the coil and the direction of the magnetic field as demonstrated by

Fig. 5.2. By adding a second, large perpendicular magnetic field and a second coil on the contact lens, movements about all 3 axes could be recorded. An accuracy of 2 percent of FSD, or 15 seconds of arc and a bandwidth of 1000Hz was claimed by Robinson (1963). As well as embedding the coil into the contact lens, Robinson also attempted to move it onto a scleral ring, fitted in the same way as a contact lens. With an appropriate frequency for the magnetic field a great sensitivity could be achieved for the measurements.

However, one of main sources of error was found to be the leads joining the contact lens coil to the amplifier which could be reduced by tight twisting.

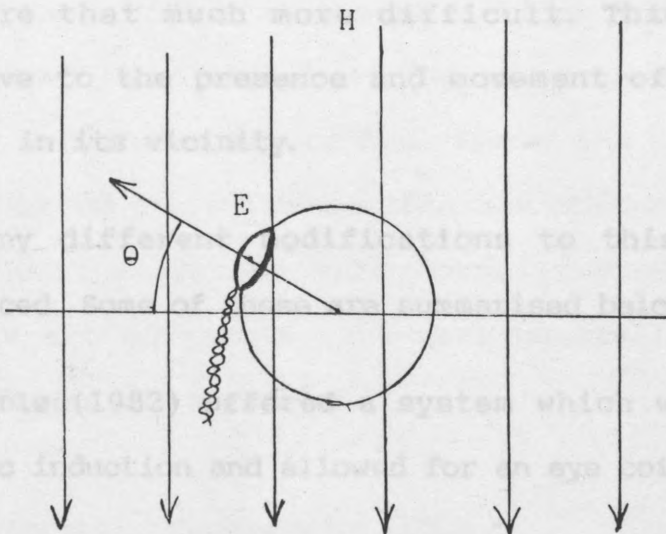


Fig. 5.2 Electromagnetic Contact Lens

Collewijw (1975) replaced the coils in the contact lens by flexible ferromagnetic rings which were fitted onto the limbic area. The ring was cast out of silicone rubber with an induction coil of 9 windings embedded within it. Once placed in the eye, the ring became firmly attached and could only be removed by lifting its edge. Because of the special design of the ring there

were no movements of the ring over the surface of the eye. However, the application of the ring required the use of anaesthetic and the method still involved the attachment of a foreign object to the eye.

Zeevi (1982) used the differential inductance variations of two C-shape coils resulting from the movement of a ferromagnetic ring attached to the sclera. A tuned bridge and a synchronous detector, were also used to attain a higher sensitivity over a wide range of 80 degrees with linearity of ± 4 percent deviation reducing to ± 0.6 percent over the range of 20 degrees.

The two symmetrical coils, wound on the ferromagnetic C-shape cores, had to be about 4mm from the ring which made the procedure that much more difficult. This method was also sensitive to the presence and movement of any ferromagnetic objects in its vicinity.

Many different modifications to this method have been introduced. Some of these are summarised below;

Renleu(1982) offered a system which was based on double magnetic induction and allowed for an eye coil free from leads.

Peters (1982) used a magnetic dipole for measuring miniature eye movements.

Bour (1984) used a polished metal ring, placed on the sclera, to improve the signal amplitude and the patients' comfort.

Stuart (1984) replaced the contact lens coils by a gold foil hooked over the lower lid which therefore had minimal contact

with the inferior limbus area. This was particularly useful when prolonged testing periods of the retinal function was necessary. Furthermore, the electrode was so light, flexible and smooth that it hardly stimulated the corneal nerve endings.

In general, all the contact lens methods requiring attachments to the eye, cause discomfort to the patients and the very tight fitting lenses usually require the application of anesthetic. Barlow (1963), by using after image methods, revealed that scleral fitting contact lenses slipped through several mins. of arc. Although light-weight, suck-on, limbal-seating cups demonstrated much improvement, complete stabilisation could not be relied upon. The frequency response of the system was generally determined by the stability of the lens when following the eye. Fender (1964) estimated that the lens slipped behind the eye by about 1 arc min. for 1 degree of eye movement, and 6 arc min. for 9 degrees. This method offered the best resolution down to 5-10 second arc, although this was achieved at the expense of the range. The systems were normally used for the study of miniature eye movements, but were generally considered to be uncomfortable and expensive.

5.1.12 Electro - Oculography (EOG):

EOG is based on the difference in potential between the cornea and the retina; the cornea is approximately 1mV more positive than the other side of the eyeball (Du Bois - Reymond, 1849).

It was initially considered that these potentials resulted from the action of the eye muscles. However, it is now believed that there is a permanent potential difference between the fundus

and the cornea due to the higher metabolic rate of the retina. This provides an electric field, in the eye tissues, which is displaced during eye movement and can be recorded by electrodes attached to the head. Two electrodes are attached to outer canthi for horizontal measurements whilst a third electrode, attached over the bridge of the nose, measures vertical movements. The nature of the electrical system was described by Mowrer et al, (1936).

The recorded potentials range from 15 to 200uV, with 4uV for every degree of eye rotation. However, these signals are difficult to detect in the presence of large muscle-action-potential artifacts. In addition to these background noises are components produced by the contacts between the electrodes and the skin. The system also requires to be shielded against external electrical interference. Furthermore, EOG is also far from being constant in magnitude, since it is influenced not only by the metabolic state of the eye, but also by visual stimulation. Byford (1963) recorded eye movements simultaneously by electro-oculography and with contact lenses, and concluded that the "Corneo-retinal potentials in no way reflect faithfully the time-course of saccadic movements". He also showed that changes in potential were not always associated with eye movements.

Fisher (1982) used the EOG method, in conjunction with an on-line mini-computer, to automate the recording of eye movements during the reading of text by the subject.

The system works upto ± 90 degrees, over a bandwidth of 0 to 10Hz, but due to the noise level of records taken by EOG, the accuracy is limited to between 1 and 1.5 degrees. However, EOG

has the largest range for eye movement measurements, especially in the vertical direction. Other problems associated with the system are as follows:

- 1) Cross coupling between the vertical and horizontal electrodes.
- 2) The non-linearity of the field.
- 3) The overshoots in the signal due to the motion of the upper eyelid.
- 4) The drift voltage in both electrodes and the d.c. amplifiers during d.c. recording.
- 5) The basic non-linearity after 30 degrees deviation of the eye.
- 6) Variation in light intensities and electrostatic potentials and the patients state of alertness.
- 7) The general background noise due to low voltages.
- 8) The preparation of the patient's skin for electrode attachment.
- 9) The earthing of the body of the patient, usually through his ear.

All the above disadvantages required too frequent calibration of the system (Schlag, 1983).

5.1.13 Impedance Oculogram:

Sullivan & Weltman (1963) introduced an alternative method of electrical measurements of the eye position called impedance oculogram. This system uses skin electrodes to pass small high frequency currents through the eyeball to measure the electrical impedance changes due to eye movements. Its advantage over the EOG method is that it avoids the artifacts of the muscle-action potential.

5.1.14 Photoelectric Methods:

As electrical signals can easily be amplified, displayed and stored, the use of photoelectric cells in the direct-viewing method may prove to be very advantageous.

The sharp boundary between the iris and the sclera (the limbus) is easily identifiable and can be detected optically and tracked by a variety of methods, as discussed below. A dark circle painted on the upper lid, when the eyes are closed, could also provide a clear sharp edge for the photocells.

The entire iris is not always visible since it is partially hidden by the eyelids. For this reason the circumference of the iris cannot be traced and its centre determined; otherwise the tracking would be a relatively simple procedure. Therefore other methods, such as pupil tracking, are necessary to determine its centre.

If only horizontal eye movements are to be measured, the left or the right edge (limbus) of the iris can be detected by either measuring the differential reflected light from a fixed area of the eye, or by tracking the limbus with scanning systems.

For vertical movements, either the level of the eyelid, the pupil position or the vertical motion of a visible part of the limbus can be tracked.

All previous limbus tracking systems measure the position of the limbus relative to the photodetector. In animals, the perimeter of the sclera is generally invisible so that limbus detection becomes a rather difficult procedure. In such circumstances pupil detection becomes a more feasible alternative.

The pupil offers a number of distinct advantages over the limbus. It is smaller and hence unobscured by the eyelids for a greater range of eye movement. Furthermore, if collimated illumination is used, the light reflected from the interior of the eye produces a bright pupil to an observer looking along the illumination axis (Merchant & Morrissette, 1974). This can be used in pupil detection systems for tracking the circumference of the pupil and hence determining its centre for eye tracking. However, although the edge of the pupil is usually crisper and forms a sharper boundary than that between the sclera and the iris, the contrast between the cornea and the pupil is not as great as the contrast between the cornea and the sclera, especially in black-eyed subjects. Hence in scanning methods, the video can not always detect the boundary between the cornea and the pupil. The method is described in detail in chapter 6.

All photoelectric limbus tracking systems use invisible, usually infrared, illumination which does not interfere with the patient's sight or the sensitivity of the system. The results are usually good with a high level of accuracy through a reasonable range. As the output is an electrical signal it may be of high frequency response.

In the pupil detection system, the centre of the pupil is not strictly the optical axis of the eye. However, the deviation of 5 to 6 degrees between the two, can generally be calibrated out. Furthermore, the diameter of the pupil is not constant and may vary as a result of both psychological and physiological influences.

These photoelectric systems are quite simple to set-up and

cause minimum discomfort to the subject. They all share a common disadvantage that head movements, relative to the transducer, will be interpreted as eye rotation.

For example, if the rotational radius of the eye is considered to be 13mm, then a displacement of 100 microns of the head will be read as an angular deviation of 0.5 degree of the eye. This problem could, however, be reduced by using Rashbass & Westheimer's (1960) method and also by using light-weight head attachments.

Photoelectric measurements can be sub-divided into the three following procedures: scanning methods, feedback methods and differential systems.

5.1.14.a Scanning Systems:

This method involves scanning a part of the eye with an electron beam, and observing the changes in the intensity of the reflected beam.

One such scanning method uses a very small spot of light, focused on the subject's retina, which is respectively scanned across the optical disk (Cornsweet, 1958). The reflected light is projected on to a photomultiplier, which translates it into an electrical voltage applied to the vertical amplifiers of a C.R.O. The horizontal sweep of the C.R.O. represents the sweep of the scanning spot. The differential light absorbance of blood capillaries and the white sclera background gives a vertical deflection on the oscilloscope whenever the scanning beam crosses a blood capillary. Hence the distance between the start of the scan and the oscilloscope deflection, due to the presence of a

blood capillary provides a measure of the position of the eye, and any variation in this represents eye movements.

Since an ophthalmoscope is used in this method, a smaller area of the eye is observed, so that the blood capillary is scanned more closely and results in a more accurate measurement.

An alternative scanning method is by using a T.V. system to monitor the position of the limbus, as suggested by Bechai (1977) and as further explained in chapter 6. It is based on the same principles as for the previous method, but the limbus is scanned instead of the blood vessel, and a T.V. camera is used in place of the light beam and the photomultiplier.

In a later section of this chapter a method is described which uses a T.V. camera with an image dissector for precise tracking of the corneal reflex (Ishikawa, 1971).

Another method used by Rashbass & Westheimer (1960) is to simultaneously record both reflected and scattered light from the eye by the use of two photodiodes. The waveform from the diodes, during a single sweep of the light beam generated by an oscilloscope, shows two clearly differentiated components; one is a step, caused by the beam crossing the limbus, whilst the other is a pulse generated when the reflected beam is detected by the photodiode. Under translational movements, both waveforms are equally displaced from the start of the sweep. However, if the eye rotates; the waveforms move relative to one another and give a measure of the rotation of the eye. Although this method allows small head movements, it only has a linear range of about 8 degrees.

In general, scanning methods are very promising since they

have a high level of accuracy without requiring any attachments to the eye or the head, or necessitating any elaborate calibration or modification of the equipment. This method is favoured in our case of tremor measurement and will be later discussed in detail.

5.1.14.b Feedback Method:

Rashbass (1960) also used the feedback technique for tracking the limbus. In this method a spot of light, generated from a C.R.O., is transposed onto the limbus, so that any eye movements either increase or decrease the intensity of the reflected light. This difference of intensity is then used to deflect the spot back onto the limbus, so that in effect the beam follows the movement of the limbus.

5.1.14.c Differential Reflection Methods:

The position of the eye can also be recorded by allowing the moving iris to vary the total light reflected back onto either a single photodiode or, two or more photodiodes. This measurement can be achieved either by using broad illumination with constrained fields for photodetection, or by focusing slits or circles of incident light with broad detection regions onto the eye.

Torok (1951) imaged one half of the eye onto a small horizontal slit placed in front of a photomultiplier. Horizontal eye movements, therefore altered the amount of white sclera visible to the photomultiplier which measured the position and movement of the eye. This simple device, which has a linear range

of only about 10 degrees, can give 10mV degree^{-1} and a time resolution of only about 10ms (Carpenter, 1977).

This crude system can be improved by using infrared instead of visible light which would reduce the effect of ambient light and would not disturb the natural movement of the patient's eye. It can also be improved by using two photodiodes instead of one suggested by Stark & Sandberg (1961) and Brown (1977). The method is based on differential light reflected from the sclera, on either side of the iris. The whole assembly is mounted on goggles worn by the patient, and although this eliminates the need for a head rest, the goggles may obscure the patient's vision. The method also eliminates the requirement of slits. The system has been claimed to have a high sensitivity performance (Findlay, 1974).

Eizenman (1984) used an array of sensor photodiodes to receive reflected infrared light from the eye. Light energy in the 1st Purkinje image, at the sensor plane, was converted to an electric current by a one dimensional array of 18 tightly-packed photo-transistors. Although the system has a low dynamic range, system noise is less than 30 arc-sec. and linearity is $2 \text{ degrees second}^{-1}$.

This method was improved by Jones (1973) and Brown (1980) who carefully positioned the slits of the two photodiodes so that both vertical and horizontal movements could be recorded. The slits were positioned at an angle of 45 degrees to the horizontal, and at right angle to each other. This method eliminates the problem of the upper and lower parts of the limbus being hidden by the eye-lids. The system is relatively accurate and cheap to construct although it requires a sensitive

calibration procedure.

The photoelectric technique was also used by Wheelless (1965) for monitoring horizontal and vertical eye movements. He used fibre optics to focus two horizontal slits on the limbus and two vertical slits on the boundary of the iris and pupil. He also modulated the light from the photodiode by the use of chopper wheels. This light was then demodulated at the same frequency so as to prevent interference from fluctuations in ambient illumination.

Other researchers, such as Comet (1983), also measured eye movements by the same photoelectric method, but this time through a closed eye. Comet used three photodiodes as proximity sensors. A layer of white make-up on the eye-lid was required to give a good reflective area. Corneal movements, behind the eye-lid, altered the distance between the eye-lid and the photodiode, so that the voltage of the photodiode was accordingly altered. This method has been extensively utilized in studies of eye movement using after-image phenomena. It is relatively cheap to use and can measure both horizontal and vertical eye movements although the eye under the test has to be closed. The system is, however, not very accurate or sensitive, with the linear range for horizontal eye movements varying from -15 degrees to +20 degrees, and for vertical movements ranging from -10 degrees to +10 degrees.

Shirley (1980) used a similar method by creating a light-to-dark surface on the eye-lid by the use of a black eye-pencil and a strip of aluminium foil. To overcome the problem of head movements the optical fibre, used to direct the reflected light,

could be attached to the head so as to hang over the eye-lids. Because of the lack of direct contact with the patient's eye, the method did not suffer from any hygiene problem.

5.1.15 T.V. Methods:

The use of television (T.V.) systems for recording eye movements has continually increased over the last few years. It is apparent that the use of video and T.V. circuits has modified and, indeed, simplified almost all the older preceding methods.

Mackworth and Mackworth (1958) employed T.V. techniques to record the position of the patient's eye when focused upon a particular scene. Whilst one T.V. camera was used to view the scene, another camera was used to pick up and magnify, by about 100 fold, the displacement of the corneal reflection of an incident light source. Outputs from these two cameras were combined to give a picture of the scene with a bright light, which indicated the position and movement of the patient's eye, superimposed onto it.

Lewellyn and Thomas (1960) and also Haith (1969) continued along similar lines and eventually developed a method for recording ocular movements in infants. The advantage of their method was that no attachment to the eye or the head was necessary, although the manual measurements of the eye positions were generally cumbersome. A further restriction was that the T.V. cameras had to accept infrared light which was used as the light source.

Ishikawa (1971) used a modified T.V. camera with two types of sweep. The main sweep was the same as a normal T.V., with

312.5 lines per field. The second sub-sweep, was at, or near, the corneal reflection and had a frequency of 15.75KHz. The main sweep was used for monitoring purposes whilst the sub-sweep was used for the accurate measurement of the corneal reflection. The instrument was claimed to instantaneously measure the position of the eye with a linearity of upto ± 15 degrees in both the vertical and horizontal directions. Furthermore, the minimum, detectable eye movement was claimed to be about 0.01 degrees with a frequency of up to 15KHz. However, the high cost of production and the complexity of the instrument limited its widespread use.

Sheena (1973) proposed two digital methods for measuring eye positions. One method was to view the eye with a video camera in which the contrast level had been increased to such an extent that only the black iris and the white sclera were displayed by the monitors. It was further suggested that with the use of mathematical computation circuits the centre of the iris could be located and also the position of the gaze.

The second method proposed by Sheena was to use a standard T.V. camera with suitable contrast and level detection circuits to extract the crossing points between the iris and pupil from the video signal. Digital circuits would then be able to locate the T.V. line which crossed the vertical centre of the pupil. This signal could then be superimposed on the output from a second camera viewing a scene, which represented the subject's point of regard. Unfortunately no data or description of the circuits was provided for either of the methods for further reproduction or analysis.

Monty (1975) also suggested the use of EG & G/HEL oculometer systems, although these may encompass an entire laboratory. For

example, a studio was required to serve as a test room, a camera room was necessary to house both the optical devices for monitoring eye movements and also the apparatus for projecting stimuli, whilst a control room was needed to contain the computers and devices for controlling the experiment. The high cost of the system and the large amount of space required to house the system, limited its use.

Foulds (1981) used a custom-built, charge-coupled device (C.C.D.) video camera, for monitoring eye movements. The C.C.D. camera was placed on a pair of eye glasses to remove the confounding effects of head movements. Furthermore, the main circuits of the camera were connected to the C.C.D. via a light cable, so that the weight of the camera did not pose any problem. An accuracy of ± 0.5 degrees was claimed but, in practice, an accuracy of only ± 2 degrees was achieved.

As discussed in the section on scanning systems, such methods could be expanded to also utilize T.V. systems so as to monitor the rotation of the eye.

Hainline (1981) used a commercially available infrared video eye-movement monitoring system (Applied Science Laboratories, Model 1994), but with extensive modifications to measure eye movement. In this technique corneal reflections are generated by collimated infrared rays reflected onto an infrared T.V. camera. Part of the incident light is also reflected by the retina giving a very bright pupil. As the cornea is a different radius of curvature to the rest of the eye, the reflection from the pupil and the cornea move differentially during eye movement, but together during head movement. The reflections from the pupil and

cornea form an image on the T.V. camera, and from the X and Y positional coordinates of the eye, its movement can be monitored.

Kasai (1982) used C.C.D. cameras to monitor images at 200 frames per second for both eyes. The measurements were of a very high resolution of up to ± 0.06 degrees for methods extracting the pupil edge, ± 0.1 degrees for using binary images and ± 0.13 degrees for detecting the corneal reflections. However, this method, due to complex design modification, was highly expensive to produce and did not use commercially available instruments.

Bechai (1977) used a mathematical model which measured the degree of rotation of an ellipse in space (a projection of a circle), to calculate the extent of movement of the iris or pupil projected onto the face of a very precise video camera. A T.V. line through the centre of the iris was selected and processed through a high-pass filter and a differentiator. A pulse, generated by a level detector, turned a counter on with its leading edge and turned it off with its trailing edge. Hence, the horizontal coordinates for the two points determined the length of the ellipse and so, with the aid of a microprocessor, the degree of movement of the iris could be found.

A few other researchers tried to measure eye movements using the ellipticity of the pupil during eye rotation. The pupil is found to be circular in shape when viewed perpendicularly, but elliptical during eye rotation. Hence by measuring the eccentricity of the pupil, the extent of eye rotation can be determined (Young, 1975).

Robinson (1963) embedded a plane mirror and, in a separate experiment, a search coil in a contact lens and determined their

apparent ellipticity during eye movement. The advantage of both the above methods is that they are only dependent on eye rotation and are independent of head translation.

5.1.16 Conclusions and Summaries:

Despite the large number of different methods surveyed here, and modifications of these methods for measuring eye movements, no single technique can be identified as the most superior, possessing all the advantages of the ideal method, yet lacking all the associated disadvantages. The suitability of the different methods and techniques described above is clearly dependent on the features required from the system. The subsequent paragraphs are the summaries of the performance of these methods (Young, 1975).

Measurement Range was found to be about ± 10 degrees for corneal reflection, contact lens and photoelectric methods. T.V. methods had ranges from ± 10 to ± 30 degrees while E.O.G. methods enjoyed ranges of up to ± 50 degrees.

Accuracy was high (about 3 to 15 seconds) for contact lens methods and for the rest between 1 to 2.5 degrees.

Frequency Response for the T.V. methods was limited by the frequency response of the T.V. frames and, for corneal reflection methods, by the speed of the film. Double Purkinje image methods had a frequency response of as high as 300Hz and for contact lens method was good, depending on the negative pressure between the eye and the lens. E.O.G. frequency response was low, of the order of 0.01 to 15Hz.

Interference with Normal Vision was worst for contact lens method, medium for corneal reflex and photoelectric methods, low for T.V. and double Purkinje methods and no interference was encountered for E.O.G.

Patient's cooperation was essential for contact lens, corneal reflex and photoelectric methods. E.O.G. needed some cooperation and T.V. methods very little.

Training of the Patient was necessary for almost all the methods, especially for the contact lens, but this could not really make a difference to the validity of the tests. Except contact lens and corneal reflex methods, children could be tested on almost all the other systems.

Calibration and Set Up Time was found to be long for corneal reflex, E.O.G. and contact lens, but not so long for the others.

Attachment to the Head or the eye was a bite board or a chin-rest for corneal reflex, double Purkinje, photoelectric and T.V. methods, although for the latter two this could be replaced by spectacles carrying the photodiodes or the video camera. E.O.G. needed electrodes and contact lens method contact lenses.

Head Stabilisation was critical for corneal reflex, contact lens and photoelectric methods. However, E.O.G. and double Purkinje methods did not require this. For T.V. methods a bite board sufficed.

Patient's Discomfort was high for contact lens method, medium for the corneal reflex and low for the rest.

Cost of Operation was high for corneal reflex if hard copy of the results was required. Also for contact lens it could be

high due to the cost of grinding the lenses. Other methods carried very little operating cost.

Young (1975) also remarked that negative pressure for the contact lens method could be hazardous and that the E.O.G. is more suitable for the eye velocity measurements than eye position.

E.O.G. methods of recording eye movements are very commonly used and they satisfy the ideal requirements d, e and particularly h as set out in the introduction of this chapter.

Corneal reflections are generally thought to be good methods but do not satisfy requirements b, d, e and g. Also vertical movements are problematic and impossible for torsional movements. Optical contact lens methods are good when used by experts but require rigid optical alignment for general use.

As photoelectric methods are now commercially available they are becoming increasingly popular and they satisfy requirements a, c, g and h. T.V. methods are rather new and still in the developmental stage. They satisfy all the requirements mentioned in the introduction with the exception of e, f and g. However, with some modifications, they could also measure vertical eye movements.

In this survey it is evident that the two methods with the most potential for further research are the T.V. and photoelectric methods. They are capable of providing tests with minimum discomfort to the patient leading to true results obtained under normal and relaxed conditions.

5.2 Initial Design Consideration

In the last section the extent to which research was conducted into the recording of eye movements, was demonstrated.

Here, it was envisaged to design a system which, with minimum cost and simple circuits, would record the eye tremor movement whilst the relative Hess chart test was being performed. Hence, the environmental condition of the latter test should also be made adequate for the detection of eye tremor. Listing some of the initial design considerations, would be as follows:

1. In the last section it was shown that one of the most suitable and attachment-free methods of detecting eye tremor was using a T.V. camera. The contrast between the luminance of the iris and the sclera was particularly of interest when using a black and white video system.

2. As the direction of gaze was to be determined by the relative movement test, the main objective of the tremor movement test was to detect the amplitude and the frequency of the tremor.

3. As explained in the last section, nystagmus is characterised as a saw-tooth pattern of eye movements with finite amplitude and frequency. Changes in direction of gaze would cause changes in nystagmus amplitude and therefore, it would be of the utmost interest to ophthalmologists to be able to measure nystagmus amplitude and frequency at different positions of gaze where the relative movement test is done, i.e. at the direction of each square dot.

4. As the nystagmus amplitude was considered to be more than one degree of eye rotation, the system was to be able to detect

at least $\frac{1}{2}$ degree oscillations without any difficulties.

5. As far as possible it was intended not to make any electrical and mechanical modification to the external equipment used. However, if such a modification were necessary this was to be kept to its minimum for obvious reasons. Although changes in the frame or line frequency of the video signal improved the results, due to high cost this was not considered.

6. The relative eye movement test was to be conducted under normal lighting conditions. In practice the available amount of light directed onto the patient's face during the test was to be the illumination radiated out of the blank monitor due to its raster, where the light pen is situated. Fortunately, the patient would be facing this monitor directly and not through the mirror. Therefore, the raster of the blank monitor should be bright enough and the camera, hidden behind the instruments, sensitive enough to be able to pick up the necessary signals for detection of tremor.

7. As the tremor measurements are to be made in the direction of each square dot, the tremor system was to be designed so as to enable detection when the direction of gaze is at ± 30 degrees horizontally and ± 20 degrees vertically.

8. A similar design consideration to the relative movement system was the question of available space in hospitals. The intention was to be able to detect nystagmus and record the result without extending the size of the system to more than an ordinary desk. This was to be achieved by situating the camera under the chart monitor and keeping the designed hardware to its minimum.

9. The use of a laser was not favoured because of its unknown side effects to the eye, and its dislike by the patient. 90% of laser light is absorbed by the cornea (Riva, 1979).

10. The distance between the camera and the eye was to be such that the camera would not interfere with the vision and possibly be even hidden away, and that the image of the eye should be large enough not to decrease the sensitivity of the system. Possible use of zoom lenses was also to be considered.

11. The duration of the test is dictated by the time taken to conduct the relative movement test because both are conducted concurrently.

12. The designed system should be linear for measurements at different directions of gaze.

13. It should also be a stable system with variable sensitivity.

14. As in the relative eye movement measurement a chin rest was to be used. Here the condition of the head to be fixed was also necessary.

Other considerations are to be discussed later, as their importance and applications become more apparent.

5.3 Introduction to the Automated System

Psychologists believe that most human beings will be more conscious when observed directly and may act differently to when they are in a natural environment without any external interference. This means that for obtaining true results on eye

movements, the patient must be totally unaware of the test which he is undergoing. Hence, looking back to the methods described in section 5.1, one cannot fail but to recognise that the T.V. method was the most suitable way to observe, detect and record eye movements without attracting the attention of the subject.

Using a T.V. camera to detect and measure Nystagmus had the advantage of not connecting any electrode to the patient's head or any attachment to the eyeball and performing the test under normal lighting conditions. These are important factors for detecting eye tremor, without creating an artificial situation which deters the patient from behaving naturally. The use of a hidden T.V. camera will certainly provide the best means for a quick test and without too many calibration procedures.

The aim in this part of the research was to utilise a T.V. camera for this purpose and keep the instrumentation simple and without major modifications to the commercial components used.

Another objective was to perform the test whilst the relative movement test was being made. In this way the patient would be busy concentrating on the latter one and would not notice the procedure of the tremor detection test. This also would help in keeping the whole instrumentation as compact, and the cost of production as low as possible, especially where almost all the previous approaches in T.V. tremor detection have been either costly or required the use of one or two rooms.

Although, T.V. methods were not as accurate as some other methods, such as Double Purkinje Image, for the purposes of recording nystagmus, they have proven to be more than adequate. Most nystagmus measuring instruments have an accuracy of one

degree or less (Mellers, 1980) so the instruments were to be designed for an accuracy of ± 0.5 degree eye rotation. Close-up lenses were also to be used to improve accuracy and minimise the effect of noise in the video circuits. Here, it was intended to facilitate the recording of eye tremor or nystagmus in all directions of gaze, and the Hess chart was to be used to record this at 5 degree steps of eye rotation in all four directions from the primary position.

In T.V. methods physical characteristics of the eye must be used to measure eye movements (section 1.4). The limbus is the most distinct feature of the eye which clearly shows eye movements and its contrast and size remain very much the same between different people. This landmark was to be used in search of eye movements.

The eye was to be observed by a T.V. camera and the picture was to be displayed on a T.V. monitor. To be able to detect the position of the limbus and track its movement accurately, the area of sensitivity for detection was to be confined to a very small part of the video waveform. The horizontal position of the limbus was to be determined by the horizontal sweep of the T.V. line crossing the centre of the iris. The time from the beginning of the line or sweep to the limbus is a measure of the horizontal position of the eye. To improve the accuracy of this measure the time was not to be measured from the start of the sweep but from the beginning of a generated "Data Allow" (A short horizontal white line) which is shorter than a T.V. line (64us) and is placed manually over the line crossing the centre of the iris (Fig. 5.3).

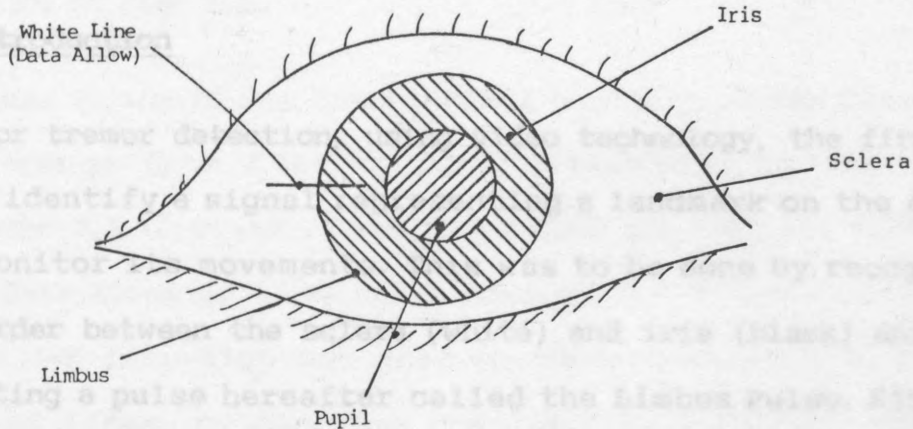


Fig.5.3 A Human Eye together with the Data Allow

Three potentiometers were to be used in placing the Data Allow. Two of the potentiometers were to control its horizontal and vertical position and the third one was to control its length.

Any movement within the cross section of this white line (Data Allow) would be measured relative to a fixed point (the beginning of the Data Allow) and hence the waveform of the eye movement was to be plotted on a moving graph paper. From this plotted curve the amplitude and the frequency of any nystagmus was to be measured. This of course would only give the measurement of horizontal nystagmus and not of the vertical or oblique ones. However, nystagmus usually appears in the horizontal direction and hence most nystagmometers are designed accordingly (Barber, 1980).

Another specification for the Data Allow was the ability to be moved vertically and horizontally so that it could be placed over the limbus of the eye. Also its length was to be made variable so as to increase the detection sensitivity, without the

CHAPTER 6 HARDWARE DESIGN

6.1 Introduction

For tremor detection, using video technology, the first step was to identify a signal representing a landmark on the eye and then monitor its movements. This was to be done by recognising the border between the sclera (white) and iris (black) and hence generating a pulse hereafter called the Limbus Pulse. Since the eye movement was represented by the movement of the limbus pulse, this was to be monitored and recorded.

In this chapter, after the generation of the Data Allow signal, the use of the limbus pulse and three methods of processing the analysis of its position (or its tracking) are discussed and the design adopted described.

6.2 Data Allow Generation

As explained in the previous chapter the Data Allow line was white a line on the T.V. screen which allowed the video information to pass through to the tremor detection circuits.

Any change of waveform during the Data Allow was detected in the circuit to be explained later. Due to the design characteristic of this detection circuit the Data Allow had to be very stable.

Another specification for the Data Allow was the ability to be moved vertically and horizontally so that it could be placed over the limbus of the eye. Also its length was to be made variable so as to increase the detection sensitivity, without the

danger of going over the range of the Data Allow. The circuit for the generation of the Data Allow is in Fig. 6.1 and its waveforms are shown in Fig. 6.2.

Timer T_1 would set the vertical position of the Data Allow with a range from 64 μ s to 20ms determined by its timing components R & C. Timer T_1 would not give the vertical coordinate of the Data Allow in terms of "number of lines" but in "seconds". Hence a J-K flip-flop was used to convert this given time to number of lines, by clocking the J-K flip-flop with the line drive waveform, so that the trailing edge of the vertical delay T_1 was for example either at the beginning of line 128 or line 127 and not somewhere in between the two. (All 558 timers needed a 2 K-ohms pull-up resistor).

The output of the J-K flip-flop was then fed into a second timer T_2 to set the horizontal coordinate from the beginning of the line to the start of the Data Allow. This was variable from 0 to 64 μ s with the use of variable timing components.

Because of the design of the tremor circuit, the length of the Data Allow would affect the sensitivity of the test. Therefore, for optimum performance, the length of the Data Allow was made to be variable. This alterable length helped in adjustment according to the size of the eye appearing on the T.V. screen. Timer T_3 was to set this length.

If the eye tremor was a measure of the time between the beginning of the Data Allow and the limbus pulse, then the stability of the Data Allow waveform was critical to the accuracy of the results. Timers 558 were tested and proved to be stable enough, however, the first timer T_1 was set in the order of

milli-seconds (for a maximum of 20ms), therefore the amount of instability, when T_1 was at its maximum, was very high compared to the values of T_2 and T_3 which were set in the order of nano-seconds and micro-seconds.

This was overcome by using the J-K flip-flop as a buffer stage between T_1 and T_2 timers. Although the output of T_1 suffered from instability, the flip-flop was only to be set by this output and reset by the line drive, thus the trailing edge of the Q-output of the flip-flop was as stable as the line drive which was generated by the central sync. generator chip.

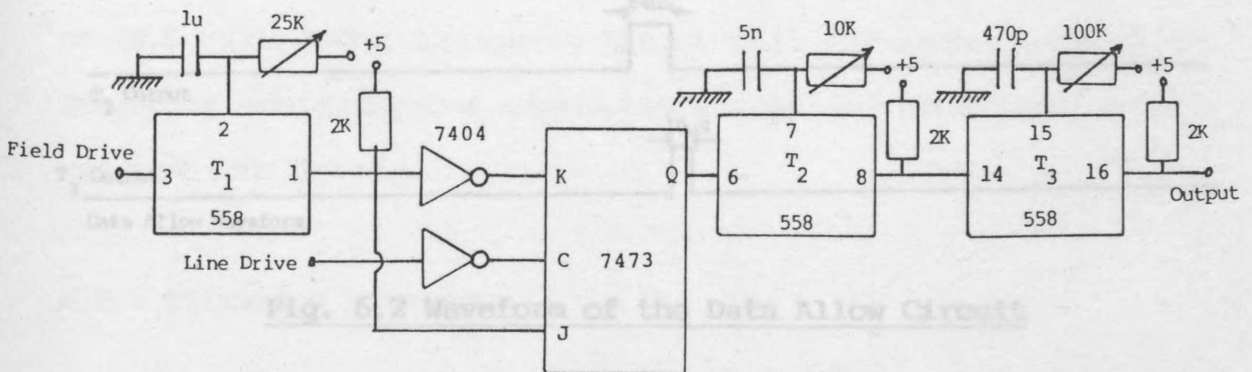


Fig. 6.1 DATA ALLOW Circuits

Through experiment it was discovered that if T_1 , T_2 and T_3 were all on a single chip, the instability of T_1 was transferred to T_2 and T_3 internally hence giving a very unstable Data Allow. Thus a separate timer chip was used for T_1 which stopped it interacting with the functioning of T_2 and T_3 . This produced a very stable T_2 and T_3 , hence producing a stable Data Allow waveform (Fig. 6.2).

6.3.1 Digital Methods:

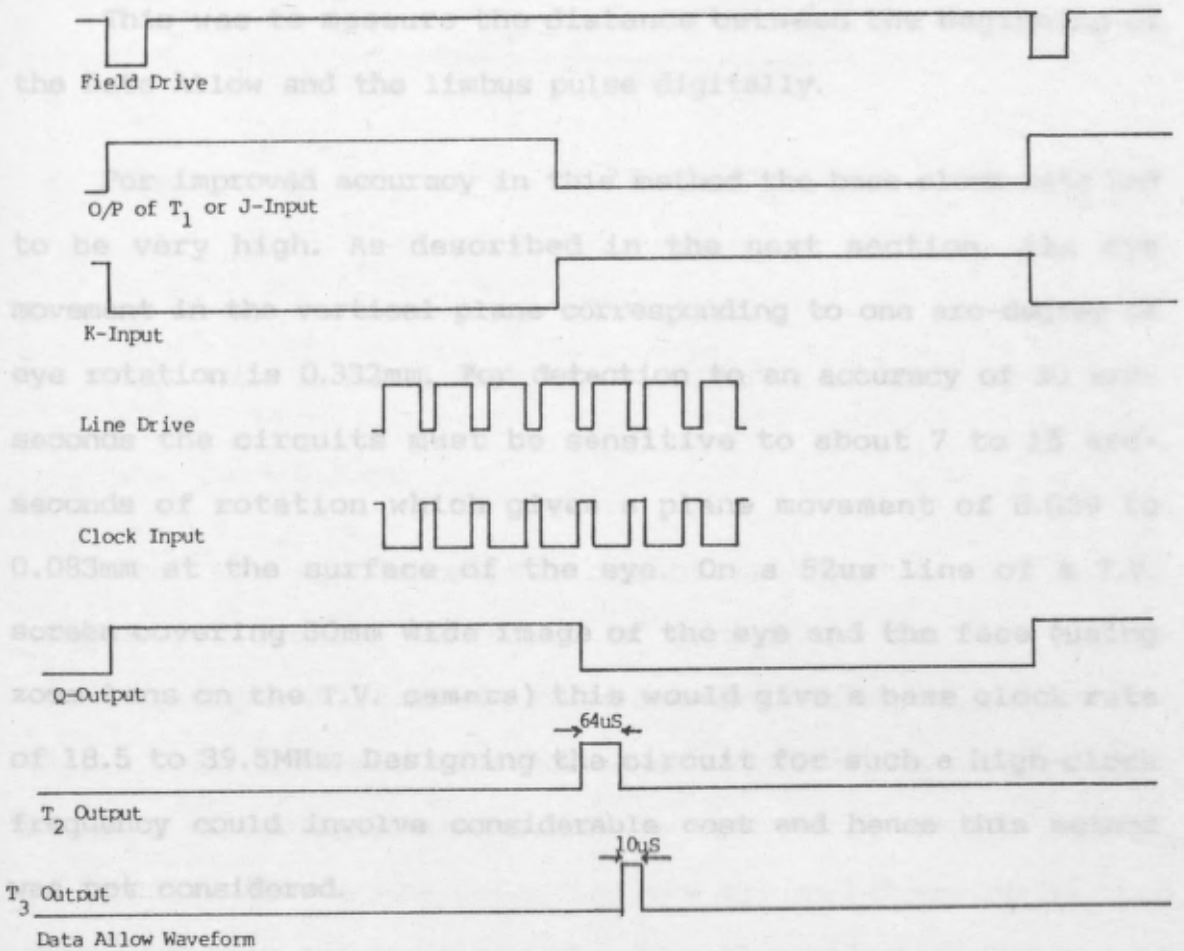


Fig. 6.2 Waveform of the Data Allow Circuit

6.3 Design Concept

As already explained in section 5.3, the idea was to generate a pulse from the limbus of the eye so that by the movement of the limbus the pulse would also move. This was done by recognising the limbus and hence generating the Limbus Pulse. After this generation the task of extracting the amount of movement from the limbus pulse is discussed under the following three categories:

6.3.1 Digital Methods:

This was to measure the distance between the beginning of the Data Allow and the limbus pulse digitally.

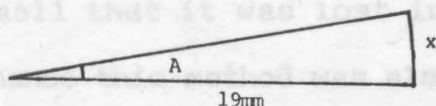
For improved accuracy in this method the base clock rate had to be very high. As described in the next section, the eye movement in the vertical plane corresponding to one arc-degree of eye rotation is 0.332mm. For detection to an accuracy of 30 arc-seconds the circuits must be sensitive to about 7 to 15 arc-seconds of rotation which gives a plane movement of 0.039 to 0.083mm at the surface of the eye. On a 52us line of a T.V. screen covering 80mm wide image of the eye and the face (using zoom lens on the T.V. camera) this would give a base clock rate of 18.5 to 39.5MHz. Designing the circuit for such a high clock frequency could involve considerable cost and hence this method was not considered.

6.3.2 Filtering Methods:

Another way of extracting movement information from the limbus pulse was to use filters. The pulse generated at the limbus of the eye was repeated every 20ms (one field). Assuming that the frequency of Nystagmus of the eye was in the order of 5Hz, then these narrow pulses were varied in width by a few nano-seconds at that frequency. Using a band-pass or a low-pass filter one was able to measure the amplitude of the 5Hz component and hence the movement of the eye.

The radius of the rotation of a human eye is 19mm and if the eye moves 1 degree, then the eye has moved in its plane by about 0.33mm.

the Limbus Pulse changed by 57ns (0.0003% of the 20ms field). This change was so small that it was lost in the noise at the output of the filter.



6.3.3 Tan A = $\frac{x}{19}$ \therefore Tan 1 degree. = $\frac{x}{19}$

In this method the movement of the limbus in 19ms was converted into voltage using a Sample & Hold circuit. \therefore $x = 19 \text{ Tan } 1 \text{ degrees}$ when A is small with a ramp which was generated by integrating the 50Hz wave. \therefore $x = 0.33\text{mm}$ (length of the Data Allow) gives the full

range of voltage at the output of the Sample & Hold. When the eye moved for one cycle the T.V. system had completed 5 cycles. Therefore in each field the T.V. system should recognise 1/5 of the total movement of the eye which was (1/5 x 0.33) 0.066mm. In other words 0.066mm was the maximum movement of Nystagmus that had to be measured by the T.V. system. If the T.V. camera was observing the eye and covering an area 60mm wide then one could say that 52us (the effective length of a T.V. line) was covering 60mm, thus:

The percentage of movement of the eye in the T.V. system was much greater in this method. Thus it was chosen as the method to detect the Nystagmus. The method is explained fully in section 6.4.

$$\frac{60\text{mm}}{0.066} = \frac{52 \times 10^{-6} \text{ s}}{x = 5.72 \times 10^{-8} \text{ s}}$$

This was the corresponding movement of the eye on the T.V. system in terms of seconds. But using filters meant that the amplitude of the 5Hz component was sampled every 20ms which was once every field, thus:

$$\frac{20 \times 10^{-3} \text{ s}}{5.72 \times 10^{-8} \text{ s}} = \frac{100\%}{x = 0.000286\%}$$

This was a very small percentage of the amplitude for the measurement by the filter method, which meant that the width of

the Limbus Pulse changed by 57ns (0.0003% of the 20ms field). This change was so small that it was lost in the noise at the output of the filter hence this method was also not considered.

6.3.3 Analogue Methods:

In this method the movement of the Limbus in terms of time was converted into voltage using a Sample & Hold circuit together with a ramp which was generated by integrating the Data Allow waveform. Since 10us (length of the Data Allow) gives the full range of voltage at the output of the Sample & Hold, this reduced the period in which the limbus movement was sampled to only 10us as oppose to 20ms of the field in the previous method. The Sample & Hold circuit held the sampled voltage for 20ms until the next Limbus Pulse appeared. Hence, if the length of the Data Allow was 10us:

$$\frac{10 \times 10^{-6} \text{ s}}{5.72 \times 10^{-8}} \times 100\% = \underline{x = 0.572\%}$$

The percentage of movement of the eye in the T.V. system was much greater in this method. Thus it was chosen as the method to detect the Nystagmus. The method is explained fully in section 6.4. This entailed producing a pulse (limbus pulse) the leading edge of which was at the same position as the leading edge of the Data Allow line. The position of this edge was constant and the trailing edge of the limbus pulse was the position of the limbus itself which moved due to Nystagmus (shown in Fig.6.3).

The construction of such a pulse could prove to be difficult since the recognition of the limbus (which is an area of transition between two colours fading into each other) from a

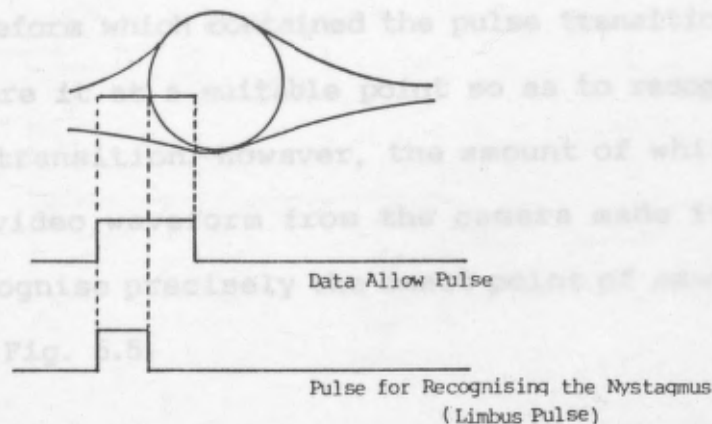


Fig. 6.3 Data Allow and Measuring Pulse.

video waveform was not easy. This is because the edge of the pulse produced by the limbus is not relatively fast enough and also there is too much noise in the video waveform.

One way of recognising the limbus was to differentiate the video waveform so that spikes were produced from the fast transitions in the waveform. The circuit in Fig. 6.4 was tested for this method but proved to be inadequate. Differentiation unlike integration is a noise amplifying process. Also an ideal differentiator as shown in Fig. 6.4 was far different to a practical differentiator (Clayton, 1979).

For the reasons stated above, the differentiation method was not reconsidered because the video waveform out of the camera was already too noisy and any more amplification would hamper the recognition of the limbus.

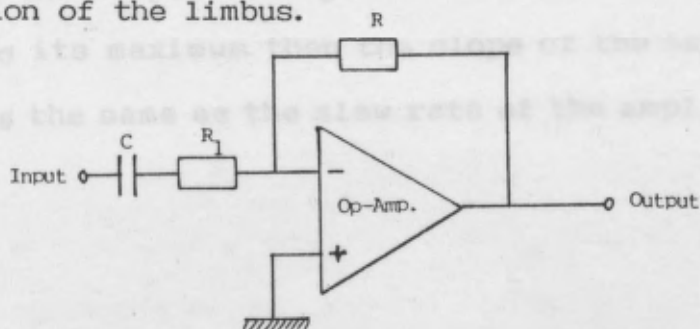


Fig. 6.4 A Differentiator

Another simple method was to raise the voltage of that part of the video waveform which contained the pulse transition of the limbus and compare it at a suitable point so as to recognise any movement of the transition. However, the amount of white noise sitting on the video waveform from the camera made it rather difficult to recognise precisely the exact point of sampling by the comparator. Fig. 6.5.

To overcome this problem one could amplify the video waveform to clip* both at top and bottom of the waveform and hence increase the slope of the transition due to the limbus. Also a comparator could be designed having a positive feedback to act like a Schmitt trigger.

The results of the above two methods are shown in Fig. 6.6 (a) & (b). The waveforms shown were recorded when the eye was stationary and the variations were simply due to the noise of the video waveform from the camera being transferred through the system.

Another problem considered was that the system was to be designed for the Data Allow to be placed over the limbus to the right of the eye. Then the transition of the video waveform, due to the limbus, was negative going. If, however, the Data Allow

* Because the output voltage of the amplifier jumped from its minimum to its maximum then the slope of the transition of the limbus was the same as the slew rate of the amplifier which was 9V/us.

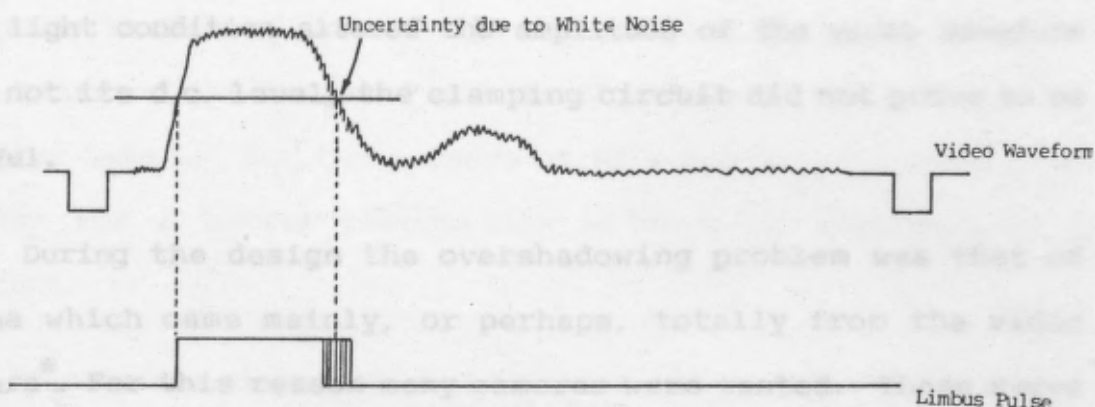
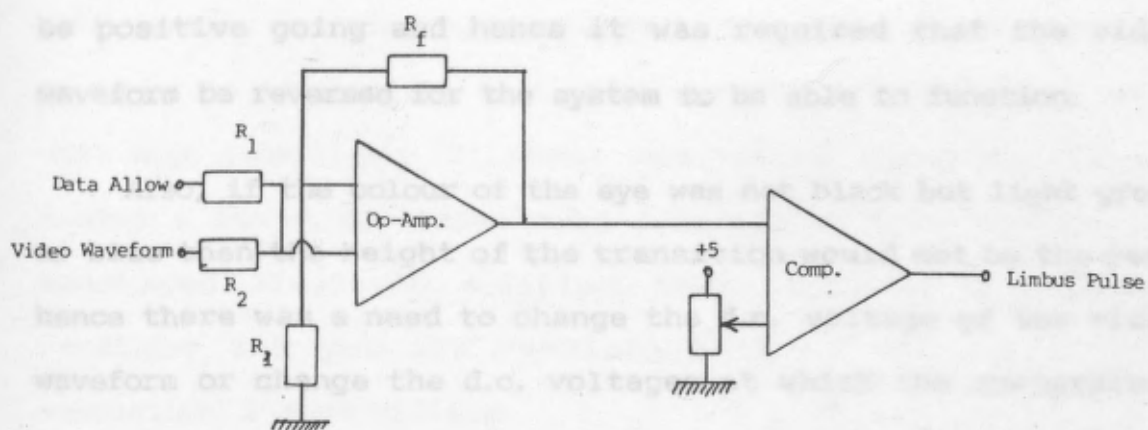


Fig. 6.5 Noise Problem Illustration

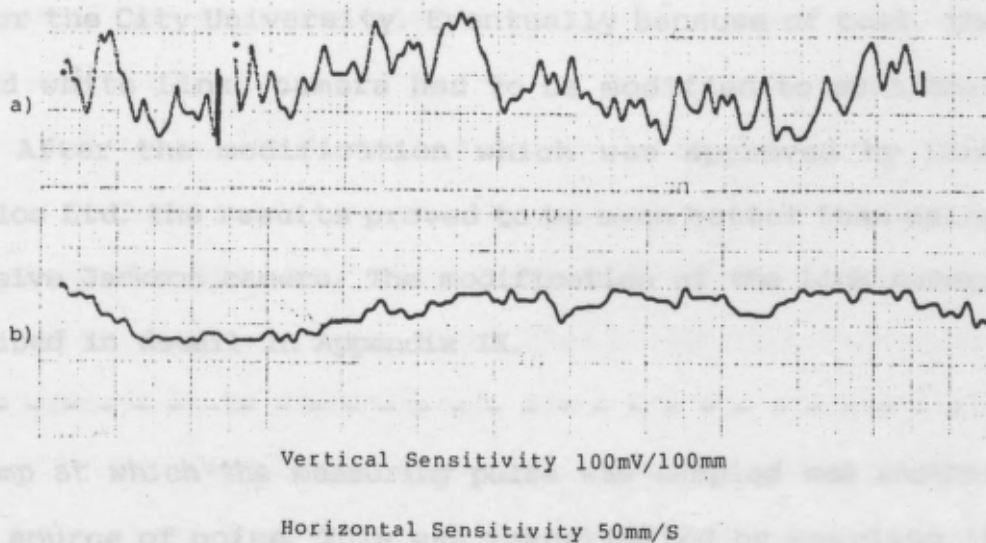


Fig. 6.6 The Noise of the System when:

- Amplification Method was used.
- Comparator with Positive Feedback was used.

was to be placed at the left of the eye then the transition would be positive going and hence it was required that the video waveform be reversed for the system to be able to function.

Also, if the colour of the eye was not black but light green or blue then the height of the transition would not be the same hence there was a need to change the d.c. voltage of the video waveform or change the d.c. voltages at which the comparators were sampling. The use of a clamping circuit was considered. However, since the change of colour of the eye or the change in the light condition altered the amplitude of the video waveform and not its d.c. level, the clamping circuit did not prove to be useful.

During the design the overshadowing problem was that of noise which came mainly, or perhaps, totally from the video camera*. For this reason many cameras were tested. These were; Link type 109B, black and white Sony AVC3250CE, Marconi V-00-3305-01, colour J.V.C. KY1900 and a specially designed Jackson camera for the City University. Eventually because of cost, the black and white Link camera had to be modified to suit this project. After the modification which was approved by Link Electronics Ltd. the results proved to be even better than using an expensive Jackson camera. The modification of the Link camera is described in detail in Appendix IX.

* The ramp at which the measuring pulse was sampled was another possible source of noise. This was investigated by sampling it against an artificial digital pulse representing the limbus. The ramp was found to be extremely stable and no noise was detected at the output of the system.

The use of different video camera tubes made some contribution in reducing the noise in the video waveforms. Also in order to perform the test under normal light conditions tubes with high sensitivity (Silicons) were tested. Among the vidicons tested a newly developed tube (Chalnicon) from Toshiba was considered. Similar to a Silicon tube, Chalnicon is extremely sensitive and yet its resolution is as high as a 'high resolution' 1-inch vidicon.

In the final design provisions were made for a U-Matic video recorder to be used in order to record the eye movements. This was to obtain the frequency and the amplitude of the Nystagmus at a later date or, for the purpose of this project, to modify the design for a better recognition without the presence of a patient.

The system designed would attain its objectives with the help of video field syncs. and line syncs. waveforms out of a T.V. sync. generator. These syncs. also drove the video camera which observed the eye movements. If the eye movements were to be recorded and analyzed at a later date, then either the sync. generator had to be synchronised to the video player or the syncs. were to be recorded on the tape at the time of recording the eye movements. Two sound channels on the video recorder were considered for this purpose, but their limited frequency bandwidth proved to be insufficient. Hence the eye movement was recorded with the Data Allow line superimposed on the picture. Then the Data Allow waveform was extracted from the recorded video and was used to synchronise the system to the video recorder. The amount of noise introduced due to the video recorder is illustrated in Fig. 6.7.

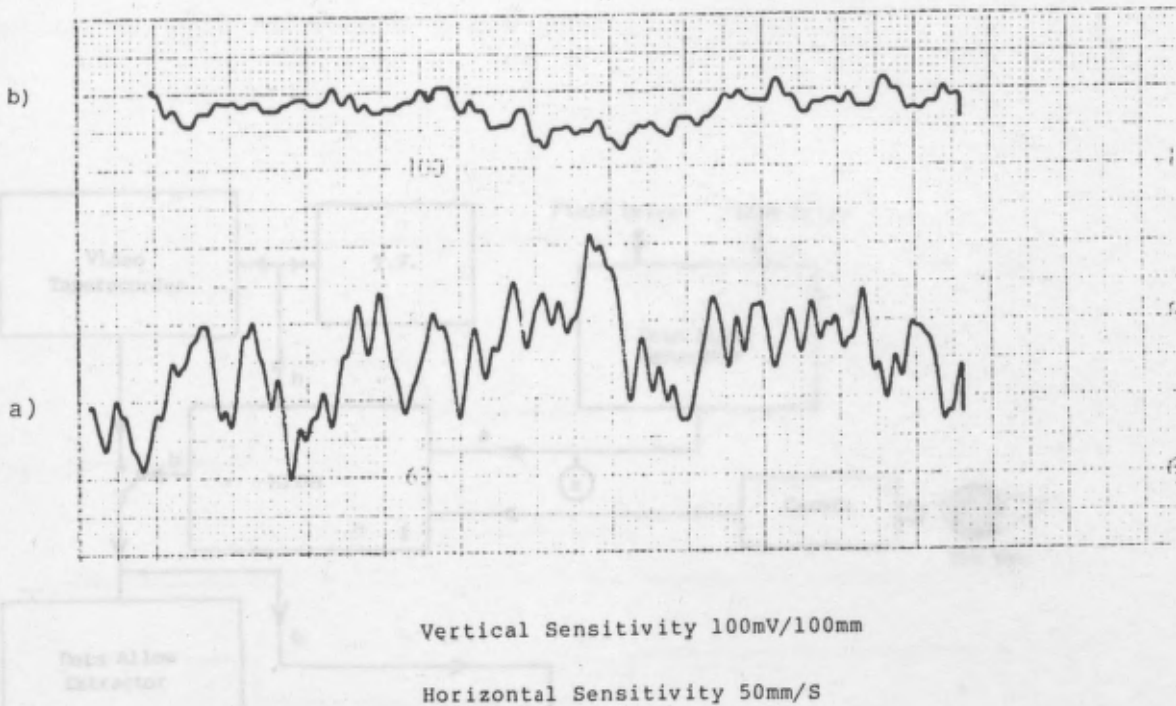


Fig. 6.7 Comparison of Noise When There is No Eye Movements:

a) With the Video Recorder

b) Without the Video Recorder

6.4 Adopted Design

The designed system for detection of the eye tremor is illustrated in Fig. 6.8 and its respective waveforms are shown in Fig. 6.9.

The Data Allow waveform was generated using the Field and the Line Drive waveforms as explained in section 6.2. The Data Allow was then mixed with the video waveform from a camera directed at an eye (waveform 'b', Fig 6.9). This mixed waveform was then fed to a T.V. monitor for observing and controlling the position of the Data Allow over the image of the eye. It was further fed to a video taperecorder in order to record the

movements of the eye together with the Data Allow waveform. This allowed the detection and measurement of nystagmus for future experiments. Waveform 'b' (Fig. 6.8) was also fed to an analogue switch as well as a Data Allow extractor circuit.

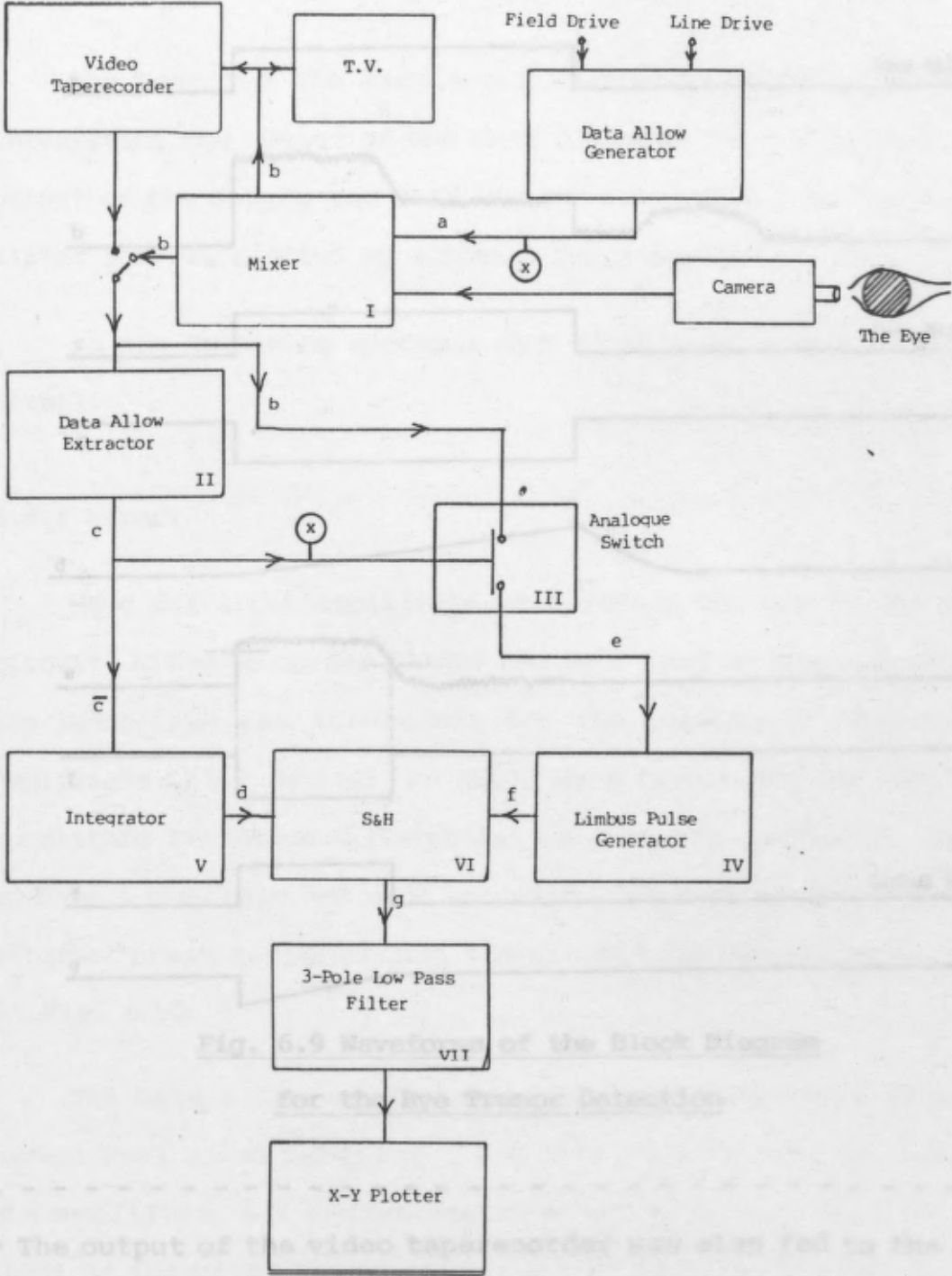
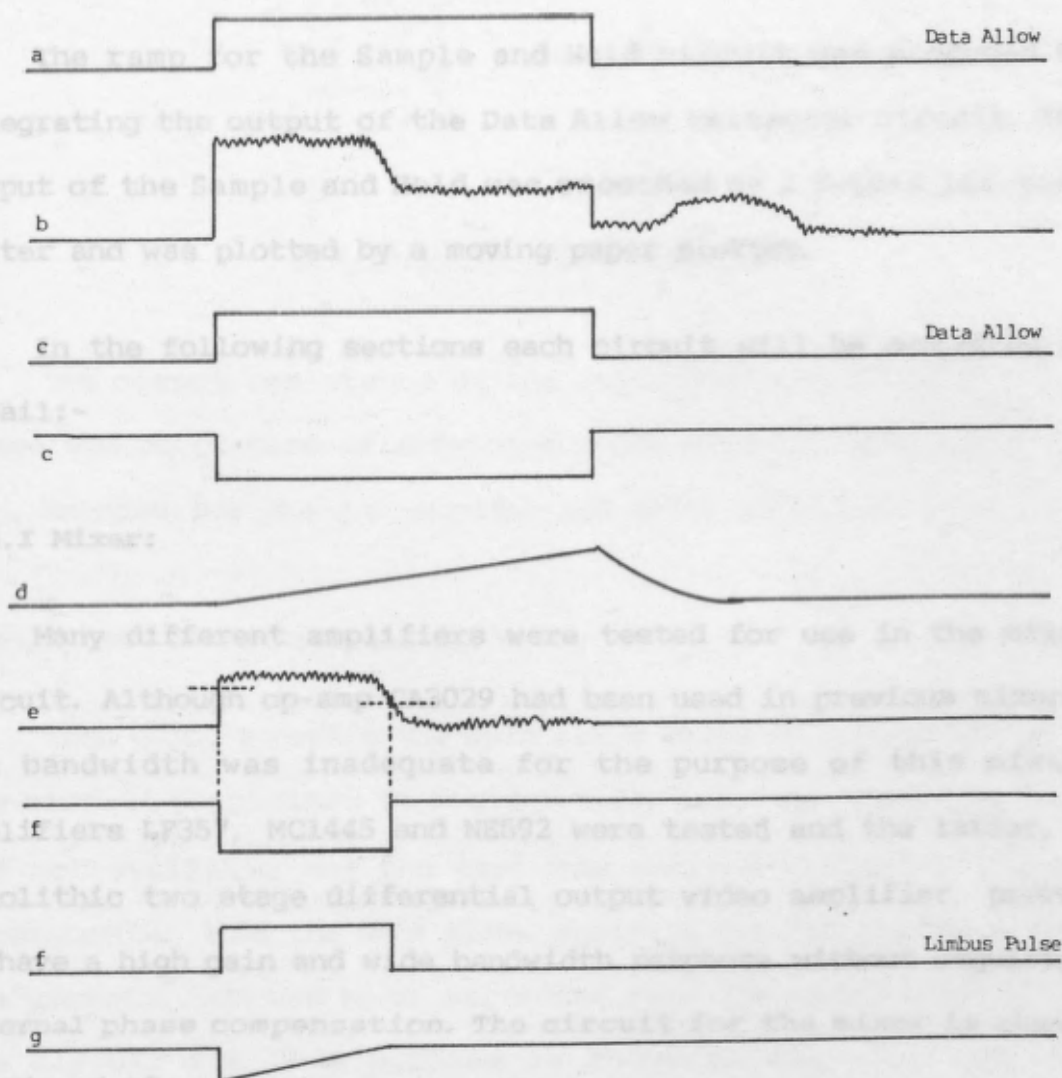


Fig. 6.8 Block Diagram for the Eye Tremor Detection

movements of the eye together with the Data Allow waveform. This allowed the detection and measurement of Nystagmus for future experiments. Waveform 'b' (Fig. 6.8) was also fed to an analogue switch as well as a Data Allow extractor circuit.*



**Fig. 6.9 Waveforms of the Block Diagram
for the Eye Tremor Detection**

* The output of the video taperecorder was also fed to the Data Allow extractor circuit when the camera was switched 'OFF' and the taperecorder was providing the video waveform.

Once the Data Allow was extracted it was used for switching the mixed waveform 'b' "ON" during its period and "OFF" for the rest of the field. This produced a video waveform with a duration the same as the Data Allow (waveform 'e') and in turn was fed to a circuit to produce a limbus pulse for use in the Sample and Hold circuit.

The ramp for the Sample and Hold circuit was produced by integrating the output of the Data Allow extractor circuit. The output of the Sample and Hold was smoothed by a 3-pole low-pass filter and was plotted by a moving paper plotter.

In the following sections each circuit will be described in detail:-

6.4.I Mixer:

Many different amplifiers were tested for use in the mixer circuit. Although op-amp CA3029 had been used in previous mixers, its bandwidth was inadequate for the purpose of this mixer. Amplifiers LF357, MC1445 and NE592 were tested and the latter, a monolithic two stage differential output video amplifier, proved to have a high gain and wide bandwidth response without requiring external phase compensation. The circuit for the mixer is shown in Fig. 6.10.

The Data Allow waveform and the video waveform from the camera were mixed using two 3.4 K-ohms resistors at the input of the amplifier. A 1 K-ohms resistor was used to adjust the d.c. level of the mixed waveform. Using a 20 K-ohm variable resistor the gain of the amplifier could be changed from 0 to 400. This resistor was adjusted for a suitable gain so that the Data Allow

in the mixed waveform was just before clipping. The output was also inverted and fed to the integrator circuit.

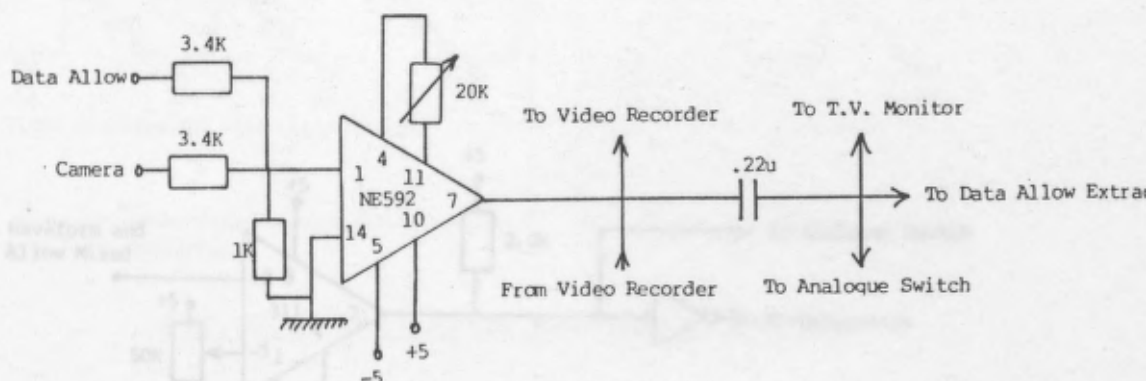


Fig. 6.10 The Mixer Circuit

The output resistance of the amplifier was 20 ohms, hence there was no problem of driving a video recorder. The output was a.c. coupled for the T.V. monitor and other circuits.

6.4.II Data Allow Extractor:

When using a camera the Data Allow waveform was generated by its circuit (explained in section 6.2). However, when a patient was not available and the test was carried out using a video taperecorder, then the Data Allow waveform was not available from its circuit* and had to be extracted from the video recordings. The circuit for this purpose is shown in Fig. 6.11 and its waveforms are shown in Fig. 6.12.

For this purpose an LM311 voltage comparator was used with a pull-up resistor of 2.2 K-ohms. The output of the comparator was

* Because the Data Allow Generator was not synchronous with the output of the video taperecorder.

fed to the logic input of the Analogue switch. The output was also inverted and fed to the integrator circuit.

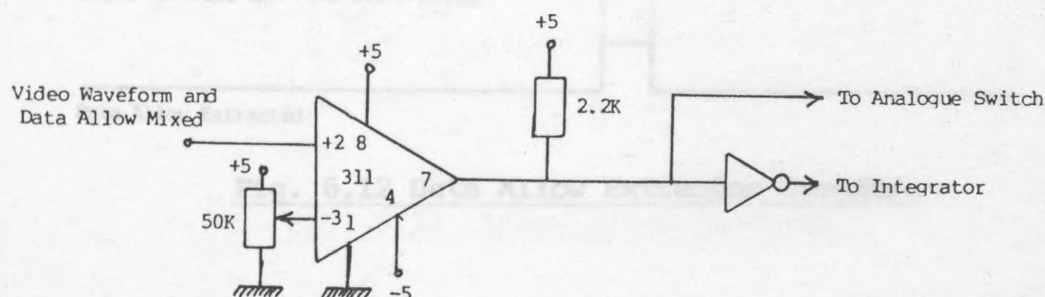


Fig. 6.11 Data Allow Extractor

6.4.III Analogue Switch

The purpose of this switch was that any bright spot on the T.V. screen (sometimes due to reflection of light in the eye or cornea reflections) would not be processed for tremor detection and only the information during the Data Allow would be processed*. When the test was being carried out live, the signal for opening and closing the analogue switch was provided by the Data Allow Generator by linking points X in Fig. 6.8. But when the video waveform was provided by the video recorder and not the camera then the link between points X was broken and the Data Allow Generator provided the input signal to the switch. In this case the analogue switch could not act as a safety circuit any

* Any bright spot on the T.V. screen corresponds to a high voltage section of the video waveform. Hence this high amplitude video waveform could be incorrectly recognised as the position of the limbus in the Limbus Pulse Generator circuit.

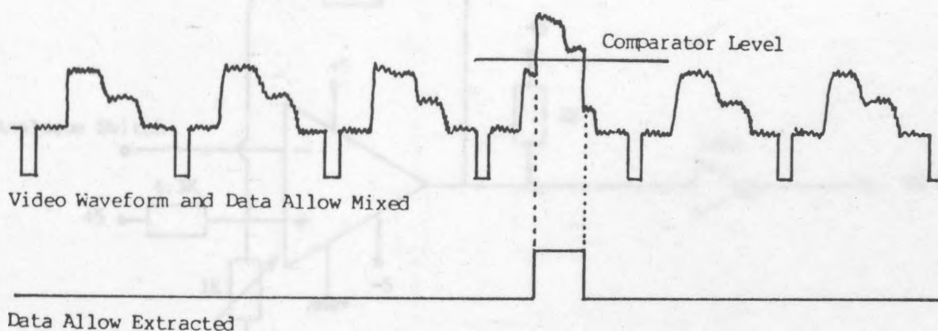


Fig. 6.12 Data Allow Extractor Waveform

more. However, in practice this did not cause a major problem and the bright spots did not affect the operation of the circuit.

An analogue switch type DG200 was first used. Its switching time was $1\mu s$ which was too long compared to a $10\mu s$ Data Allow. Hence a faster analogue switch type TL610 with a switching time of only $100ns$ was finally used.

6.4.IV Limbus Pulse Generator:

The Limbus Pulse is a pulse the leading edge of which was set at the same position as the leading edge of the Data Allow line. The trailing edge was the position of the limbus on the T.V. screen.

The circuit to produce the Limbus Pulse is illustrated in Fig. 6.13, and its waveform in Fig. 6.14.

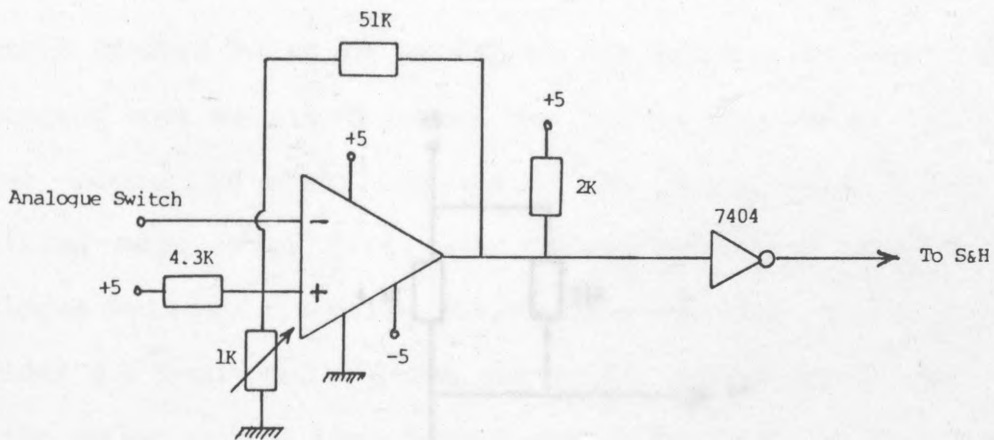


Fig. 6.13 Limbus Pulse Generator

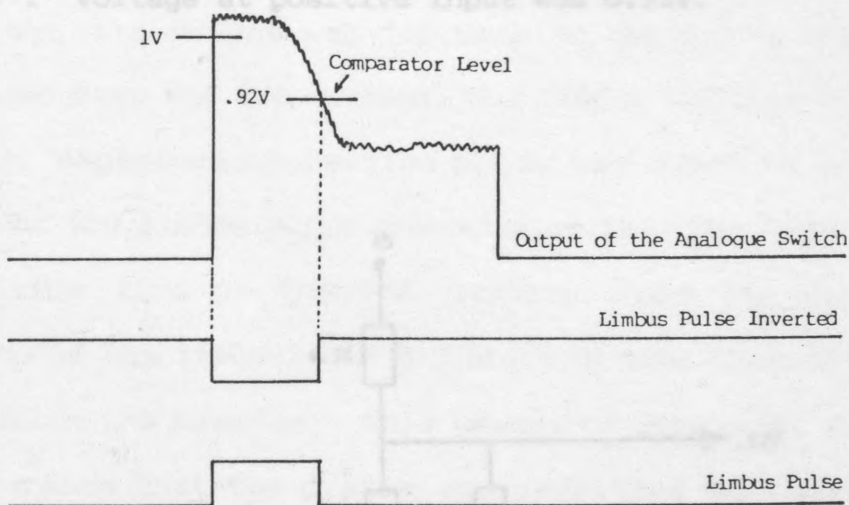


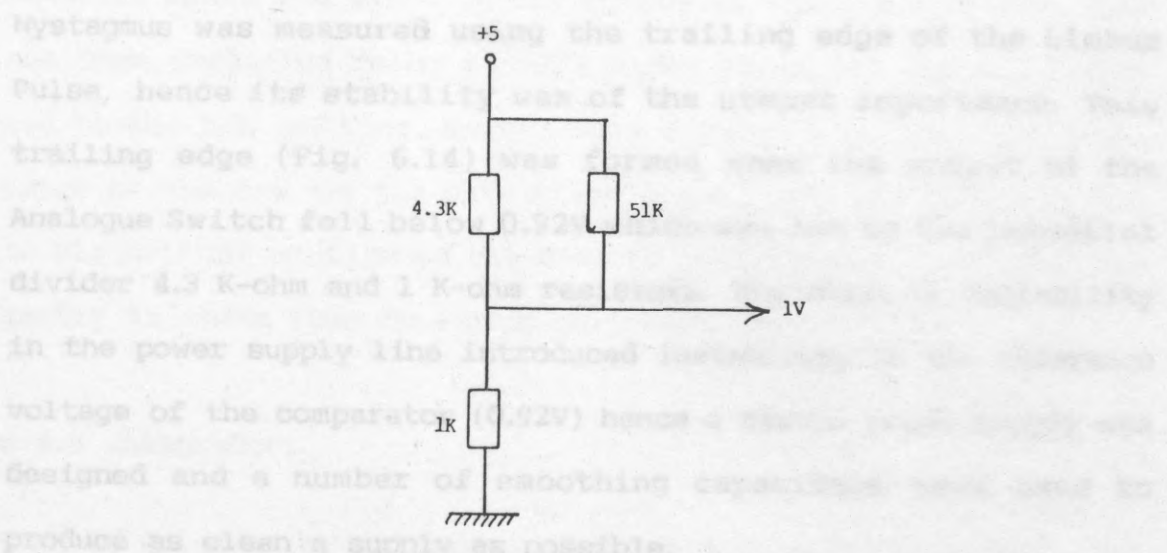
Fig. 6.14 Waveform of Limbus Pulse Generator

From the circuit in Fig. 6.13 when the 1 K-ohms variable resistor was set at 1 K-ohms:

If the negative input was low then the output was 5V.

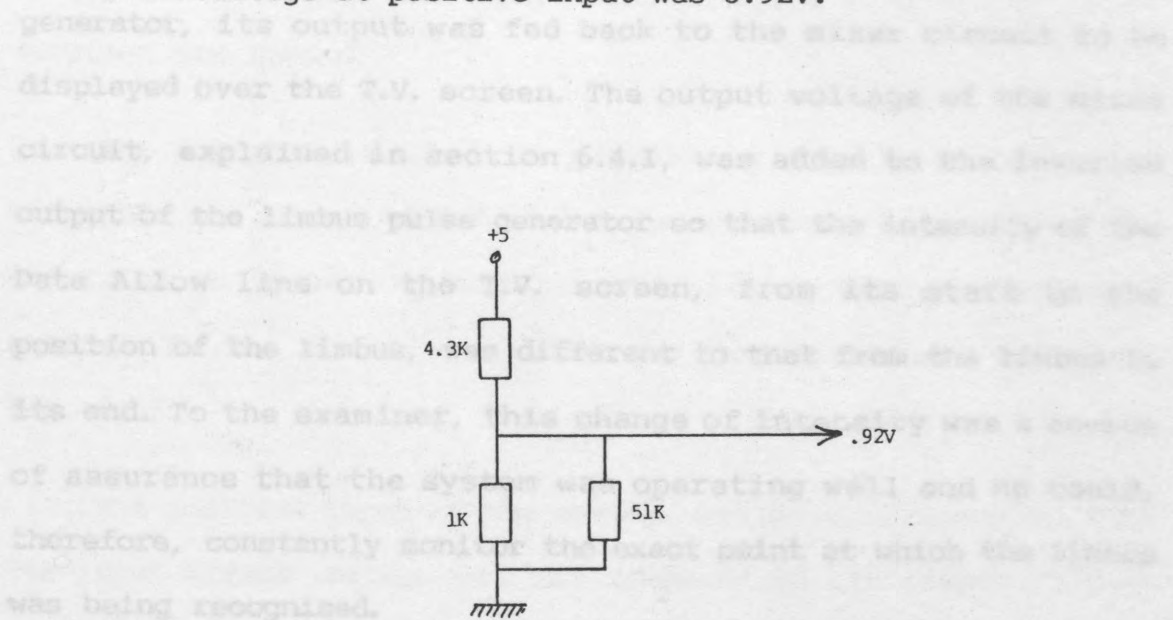
∴ voltage at positive input was 1V.

The output of the comparator was then inverted for an upright Limbus Pulse to be fed to the Sample and Hold circuit.



If the negative input was high then the output was 0V.

To be able to monitor the output of the Limbus pulse generator, its output was fed back to the mixer circuit to be displayed over the V. screen. The output voltage of the mixer circuit, explained in section 6.4.1, was added to the inverted output of the Limbus pulse generator so that the intensity of the



Hence using a comparator LM311 with a positive feedback (51 K-ohms resistor), any rising voltage which exceeded 1V and any falling voltage which exceeded 0.92V was detected. This produced the Limbus Pulse in an inverted form and using this hysteresis method of voltage comparing, eliminated wobbling of the trailing edge of the Limbus pulse due to small white noise sitting on the video waveform.

Fig. 6.15 Limbus Pulse, Data Allow 5 Video Signal Mixer

The output of the comparator was then inverted for an upright Limbus Pulse to be fed to the Sample and Hold circuit. As shown in Fig. 6.13 the output of the Limbus Pulse generator was inverted again and added to the output of the Sample and Hold circuit. Nystagmus was measured using the trailing edge of the Limbus Pulse, hence its stability was of the utmost importance. This trailing edge (Fig. 6.14) was formed when the output of the Analogue Switch fell below 0.92V which was set by the potential divider 4.3 K-ohm and 1 K-ohm resistors. Any noise or instability in the power supply line introduced instability in the reference voltage of the comparator (0.92V) hence a stable power supply was designed and a number of smoothing capacitors were used to produce as clean a supply as possible.

To be able to monitor the output of the limbus pulse generator, its output was fed back to the mixer circuit to be displayed over the T.V. screen. The output voltage of the mixer circuit, explained in section 6.4.I, was added to the inverted output of the limbus pulse generator so that the intensity of the Data Allow line on the T.V. screen, from its start to the position of the limbus, was different to that from the limbus to its end. To the examiner, this change of intensity was a source of assurance that the system was operating well and he could, therefore, constantly monitor the exact point at which the limbus was being recognised.

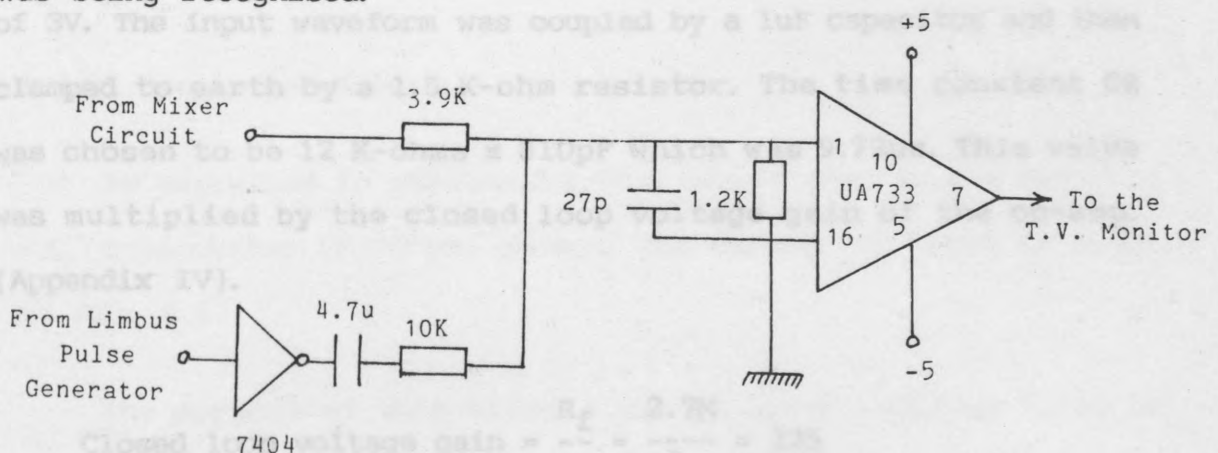


Fig. 6.15 Limbus Pulse, Data Allow & Video Signal Mixer

As shown in Fig. 6.15 the output of the limbus generator was inverted again and added to the output of the video mixer. This was then amplified using a uA733 video amplifier and its output fed to the T.V. monitor. Hence, this monitor was displaying the image of the eye and the Data Allow placed over the limbus partly in black (that portion of the data allow before the limbus) and partly in white (the remaining part after the limbus).

6.4.V Integrator:

To be able to determine the position of the Limbus, the Limbus Pulse was used to sample a linear ramp. Nystagmus was to be measured during the Data Allow hence a ramp of the same duration was needed.

The simplest method of generating such a ramp was to integrate the inverted Data Allow pulse using an op-amp.. The theory of an op-amp. integrator has already been explained in section 3.4.II. The circuit and the waveforms are shown in Fig. 6.16.

The positive input of the op-amp. was shorted to earth since its input offset voltage was 5mV compared to its output voltage of 3V. The input waveform was coupled by a 1uF capacitor and then clamped to earth by a 1.5 K-ohm resistor. The time constant CR was chosen to be 12 K-ohms x 810pF which was 9.72us. This value was multiplied by the closed loop voltage gain of the op-amp. (Appendix IV).

$$\text{Closed loop voltage gain} = \frac{R_f}{R_1} = \frac{2.7M}{12K} = 225$$

$$\therefore CR = 9.72 \times 10^{-6} \times 225$$

sampling and when it was low it held the last value of the ramp until the next T.V. field (Fig. 6.18). Hence the trailing edge of the Limbus Pulse determined the value of the ramp and any movement of this edge caused the 'held' value of the ramp to change.

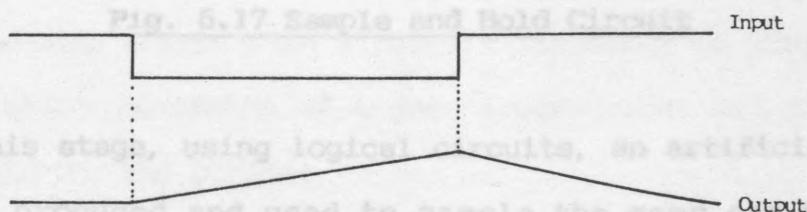
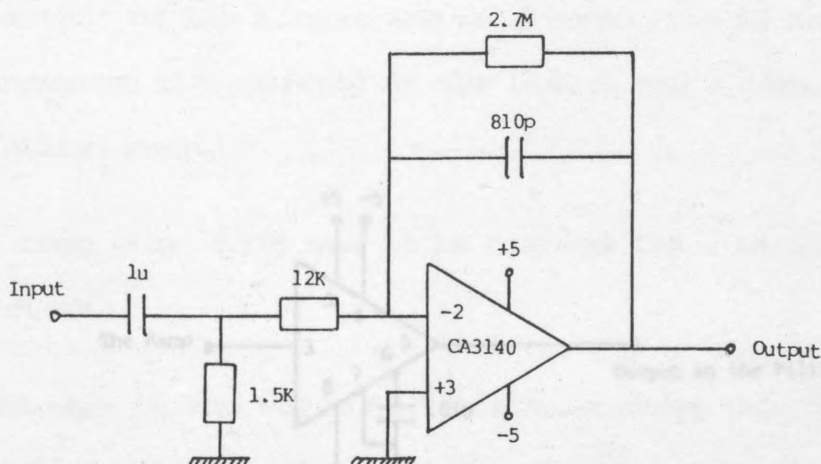


Fig. 6.16 Integrator Circuit and its Waveforms

This is much greater than the period of the Data Allow (10us), hence producing a linear ramp during this period which was then fed to the Sample and Hold circuit.

6.4.VI Sample and Hold:

As explained in section 3.4.IV a single chip Sample and Hold I.C. type number LF398 was chosen, the circuit of which is shown in Fig. 6.17.

The purpose of this circuit was to use the Limbus Pulse to sample a ramp. When the Limbus Pulse was high the circuit was

sampling and when it was low it held the last value of the ramp until the next T.V. field (Fig. 6.18). Hence the trailing edge of the Limbus Pulse determined the value of the ramp and any movement of this edge caused the 'held' value of the ramp to change.

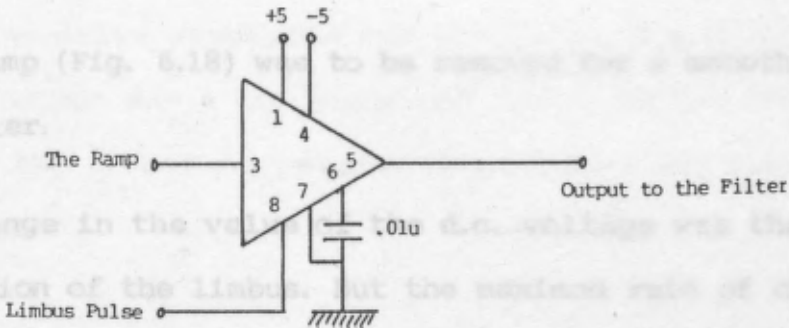


Fig. 6.17 Sample and Hold Circuit

At this stage, using logical circuits, an artificial Limbus Pulse was produced and used to sample the ramp and hence the linearity and the stability of the ramp was confirmed. This also established the stability of the whole system, and verified the low level of the system noise.

6.5 Summary

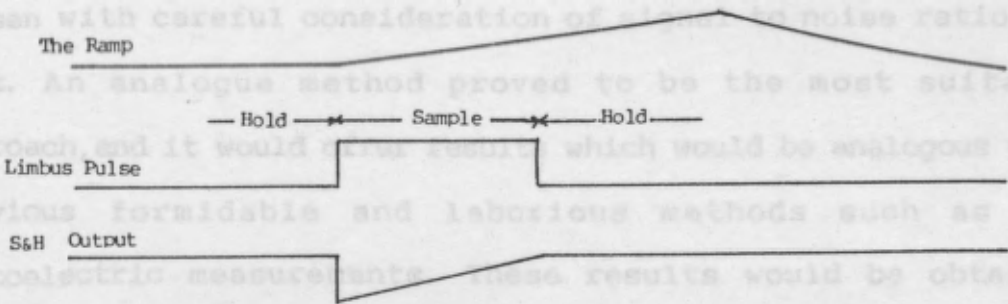


Fig. 6.18 Inputs and Output of the Sample and Hold I.C.

The output of this circuit was then fed to a 3-Pole Low-Pass filter.

6.4.VII 3-Pole Low-Pass Filter:

The output of the Sample and Hold consisted of a d.c. value which represented the position of the Limbus and a 10 μ s (width of the Data Allow) ramp.

This ramp (Fig. 6.18) was to be removed for a smooth reading on the plotter.

The change in the value of the d.c. voltage was the change in the position of the limbus. But the maximum rate of change of the Limbus (Nystagmus) was not more than 10 cycles per second. Hence a low-pass filter with a cut-off frequency of 10Hz removed the ramp (which consisted of higher frequencies) and provided a smooth output to the plotter.

The design used in section 3.4.VIII was also used here. The circuit and the frequency response are shown in Fig. 6.19 (Appendix XI).

6.5 Summary

The method of detection of the eye tremor movements was chosen with careful consideration of signal to noise ratio and cost. An analogue method proved to be the most suitable approach, and it would offer results which would be analogous with previous formidable and laborious methods such as the photoelectric measurements. These results would be obtained without the knowledge of the patient or obstruction to his vision, and hence his eye behaviour would be under natural

conditions.

Besides the modified black and white T.V. camera other commercially available instruments used were: a black and white monitor, a moving paper X-Y plotter and a U-Matic video taperecorder.

The inputs to the system consisted of the power supply, field and line drive waveforms and the video signal out of the camera. Its output was a low frequency signal to the X-Y plotter representing the tremor movements. Conclusions and discussions are in chapter 8.

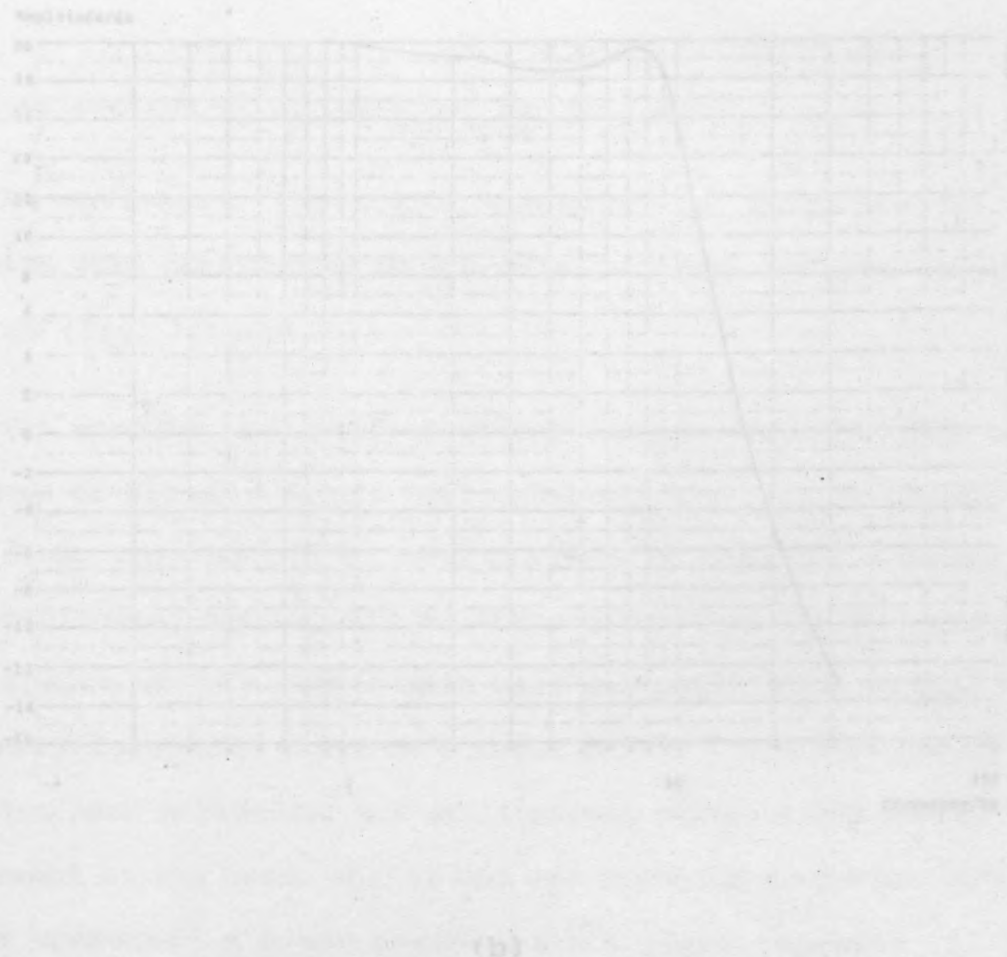
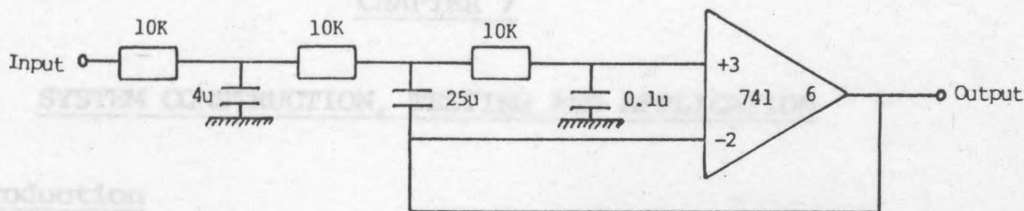
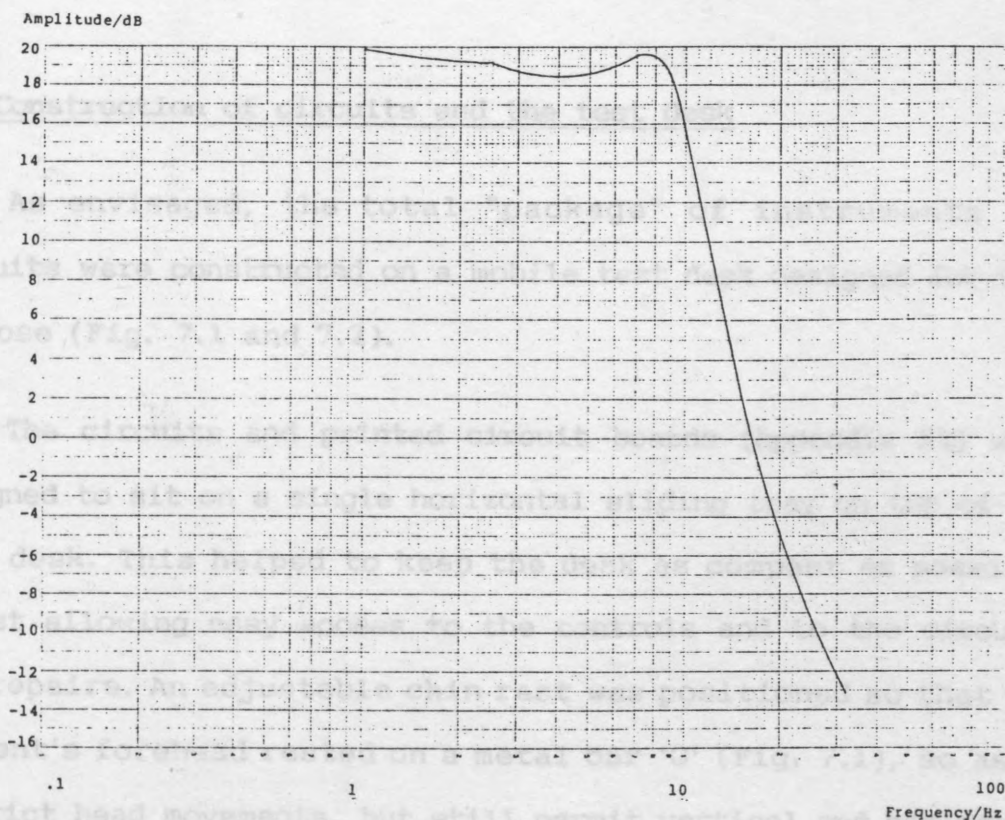


Fig. 5.19 3-Pole Low-Pass Filter
(a) The Circuit
(b) Frequency Response



(a)



(b)

Fig. 6.19 3-Pole Low-Pass Filter

(a) The Circuit

(b) Frequency Response

CHAPTER 7

SYSTEM CONSTRUCTION, TESTING AND APPLICATION

7.1 Introduction

The integration and amalgamation of the two systems, namely, the detection of relative and also tremor eye movements facilitated the simultaneous operation of the two tests. This involved designing a suitable structure to house all the instruments, placing the patient in a comfortable position for the test, supplying the correct voltage to all the instruments and circuits, and also driving all the monitors with the necessary waveforms.

7.2 Construction of circuits and the test desk

As envisaged, the total "package" of instruments and circuits were constructed on a mobile test desk designed for this purpose (Fig. 7.1 and 7.2).

The circuits and printed circuit boards (Appendix XII) were designed to sit on a single horizontal sliding tray on top of the test desk. This helped to keep the desk as compact as possible whilst allowing easy access to the controls and to the circuits for repairs. An adjustable chin rest was positioned so that the patient's forehead rested on a metal bar 'G' (Fig. 7.1), so as to restrict head movements, but still permit vertical and horizontal alignment of the head. Whilst one eye directly faced monitor A, which presented a plain raster with a light pen over it, the other eye, via a small mirror, faced monitor B which displayed the Hess chart. The mirror, chin rest and both monitors

were attached to metal bars so that they could all be aligned horizontally, for testing each eye separately. For accommodating the patient's particular requirements, the 1-X plotter 'D', and the monitor 'C', which was used for the tremor test and which displayed the results of the test, were superimposed on the image of the patient's eye which was shown on top of the test desk. The eye which was shown with the

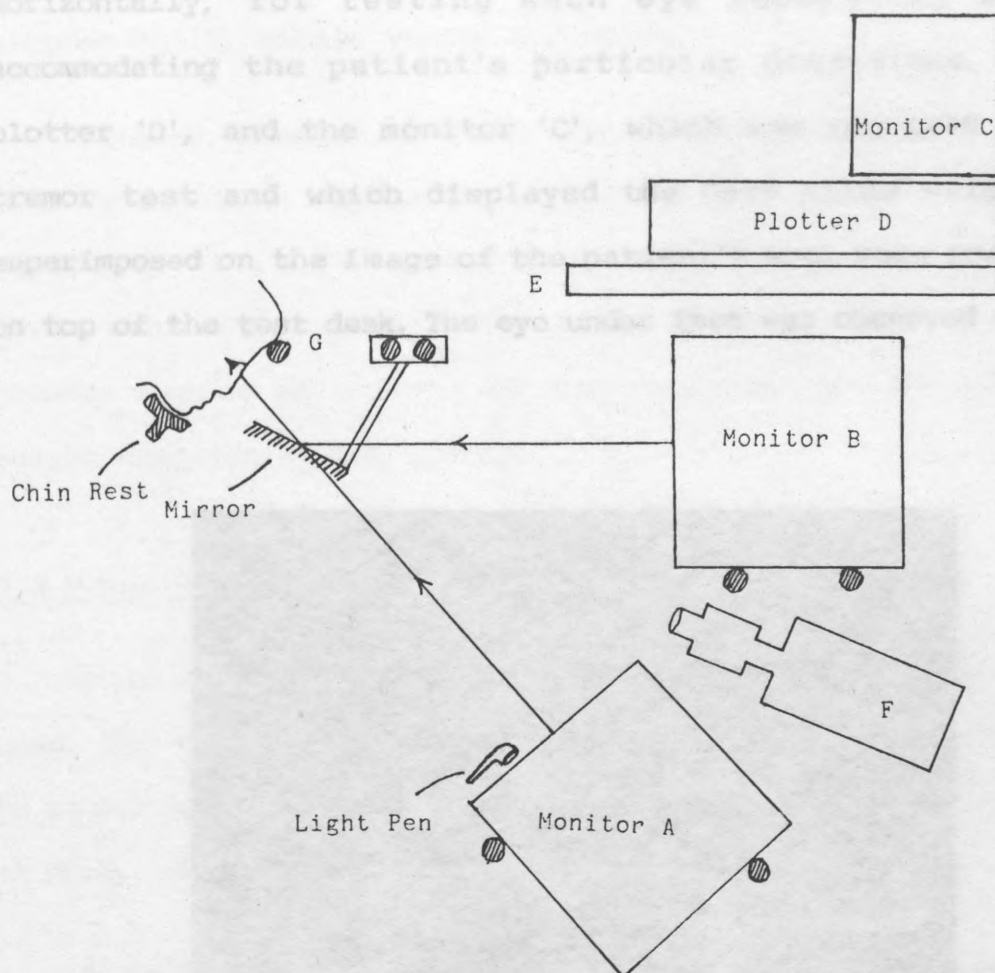


Fig. 7.1 Elevation view of the test desk

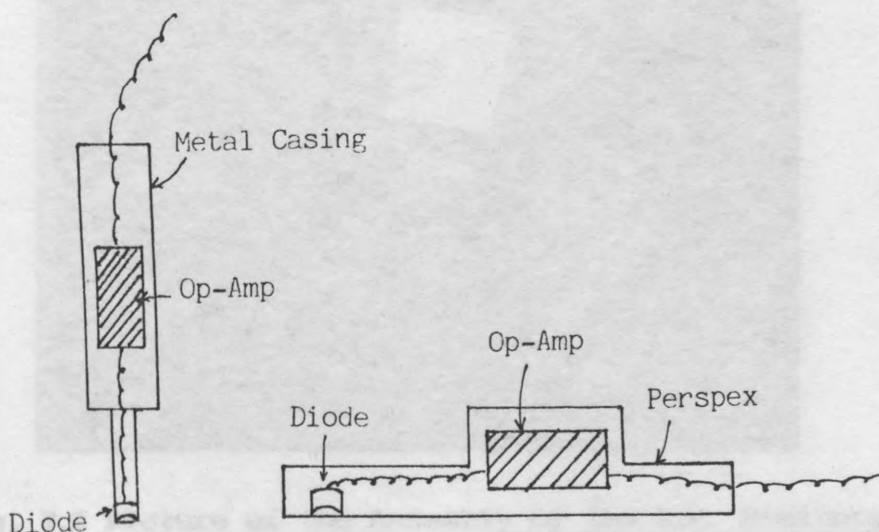


Fig. 7.1.a Light Pen Casing Modification

were attached to metal bars so that they could all be slid horizontally, for testing each eye separately and for accommodating the patient's particular dimensions. The X-Y plotter 'D', and the monitor 'C', which was required for the tremor test and which displayed the Data Allow bright line superimposed on the image of the patient's eye, were positioned on top of the test desk. The eye under test was observed with the greater degree of control of the modified pen and permitted easier scanning by the patient.



Fig. 7.2 Picture of the Assembly of the T.V. Monitors
and the test desk

aid of a black and white camera 'F', hidden between the two monitors 'A' and 'B'. All these components were constructed on a purpose-built, mobile wooden structure.

Finally, changes in the construction of the light pen were made by substituting the pen-shaped metal casing surrounding the photodiode with a flat piece of perspex (Fig. 7.1.a) which could hover over the surface of the T.V. monitor. This enabled a greater degree of control of the modified pen and permitted easier scanning by the patient.

7.3 Power Supply:

Four voltages were required to supply all the circuits used. The total maximum current for each voltage was calculated to be 1.2 A (for +5V); 200 mA (for -5V); 250 mA (for +12V) and 20 mA (for -12V).

A suitable power supply unit was designed so that when switched on, both -5V and -12V voltages were instantly available and then, with the aid of two relays, +5V and +12V voltages were turned on. Moreover, the design allowed the +5V and +12V to switch off first, and also made provisions for the +5V to be short-circuited in case the +12V was short-circuited.

The above provisions were necessary because, in the circuits, four 2708 EPROMs were used with specifications stating that the -5V should be applied prior to +5V and +12V, and -5V must also be the last power supply switched off.

The circuit of the power supply is shown in Fig. 7.3.

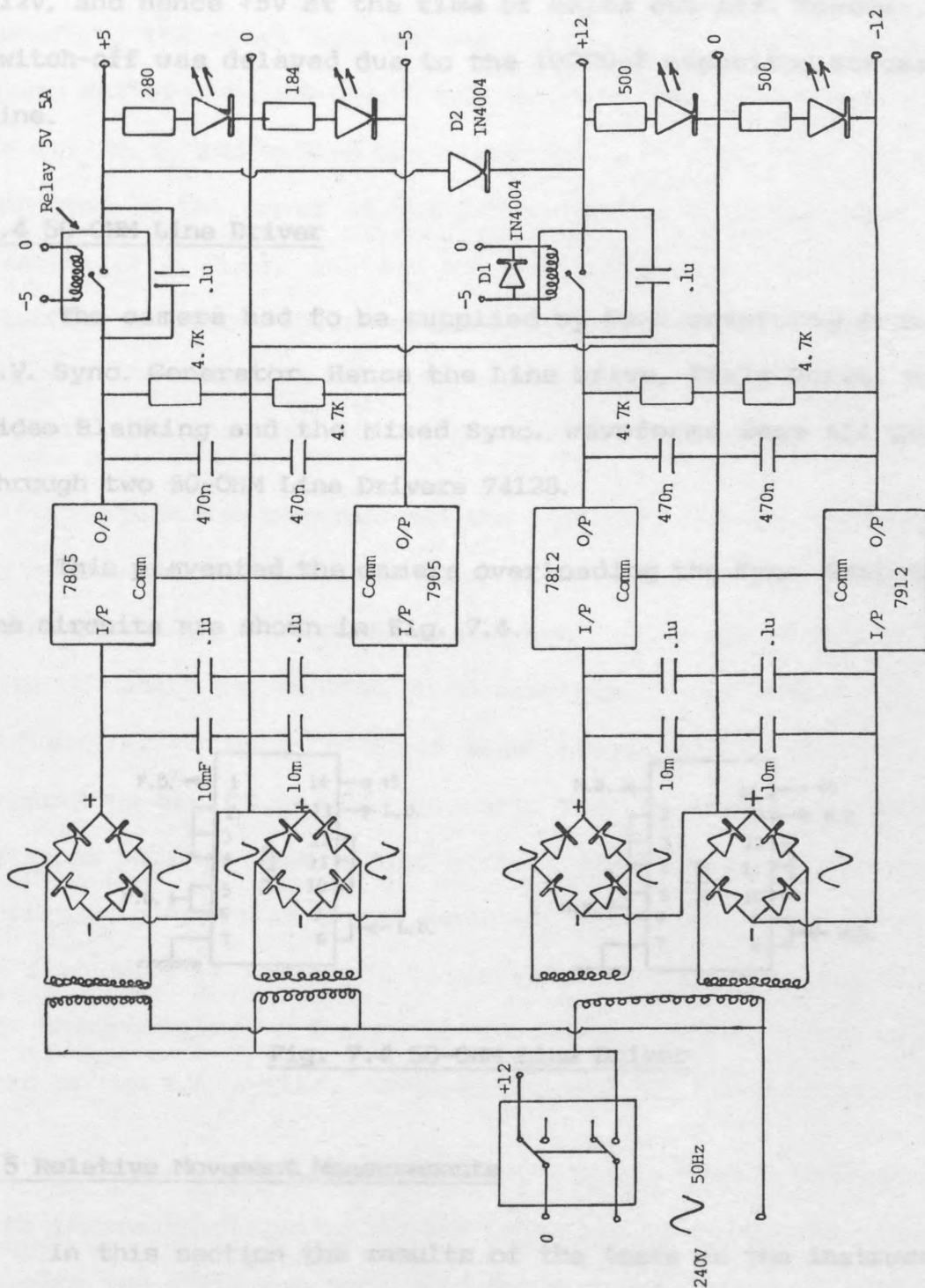


Fig.7.3 Power Supply Circuit

Diode D_2 was to ensure that +5V was short-circuited when +12V was shorted. Diode D_1 and the 0.1uF capacitors were used to suppress any spikes generated by the relays. The double-pole switch, used for the mains, was to ensure that the +12V and +5V supplies were switched off before -5V. This was done by shorting +12V, and hence +5V at the time of mains cut-off. However, -5V switch-off was delayed due to the 10000uF capacitor across its line.

7.4 50-OHM Line Driver

The camera had to be supplied by four waveforms from the T.V. Sync. Generator. Hence the Line Drive, Field Drive, Mixed Video Blanking and the Mixed Sync. waveforms were all passed through two 50-OHM Line Drivers 74128.

This prevented the camera overloading the Sync. Generator. The circuits are shown in Fig. 7.4.

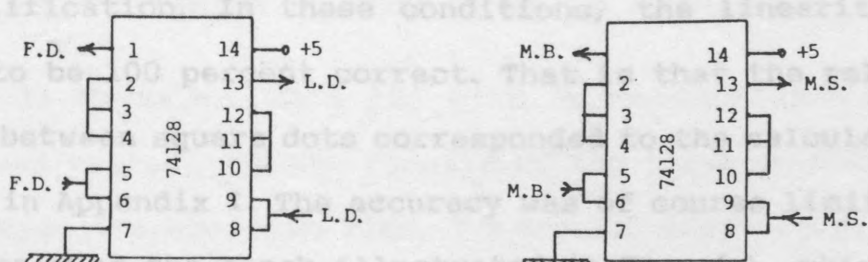


Fig. 7.4 50-OHM Line Driver

7.5 Relative Movement Measurements

In this section the results of the tests on the instruments designed for the measurements of the relative eye movements are presented. Printed circuit boards were prepared and the T.V.

monitors were set up as outlined in chapters 3 & 4 and also in Fig. 7.2.

The first task was to plot the Hess chart, as generated by the circuits shown in Fig. 4.1. This was then used as the small, diagnostic chart onto which the test results were transferred. Therefore, the chart monitor was set so as to display only one square dot of the Hess Chart. The output of the generator, after the switch S_1 and before the mixer section (Fig. 4.1), was then connected to the input of the S-R flip-flop, in the light pen circuits (Fig. 3.6), instead of the light pen. Therefore, by selecting different square dots, the pen of the X-Y plotter could indicate the position of that square dot, and hence plot the complete Hess Chart on the X-Y plotter with a red pen.

This plot was measured and the linearity and the accuracy of the system was checked, and found to be satisfactory. Initially, the chart was plotted on A3 size paper, although in day to day tests the chart was plotted on A5 size paper resulting in a four-fold amplification. In these conditions, the linearity was measured to be 100 percent correct. That is that the relative distances between square dots corresponded to the calculations presented in Appendix I. The accuracy was of course limited by the frequency of the clock illustrated in Fig. 4.1, which was 4MHz horizontally, and also to the number of T.V. lines in one field of the T.V. system, which was around 300 lines vertically.

After the above linearity check, the connection between the chart generator circuits and the light pen circuits was broken. The same red chart was then used for a control group of patients who had normal vision, and also for six patients with known eye

disorders on whom the test was carried out. Each of the patients, with their heads resting on a chin rest, looked through a mirror with their left eye at Monitor 'A' (Figs. 7.1 & 7.2) , and at Monitor 'B' with their right eye. They then placed the light pen over the Blank Monitor (Monitor 'B') so as to reproduce the chart on the X-Y plotter in black. The discrepancy between the black and the red charts was a measure of the imbalance in the action of the extraocular muscles of their two eyes.

Before the start of the test, the patients were informed that if, during the procedures, they missed or were unhappy about the recording of some of the square dots, they should not be concerned as the practitioner could always return and repeat those points again. The psychological effects of this assurance on the patient are considered important, as anxiety could have affected the results.

7.5.1 Case Studies

**Case studies (p. 191-204)
have been removed for
data protection reasons**

7.6 Tremor Measurements

In this section the results of tests on the instruments designed for the measurements of the eye tremor movements are presented. The circuits were constructed and set up as explained in chapter 6 and Fig. 7.2.

7.6.1 T.V. Method Test using an Artificial Model Eye

The validity of the instrument, its calibration and a check on its freedom from noise were made possible by the simulation of eye tremors produced on an artificial model eye. These movements were produced by a vibrator whose frequency and amplitude were controlled and monitored by an oscillator. The first task was to examine the linearity of the circuits and to make a few preliminary tests. A Link camera was placed in front of, and about 10cm away from, an artificial eye mounted on a rotary assembly connected to a mechanical vibrator. The block diagram of this is shown in Fig. 7.16 and its picture in Fig. 7.17. The oscillator was set at a frequency of 3Hz, with a voltage amplitude giving a rotation of 0.5 degree to the eye.

The plastic model eye used was shaped and coloured exactly as a real eye, and was placed on a rotary dish 19mm away from the centre of rotation. As the centre of the dish was the centre of a protractor, it was easy to measure the amplitude, in degrees, of rotary eye movements. In this way the voltage of the oscillator directly controlled the amplitude of the vibrators' movement and hence of the eye.

The oscillation of the artificial model eye was detected by the system and plotted on a moving paper plotter. The plot is

shown in Fig. 7.18.

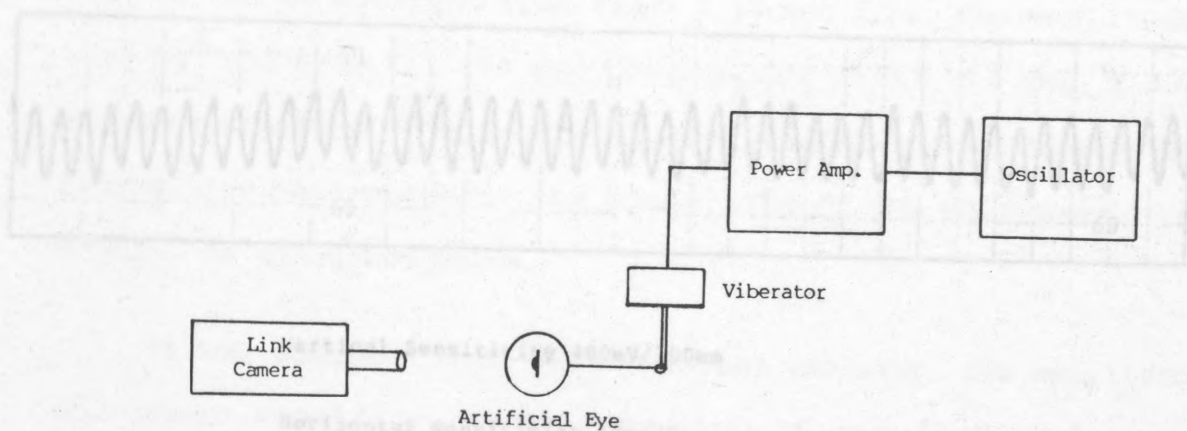


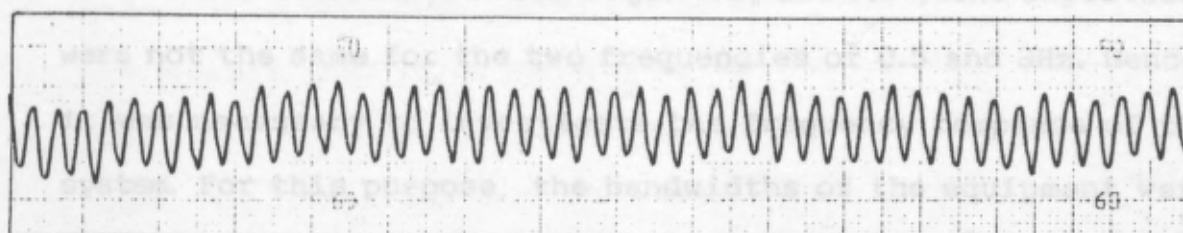
Fig. 7.16 Block Diagram of the Artificial Eye Assembly



Fig. 7.17 Picture of the Artificial Eye Assembly

The system was also tested with both 1.0 and 1.5 degrees rotation of the artificial eye (Fig. 7.19).

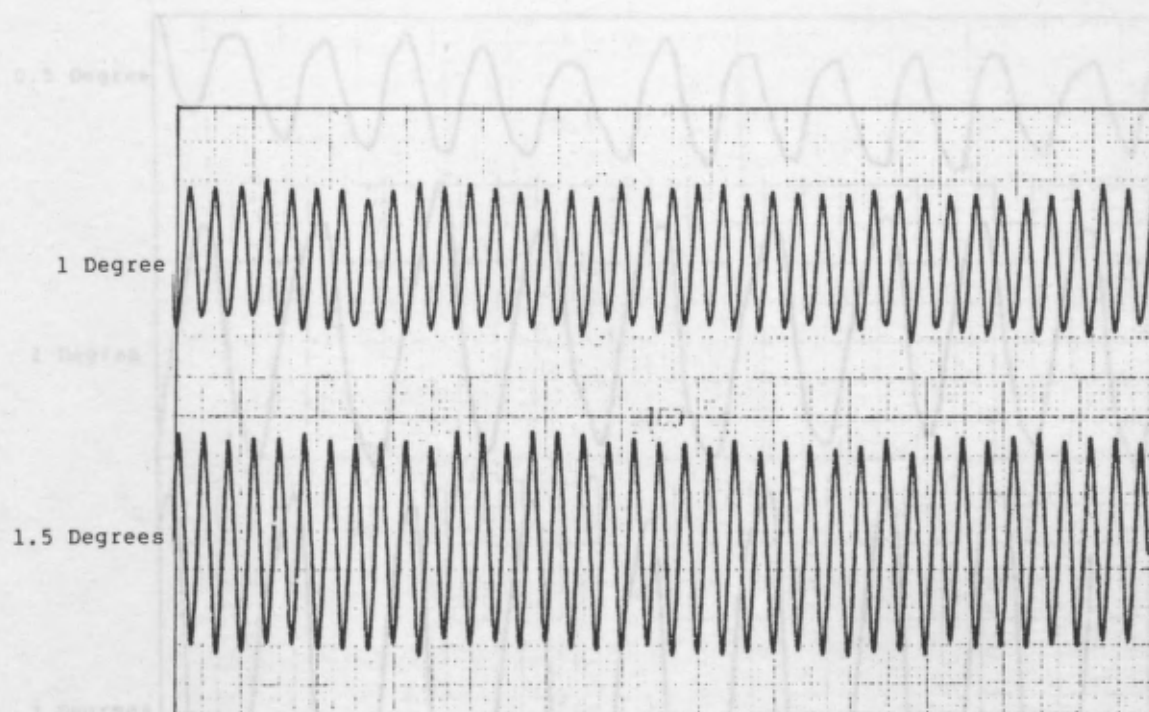
The artificial eye was also manually rotated by 0.5, 1.0 & 2.0 degrees at an approximate frequency of 0.5KHz, as shown in Fig. 7.20.



Vertical Sensitivity 400mV/100mm

Horizontal Sensitivity 10mm/S

Fig. 7.18 Artificial Eye Rotation of 0.5° at 3Hz



Vertical Sensitivity 400mV/100mm

Horizontal Sensitivity 10mm/S

Fig. 7.19 Artificial Eye Rotation of 1.0° & 1.5° at 3Hz

The artificial eye was also manually rotated by 0.5° , 1.0° & 2.0° degrees at an approximate frequency of 0.5Hz, as shown in Fig. 7.20.

To be able to test the frequency response of the designed

As can be observed from Figs. 7.19 and 7.20, the amplitudes were not the same for the two frequencies of 0.5 and 3Hz. Hence, it was necessary to investigate the frequency response of the system. For this purpose, the bandwidths of the equipment were studied as discussed below.

It was possible that the mechanical vibrator, its oscillator and power amplifier could introduce a non-flat frequency response. So as to overcome this problem, the amplitude of eye rotation was set at 1.0 degree, as read on the protractor, each time the frequency was varied.

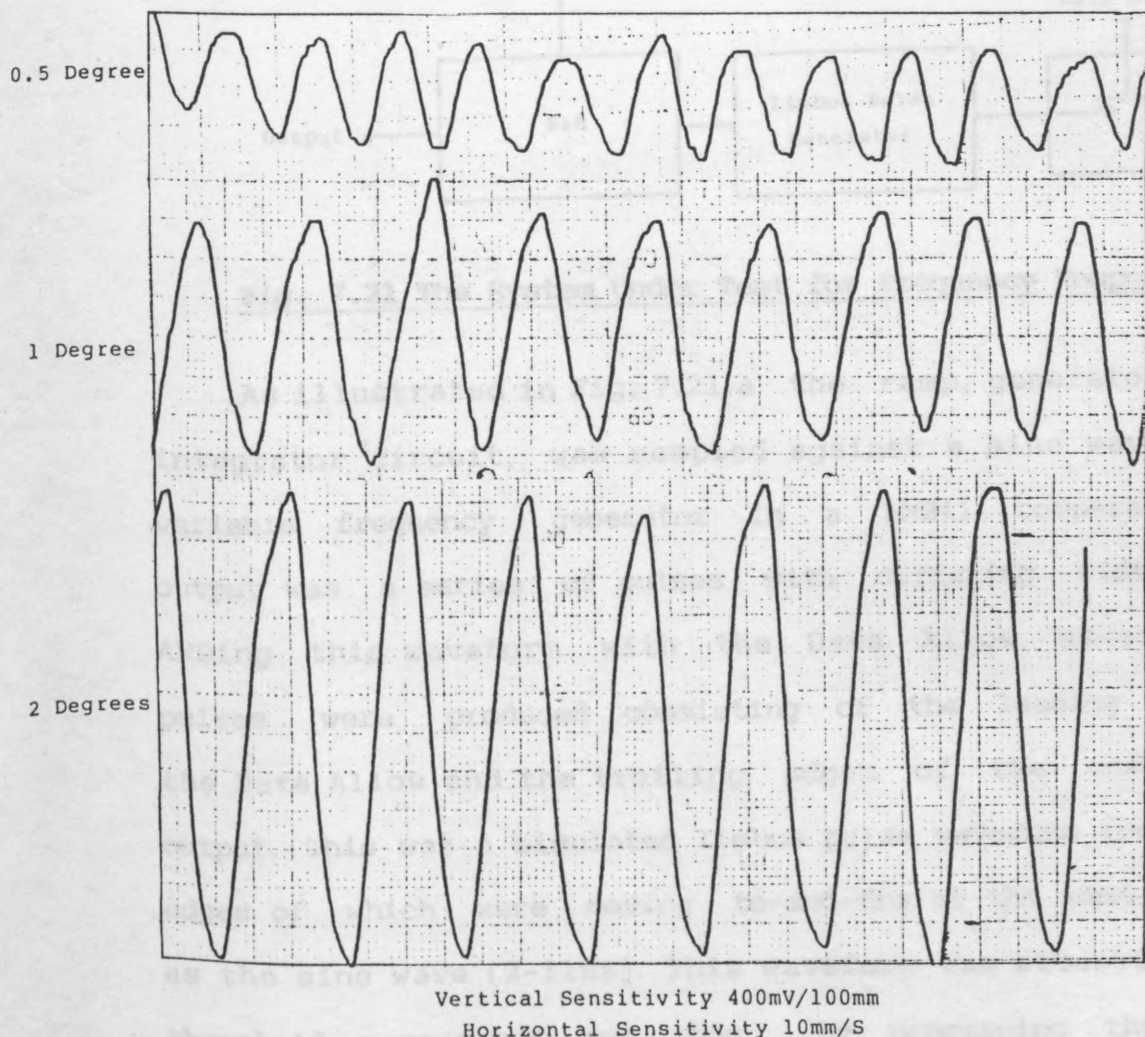


Fig. 7.20 Artificial Eye Rotation of 0.5, 1.0 & 2.0° at 0.5Hz

To be able to test the frequency response of the designed circuits, a simulated limbus pulse, free from the limitations of the camera, had to be generated. In the circuit shown in Fig. 7.21, this simulated limbus pulse was fed into the circuit under test. For the purposes of this test, the 3-Pole Low Pass Filter was excluded.

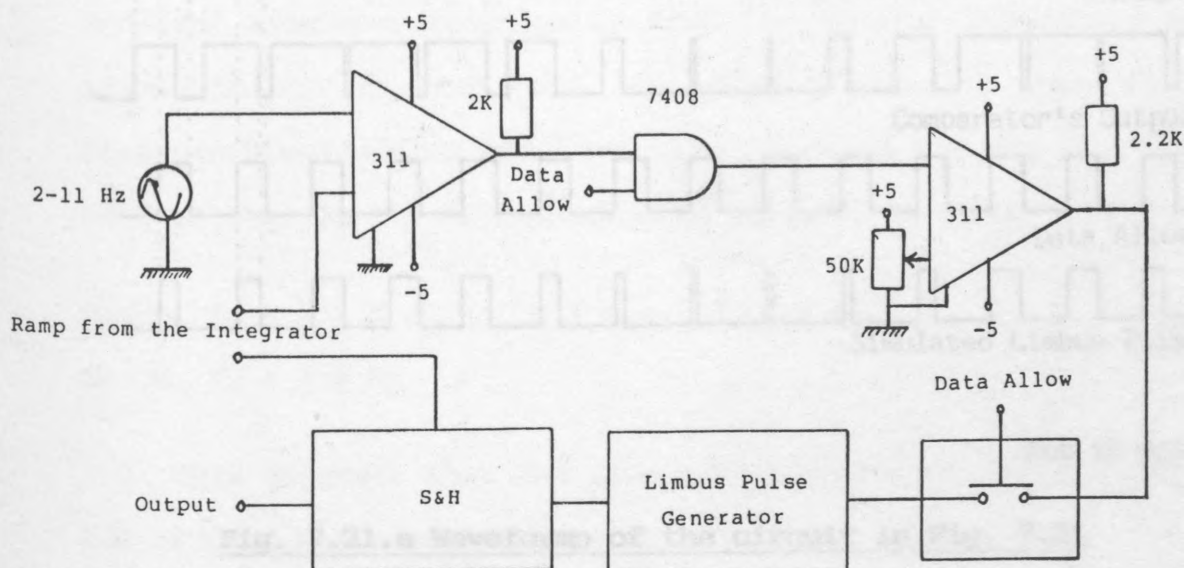
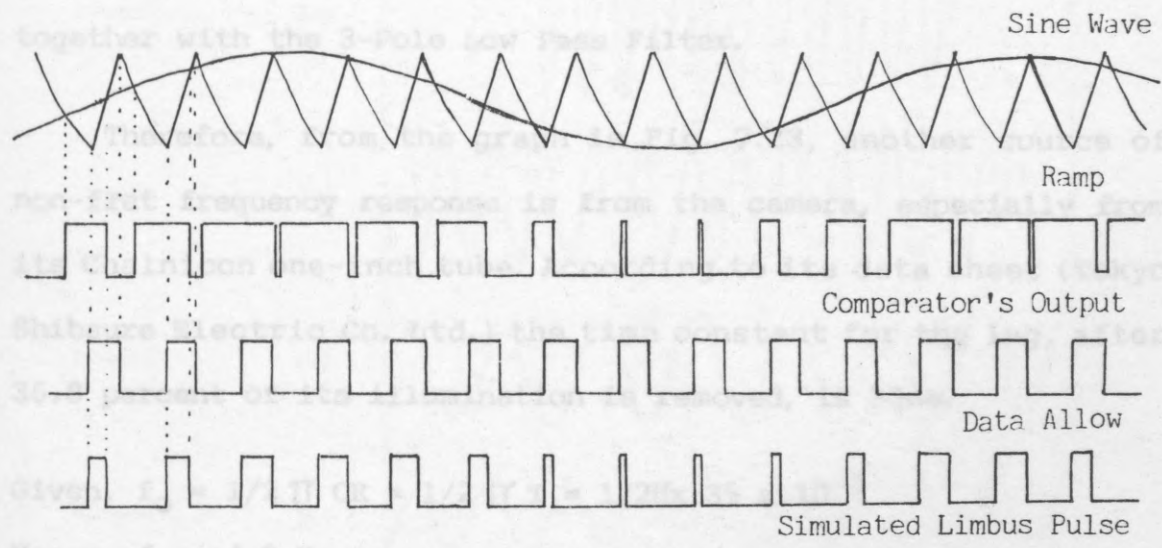


Fig. 7.21 The System Under Test for Frequency Response

As illustrated in Fig. 7.21.a the ramp, generated by the integrator circuit, was sampled against a sine wave from a variable frequency generator in a LM311 comparator. The output was a series of pulses with differing widths. After ANDing this waveform with the Data Allow waveform, new pulses were produced consisting of the leading edges of the Data Allow and the trailing edges of the comparator's output. This was a simulated limbus pulse waveform the trailing edges of which were moving to-and-fro at the same frequency as the sine wave (2-11Hz). This waveform was cleaned, using a threshold comparator, and then, by processing through the system under test, its frequency response was evaluated by

measuring the output voltage of the Sample and Hold I.C. The results of the test are shown in the table 7.1. Curve 'a' in Fig. 7.23 represents the frequency response of the designed circuits and curve 'b' represents the frequency response of the circuits together with the 3-Pole Low Pass Filter.



Not to Scale

Fig. 7.21.a Waveforms of the circuit in Fig. 7.21

Fre- quency	Amplitude		Amplitude		Amplitude			Amplitude
	Circuits		Circuits + Filters		Circuits + Filter + Camera			Camera
Hz	volt	dB'a'	volt	dB 'b'	mm	mV	dB'c'	dB'd' (='c'-'b')
2.0	.51	-.97	.44	-2.25	22.5	90.2	-5.2	-3.00
3.0	.51	-.97	.39	-3.30	16.8	67.2	-7.80	-4.50
4.0	.50	-1.14	.34	-4.49	14.1	56.4	-9.32	-4.83
5.0	.49	-1.31	.32	-5.01	9.5	38	-12.75	-7.74
6.0	.48	-1.49	.30	-5.58	8.2	32.8	-14.03	-8.45
7.0	.47	-1.68	.29	-5.87	7	28	-15.41	-9.54
8.0	.46	-1.86	.30	-5.58	5.3	21.2	-17.82	-12.24
9.0	.45	-2.05	.31	-5.29	5.6	22.2	-17.42	-12.13
9.5			.32	-5.01				
10.0	.45	-2.05	.31	-5.29	6.0	24	-16.75	-11.46
10.5			.31	-5.58				
11.0	.44	-2.25	.27	-6.49	5.0	20	-18.32	-11.83

Table 7.1 Results of the Amplitudes of The Circuits ('a'),
The Circuits + Filter ('b'),
The Circuits + Filter + Camera ('c'), The Camera ('d'),
With Frequencies from 2 to 11Hz and an Eye Rotation of 1°

measuring the output voltage of the Sample and Hold I.C. The results of the test are shown in the table 7.1. Curve 'a' in Fig. 7.23 represents the frequency response of the designed circuits and curve 'b' represents the frequency response of the circuits together with the 3-Pole Low Pass Filter.

Therefore, from the graph in Fig. 7.23, another source of non-flat frequency response is from the camera, especially from its Chalnicon one-inch tube. According to its data sheet (Tokyo Shibaura Electric Co. Ltd.) the time constant for the lag, after 36.8 percent of its illumination is removed, is 35ms.

$$\text{Given, } f_o = 1/2 \pi CR = 1/2 \pi T = 1/2\pi \times 35 \times 10^{-3}$$

$$\text{Hence, } f_o = 4.5 \text{ Hz}$$

This suggests that the frequency response of the tube would not be flat between 2 and 11Hz .

The last possible stage for the introduction of non-linearity in the frequency response is from the moving paper plotter. To ensure that this is not included in the final results, a 10MHz digital storage oscilloscope was used to store the waveforms digitally and thus plot them on the plotter at a frequency much lower than 2Hz. The waveforms are shown in Fig. 7.22, and the results in the table 7.1. The curve 'c', in Fig. 7.23 represents the frequency response of the system, the filter and the camera. However, as stated above, the frequency response of the plotter was excluded in curve 'c' as a digital storage oscilloscope was used.

Fig. 7.22 The Waveforms 2 to 11Hz using Digital

The frequency response of the camera together with its tube (curve 'd'), was given by the difference between the results of

Horizontal Sensitivities

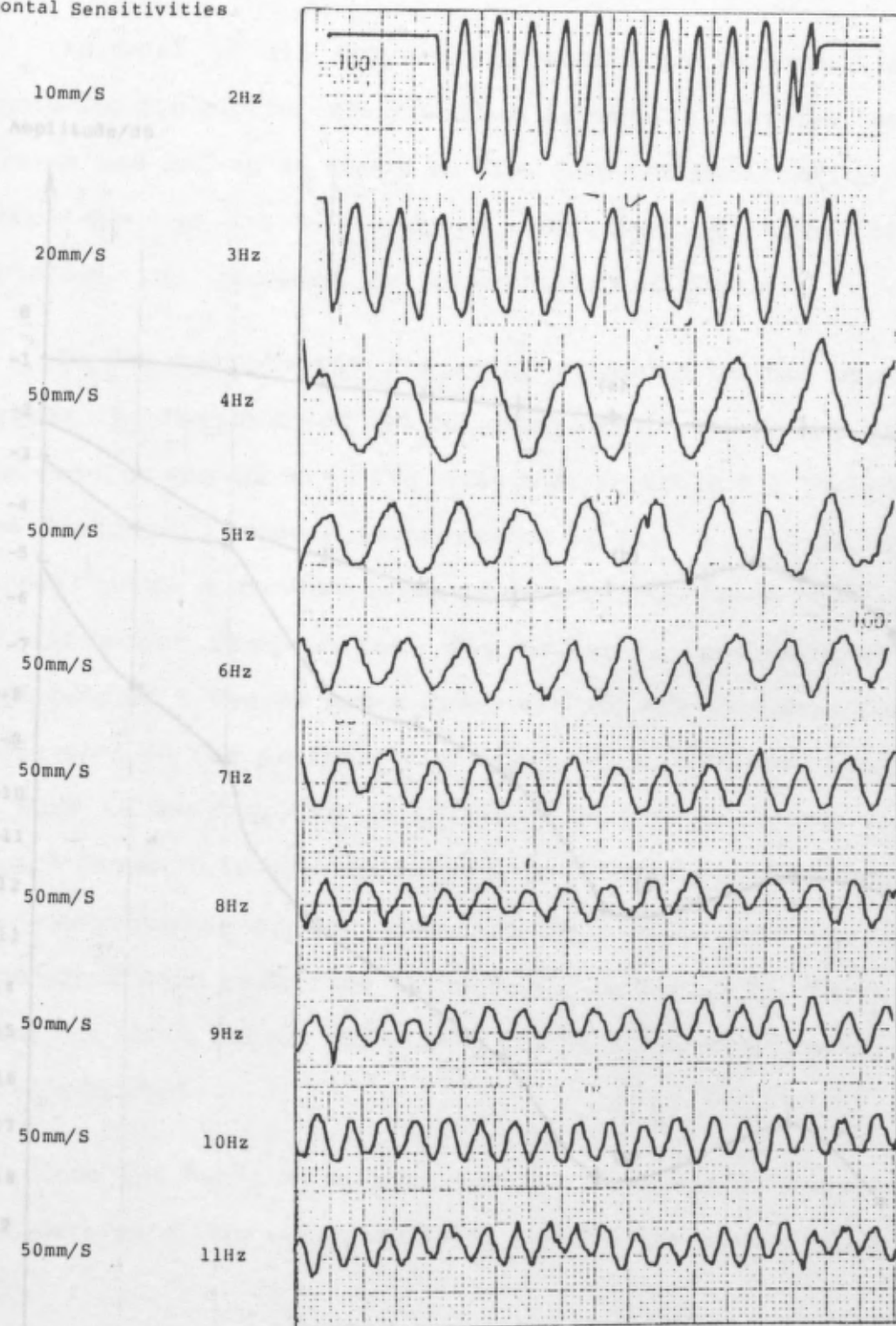


Fig. 7.22 The Waveforms 2 to 11Hz using Digital Storage Oscilloscope

Fig. 7.23 Vertical Sensitivity 400mV/100mm

'c' and 'd'. A full investigation and discussion of the capability of the camera tube can be found in the next Chapter.

As well as all the above precautions the total system including the plotter was tested as if under a real eye test. The system was set-up as shown in Fig. 7.16 The oscillation of the plotter was set at 1 degree and the amplitude of its rotation was recorded on paper moving at 10 cm s^{-1} .

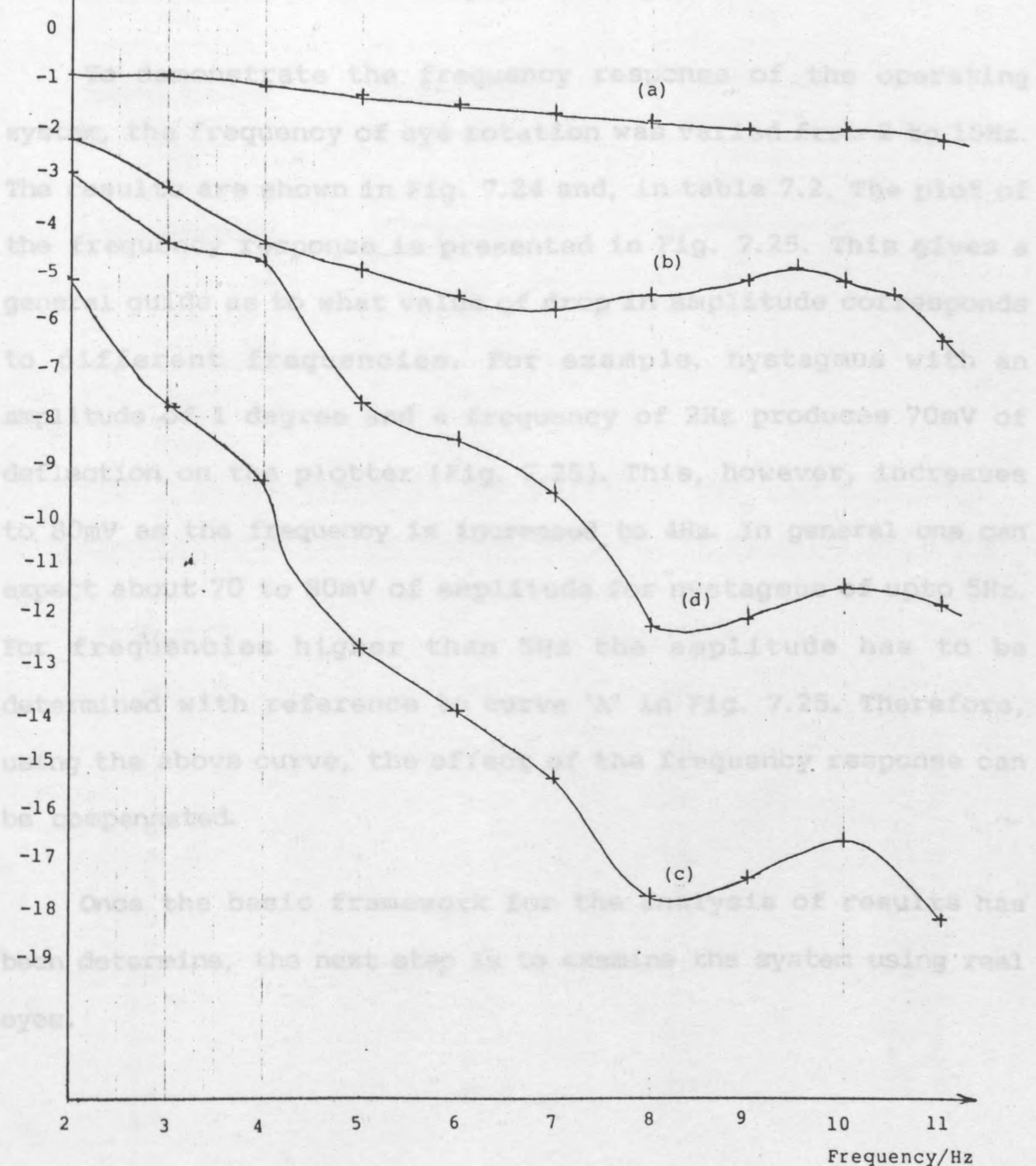


Fig. 7.23 Amplitude vs Frequency response for the Circuits

Filter and Camera

'c' and 'b'. A full investigation and discussion of the capability of the camera tube can be found in the next Chapter.

As well as all the above precautions the total system including the plotter was tested as if under a real eye test. The system was set-up as shown in Fig. 7.16 The oscillation of the model eye was set at 1 degree, and the amplitude of its rotation was recorded on paper moving at 10mm s⁻¹.

To demonstrate the frequency response of the operating system, the frequency of eye rotation was varied from 2 to 15Hz. The results are shown in Fig. 7.24 and, in table 7.2. The plot of the frequency response is presented in Fig. 7.25. This gives a general guide as to what value of drop in amplitude corresponds to different frequencies. For example, nystagmus with an amplitude of 1 degree and a frequency of 2Hz produces 70mV of deflection on the plotter (Fig. 7.25). This, however, increases to 80mV as the frequency is increased to 4Hz. In general one can expect about 70 to 80mV of amplitude for nystagmus of upto 5Hz. For frequencies higher than 5Hz the amplitude has to be determined with reference to curve 'A' in Fig. 7.25. Therefore, using the above curve, the effect of the frequency response can be compensated.

Once the basic framework for the analysis of results has been determine, the next step is to examine the system using real eyes.

Table 7.2 The Result of the Frequency Response of the Total System, Including the Plotter, for 1° Eye Movement

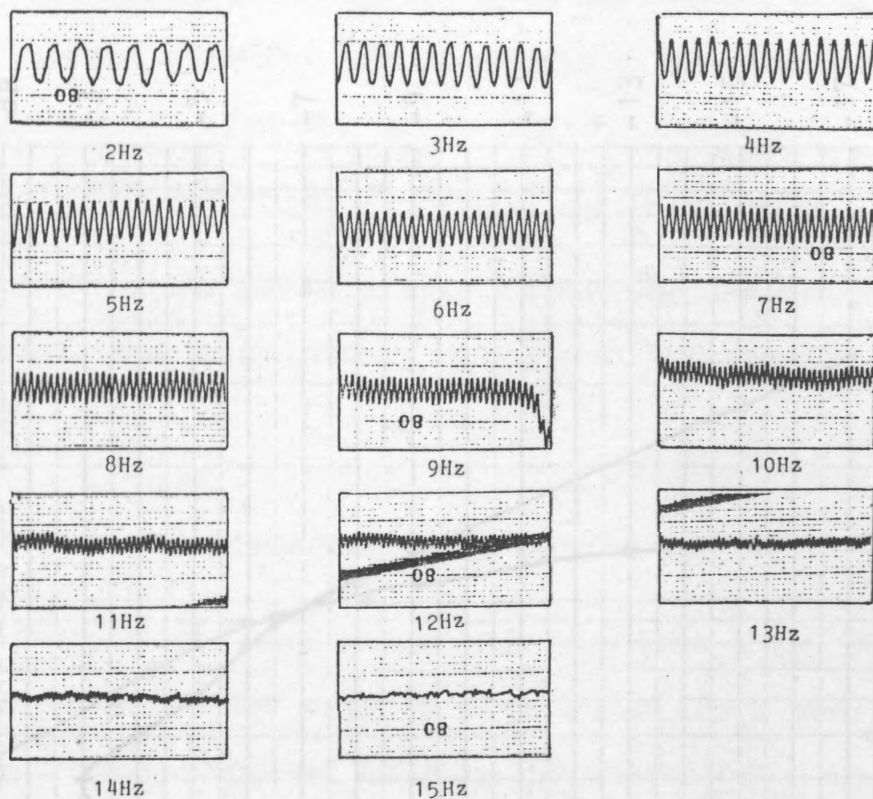


Fig. 7.24 The Traces of the Artificial Eye from 2 to 15Hz
Horizontal Sensitivity 10mm/s, Vertical Sensitivity 1V/100mm

Frequency		Amplitude	
Hz	mm	mV	dB
2	7.0	70	-2.2
3	7.5	75	-1.6
4	8.0	80	-1.0
5	7.0	70	-2.2
6	6.0	60	-3.5
7	5.5	55	-4.3
8	5.0	50	-5.1
9	4.5	45	-6.0
10	3.5	35	-8.2
11	3.0	30	-9.5
12	2.5	25	-11.1
13	2.0	20	-13.0
14	1.0	10	-19.0
15	-	-	-

Table 7.2 The Result of the Frequency Response of the Total
System, Including the Plotter, for 1° Eye Movement

7.6.2 Patient's Eye Tests

The eye movements of ten cases were tested with the designed T.V. tremor detector and also with a commercially available photoelectric system, made by [REDACTED], Development Optoelectronic Ltd., model 53.

Most of the patients were supplied by the London Refraction Hospital, and their history is reported individually (see section 7.6.3).

7.6.2.a Photoelectric Test (c.f. Section 5.1.14)

The patients were seated 55cm away from a T.V. monitor which displayed a red dot aligned with the primary position of the patient's eye. Goggles, holding the photodiodes, were worn and the movement of each eye recorded on a moving paper plotter. The results of all the patients, except Case number 1, are presented below.

As illustrated in Fig. 7.26, for one degree of eye movement to the right, an upward deflection of 10mm was registered by the plotter when set for 4V per 100mm in the Y-deflection; giving 400mV degree^{-1} .

7.6.2.b T.V. Method Test

Patients were seated 75cm away from the lens of a T.V. camera placed in front of their eyes. The lighting conditions of the room were normal, and illuminations from monitors 'A' and 'B', shown in Fig. 7.1, lit the patient's faces in such a way that there were no bright reflections in their eyes. The existence of

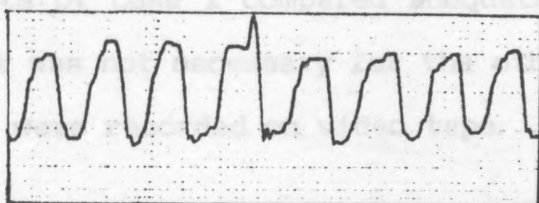


Fig 7.26 A 1° Oscillation of the Model Eye
on the-Photoelectric System Energised by Hand
Horizontal Sensitivity 10mm/s, Vertical Sensitivity 4V/100mm

such a corneal reflection did not however cause any real problems, and the Data Allow line was adjusted so as not to coincide with these. Each patient's head was placed on a chin rest, with their forehead resting against a bar so that the head was completely stationary.

The Link camera was focused, and the Data Allow placed over the limbus so that they were mutually perpendicular to each other (i.e. with the Data Allow passing through the centre of the pupil, Fig. 5.3). A significant point to note for the calibration procedure of the tremor movement system was that its sensitivity to the eye movement was inversely proportional to the length of the Data Allow line. This meant that the sensitivity was doubled if the Data Allow line was halved. In this chapter, all the results were collected when this length was set at 10us.

Whilst the tests were being carried out, a U-Matic video recorder was switched on. The waveforms of the eye movements were recorded on the moving paper plotter and the frequency and amplitude of nystagmus determined from the waveforms.

For Case 1, the video tape was replayed at a later date, and the test repeated. This showed that the results of both the live and recorded tests of Case 1 compared adequately, and therefore the recorded test was not necessary for the other cases. However, their live tests were recorded on video tape.

The Y-deflection setting and the speed of the plotter's paper are indicated in all the figures. In all cases, the iris of the eye covered approximately 47 percent of the T.V. screen.

From the traces obtained in the T.V. test system, downward plots represent eye rotation to the right and upward plots represent eye rotation to the left and vice-versa for the photoelectric system.

Analysis of the nystagmus curves, obtained from the following cases by the X-Y plotter, yields information as to the direction of the nystagmus, its frequency and amplitude, and also on the speed of the fast and slow phases of each cycle of nystagmus.

**Case studies (p.219-246)
have been removed for
data protection reasons**

CHAPTER 8

DISCUSSION AND CONCLUSIONS

In the preceding chapters the different methods of monitoring relative and tremor eye movements, ranging from the early, simple and unsophisticated methods to the modern, highly complex and relatively expensive systems, have been discussed. From an understanding of the concepts involved in measuring ocular movements, and an appreciation of the video technology now available, a new system has been designed which automates the measurement of relative eye movements and, at the same time, provides a more sophisticated method for monitoring and recording eye tremor movements than those previously used.

The results obtained from the use of this system suggest that the system may contribute further to research into particular areas of eye anomalies. However, a more critical appraisal is required to establish its true limits and potentials, especially in terms of its feasibility and effectiveness in the light of the previous methods used for monitoring ocular eye movements. A number of problems are known to be associated with earlier methods and these are contrasted and compared with the value, speed of operation, expense, accuracy and precision of this new system.

Various aspects of the system including its ease and simplicity of use, its setting-up time, and space and calibration requirements, will be discussed and a number of modifications to the system with a view to enhance its efficiency further will be suggested.

8.1 Relative Eye Movements

8.1.1 Observations Arising from Case Studies

The automated system proved to be capable of producing accurate results when tested on normal eyes, as shown for example by Cases 1 and 2. Differences between the results of these two latter cases were due to certain muscle imbalances, within the acceptable normal range.

The results also indicated that the system was capable of detecting muscle imbalances in the subjects. For example, the subject in case 3, displayed over-action in the left inferior oblique muscle of her right eye (Fig. 7.8) which appeared to compensate for the under-action of her left eye (Fig.7.9).

For some subjects, the field of the test had to be extended beyond ± 15 degrees. In Cases 6 and 7, the examination and plots were extended even further to isolate the action of the muscle with possible paresis. This extension was only recorded when a more detailed result was required.

A comparison of the results obtained using the designed, automated system with the Lees screen test confirmed the validity and accuracy of the former. Furthermore, the described system whilst being useful for subjects suffering from multiple sclerosis, may also prove valuable for further research into more complex eye muscle disorders (for example subject in Case 8).

8.1.2 Further Points for Discussion

1. High frequency micro-processors operate at about 11MHz, but the time needed to acquire, process and execute the data is about

lus, which is too slow to produce the Hess chart. The use of Video Display Generators and other ancillary I.C.s, together with a fast microprocessor would, however, enable the chart to be generated. The advantage of the current design is that the chart was generated in real time with the minimum number of I.C.s, thus helping to keep production costs down.

2. The use of computers in producing the Hess chart was also considered by Thomson (1985). He confirmed that an automated system would retrench the costs, but expressed his preference for a dedicated system (Appendix XIV). However, there are many advantages of using a microprocessor, including the printing of alpha-numerics on the chart, and the expansion or reduction of particular sections of the chart.

3. In the test, the Hess chart could have been presented to the patient as an ordinary cardboard drawing, but was instead presented on a T.V. screen. This had a number of distinct advantages which included the ability to show one square dot at a time, allow the square dots to be presented in different sequences, give the flexibility of changes to the design, keep the running costs down, and provide other services such as presenting reading text to the patient. Furthermore, the flexibility of printing alpha-numerics, using a micro-computer, and the adjustable brightness and width of the square dots according to personal requirements and preference of the patient was catered for.

4. The light pen, which was constructed especially for this purpose, hovered over the surface of the monitor. The patient's hand was, therefore, able to rest comfortably against the face of the T.V. monitor, instead of being suspended in mid air, allowing

for a more accurate positioning of the pen This was particularly true in the case of children.

5. Accurate printing of the dots of the Hess Chart by the system, (Fig. 7.5), was achieved by feeding the chart signal to the light pen circuits, thus verifying the accuracy and linearity of both the chart generator and light pen circuits.

For the purpose of research, however, it should be noted that the patients in Cases 2, 4, 5, 6 and 7, whilst wearing polarized goggles, were tested when each T.V. screen was polarised in one direction and a semi-reflecting mirror was used to combine the images of both T.V. screens. This improvement was helpful in that the use of different goggles for testing each eye, obviated the need for movement and alignment of the mirror or of the T.V. screens. Furthermore, the system could be rapidly checked for calibration by skimming over the test procedure without the need for the patient to wear goggles. This modification did not pose any problem for the patients, but the associated disadvantages of wearing goggles remained.

8.1.3 Comparisons of the Automated system

and Previous Methods

The design of the system used to monitor relative eye movements was based on the information presented (Chapter 2). The advantages of the automated system, over the previous methods, are outlined below:

1. The accuracy of the Hess-Lancaster screen or the Lees screen tests were limited by:

- a) The relative sizes of the pointer and screen,

b) the positioning of the 50cm long rod or green torch on the Hess screen, and

c) the estimation of the position of the pointer rod and its transfer onto the diagnosis tangent chart by the orthoptist.

In general, ophthalmologists consider an accuracy of ± 5 degrees to be acceptable for the test. In the automated system, however, the accuracy was increased to ± 0.5 degree since the pointer rod was replaced by a more controllable light pen. This was also due to the results being directly plotted onto the screen, without human interference or misjudgement.

Furthermore, as discussed in section 2.1.10, the accuracy of the Lees screen test was found to be mainly dependent on the orthoptists' experience. Orthoptists with little experience may inaccurately estimate the position of the patient's pointer, compared with experienced orthoptists who may look for previously defined trends and tendencies. However, since the use of the automated system did not depend upon the previous experience of the orthoptist, many of these discrepancies were removed, thus contributing to a more accurate measurement of relative eye movement.

2. Although the capital cost of the automated system is comparable to the Lees screen system (approximately £300), it may have a higher initial cost than some of the other methods mentioned previously. Undoubtedly, however, its running costs are lower than the other systems since its automation removes the need for an orthoptist to be present during the test (Appendix XIV).

3. The speed of performance was greatly increased by the automated sequences of the test, which reduced the running costs of the test even further. For example, each of the patients, except in Cases 1 and 3, were tested in only 3 to 4 minutes. In contrast, the duration of the test for the patients in cases 1 and 3 lasted about 7 to 10 minutes because all the available points in the chart were plotted. The procedure of the test was explained to the patients in only 2 to 3 minutes.

In addition to the rapidity of the test, only small and simple alterations are required to test the other eye. For the mirror system, it was only necessary to slide Monitor B and its mirror horizontally over their supporting rails (Fig. 7.2), compared with the goggle system, whilst only the goggles needed to be changed. The simplicity of these changes helped considerably to keep the duration of the test short.

4. This rapid test required a shorter period of concentration by the patient. This helped the patient to remain relaxed whilst producing more accurate measurements. In addition, the concentration of the patient was further maintained during the test by superimposing the light pen over the square dot.

5. For both the patient and orthoptist, the automated system proved to be an easier method to use, to the extent that the orthoptist can even test his own relative eye movements. Indeed, the patient is only required to place the light pen on the target and press a button to record its position, without the assistance of the orthoptist. The ease with which the test is conducted, contributed further to the reduction in test duration.

for further analysis.

6. The amount of space required by the system was also greatly reduced. In contrast to the Lees screen test, for example, which requires at least 4m^2 , the automated system was neatly packed into a mobile desk-sized apparatus which occupied less than 1m^2 .

7. As in the Lees screen test, complete dissociation between the two eyes was maintained by the use of mirrors.

8. For any practical monitoring system, the permitted eye rotation must extend by at least 20 degrees (section 1.2.3.d). The automated system allowed eye rotations of upto ± 20 degrees vertically, and ± 30 degrees horizontally.

9. The calibration and setting-up time of the system was minimal and relatively simple. With the degree of accuracy, and the amount of information generated, this system proved to have required a very short calibration period. For the purpose of the current tests, the system was calibrated for each individual with a testing period of only 2 minutes for the use of polarized goggles or 5 minutes for the mirror system. The system also benefited from a brief periodical check on the horizontal and vertical linearity of the T.V. monitors.

10. The operating system was also found to be highly flexible and versatile, allowing any part(s) of the test to be carried out without the need to proceed with the entire test. This also allowed other tests to be conducted simultaneously.

11. The results of the test were presented in a form familiar to and acceptable by ophthalmologists. In addition, it was also possible for the results to be fed into a micro-computer

for further analysis.

12. The results of the test were obtained in real time, thus increasing the swiftness of the test.

13. The patients did not experience any pain or discomfort during the test.

14. The accuracy of the test was not dependent upon the degree of intelligence of the patient. The test proved to be valuable within a wide age range of patients (11 to 76 years old).

15. The test did not require any specific lighting conditions. The T.V. monitors provided the necessary ambient light. The lack of sufficient light in the Lees or the Hess-Lancaster screen tests was often a cause for concern, since the transfer of the patient's response had to be recorded onto the diagnostic chart under dim illumination.

16. The Hess diagnostic chart was automatically plotted by the system which obviated the need to purchase pre-printed paper or to spend time aligning the chart on the X-Y plotter.

17. The automated system was not based on an equi-distant chart, but rather on the Hess tangent screen which is known to produce a more representative measure of eye rotation.

18. No modifications to the commercial components used in the system were necessary. An ordinary T.V. monitor and an X-Y plotter were adequate to produce the necessary results.

19. It is hoped that the results will contribute to further research into the anomalies of ocular movements (Appendix

XIII).

Many of the disadvantageous features of the previous methods of measuring relative eye movements have been avoided in the design of the automated system, without compromising any of the other beneficial features. Indeed, the automated system appeared to be as valuable as, if not more valuable than, the previous methods.

8.2 Eye Tremor Movements

By using the designed system nystagmus was, for the first time, measured with a high accuracy under normal lighting conditions, without any attachments to the eye and in the absence of the patients' goggles.

8.2.1 Observations Arising from Case Studies

It is not the intention of this thesis to interpret the diagnostic results obtained from the case studies but rather to use the results obtained in order to assess the value of the system.

The negligible differences between the live and recorded test results for Case 1 (Figs. 7.27 and 7.28) demonstrated that the system's ability to record the movements of the subject's eye and to perform the test at a later date served as a powerful tool; provided freedom to the orthoptist and reduced doubts over the interpretation of the results.

The testing of subjects wearing reading spectacles by the photoelectric system, proved to be a difficult task especially for eye deflections over 10 degrees. However, as shown by the

results from Case 2, the designed T.V. system was not hampered by such obstacles (Figs. 7.30 and 7.31).

It was also found that the output from the photoelectric system drifted as the upper eye-lid of the subject moved during fixation. However, the results from the patient in Case 4 indicated that this problem was also eliminated in the newly designed T.V. method.

It was evident, as shown by the study of Case 5, that the test procedure could not be standardised. The outcome from one set of results determined the pattern of the next stage of the test. It was therefore necessary for the test results to be available in real time.

The equipment and test procedure were also observed to induce behavioural changes in the patients. There was a direct relationship between concentration and nystagmus frequency as well as amplitude. This was demonstrated by the subject in Case 6, where there was a decrease in nystagmus amplitude and increase in frequency during periods of concentration. Concealing the T.V. camera was, therefore, necessary for any reliable results.

In patients with squints, (Cases 4 and 7) drifts were observed in the eye under test, whilst the normal eye was fixating, which could have been avoided by covering the normal eye.

In all the Cases studied, the results obtained provided the necessary information required by an orthoptist for the diagnosis of various disorders, including the differentiation between left/right-beating or pendular types of nystagmus. In addition,

details of the presence of various components of frequencies and amplitudes, including the speed of the fast and slow phases, could be determined.

8.2.2 Further Points for Discussion

1. Although nystagmus has been taken as the main example for the application of this system, other eye measurements including the pursuit eye movements by random to-and-fro target movement (Takahashi, 1984) are also possible. In contrast, saccadic eye movements, could not be measured by this system due to their high frequencies which range from 15 to 200Hz (Bahill, 1981).

2. The system was first tested using an artificial eye with a 0.5 degree rotation (Fig. 7.18). The average amplitude of the recorded waveform was measured at 9mm. The y-deflection setting of the plotter was set at 400mV/100mm, and the speed of the paper, moving in the negative x-direction, was set at a rate of 10mm/s. The voltage applied to the plotter was therefore calculated to be 36mV, and was obtained when the eye was illuminated with a 40watt light bulb. The aperture of the lens was set at f:11, with the diameter of the iris covering 42 per cent of the width of the T.V. screen.

Similarly, the system was tested for 1.0 and 1.5 degrees eye rotation (Fig. 7.19), giving average recorded amplitudes of 18 and 27mm, respectively. As all the other settings were unchanged, the voltages applied to the plotter were calculated to be 72 and 108mV, respectively. The above measurements were all obtained when the frequency of eye rotation was set at 3Hz. Under these conditions, the system can easily detect tremors less than 0.5 degree (Fig. 7.18), although the system was initially designed

for eye rotations greater than 1 degree.

3. The artificial eye was manually oscillated at a frequency of about 0.5Hz for amplitudes of 0.5, 1 and 2 degrees, whilst maintaining all the other conditions used previously at a frequency of 3Hz (Fig. 7.20). This resulted in the recorded amplitudes measuring 14, 29 and 60mm, and giving voltages of 56, 116 and 240mV, respectively. As these values were different from the measurements at 0.5 degree rotation and 3Hz frequency, a framework was necessary to rapidly convert the vertical distances obtained from the traces into degrees of eye movement. The plot of the frequency response of the total system including the plotter (Fig. 7.25) was therefore used as a convenient conversion table. For an average nystagmus of less than 3Hz, the conversion gave a mean value of 70 to 80mV per degree of eye rotation.

4. The change in the characteristics or pattern of nystagmus with time presented another variable which required attention. To overcome this, the calibration duration had to be reduced and the subject be tested at several different intervals.

5. Amongst the many advantages of the system was its ability to simultaneously measure relative and tremor eye movements, thus helping to keep down the costs and enabling eye tremor movements to be recorded under normal behavioural conditions.

8.2.3 Comparisons of the Designed T.V. System

and Previous Methods

The eye tremor detector was designed on the basis of the considerations presented earlier (Chapter 5), together with the use of video technology. Below, the particular features of the

designed system which make it a more valuable method of monitoring eye tremors are discussed in contrast to the previous methods of detection:

1. Except for the contact lens method which had an accuracy of a few seconds of arc (Young, 1975), the previous methods had an accuracy of approximately 0.5 degree. In contrast the designed tremor detection system exhibited accuracy greater than 0.5 degree of eye movement, sufficient to monitor nystagmus movements with an amplitude of more than 1 degree of eye rotations. This accuracy can, however, be further enhanced by reducing the length of the Data Allow line or by increasing the size of the eye on the T.V. screen using zoom lenses. All the results were obtained with the iris covering 42 per cent of the width of the T.V. screen when the artificial eye was used, and 47 per cent with a real eye.

2. Although, the frequency of nystagmus seldom exceeded 3Hz, the frequency response of the designed system was tested between 2 and 11Hz to establish its full potential over this range. The results (Fig. 7.23), demonstrated the frequency response of the designed electronic circuits dropping in amplitude by only 1dB (curve 'a'), which could be due to the signal generator used. According to this curve the circuits have an excellent frequency response.

This was confirmed by the similarities between the frequency response of the circuits with the 3-Pole Low Pass filter, represented by curve 'b', and the filter.

The frequency response of the circuits together with the filter and camera was represented by curve 'c'. In this case,

however, the limbus pulse was produced by using the rotating eye, rather than being artificially produced as in the above case. By ensuring that the amplitude of rotation was 1 degree at each recorded frequency, the possibility of the rotating eye introducing non-linearity into the frequency response was removed. The fall in amplitude, which at 13dB decade^{-1} was considerably more than in curve 'b', suggested that the camera was introducing a large amount of non-linearity into the frequency response. The extent of this inefficiency was shown by the frequency response of the camera, curve 'd', obtained from the difference in amplitude between curves 'b' and 'c'.

Since the detected frequency was sampled during the Data Allow, which is only on one line in every field, then the sampling frequency and field frequency are both equivalent to 50Hz. The maximum frequency detectable by a T.V. system is half the sampling or field frequency (25Hz), and is therefore the limiting factor of the frequency response of the T.V. camera. However, from the camera's frequency response curve the fall in amplitude was found to be 9dB decade^{-1} . This suggested that the limiting factor was not only the field frequency but also the lag characteristics of the camera tube. As indicated in section 7.6, the approximate roll-off frequency of the tube was about 4.5Hz and, as a result, there was a sharp fall in the frequency response of the camera after 4Hz.

Of course, this problem can be easily overcome by differentiating the limbus pulse waveform and considering only the first pulse as the new limbus pulse (Fig. 8.1). It was found that there was no lag in the tube when the limbus travelled towards the black, but the lag showed as an exponential decay in

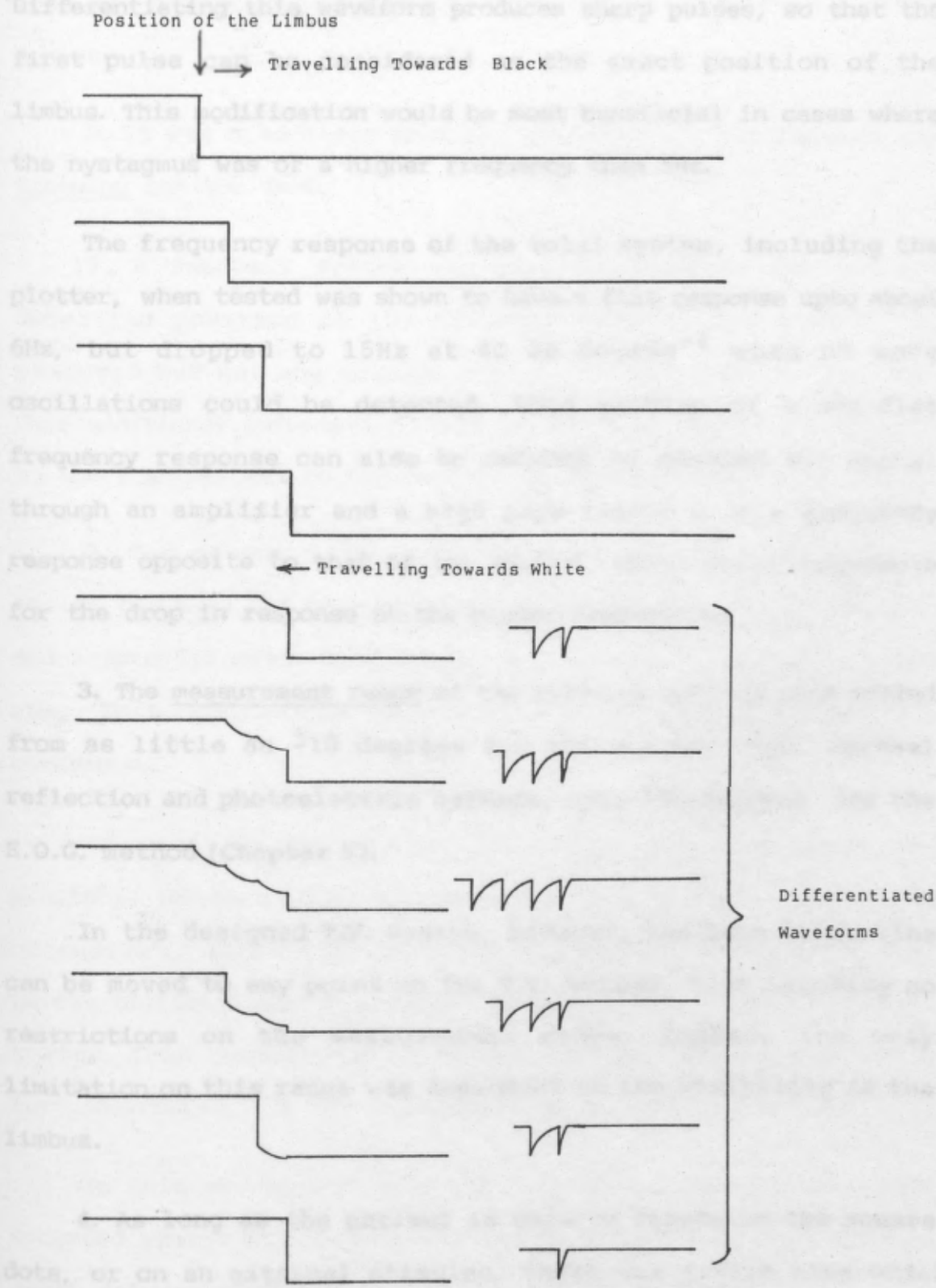


**Fig. 8.1 Limbus Pulse Waveform with Lag in the Camera Tube
and its Differentiation**

the pulse waveform when the limbus traveled towards the white. Differentiating this waveform produces sharp pulses, so that the first pulse can be considered as the exact position of the limbus. This modification would be most beneficial in cases where the nystagmus was of a higher frequency than 5Hz.

The frequency response of the total system, including the plotter, when tested was shown to have a flat response upto about 6Hz, but dropped to 15Hz at 40 dB decade⁻¹ when no more oscillations could be detected. This problem of a non-flat frequency response can also be reduced by passing the signal through an amplifier and a high pass filter with a frequency response opposite to that of the system, which would compensate for the drop in response at the higher frequencies.

3. The measurement range of the previous methods used varied from as little as ± 10 degrees for the contact lens, corneal reflection and photoelectric methods, upto ± 50 degrees for the E.O.G. method (Chapter 5).

In the designed T.V. system, however, the Data Allow line can be moved to any point on the T.V. screen, thus imposing no restrictions on the measurement range. Indeed, the only limitation on this range was dependent on the visibility of the limbus.

4. As long as the patient is able to fixate on the square dots, or on an external stimulus, there was little else which required the patient's cooperation.

5. This system enjoyed the advantage of non-interference with the subjects' vision, maintaining normal conditions for him

and assisting him to relax. The subjects used in these case studies were fully aware of the presence of the T.V. camera, but this was hidden in order not to distract or cause them further anxiety.

6. It was also clear that the patients did not require any training for the test.

7. A feedback system was used to indicate the precise detecting position of the limbus, ensuring the limbus was measured but not any corneal reflex or land-marks on the eye. This additional information shown on the T.V. monitor was helpful to the practitioner to rapidly set-up and calibrate the system.

8. One of the major advantages of this system was that whilst the head had to be stabilised with the aid of a chin rest and a forehead metal bar, no attachments were required for the eyes. This contributed considerably to the subject's normal eye behaviour.

Young (1975) stated that: "Most of the devices currently available for monitoring eye movements are by their very nature obtrusive". These previous methods generally caused discomfort to the patients, and made them aware that their eyes were being tested. This contributed to changes in eye behaviour which in turn interfered with the intended measurements.

In this new tremor detector system the measurements were recorded whilst the patient was occupied with plotting the Hess chart and was therefore unaware of the T.V. camera.

In addition, as there were no attachments to the eyes, the risk of eye infection was reduced.

9. Although the capital cost of the system was not lower than the previous methods, the more superior results obtained make it a far more cost-effective system. Apart from the practitioners' time, the only additional running expense of the system was the cost of the video tape and plotting paper.

10. Compared with the previous methods, the speed at which the test was conducted was improved. The duration of the test averaged 12 minutes for each eye deflected to ± 30 degrees. The subjects did not find the test either cumbersome or laborious.

11. The tests were conducted and the results obtained in real time which was essential for determining the next step in the test procedure.

12. The results were presented in their simplest form, ready for analysis both manually and with the aid of a computer.

13. This part of the system was designed to integrate with that used for measuring relative eye movements, and did not add to the space already occupied by the latter system. There was no special requirement for any rooms, whether dark, heavily lit or equipped with either infrared or other invisible light source. The system also obviated the need for any special or expensive apparatus or large working areas, or for a specially qualified medical practitioner or highly trained technician.

14. Neither the age nor intelligence of the subject influenced the procedure or results of the test.

15. The light emitted from the T.V. screens, used for the measurement of relative eye movements, produced sufficient

illumination for the detection of eye tremor movements. The ambient lighting conditions did not affect the procedure of the test.

16. One modification was required for the commercial instruments, which was to improve the design of the head amplifier of the T.V. camera (Appendix IX). This modification is not necessary when the newly designed and commercially available black and white cameras are to be used. The incorporation of such cameras, into the system will help to keep the capital cost of the system even lower.

17. A further advantage of this method of tremor detection was the facility to record the image of the eye on a video recorder. The recording can be reviewed repeatedly, permitting nystagmus to be detected and its waveforms to be plotted over and over again. By having the picture of the eye available during the test, the nystagmus can be differentiated from the confounding effects of blinking, head movements, eye movements and Data Allow adjustments. The video recording also provided flexibility to the orthoptist who can perform the test at a convenient time, even when the patient is absent. Recording the eye itself instead of its waveforms, as used in some existing methods, provided the opportunity to repeat the test in the event of mistakes. In addition, the audio tracks of the video recorder were also used to record relevant audio information, for example the date and personal data of the patient, together with any instructions given to him.

This also facilitated the possibility of better interpretation of the results, especially when different

sensitivities were selected on the moving paper plotter.

18. The stability of the whole system was checked by feeding an artificially generated limbus pulse to it, and measuring the system noise (section 6.4.VI). The results showed that this noise was negligible when compared to the noise from the video waveform of the T.V. camera.

19. The test was easily conducted whilst the patient continued to wear his reading glasses, as shown by the comparison of Figs. 7.30 and 7.31. Results, from two of the patients tested both with and without their spectacles, demonstrated the versatility of the T.V. system. The wearing of glasses had proved to be difficult in some of the previous methods, especially the photoelectric system where the wearing of two sets of spectacles was necessary.

20. The detection of eye movements was based on the position of the limbus, found to be the best land-mark on the surface of the eye, especially since the contrast between the sclera and the iris is known to be greater than that for the iris and the pupil. As pupil size does not remain constant, but is dependent on the intensity of the ambient light and the psychological state of the subject, the boundary between the iris and the pupil is not suitable for the detection of eye tremors.

21. It is expected that the results obtained from the use of the system will contribute considerably to further research into the anomalies of ocular movements (Appendix XIII).

8.3 Conclusions

Over the last several years, little progress has been made in successfully measuring relative and tremor eye movements. Progress in these fields had been mainly hampered because (1) the manual methods of measuring eye movements were accepted without significant modification or development and (2) any such modifications were based on existing classical methods and ignoring the modern technologies available.

The new system was designed and constructed by a better understanding of (a) physiology of the eye and its physical characteristics, (b) basic theories of ocular measurement, and (c) an appreciation of the benefits of video technology. The system automated the measurement of relative eye movements and provided a better means of measuring complex eye tremor movements, such as nystagmus.

The system, primarily designed for use in ophthalmic departments of hospitals, was relatively cheap to construct and extremely cost-effective. It was mobile, compact and easy to set up, calibrate and operate. The complete system was tested with several patients and found to be accurate, effective and versatile. The results were consistent, reproducible and objective.

The data generated permits the identification of particular ocular anomalies and, through frequent tests, determines the progress of the condition with a view to improving the diagnosis. Such information is useful in determining the natural course of recovery of conditions, such as ocular muscle paresis, and the subsequent course of action required. Consecutive ocular

used as a basis for further development which may lead to measurements for instance, must prove stable over six-month, before any surgery is undertaken to correct any residual disorder of ocular eye movements (Roper-Hall, 1978). This system would be ideal to collate such data.

The rapidity and the low running costs of the test may permit its widespread utilisation on all hospital patients suffering from various ocular disorders, and serve to provide a case history for each patient and also a more precise diagnosis of the disorder. It would also be valuable in the study of population trends and allow more extensive and comprehensive statistical analyses of particular disorders.

This system appears to provide a useful tool for advancement in the field of clinical practice and research. The equipment, and results obtained from its use, have already been used by the Bedwell Consultancy and the London Refraction Hospital. As with the more conventional methods, the use of this equipment was limited by its particular specifications. For example, the frequency response of the T.V. system, did not allow the measurement of high frequency saccadic movements. Although the use of video technology has, because of its low signal to noise ratio, been criticized in the past, the case studies have indicated that such technology, can generate highly valuable and informative data.

The overall superiority of this system over the previous methods of eye measurements can only be unequivocally demonstrated after more extensive tests conducted over a period of time. Indeed, simple modifications to the current system, as discussed in the following Chapter, may allow it to be

used as a basis for further development which may lend to commercial production.

CHAPTER 9

RECOMMENDATIONS FOR FURTHER DEVELOPMENTS

The present system was adequate in providing sufficient information for analysis, however, a number of modifications and additions can be made to improve its versatility and use further.

One of the most beneficial additions can be the incorporation of a micro-processor, which will increase the versatility of the system especially for the measurement of relative eye movements.

The production of an accurate Hess Chart, by programming the micro-processor to calculate the coordinates of each square dot, would be a very desirable feature. However, this would have to be used in conjunction with a Video Display Generator, such as A.M.I. 568047 or Motorola MC6847Y with high resolution graphics, which will considerably increase the cost of the system. Additionally, the micro-processor would enable the Hess chart to be displayed on the video screen in any size and form, and allow alphanumeric data to be printed on the chart.

The micro-processor can also be used to draw lines between the square dots of the Hess chart, in a manner similar to that used in hospitals. The results can be presented in different formats, depending on the preference of the practitioner.

For the measurement of relative eye movements an analogue output can, instead of being sent to the X-Y plotter, be fed into a computer, fitted with relevant software, so as to assist the analysis of results.

CHAPTER 9

RECOMMENDATIONS FOR FURTHER DEVELOPMENTS

The present system was adequate in providing sufficient information for analysis, however, a number of modifications and additions can be made to improve its versatility and use further.

One of the most beneficial additions can be the incorporation of a micro-processor, which will increase the versatility of the system especially for the measurement of relative eye movements.

The production of an accurate Hess Chart, by programming the micro-processor to calculate the coordinates of each square dot, would be a very desirable feature. However, this would have to be used in conjunction with a Video Display Generator, such as A.M.I. S68047 or Motorola MC6847Y with high resolution graphics, which will considerably increase the cost of the system. Additionally, the micro-processor would enable the Hess chart to be displayed on the video screen in any size and form, and allow alphanumerics to be printed on the chart.

The micro-processor can also be used to draw lines between the square dots of the Hess chart, in a manner similar to that used in hospitals. The results can be presented in different formats, depending on the preference of the practitioner.

For the measurement of relative eye movements an analogue output can, instead of being sent to the X-Y plotter, be fed into a computer, fitted with relevant software, so as to assist the analysis of results.

For tremor movements, the output of the designed system can be fed to the "Micro-computer - Based Eye Movement Automatic Analysis System", developed by Morra (1982), which analyses the fast and slow phases of the nystagmus trace using digital filtering techniques. Nystagmus can also be evaluated by its energy 'E', which is a product of its amplitude and frequency and a measure of the angular deviation of the eye in one direction per unit time (Ohms, 1939). The output of this system can, with the aid of a micro-processor, be utilised to give the value of 'E'. The frequency and amplitude of nystagmus can also be translated into digital read-outs, and be printed adjacent to the appropriate square dots of the relative diagnostic chart.

Because the camera used for measuring tremor movements did not produce a flat frequency response, a correction factor was required to compensate for the error. This factor must be a mirror image of the frequency response curve of the camera. With the aid of such a curve the exact amplitude of nystagmus can be calculated for individual patients. Such a correction factor can only be used when a micro-processor is utilised, otherwise an additional circuit will be required.

The light pen can be replaced either by a computer mouse or the use of a T.V. touch screen, both of which would require a micro-processor. Alternatively, the light pen can be replaced by a helmet method of detecting the direction of gaze. Here, the patient would be able to point at the chart by simple observation, with the plotter's pen following the patient's eye rather than the light pen.

If the need to measure relative movements under dynamic

conditions should arise, the chart monitor can be used to display a moving target. In this case the patient follows the target with his light pen, and discrepancies found between the pen and target would be a measure of dynamic relative movement.

To enhance both the ease of use of the system and improve the patient's comfort, better chin and head rests and a modified mirror system needs to be introduced. These would also increase the accuracy of the test. For further simplification, the X-Y plotter pen switch and the switch used for moving to the next square dot can be combined into a single switch incorporating an automatic delay circuit. Such a switch can be constructed on an infra-red remote control unit, which would be especially useful when certain areas of the chart need to be rechecked.

For improved tremor detection, several modifications can be incorporated into the system. Nystagmus is only detected when the Data Allow line is placed over the limbus, where there is a voltage level change moving from the white into the black. However, the circuits can be slightly modified so that the Data Allow can be placed over the limbus where the opposite changes of voltage occur. Vertical nystagmus can also be measured if a vertical Data Allow line is generated by the system.

Additionally, automatic tracking of the eye and head can be accomplished by the use of a circuit which tracks a bright point on the video waveform. Hence, there would be no need for the Data Allow line to be manually positioned over the limbus. Attempts have already been made, at The City University, to produce such a tracking system. The automatic positioning of the Data Allow can also be accomplished by a feedback technique (Rashbass, 1960).

The system can also be further improved by the use of C.C.D. camera tubes with reduced noise under low light conditions.

The results were adequate for clinical evaluation, but for purpose of research, the determination of the exact position of the datum-line would be needed. It would be more advantageous to move the camera to the position where eye fixation is required, and allow the eyes to follow a bright dot suspended over the centre of the camera lens. By observing the image of the eye in the monitor, the approximate position of the datum-line can then be determined.

The U-Matic recorder, already utilised in the system, can be employed to record additional information such as the patient's personal data, the position of the eye being tested and details of the camera. These additional data may either be directly recorded on the two available audio channels, or be modulated, multiplexed and then recorded on the tape.

The method used in this system to detect eye tremor movements can also be adopted on both eyes simultaneously, so as to determine their instantaneous positions. The difference between the two output signals would thus represent a measure of their relative movement.

It should be noted, however, that not all the above modifications can necessarily be introduced simultaneously into the system. Furthermore, many of the modifications may be incorporated at the expense of other more advantageous features of the system, such as its low production costs, small space requirement and simplicity of use.

APPENDIX I

Beam Chart

Beam chart equations and the calculation of the square data are demonstrated in this appendix (see, 1900).

When $x = 0$, $y = a \tan A$ and $x = a \cot A$, $y = 0$ are the coordinates of the points where the beam enters and leaves the chart. The coordinates of the points where the beam enters and leaves the chart are $x = a \cot A$, $y = 0$ and $x = 0$, $y = a \tan A$ respectively. The equations for the beam are:

$$x^2 \cot^2 A - y^2 = a^2 \quad \text{(1)}$$

$$y^2 \cot^2 B - x^2 = a^2 \quad \text{(2)}$$

When $a = 1000$, equation (1) is:

$$\cot^2 A x^2 - y^2 = 1000^2 \quad \text{(3)}$$

and multiplying equation (2) by $\cot^2 A$:

$$-\cot^2 A x^2 + \cot^2 A \cot^2 B y^2 = 1000^2 \cot^2 A \quad \text{(4)}$$

Adding (3) & (4):

$$y^2 (\cot^2 A \cot^2 B - 1) = 1000^2 (1 + \cot^2 A)$$

$$y = \sqrt{\frac{1000^2 (1 + \cot^2 A)}{\cot^2 A \cot^2 B - 1}}$$

and

$$x = \sqrt{\frac{1000^2 + y^2}{\cot^2 A}}$$

which may be evaluated by substituting the values of A and B .

When $x = 0$, $y = 1000 \tan A$ and $x = 1000 \cot A$, $y = 0$ are the coordinates of the points where the beam enters and leaves the chart. The coordinates of the points where the beam enters and leaves the chart are $x = 1000 \cot A$, $y = 0$ and $x = 0$, $y = 1000 \tan A$ respectively. The equations for the beam are:

APPENDIX I

Hess Chart

Hess chart equations and the calculations of the square dots are demonstrated in this Appendix (Hess, 1908).

When x = coordinate for angle of elevation A and y = coordinate for angle of azimuth B - Since curves are hyperbole quarters are symmetrical and x and y are replaceable on 45° axis - the equations for the Hess Screen curves are:

$$x^2 \cot^2 A - y^2 = a^2 \quad (\text{x-axis vertical}) \quad \dots (1)$$

$$y^2 \cot^2 B - x^2 = a^2 \quad (\text{y-axis horizontal}) \quad \dots (2)$$

when a = radius = 50cms equation (1) is:

$$\cot^2 A x^2 - y^2 = 2500 \quad \dots (3)$$

and multiplying equation (2) by $\cot^2 A$

$$-\cot^2 A x^2 + \cot^2 A \cot^2 B y^2 = 2500 \cot^2 A \quad \dots (4)$$

adding (3) & (4):

$$y^2 (\cot^2 A \cot^2 B - 1) = 2500 (1 + \cot^2 A)$$

$$y = \sqrt{\frac{2500(1 + \cot^2 A)}{\cot^2 A \cot^2 B - 1}}$$

and

$$x = \sqrt{\frac{2500 + y^2}{\cot^2 A}}$$

which may be evaluated by substitution when y has been found.

When $x = 0$, $y = a \tan B$ and when $y = 0$, $x = a \tan A$. The values of x 's and y 's were found when A and B were 5° , 10° , 15° , 20° , 25° and 30° . The table below is the list of the values when a is equal to 300mm.

APPENDIX II

B	A	0	5	10	15	20	25
T.V. System							
0	x = 0	0	26.3	52.9	80.4	109.2	139.9
	y = 0	0	0	0	0	0	0
5		0	26.3	53.1	80.7	109.7	140.5
		26.2	26.3	26.7	27.2	27.9	29.0
10		0	26.7	53.7	81.7	111.1	142.5
		52.9	53.1	53.7	54.7	56.4	58.6
15		0	27.2	54.8	83.4	113.6	146.0
		80.4	80.7	81.7	83.4	86.0	89.4
20		0	27.9	56.4	86.0	117.2	151.1
		109.2	109.7	111.1	113.6	117.2	122.3
25		0	29.0	58.6	89.4	122.3	158.1
		139.9	140.5	142.5	146.0	151.1	158.1
30		0	30.3	61.4	94.0	129.0	167.7
		173.2	174.1	176.8	181.5	188.5	198.4

The above table helped in reproducing the Hess chart on the screen of a T.V. monitor used in conjunction with the chart generator circuits.

There is a Field Blanking period separating every field. This period is when one field is completed and the electron beam is flying back to the top left hand corner of the T.V. screen. The duration of the Field Blanking is 1.666 μ sec. (1/600).

APPENDIX II

T.V. System

A full television picture consists of 625 lines which is termed a frame. A frame occurs every $1/25^{\text{th}}$ of a second and as this may produce flickering, the 625 lines are divided into two fields - one containing odd lines and the other even lines, so there are two fields per frame and each field is thus $1/50^{\text{th}}$ of a second. A complete field waveform with its field sync. pulses is shown in Fig.II.1.

The time between field sync. pulses is 20ms. But each field has $625/2$ lines, therefore the time taken for each line is, 20mS divided by 312.5 which gives 64uS. This is the time for the electron beam to travel from the left side of a T.V. screen to the right side and 'fly-back'.

The fly-back time is 10.5us and the screen is blanked during this time. This leaves a scanning time of 53.5us when information can be displayed over the T.V. screen.

There is a Field Blanking period separating every field. This period is when one field is completed and the electron beam is flying back to the top left hand corner of the T.V. screen. The duration of the Field Blanking is 1.6mS. (Kiver, 1973).

Fig. II.3 T.V. Video Equalizing and Broad Pulses

The diagram illustrates a complete field waveform. It shows a series of horizontal sync pulses. The line numbers are labeled above the pulses: 623, 624, 625, 1, 2, 3, 4, 15, and 16. A break symbol (two parallel diagonal lines) is placed between line 4 and line 15, indicating that the waveform continues between these lines.

Fig. II.1 A Complete Field Waveform

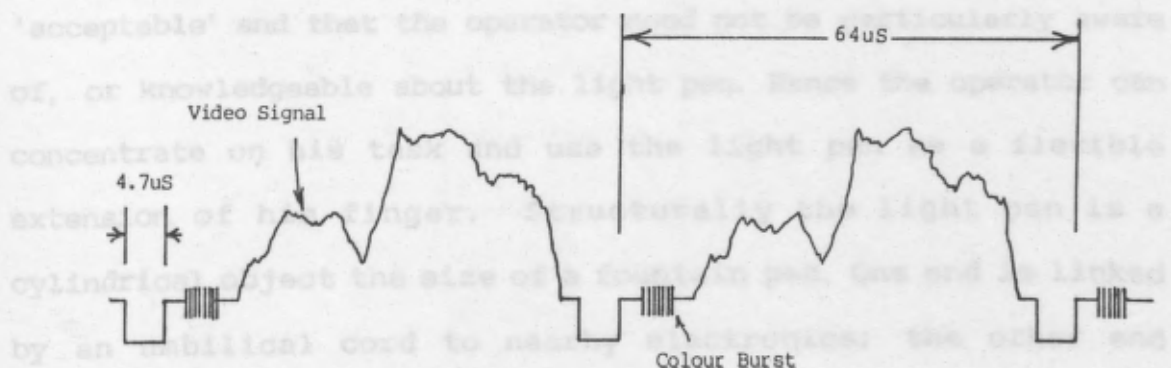


Fig. II.2 Two Lines of Video Waveform

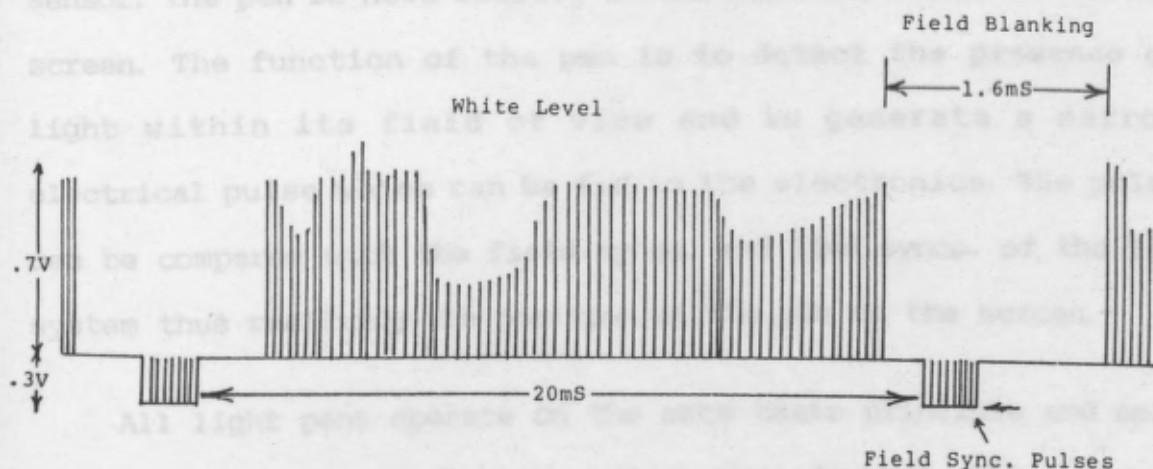


Fig. II.3 T.V. Video Equalising and Broad Pulses

APPENDIX III

Light Pen

A light pen is a special type of pointer used with cathode ray tube (CRT) displays. By using a light pen an operator can select pictures on the CRT. This is similar to drawing with a conventional pen on paper. The light pen is an effective and popular means of interfacing the human operator with the display screen. A light pen system is pleasing to the human operator in the sense that the response time to execute commands is 'acceptable' and that the operator need not be particularly aware of, or knowledgeable about the light pen. Hence the operator can concentrate on his task and use the light pen as a flexible extension of his finger. Structurally the light pen is a cylindrical object the size of a fountain pen. One end is linked by an umbilical cord to nearby electronics; the other end contains an exposed light-detecting device such as a photodiode or a phototransistor. A lens may be placed before the light sensor to collect and focus light on the active area of the sensor. The pen is held loosely in the hand and aimed at the CRT screen. The function of the pen is to detect the presence of light within its field of view and to generate a narrow electrical pulse which can be fed to the electronics. The pulse can be compared with the field syncs. and line syncs. of the T.V. system thus realizing the position of the pen on the screen.

All light pens operate on the same basic principle and only differ in structural detail rather than theory. The several functional elements required are shown diagrammatically in Figure IIIa. Light from a CRT spot enters the pen through an optical

system which collects light from the source and limits the field of view of the pen. Limiting of the field is obviously necessary so that a single CRT spot may be identified.

The simplest limiting method is to provide an aperture which permits the photodetector to "see" only a conical region in space. The deficiency herein is that the acceptance area of the pen is a function of the distance of the pen from the CRT.

Light from the CRT which passes through the optical system impinges on the photodetector. The photodetector converts the radiant energy to an electrical signal. In solid state pens, the photodetector may be either a photodiode or phototransistor. A phototransistor has the advantage of providing gain. Due to the relative slow response of a phototransistor, a photodiode coupled with a wide band amplifier replaces the phototransistor in high-speed pens.

Amplified signals are applied to a voltage comparator circuit. This circuit discriminates between random noise generated by the detector and amplifier circuit and desired signals by means of an adjustable voltage threshold. Signals which exceed the threshold produce a standard output pulse through pulse shaping and output circuits.

A light pen having a particular photodetector and other electronic circuits has a sensitivity to light from a CRT. This may be related to the following equation:

$$S = \frac{A_p \cdot A_c \cdot E}{4\pi \cdot d^2 \cdot \lambda \cdot \eta}$$

where S is considered to increase with improved sensitivity.

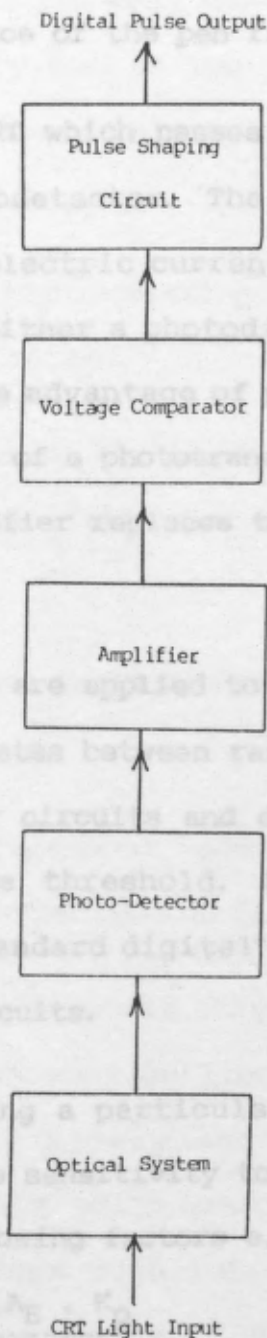


Fig. IIIa Light Pen Functional Elements

system which collects light from the source and limits the field of view of the pen. Limiting of the field is obviously necessary so that a single CRT spot may be identified.

The simplest limiting method is to provide an aperture which permits the photodetector to "see" only a conical region in space. The deficiency herein is that the acceptance area of the pen is a function of the distance of the pen from the CRT.

Light from the CRT which passes through the optical system impinges on the photodetector. The photodetector converts the radiant energy to an electric current. In solid state pens, the photodetector may be either a photodiode or phototransistor. A phototransistor has the advantage of providing gain. Due to the relative slow response of a phototransistor, a photodiode coupled with a wide band amplifier replaces the phototransistor in high-speed pens.

Amplified signals are applied to voltage comparator circuit. This circuit discriminates between random noise generated by the detector and amplifier circuits and desired signals by means of an adjustable voltage threshold. Signals which exceed the threshold produce a standard digital output pulse through pulse shaping and output circuits.

A light pen having a particular photodetector and other electronic circuits has sensitivity to light from a CRT. This may be related to the following factors e.g:

$$S \propto \frac{A_R \cdot A_E \cdot K_P}{l^2 \cdot f \cdot T}$$

In general, a light pen is activated when its photodiode is subjected to photons radiating from a CRT screen. The position

The factors are:

A_R - Area of pen that is capable of receiving light. The advantage of a lens system is immediately obvious. Without lenses, A_R is simply the area of the photodetector.

l - Distance of the pen from the light source, which strongly influences sensitivity due to the spreading of the available light energy over an area. This increases as the square of the distance.

A_E - Area of the light-emitting source, which is related to the brightness of the screen.

f - Frequency at which the light source is refreshed which is related to the average light output proportional to the peak light intensity.

T - Time delay from excitation of source until a pen output is obtained.

K_p - A constant dependent upon the characteristics of the phosphor and more importantly, the persistence characteristics.

Operation of a light pen is only possible because of a very large ratio of peak to average light output of the phosphor. Phosphors which decay slowly and are classified as 'long' persisting are normally quite poor for light pen operation whereas 'short' phosphors with rapid decay are most suitable (Information Control Corporation, IBM).

In general, a light pen is activated when its photodiode is subjected to photons radiating from a T.V. screen. The position

of the output pulse, from the light pen, relative to the line and field drive waveforms driving the T.V. system, is an indication of the location of the light pen on the T.V. screen.

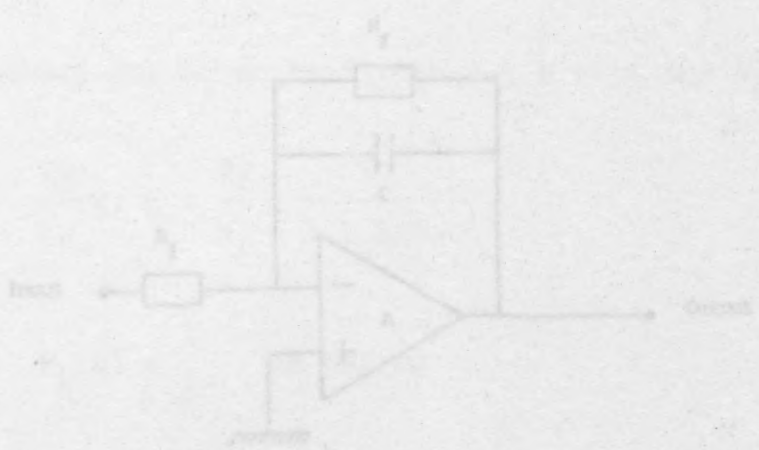
The circuit for a simple RC integrator is shown below:



Its step function is:

$$\frac{V_o}{V_i}(t) = 1 - e^{-\frac{t}{CR}} \quad \text{when } CR = \text{time constant}$$

The circuit for an integrator using an op-amp. is shown below:

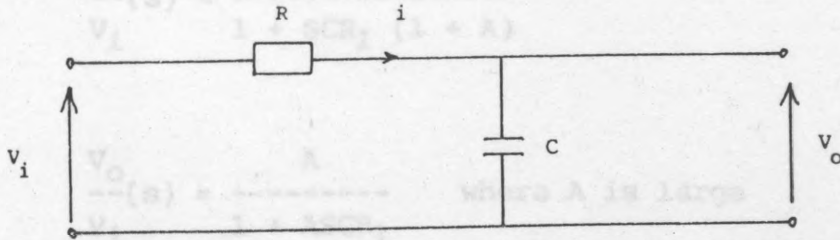


Its transfer function is:

APPENDIX IV

Integrators

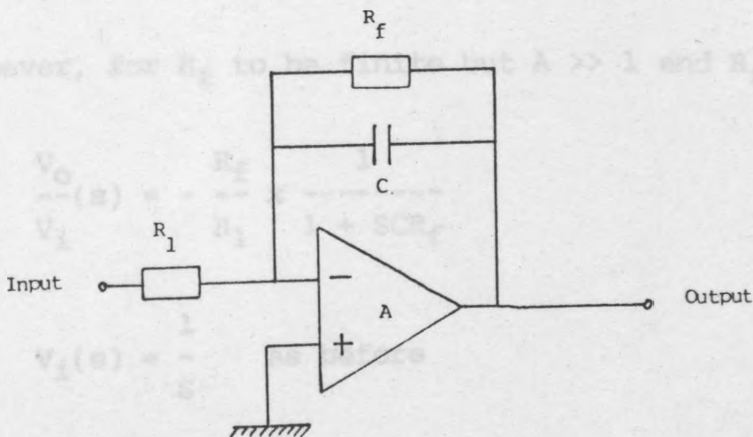
The circuit for a simple RC integrator is shown below:



Its step function is:

$$V_o(t) = V_i \left(1 - e^{-\frac{t}{CR}} \right) \quad \text{when } CR = \text{time constant}$$

The circuit for an integrator using an op-amp. is shown below:



Its transfer function is:

$$\frac{V_O}{V_i}(s) = - \frac{1}{R_1} \times \frac{1}{sC + \frac{1}{R_f} + \frac{1}{A} \left(\frac{1}{R_1} + sC + \frac{1}{R_f} \right)}$$

Hence, using a d.c. negative feedback the transfer function

and the time constant were multiplied by the closed loop voltage

then $\left(R_f/R_1 \right)$ of the op-amp.

$$\frac{V_O}{V_i}(s) = \frac{A}{1 + sCR_1 (1 + A)}$$

$$\frac{V_O}{V_i}(s) = \frac{A}{1 + ASCR_1} \quad \text{where } A \text{ is large}$$

for $V_i(s) = \frac{1}{s}$ a step

$$V_O(t) = -A \left(1 - e^{-\frac{t}{ACR_1}} \right)$$

Thus using an op-amp. had the advantage of the transfer function and the time constant CR_1 being multiplied by the open loop voltage gain (A) of the amplifier.

However, for R_f to be finite but $A \gg 1$ and $R_f/R_1 = a$

then
$$\frac{V_O}{V_i}(s) = - \frac{R_f}{R_1} \times \frac{1}{1 + sCR_f}$$

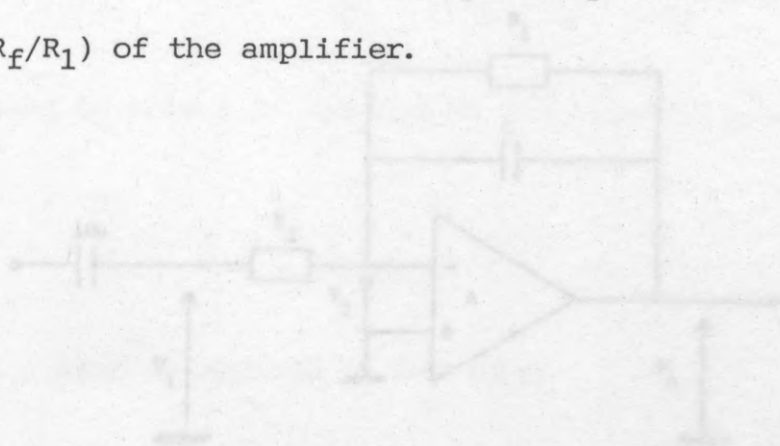
for $V_i(s) = \frac{1}{s}$ as before

$$V_O(t) = - \frac{R_f}{R_1} \left(1 - e^{-\frac{t}{CR_f}} \right)$$

$$V_O(t) = -a \left(1 - e^{-\frac{1}{aCR_1} t} \right)$$

Op-Amp Integrator and Amp Non-Linearity

Hence, using a d.c. negative feedback the transfer function and the time constant were multiplied by the closed loop voltage gain (R_f/R_1) of the amplifier.



$$R_f = 2.7M\Omega$$

$$C = 1nF$$

$$R_1 = 7.35k\Omega$$

$$A = \text{open loop gain} = 10^5$$

$$[V_2(s) - V_1(s)] \frac{1}{R_1} + [V_2(s) - V_O(s)] \left(sC + \frac{1}{R_f} \right) = 0$$

$$V_2(s) \left(\frac{1}{R_1} + sC + \frac{1}{R_f} \right) - V_1(s) \frac{1}{R_1} - V_O(s) \left(sC + \frac{1}{R_f} \right) = 0 \quad (1)$$

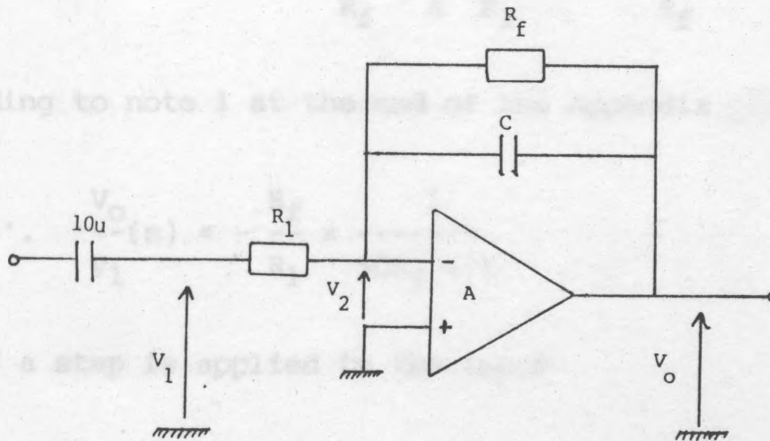
$$\text{but } V_O(s) = -AV_2(s)$$

$$-\frac{V_O(s)}{A} \left(\frac{1}{R_1} + sC + \frac{1}{R_f} \right) - V_1(s) \frac{1}{R_1} + V_O(s) \left(sC + \frac{1}{R_f} \right) = 0$$

collecting terms:

APPENDIX V

Op-Amp Integrator and Ramp Non-Linearity



$$R_f = 2.7\text{M-Ohms}$$

$$C = 1\text{nF}$$

$$R_1 = 7.5\text{K-Ohms}$$

$$A = \text{open loop gain} = 10^5$$

$$[V_2(s) - V_1(s)] \frac{1}{R_1} + [V_2(s) - V_0(s)] \left(sC + \frac{1}{R_f} \right) = 0$$

$$V_2(s) \left(\frac{1}{R_1} + sC + \frac{1}{R_f} \right) - V_1(s) \frac{1}{R_1} - V_0(s) \left(sC + \frac{1}{R_f} \right) = 0 \quad (1)$$

$$\text{but } V_0(s) = -AV_2(s)$$

$$- \frac{V_0(s)}{A} \left(\frac{1}{R_1} + sC + \frac{1}{R_f} \right) - \frac{V_1(s)}{R_1} - V_0(s) \left(sC + \frac{1}{R_f} \right) = 0$$

collecting terms:

$$V_O(s) \left[SC + \frac{1}{R_f} + \frac{1}{A} \left(\frac{1}{R_1} + SC + \frac{1}{R_f} \right) \right] = - \frac{V_1}{R_1}(s)$$

$$\frac{V_O}{V_1}(s) = - \frac{1}{R_1} \times \frac{1}{SC + \frac{1}{R_f} + \frac{1}{A} \left(\frac{1}{R_1} + SC + \frac{1}{R_f} \right)}$$

According to note 1 at the end of the Appendix when $A \gg 1$.

$$\therefore \frac{V_O}{V_1}(s) = - \frac{R_f}{R_1} \times \frac{1}{SCR_f + 1} = 0.01185$$

Now if a step is applied to the input

$$d_1(s) = \frac{1}{s}$$

$$\therefore V_O(s) = - \frac{R_f}{R_1} \times \frac{1}{s} \times \frac{1}{1 + SCR_f} = - \frac{R_f}{R_1} \left(\frac{1}{s} - \frac{CR_f}{1 + SCR_f} \right)$$

Transforming from S plane to T plane using Laplace transforms

$$\therefore V_O(t) = - \frac{R_f}{R_1} \left(1 - e^{-\frac{t}{CR_f}} \right)$$

expanding the bracket :

$$V_O(t) = - \frac{R_f}{R_1} \left\{ 1 - \left[1 - \frac{t}{CR_f} + \frac{1}{2} \left(\frac{t}{CR_f} \right)^2 + \dots \right] \right\}$$

$$V_O(t) = - \frac{R_f}{R_1} \left[\frac{t}{CR_f} - \frac{1}{2} \left(\frac{t}{CR_f} \right)^2 + \dots \right]$$

Higher terms are too small relative to first and second terms.

$$V_O(t) = - \frac{t}{CR_1} \left[1 - \frac{1}{2} \times \frac{t}{CR_f} \right]$$

∴ for non-linearity to be zero:

$$\frac{1}{2} \times \frac{t}{CR_f} \rightarrow 0 \quad t = \frac{1}{f} = \frac{1}{15.625 \text{ KHz}} \dots \text{line frequency}$$

$$C = 1nF \quad R_f = 2.7M\text{-Ohms}$$

$$\therefore \text{Non-linearity} = \frac{1}{2 \times 15625 \times 1 \times 10^{-9} \times 2.7 \times 10^6} = 0.01185$$

∴ Non-linearity is 1.2%

This was very small and had proven to be of no effect in practical terms.

To prevent the input offset voltage in the normal use of an op-amp introducing inaccuracy in the output, the impedances of the differential inputs were made equal. Since a 10uF d.c. decoupling capacitor was used then the only path to the earth on the negative input was through R_f and therefore the resistor in the positive input should be of the same order of R_f . However, since the input offset voltage was only 5mV and not amplified, the positive input was left shorted to the earth.

Note 1:

The ratio of output voltage to the input was found to be:

$$\frac{V_O}{V_1}(s) = - \frac{1}{R_1} \times \frac{1}{\left(\frac{1}{R_f} + sC \right) + \frac{1}{A} \left(\frac{1}{R_1} + sC + \frac{1}{R_f} \right)}$$

If $A \gg 1$:

and the pole is at $\frac{SCAR_f R_1 (1 + 1/A)}{AR_1 + R_f + R_1} = 1$

$$\frac{V_O}{V_1}(s) = - \frac{1}{R_1} \times \frac{1}{SC + \frac{1}{R_f} + \frac{1}{AR_1} + \frac{SC}{A} + \frac{1}{AR_f}}$$

and when $A = 10^4$ the constant $k = 50.8$ dB and the pole is at $\omega = 383$ Hz. Thus if $A > 10^4$ the value of the constant k and the pole

$$\frac{V_O}{V_1}(s) = - \frac{1}{R_1} \times \frac{1}{SC(1 + 1/A) + (\frac{1}{R_f} + \frac{1}{AR_1} + \frac{1}{AR_f})}$$

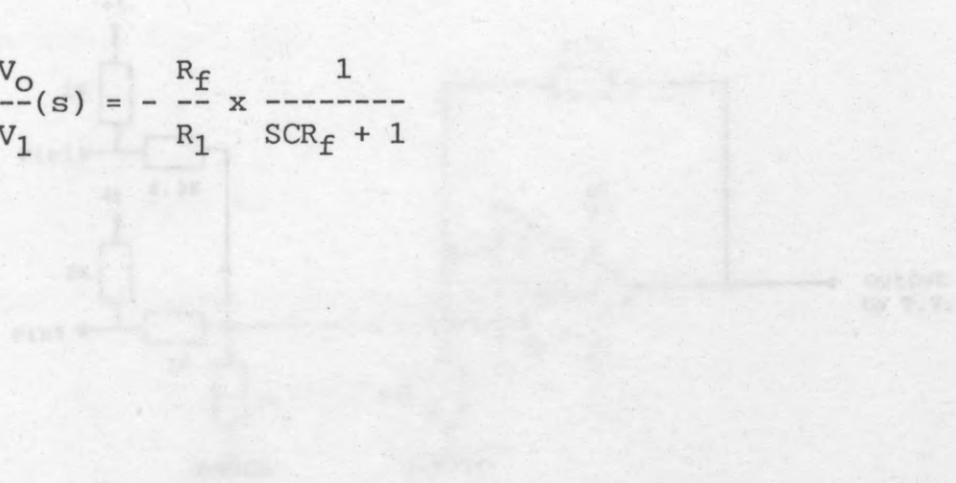
then we can write:

$$\frac{V_O}{V_1}(s) = - \frac{1}{R_1} \times \frac{1}{SC(1 + 1/A) + \frac{1}{\frac{1}{R_f} + \frac{1}{AR_1} + \frac{1}{AR_f}}}$$

$$\frac{V_O}{V_1}(s) = - \frac{1}{R_1} \times \frac{\frac{AR_f R_1}{AR_1 + R_f + R_1}}{\frac{SCAR_f R_1 (1 + 1/A)}{AR_1 + R_f + R_1} + 1}$$

$$\frac{V_O}{V_1}(s) = - \frac{AR_f}{AR_1 + R_f + R_1} \times \frac{1}{1 + \frac{SCAR_f R_1 (1 + 1/A)}{AR_1 + R_f + R_1}}$$

$$\text{the constant } k = \frac{AR_f}{AR_1 + R_f + R_1} = 51 \text{ dB}$$

$$\frac{\text{SCAR}_f R_1 (1 + 1/A)}{AR_1 + R_f + R_1} = 1$$
$$\frac{V_O}{V_1}(s) = -\frac{R_f}{R_1} \times \frac{1}{SCR_f + 1}$$


APPENDIX VI

Voltage Summation of an Op-Amp.

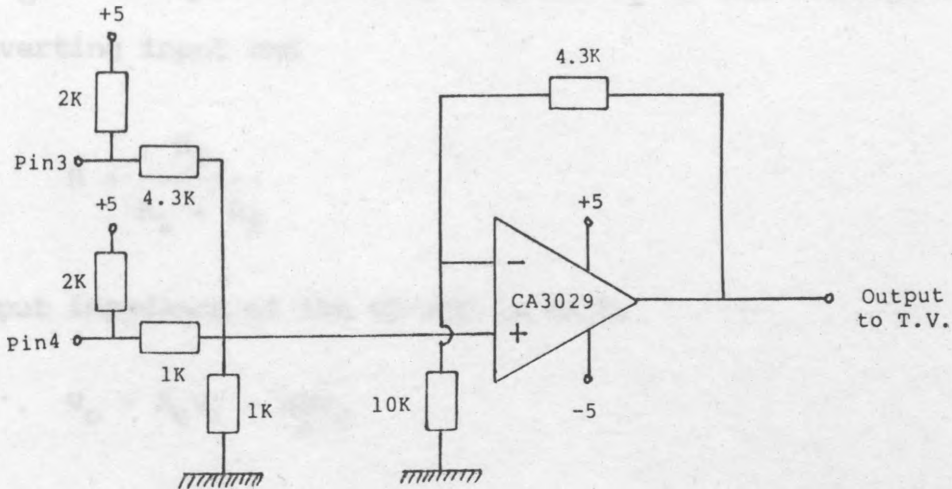


Fig. VI Raster Mix Circuit

The conventional op-amp adders use the inverting input because it is at virtual earth. However, since the output of the op-amp was not required to be inverted, and in order to save an inverting stage, the non-inverting input of the op-amp was used. The Ferranti T.V. pulse generator chip was an open collector output I.C. and the pull-up resistors were 2K-ohms, thus when the outputs were low the output resistances were zero and when they were high the output resistance were 2K-ohms.

The output of pins 3 & 4 were mixed by a matrix of resistors and an op-amp was used as a buffer stage between the T.V. pulse generator and the T.V. input. The values of the resistors were chosen experimentally to produce an optimum raster on the blank

monitor so that it was bright enough for the light pen to pick up the raster signal but meanwhile not too bright to hurt the eye of the patient.

The output voltage is

$$V_O = A_O (V_i - BV_O)$$

where A_O is the gain of the op-amp and V_i is the voltage at the non-inverting input and

$$B = \frac{R_1}{R_1 + R_f}$$

and input impedance of the op-amp is high.

$$\therefore V_O = A_O V_i - ABV_O$$

$$V_O = \frac{A_O V_i}{1 + A_O B}$$

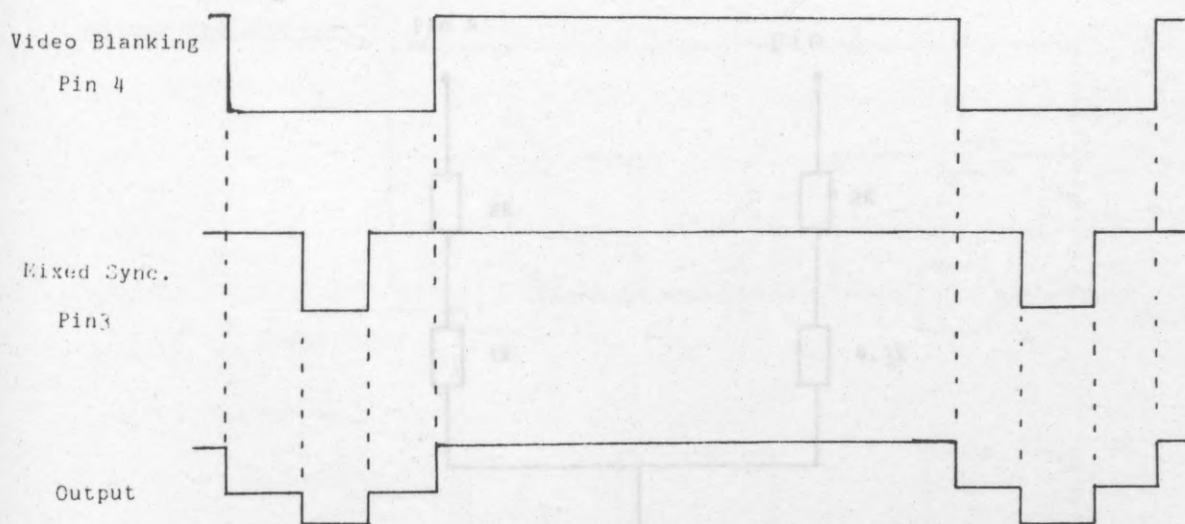
$$A_f = \frac{V_O}{V_i} = \frac{A_O}{1 + A_O B}$$

when $A_O \gg 1$ then

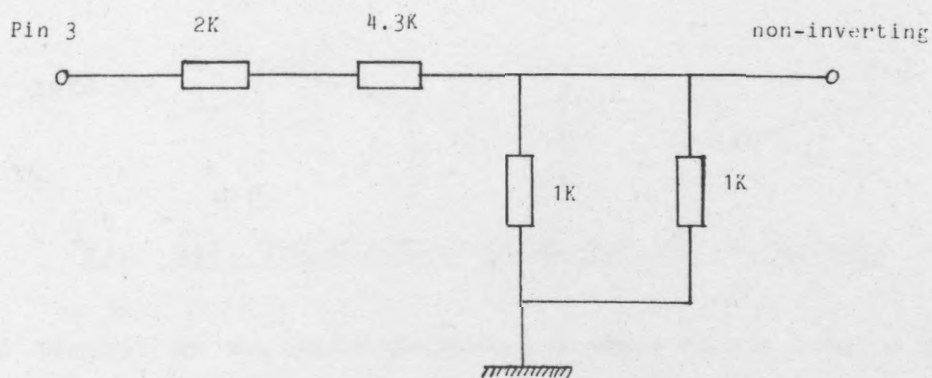
$$A_f = \frac{1}{B} = \frac{R_1 + R_f}{R_1} = \frac{10 + 4.3}{10}$$

$$\therefore \underline{A_f = 1.43}$$

Therefore the voltage at the non-inverting input was 1/14 of the voltage at pin 3 (5 Volts) which is 0.36V. When both pins 3 & 4 were high:



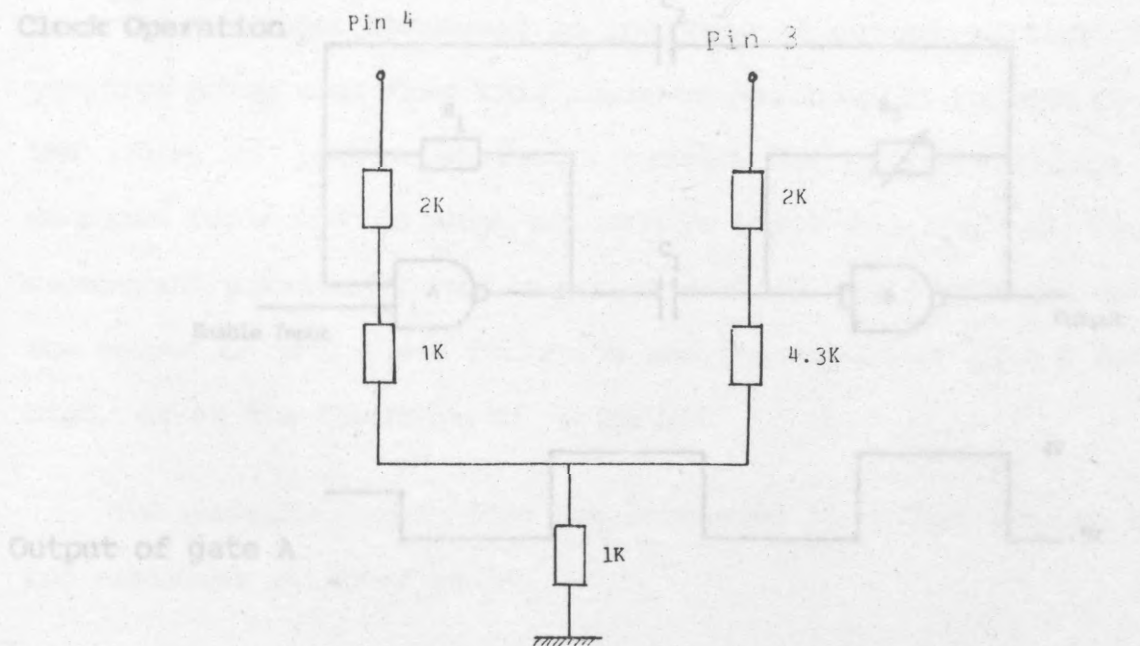
When both pins 3 & 4 were low the voltage at the non-inverting input of the op-amp was zero. When pin 3 was high and pin 4 was low: the voltage at the non-inverting input of the op-amp was $1/3$ of the voltage at pins 3 & 4, which is 1.7V.



Therefore the voltage at the non-inverting input was $1/14$ of the voltage at pin 3 (5 Volts) which is 0.36V. When both pins 3 & 4 were high:

APPENDIX VII

Clock Operation



Therefore the voltage at the non-inverting input of the op-am was $1/3$ of the voltages at pins 3 & 4, which is 1.7V.

Fig. VII The Clock Circuit and its Waveforms

The circuit shown above provided a 4kHz clock source to the clock divider. The waveforms showed that it was a form of multivibrator and that it thus used regenerative switching between its two output states. A qualitative description of the operation is as follows:

Initially both gates were in a state of equilibrium with their output voltages equal to their input voltages. When the enable input was put to logical 1, the output voltage of gate A

APPENDIX VII

Clock Operation

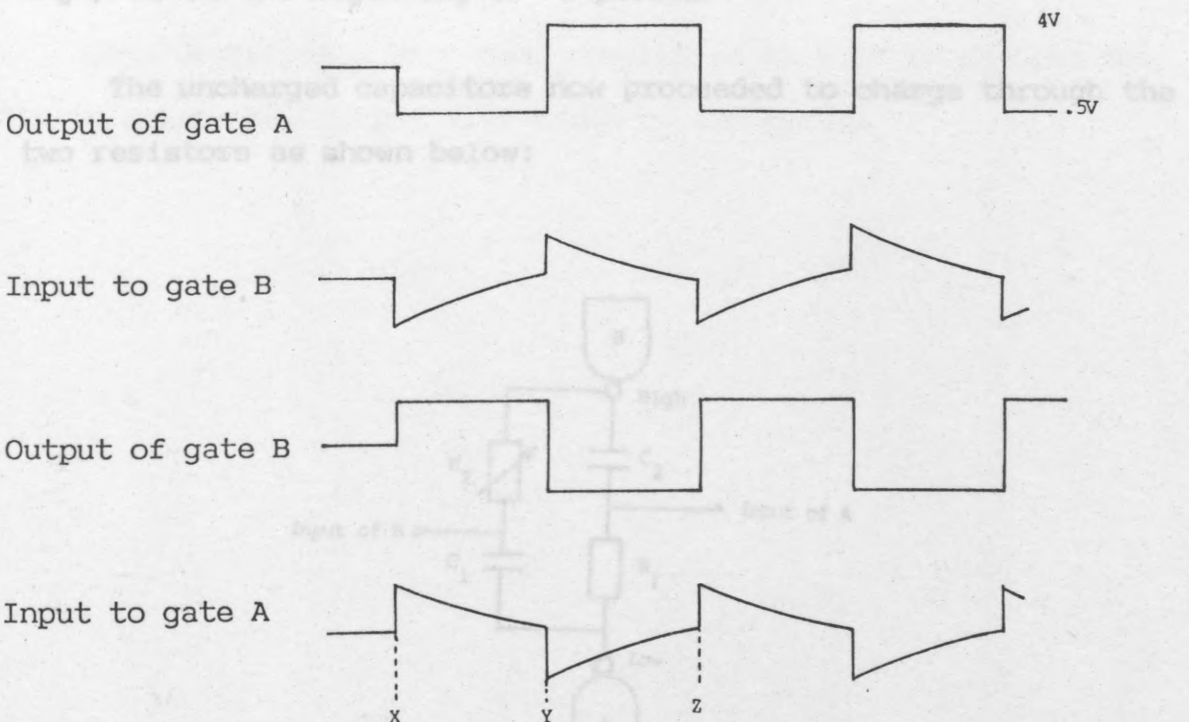
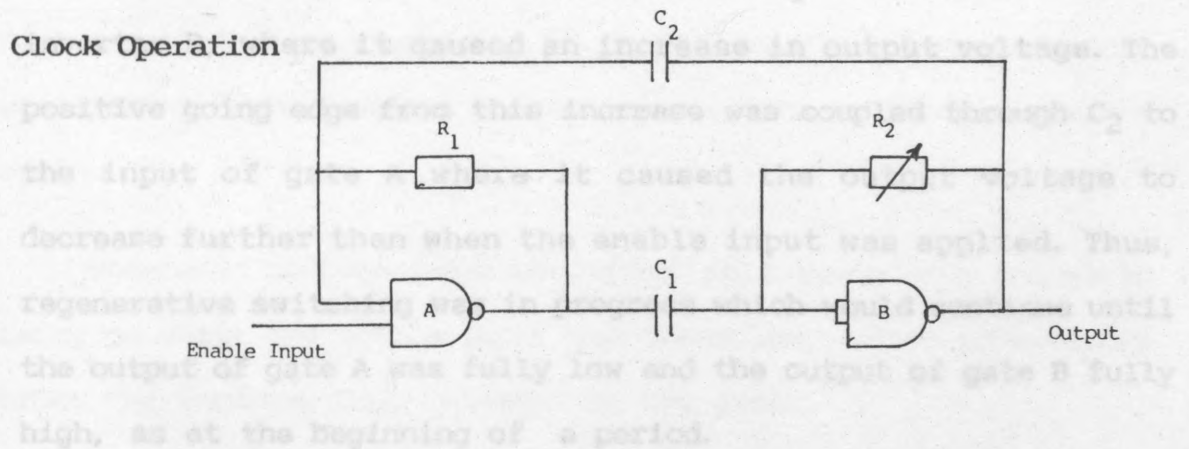


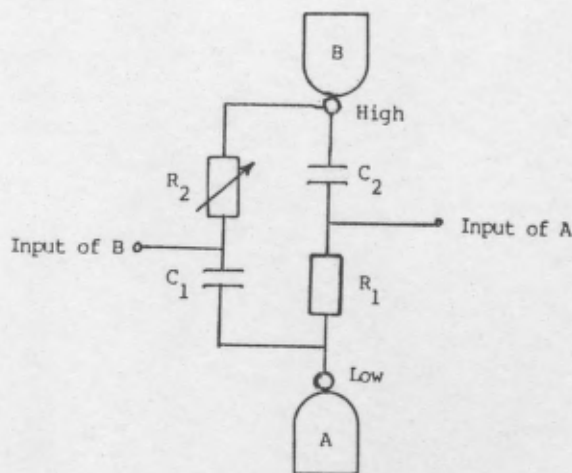
Fig. VII The Clock Circuit and its Waveforms

The circuit shown above provided a 4MHz clock source to the clock divider. The waveforms showed that it was a form of multivibrator and that it thus used regenerative switching between its two output states. A qualitative description of the operation is as follows:

Initially both gates were in a state of equilibrium with their output voltages equal to their input voltages. When the enable input was put to logical 1, the output voltage of gate A

would slightly decrease, though not fully to the '0' state. This negative going edge was coupled through C_1 to the input of the inverter B, where it caused an increase in output voltage. The positive going edge from this increase was coupled through C_2 to the input of gate A where it caused the output voltage to decrease further than when the enable input was applied. Thus, regenerative switching was in progress which would continue until the output of gate A was fully low and the output of gate B fully high, as at the beginning of a period.

The uncharged capacitors now proceeded to charge through the two resistors as shown below:



C_2 charged through R_1 with a time constant of $0.22\mu\text{s}$ and C_1 charged through R_2 with a variable time constant. Thus, the input voltage to gate A decayed and the input voltage to gate B rose as shown in the period of XY of the waveforms in Fig. VII, until the input voltages to the gates reached the threshold at which their outputs started to rapidly swing (i.e. the gates were in their active region where they had forward gain). Regenerative switching in the opposite direction to that previously occurred. This changed the output states of the two gates as shown at point

Y. After this, the capacitors started to charge again, though this time the output of gate B was low and the output of gate A high, so that they charged in the opposite directions to before until point Z was reached, where regenerative switching occurred again.

The oscillations were therefore self-sustaining and would carry on until the enable input was taken low, which effectively broke the feedback loop between the two gates.

This description is rather simplified in that it ignores the finite delays and output rise times of the gates.

Location	Data	Address(Hexa Dec.)	Data(Hexa Dec.)
00	10	60	A
01	11	61	B
02	12	62	C
03	13	63	D
04	14	64	E
05	15	65	F
06	16	66	10
07	17	67	11
08	18	68	12
09	19	69	13
10	20	70	14
11	21	71	15
12	22	72	16
13	23	73	17
14	24	74	18
15	25	75	19
16	26	76	1A
17	27	77	1B
18	28	78	1C
19	29	79	1D
20	30	80	1E
21	31	81	1F
22	32	82	20
23	33	83	21
24	34	84	22
25	35	85	23
26	36	86	24
27	37	87	25
28	38	88	26
29	39	89	27
30	40	90	28
31	41	91	29
32	42	92	2A
33	43	93	2B
34	44	94	2C
35	45	95	2D
36	46	96	2E
37	47	97	2F
38	48	98	30
39	49	99	31
40	50	100	32
41	51	101	33
42	52	102	34
43	53	103	35
44	54	104	36
45	55	105	37
46	56	106	38
47	57	107	39
48	58	108	3A
49	59	109	3B
50	60	110	3C
51	61	111	3D
52	62	112	3E
53	63	113	3F
54	64	114	40
55	65	115	41
56	66	116	42
57	67	117	43
58	68	118	44
59	69	119	45
60	70	120	46
61	71	121	47
62	72	122	48
63	73	123	49
64	74	124	4A
65	75	125	4B
66	76	126	4C
67	77	127	4D
68	78	128	4E
69	79	129	4F
70	80	130	50
71	81	131	51
72	82	132	52
73	83	133	53
74	84	134	54
75	85	135	55
76	86	136	56
77	87	137	57
78	88	138	58
79	89	139	59
80	90	140	5A
81	91	141	5B
82	92	142	5C
83	93	143	5D
84	94	144	5E
85	95	145	5F
86	96	146	60
87	97	147	61
88	98	148	62
89	99	149	63
90	100	150	64
91	101	151	65
92	102	152	66
93	103	153	67
94	104	154	68
95	105	155	69
96	106	156	6A
97	107	157	6B
98	108	158	6C
99	109	159	6D
100	110	160	6E
101	111	161	6F
102	112	162	70
103	113	163	71
104	114	164	72
105	115	165	73
106	116	166	74
107	117	167	75
108	118	168	76
109	119	169	77
110	120	170	78
111	121	171	79
112	122	172	7A
113	123	173	7B
114	124	174	7C
115	125	175	7D
116	126	176	7E
117	127	177	7F
118	128	178	80
119	129	179	81
120	130	180	82
121	131	181	83
122	132	182	84
123	133	183	85
124	134	184	86
125	135	185	87
126	136	186	88
127	137	187	89
128	138	188	8A
129	139	189	8B
130	140	190	8C
131	141	191	8D
132	142	192	8E
133	143	193	8F
134	144	194	90
135	145	195	91
136	146	196	92
137	147	197	93
138	148	198	94
139	149	199	95
140	150	200	96
141	151	201	97
142	152	202	98
143	153	203	99
144	154	204	9A
145	155	205	9B
146	156	206	9C
147	157	207	9D
148	158	208	9E
149	159	209	9F
150	160	210	90
151	161	211	91
152	162	212	92
153	163	213	93
154	164	214	94
155	165	215	95
156	166	216	96
157	167	217	97
158	168	218	98
159	169	219	99
160	170	220	9A
161	171	221	9B
162	172	222	9C
163	173	223	9D
164	174	224	9E
165	175	225	9F
166	176	226	A0
167	177	227	A1
168	178	228	A2
169	179	229	A3
170	180	230	A4
171	181	231	A5
172	182	232	A6
173	183	233	A7
174	184	234	A8
175	185	235	A9
176	186	236	AA
177	187	237	AB
178	188	238	AC
179	189	239	AD
180	190	240	AE
181	191	241	AF
182	192	242	B0
183	193	243	B1
184	194	244	B2
185	195	245	B3
186	196	246	B4
187	197	247	B5
188	198	248	B6
189	199	249	B7
190	200	250	B8
191	201	251	B9
192	202	252	BA
193	203	253	BB
194	204	254	BC
195	205	255	BD
196	206	256	BE
197	207	257	BF
198	208	258	C0
199	209	259	C1
200	210	260	C2
201	211	261	C3
202	212	262	C4
203	213	263	C5
204	214	264	C6
205	215	265	C7
206	216	266	C8
207	217	267	C9
208	218	268	CA
209	219	269	CB
210	220	270	CC
211	221	271	CD
212	222	272	CE
213	223	273	CF
214	224	274	D0
215	225	275	D1
216	226	276	D2
217	227	277	D3
218	228	278	D4
219	229	279	D5
220	230	280	D6
221	231	281	D7
222	232	282	D8
223	233	283	D9
224	234	284	DA
225	235	285	DB
226	236	286	DC
227	237	287	DD
228	238	288	DE
229	239	289	DF
230	240	290	E0
231	241	291	E1
232	242	292	E2
233	243	293	E3
234	244	294	E4
235	245	295	E5
236	246	296	E6
237	247	297	E7
238	248	298	E8
239	249	299	E9
240	250	300	EA
241	251	301	EB
242	252	302	EC
243	253	303	ED
244	254	304	EE
245	255	305	EF
246	256	306	F0
247	257	307	F1
248	258	308	F2
249	259	309	F3
250	260	310	F4
251	261	311	F5
252	262	312	F6
253	263	313	F7
254	264	314	F8
255	265	315	F9
256	266	316	FA
257	267	317	FB
258	268	318	FC
259	269	319	FD
260	270	320	FE
261	271	321	FF

APPENDIX VIII

Memories Contents

1. Memory A. in Hexa Decimal

Location	Data	Address(Hexa Dec.)	Data(Hexa Dec.)
00	10	00	A
01	11	01	B
02	12	02	C
03	16	03	10
04	17	04	11
05	20	05	14
06	21	06	15
07	22	07	16
08	23	08	17
09	24	09	18
10	25	A	19
11	26	B	1A
12	27	C	1B
13	34	D	22
14	35	E	23
15	36	F	24
16	37	10	25
17	38	11	26
18	39	12	27
19	40	13	28
20	41	14	29
21	42	15	2A
22	FF	16	FF
23	50	17	32
24	51	18	33
25	52	19	34
26	53	1A	35
27	54	1B	36
28	55	1C	37
29	56	1D	38
30	FF	1E	FF
31	66	1F	42
32	67	20	43
33	68	21	44
34	69	22	45
35	81	23	51
36	82	24	52
37	94	25	5E
38	95	26	5F
39	96	27	60
40	97	28	61
41	107	29	6B
42	108	2A	6C
43	109	2B	6D
44	110	2C	6E
45	111	2D	6F
46	112	2E	70
47	113	2F	71
48	121	30	79

49	122	31	7A
50	123	32	7B
51	124	33	7C
52	125	34	7D
53	126	35	7E
54	127	36	7F
55	128	37	80
56	129	38	81
57	136	39	88
58	137	3A	89
59	138	3B	8A
60	139	3C	8B
61	140	3D	8C
62	141	3E	8D
63	142	3F	8E
64	143	40	8F
65	146	41	92
66	147	42	93
67	151	43	97
68	152	44	98
69	153	45	99

2. Memory B in Hexa Decimal

000	51	8D	51	8D	51	60	6F	7E	8D	51	60	6F	7E	8D	60	6F
010	7E	60	6F	7E	11	CC	11	CC	11	CC	11	CC	23	BB	23	BB
020	23	BB	23	BB	34	AA	34	AA	34	AA	34	AA	44	9A	44	9A
030	44	52	8B	9A	44	52	8B	9A	52	61	6F	7D	8B	52	61	6F
040	7D	8B	61	6F	7D	61	6F	7D	14	CA	14	CA	14	CA	14	CA
050	26	B8	26	B8	26	B8	26	B8	36	A8	36	A8	36	45	99	A8
060	36	45	99	A8	45	53	8B	99	45	53	8B	99	53	61	6F	7D
070	8B	53	61	6F	7D	8B	61	6F	7D	61	6F	7D	16	C8	16	C8
080	16	C8	16	C8	27	B7	27	B7	27	37	46	98	A7	B7	27	37
090	46	98	A7	B7	37	46	54	61	7D	8A	98	A7	37	46	54	61
0A0	7D	8A	98	A7	54	61	6F	7D	8A	54	61	6F	7D	8A	6F	6F
0B0	17	28	B6	C7	17	28	B6	C7	17	28	38	46	54	8A	98	A6
0C0	B6	C7	17	28	38	46	54	8A	98	A6	B6	C7	38	46	54	61
0D0	6F	7D	8A	98	A6	38	46	54	61	6F	7D	8A	98	A6	61	6F
0E0	7D	61	6F	7D	18	29	38	46	54	61	6F	7D	8A	98	A6	B5
0F0	C6	18	29	38	46	54	61	6F	7D	8A	98	A6	B5	C6	18	29
100	38	46	54	61	6F	7D	8A	98	A6	B5	C6	18	29	38	46	54
110	61	6F	7D	8A	98	A6	B5	C6	61	6F	7D	61	6F	7D	38	46
120	54	61	6F	7D	8A	98	A6	38	46	54	61	6F	7D	8A	98	A6
130	17	28	38	46	54	8A	98	A6	B6	C7	17	28	38	46	54	8A
140	98	A6	B6	C7	17	28	B6	C7	17	28	B6	C7	6F	6F	54	61
150	6F	7D	8A	54	61	6F	7D	8A	37	46	54	61	7D	8A	98	A7
160	37	46	54	61	7D	8A	98	A7	27	37	46	98	A7	B7	27	37
170	46	98	A7	B7	27	B7	27	B7	16	C8	16	C8	16	C8	16	C8
180	61	6F	7D	61	6F	7D	53	61	6F	7D	8B	53	61	6F	7D	8B
190	45	53	8B	99	45	53	8B	99	36	45	99	A8	36	45	99	A8
1A0	36	A8	36	A8	26	B8	26	B8	26	B8	26	B8	14	CA	14	CA
1B0	14	CA	14	CA	61	6F	7D	61	6F	7D	52	61	6F	7D	8B	52
1C0	61	6F	7D	8B	44	52	8B	9A	44	52	8B	9A	44	9A	44	9A
1D0	34	AA	34	AA	34	AA	34	AA	23	BB	23	BB	23	BB	23	BB
1E0	11	CC	11	CC	11	CC	11	CC	60	6F	7E	60	6F	7E	51	60
1F0	6F	7E	8D	51	60	6F	7E	8D	51	8D	51	8D	00	00	00	00
200	00															

3. Memory C in Hexa Decimal

```

000 57 58 59 5A 56 55 54 47 37 27 67 77 87 48 39 2A
010 66 75 84 68 79 8A 46 35 24 5B 5C 5D 53 52 51 17
020 07 97 A7 1B 93 9B 13 49 4A 3A 4B 3B 2B 4C 3C 2C
030 1C 4D 3D 2D 1D 69 6A 7A 6B 7B 8B 6C 7C 8C 9C 6D
040 7D 8D 9D 78 88 89 98 99 9A 8A 9A 76 86 85 96 95
050 94 A6 A5 65 64 74 63 73 83 62 72 82 92 61 71 81
060 91 45 44 34 43 33 23 42 32 22 12 41 31 21 11 36
070 26 25 16 15 14 06 05 38 28 29 18 19 1A 08 09 00

```

4. Memory D in Hexa Decimal

```

000 9D FF FF FF FF FF 4D 3D 2D 1D FF 96 86 76 66 56
010 46 36 26 16 A9 95 85 75 65 55 45 35 25 15 A8 94
020 84 74 64 54 44 34 24 14 A7 93 83 73 63 53 43 33
030 23 13 A6 92 82 72 62 52 42 32 22 12 A5 91 81 71
040 FF FF FF FF FF FF 5D 6D 7D 8D 9C 8C 7C 6C 5C 4C
050 3C 2C 1C FF 9B 8B 7B 6B 5B 4B 3B 2B 1B 09 9A 8A
060 7A 6A 5A 4A 3A 2A 1A 08 99 89 79 69 59 49 39 29
070 19 07 98 88 78 68 58 48 38 28 18 06 97 87 77 67
100 61 51 41 31 21 11 FF FF FF FF FF FF FF FF FF
140 57 47 37 27 17 05 FF FF FF FF FF FF FF FF FF

```

APPENDIX IX

T.V. Camera Modification

A black and white Link camera was used. Its Signal to Noise ratio was measured to be about 17dB when the lens aperture was set to get maximum signal out just before clipping. Tests were performed to establish the source of this noise. Noise was traced back to the head amplifier. By removing the tube and performing other tests it was found that the majority of the noise was the result of the poor design of the head amplifier. The circuit of the head amplifier is shown in Fig. IX.1. The iris of the camera was opened until the output waveform of the tube was just before clipping (f:2). The Gamma correction was set at one and the Aperture correction was set for minimum noise.

To improve Signal to Noise ratio:

(a) The gain of the head amplifier had to be shifted to earlier transistors so that the noise produced by the second (S_2) and the third stage (S_3) was small compared to the signal out of the first stage.

(b) To reduce the sensitivity of the head amplifier so that the aperture of the lens had to be opened more and hence the tube being harder on. This was achieved by reducing the overall gain of the head amplifier.

It was noticed that the output of S_4 was much noisier than output of S_3 and since the d.c. voltage of 0.7V did not alter the functioning of S_6 , the collector of S_3 was shorted to the emitter

of S_4 , hence omitting S_4 .

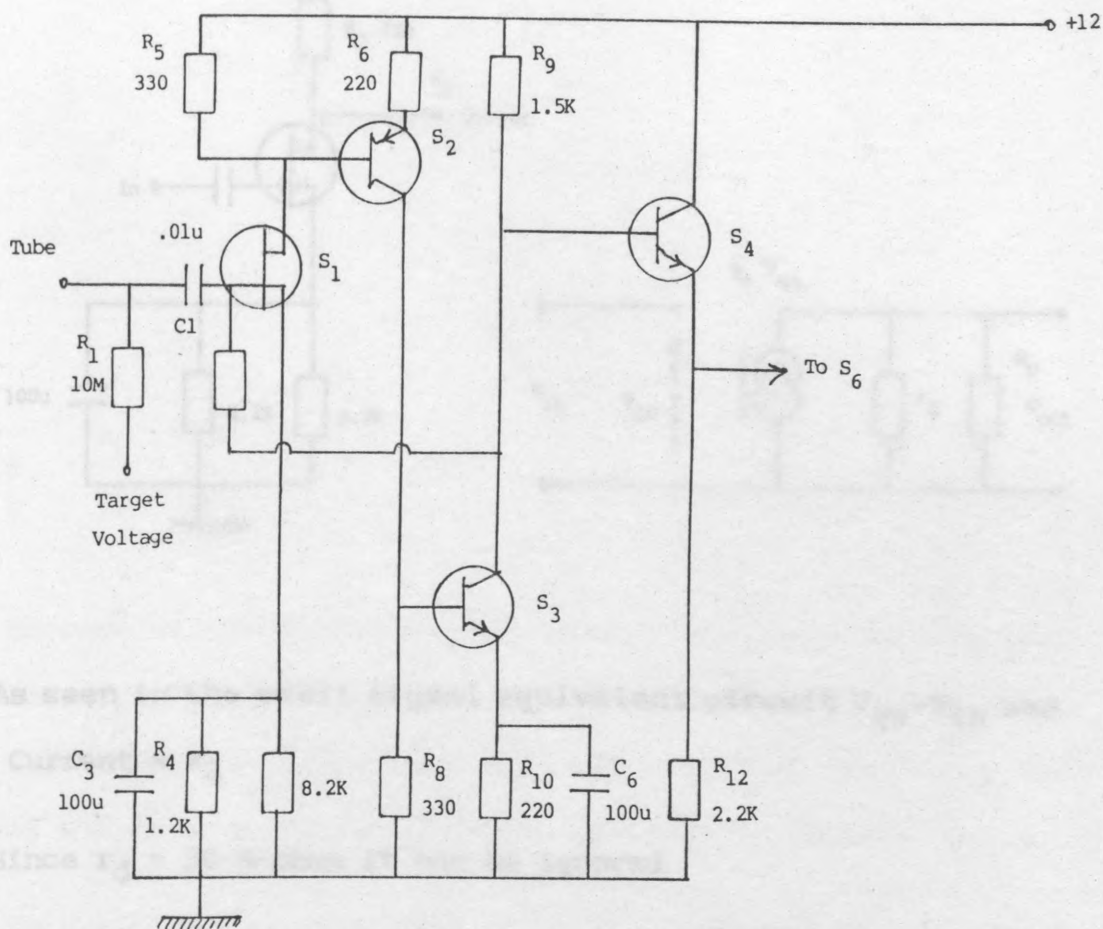
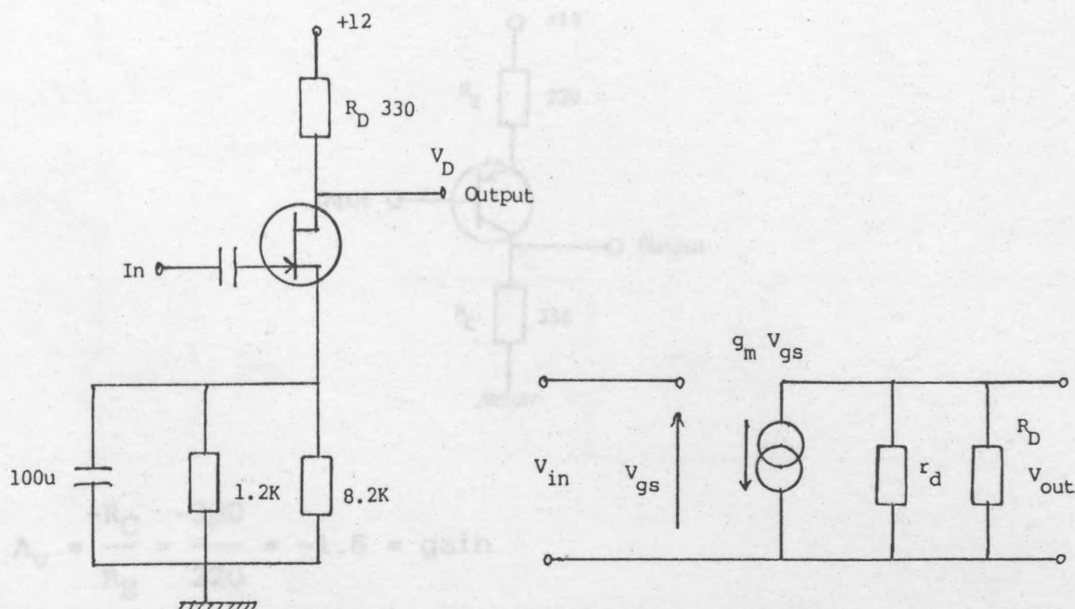


Fig. IX.1 Circuit Diagram of the Head Amplifier

(a) To reduce the noise in the head amplifier the noise of the second (S_2) and third (S_3) stages were made small relative to the output signal of the first (S_1) stage. This was achieved by increasing the voltage gain of S_1 and S_2 and reducing the gain of S_3 .

First Stage S_1



As seen in the small signal equivalent circuit $V_{gs} = V_{in}$ and $V_{out} = \text{Current} \times R_D$

Since $r_d = 30 K\text{-ohms}$ it can be ignored

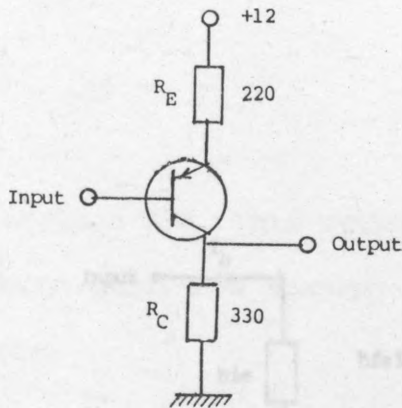
$$\therefore V_{out} = -g_m V_{gs} R_D$$

$$R_D = 330 \text{ ohms} \quad g_m = 6 \text{ mmhos}$$

$$\therefore \text{gain} = -2$$

This can be increased if R_D is increased, but there is a limit to which R_D could be increased (minimum $V_D = 5.3V$). R_D was set at $1K\text{-ohms}$ hence the gain was -6 . Also in an F.E.T transistor the lower the I_D the noisier the transistor would be, so the current I_D was also increased with the above modification.

Second Stage S₂



$$A_V = \frac{-R_C}{R_E} = \frac{-330}{220} = -1.5 = \text{gain}$$

As seen in the small signal equivalent circuit:

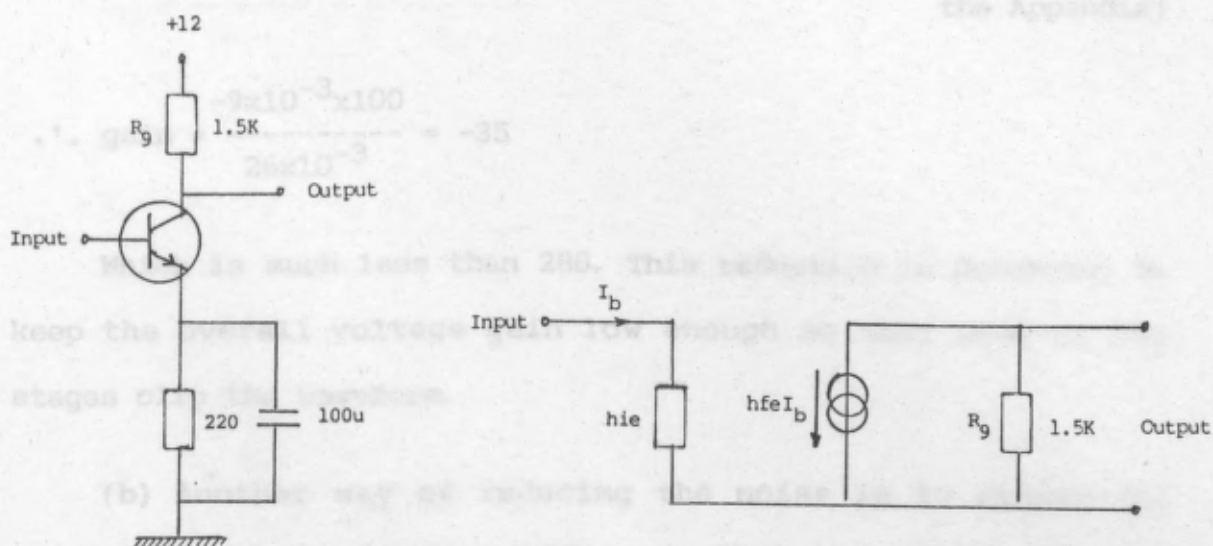
Because of the modification in S₁, V_{D1} (V_{B2}) is reduced, therefore V_{E2} has to be reduced. To achieve this R_E is divided into a 330 ohms and decoupled 7.5 K-ohms resistors. Hence V_{E2} was reduced and also R_E, in small signal equivalent, remained small.

The gain can be increased if R_C is increased to 3.3 K-ohms giving a gain of 10. This gave a collector current of 0.8 mA which was much smaller than the previous I_C of 5 mA. This resulted in less noise in S₂ since the optimum working I_C for this transistor for minimum noise is 0.5 mA.

$$\therefore \text{gain} = -288$$

To reduce this gain, R_E had to be reduced but the V_E had to remain the same. Thus a 0.5V zener diode together with a 100ohm resistor was used in place of R_E.

Third Stage S₃



As seen in the small signal equivalent circuit:

$$V_{in} = I_b h_{ie} \quad \text{and} \quad V_{out} = -h_{fe} I_b R_9$$

$$\text{Hence } \frac{V_{out}}{V_{in}} = \text{gain} = \frac{-h_{fe} R_9}{h_{ie}}$$

$$\text{but } h_{ie} = \frac{26 \times 10^{-3}}{I_b} \quad \text{and} \quad I_b = \frac{I_C}{h_{fe}}$$

$$\therefore \text{gain} = \frac{-h_{fe} R_9 I_C}{26 \times 10^{-3} h_{fe}} = \frac{-I_C R_9}{26 \times 10^{-3}} = \frac{-5 \times 10^{-3} \times 1.5 \times 10^3}{26 \times 10^{-3}}$$

$$\therefore \text{gain} = -288$$

To reduce this gain, R₉ had to be reduced but the V_C had to remain the same. Thus a 6.8V zenor diode together with a 100ohm resistor was used in place of R₉.

$$\text{gain} = \frac{-I_C R_9}{26 \times 10^{-3}}$$

When $R_9 = 100 \text{ ohms}$ $I_C = 9 \text{ mA}$ (calculations at the end of the Appendix)

$$\therefore \text{gain} = \frac{-9 \times 10^{-3} \times 100}{26 \times 10^{-3}} = -35$$

Which is much less than 288. This reduction is necessary to keep the overall voltage gain low enough so that none of the stages clip the waveform.

(b) Another way of reducing the noise is to reduce the sensitivity of the head amplifier so that the camera tube is working at a higher current output.

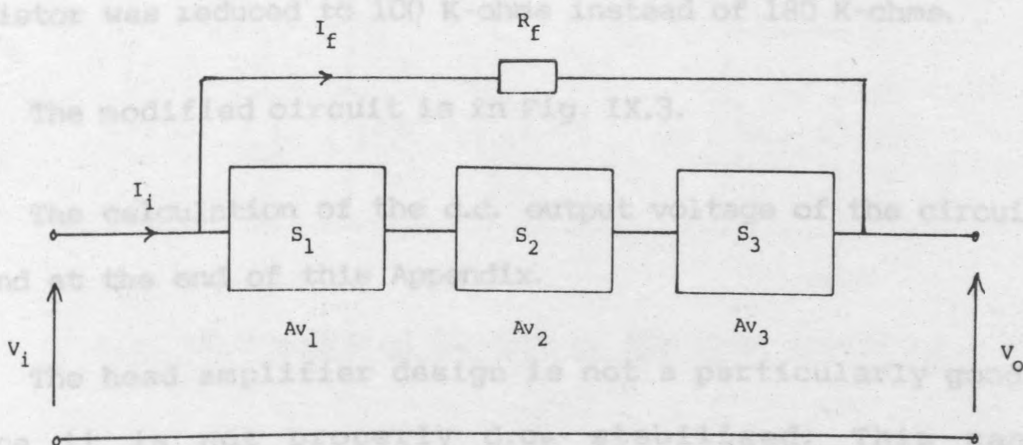


Fig. IX.2 Block Diagram of the Head Amplifier

In Fig. IX.2, Av_1 , Av_2 and Av_3 are voltage gains of stages S_1 , S_2 and S_3 respectively. Hence overall voltage gain is:

$$\frac{V_o}{V_i} = Av_1 \times Av_2 \times Av_3 = A_o$$

$I_i = I_f$ because Z_{in} of the 1st stage is very large

$$I_f = \frac{V_1 - V_O}{R_f} = \frac{V_1 (1 - A_O)}{R_f}$$

$$\therefore \frac{V_O}{I_i} = \frac{A_O V_i}{I_i} = \frac{A_O V_i R_f}{V_i (1 - A_O)}$$

$$\therefore \frac{V_O}{I_i} = \frac{A_O R_f}{1 - A_O} = R_f \text{ when } A_O \gg 1$$

Hence the overall voltage gain does not affect the sensitivity and the latter can be reduced by reducing R_f . This resistor was reduced to 100 K-ohms instead of 180 K-ohms.

The modified circuit is in Fig. IX.3.

The calculation of the d.c. output voltage of the circuit is found at the end of this Appendix.

The head amplifier design is not a particularly good one since it is not properly d.c. stabilised. This can be demonstrated by the following:

From equation IX.1 at the end of the Appendix

$$V_A \left(\frac{R_5}{R_X} + \frac{R_{10}R_6}{R_9R_8} \right) = \frac{R_S}{R_X} V_{gs} + \frac{R_{10}R_6}{R_9R_8} V_S - \frac{R_{10}R_6}{R_9R_8} V_D + \frac{R_6}{R_8} V_{BE3} + V_{BE2}$$

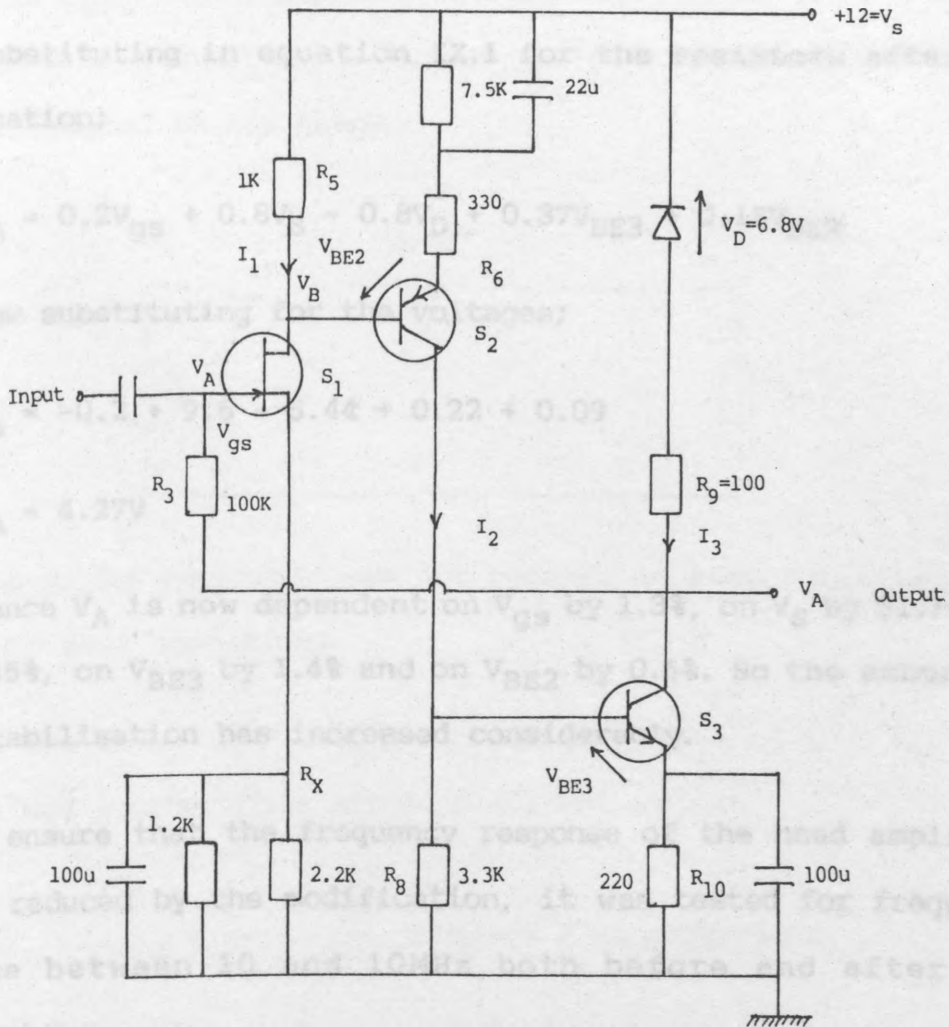


Fig. IX.3 Modified Circuit of the Head Amplifier

Substituting for the resistor values before the modification and hence omitting the term V_D ;

$$V_A = 0.77V_{gs} + 0.23V_S + 1.56V_{BE3} + 2.33V_{BE2}$$

Now substituting for the voltages;

$$V_A = -0.77 + 2.76 + 0.936 + 1.398$$

$$\therefore V_A = 4.32V$$

Hence V_A is dependent on V_{GS} by 13.1%, on V_S by 47.1%, on V_{BE3} by 16.0% and on V_{BE2} by 23%. Therefore only 47.1% is d.c. stabilised.

Substituting in equation IX.1 for the resistors after the modification;

$$V_A = 0.2V_{GS} + 0.8V_S - 0.8V_D + 0.37V_{BE3} + 0.15V_{BE2}$$

Now substituting for the voltages;

$$V_A = -0.2 + 9.6 - 5.44 + 0.22 + 0.09$$

$$\therefore V_A = 4.27V$$

Hence V_A is now dependent on V_{GS} by 1.3%, on V_S by 61.7%, on V_D by 35%, on V_{BE3} by 1.4% and on V_{BE2} by 0.6%. So the amount of d.c. stabilisation has increased considerably.

To ensure that the frequency response of the head amplifier is not reduced by the modification, it was tested for frequency response between 10 and 10MHz both before and after the modification.

This was achieved by;

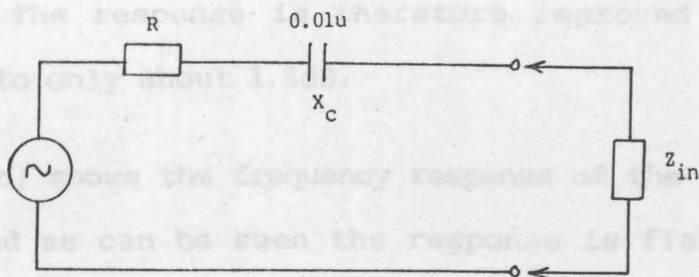
From Fig. IX.2

$$Z_{in} = \frac{V_i}{I_i} \quad \text{but} \quad I_i = \frac{V_i (1-A_O)}{R_f} \quad \text{when } A_O \text{ is -ve}$$

$$\therefore Z_{in} = \frac{R_f}{1-A_O} \quad R_f = 100 \text{ K-ohms} \quad \text{and} \quad A_O = -6 \times 10 \times 35 = -2100$$

$$Z_{in} = \frac{100 \times 10^3}{1 + 2100} = 47 \text{ ohms}$$

When Z_{in} = Input impedance of the head amplifier. The camera tube was disconnected and a voltage source with a serial resistor R was connected in its place.



The 0.01uF capacitor was not removed to keep the impedances under the same conditions.

If the value of R was ten times the value of $X_C + Z_{in}$ then the voltage source would act as a current source.

$$X_C = \frac{1}{\omega C} = \frac{1}{2\pi f C} \quad \text{minimum } f \text{ is about } 50\text{Hz}$$

$$\text{Hence minimum } X_C = \frac{1}{2\pi \times 50 \times 0.01 \times 10^{-6}} = 318 \text{ K-ohms}$$

Hence the value of Z_{in} is negligible compared to X_C . Ten times 318 K-ohms is 3.2 M-ohms. The current needed for the head amplifier is in the order of 1uA. Therefore a voltage source of 3V in series with 3.2 M-ohms will produce 1uA of current. The head amplifier was then tested for frequency response between 10 to 10 MHz.

In Fig. IX.4, Curve (a) is the frequency response for the unmodified head amplifier and as can be seen the response is flat

from 50 Hz to 100 KHz and then a peak at 4 MHz. This is due to the capacitance in the 3.2 M-ohms resistor. If this resistor is decreased the frequency response of frequencies lower than about 3 KHz ($R/10 \times 2 C = 1/f$) would not be correct but instead the response at high frequencies would be more true.

Curve (b) shows the response using a 52 K-ohms series resistor R. The response is therefore improved in the high frequencies to only about 1.5dB.

Curve (c) shows the frequency response of the modified head amplifier and as can be seen the response is flat upto 6 MHz which is more than enough for a black and white camera. Also the peak at 4 MHz is reduced to only 0.5dB. This has considerable effect in reducing the white noise since most of the power of the latter lies in higher frequencies. The frequency response is not flat below 1 KHz since the series resistor is only 52 K-ohms and thus the response is not correct below 1 KHz.

With this response it was proved that the modification to the head amplifier is not merely a low pass filter.

The modification increased the signal to noise ratio. The camera was placed in front of a test chart and the iris of the lens opened until the output of the camera was just before clipping.

Before modification

Signal	1.8V
-----	= ----- = 7.2 = 17dB
Noise	.25V

After modification

$$\frac{\text{Signal}}{\text{Noise at the black level}} = \frac{2.2\text{V}}{0.1\text{V}} = 22 = 27\text{dB}$$

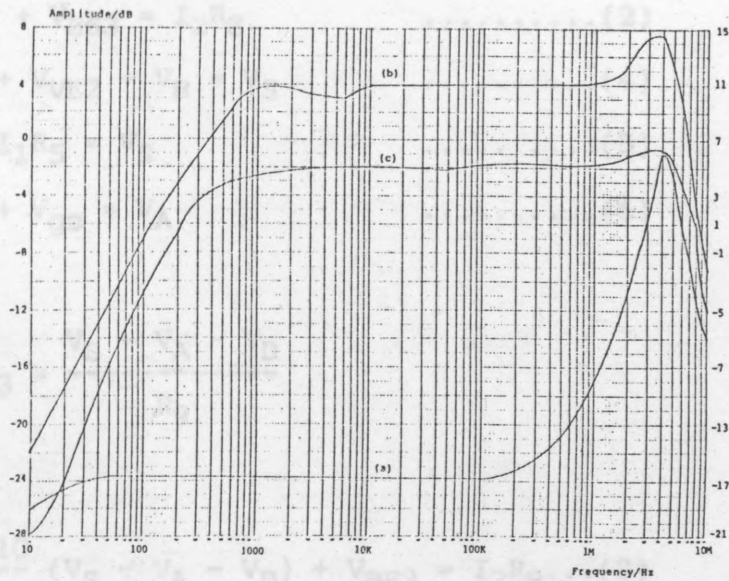


Fig. IX.4 Frequency Response of the Head Amplifier

$$\frac{\text{Signal}}{\text{Noise at the white level}} = \frac{2.2\text{V}}{.025\text{V}} = 88 = 39\text{dB}$$

The signal to noise ratio has improved considerably especially at the white level where the limbus pulse in section 6.4.IV was generated.

The reason for different noise levels at different grey levels of the signal could be due to many factors. These include, a) the Gamma Correction on the camera being not properly set at 1, b) the amplifiers in the camera working nearer to their saturation, c) the d.c. operating point of the F.E.T changing with the incoming signal, d) the tube producing more noise when the incident light on its face decreases (black level) and less noise when there is more light (white level).

Calculations of the D.C. Output of the Head Amplifier

As in Fig. IX.3

$$V_A + I_3 R_9 + V_D = V_S \quad \dots\dots\dots(1)$$

$$I_3 R_{10} + V_{BE3} = I_2 R_8 \quad \dots\dots\dots(2)$$

$$I_2 R_6 + V_{BE2} + V_B = V_S \quad \dots\dots\dots(4)$$

$$V_B + I_1 R_5 = V_S \quad \dots\dots\dots(5)$$

$$I_1 R_X + V_{GS} = V_A \quad \dots\dots\dots(6)$$

$$\text{from (1)} \quad I_3 = \frac{V_S - V_A - V_D}{R_9}$$

$$\text{in (2)} \quad \frac{R_{10}}{R_9} (V_S - V_A - V_D) + V_{BE3} = I_2 R_8 \dots(3)$$

$$\text{from (3)} \quad I_2 = \frac{R_{10}}{R_9 R_8} (V_S - V_A - V_D) + V_{BE3}/R_8$$

$$\text{in (4)} \quad \frac{R_{10} R_6}{R_9 R_8} (V_S - V_A - V_D) + \frac{R_6}{R_8} V_{BE3} + V_{BE2} + V_B = V_S$$

$$\therefore V_B = V_S - \frac{R_{10} R_6}{R_9 R_8} (V_S - V_A - V_D) - \frac{R_6}{R_8} V_{BE3} - V_{BE2}$$

$$\text{in(5)} \quad V_S - \frac{R_{10} R_6}{R_9 R_8} (V_S - V_A - V_D) - \frac{R_6}{R_8} V_{BE3} - V_{BE2} + I_1 R_5 = V_S \dots(7)$$

$$\text{From (6)} \quad I_1 = \frac{V_A - V_{GS}}{R_X} \quad \text{in (7)}$$

$$\frac{R_5}{R_X} (V_A - V_{gs}) = \frac{R_{10}R_6}{R_9R_8} (V_S - V_A - V_D) + \frac{R_6}{R_8} V_{BE3} + V_{BE2}$$

$$V_A \left(\frac{R_5}{R_X} + \frac{R_{10}R_6}{R_9R_8} \right) = \frac{R_5}{R_X} V_{gs} + \frac{R_{10}R_6}{R_9R_8} V_S - \frac{R_{10}R_6}{R_9R_8} V_D + \frac{R_6}{R_8} V_{BE3} + V_{BE2} \quad \dots(IX.1)$$

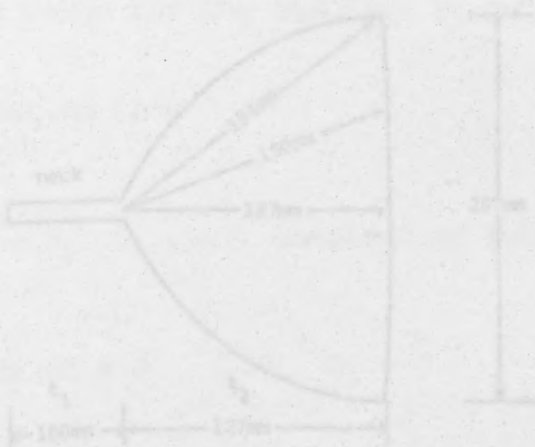
$$\text{when } R_X = \left(\frac{1}{1.2K} + \frac{1}{2.2K} \right)^{-1} = 776 \text{ ohms}$$

$$\begin{aligned} R_5 &= 1000 \text{ ohms} \\ R_{10} &= 220 \text{ ohms} \\ R_6 &= 7830 \text{ ohms} \\ R_9 &= 100 \text{ ohms} \\ R_8 &= 3300 \text{ ohms} \end{aligned}$$

$$\begin{aligned} V_D &= 6.8V \\ V_{gs} &= -1 V \\ V_S &= 12 V \\ V_{BE3} &= V_{BE2} = 0.6V \end{aligned}$$

Substituting for resistors and voltages;

$$V_A = 4.28 \text{ volts.}$$



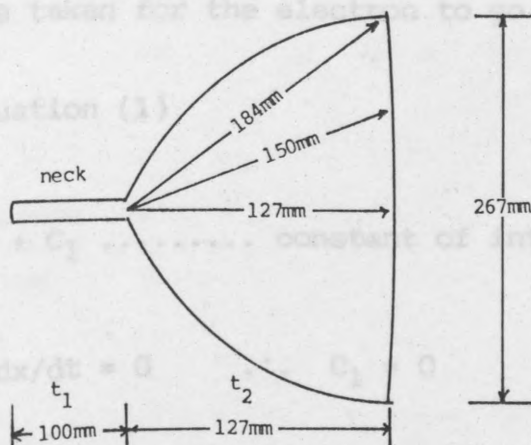
1) Calculation of time t_1 , when electrons are accelerating:

Appendix X

Delay calculations:

1) The delay in the circuit of the monitor was in the order of nanoseconds since there were only a few active stages in the vision amplifiers. These, of course, vary from monitor to monitor, but generally they consisted of few transistors or op-amp. This delay is almost negligible.

2) The delay for the electrons to travel from the cathode to anode is divided into two, t_1 and t_2 . t_1 is the time taken for the electrons to travel in the neck of the C.R.T. when they are accelerating and t_2 is the time for the electrons to travel from the neck to the screen with constant speed.



i) Calculation of time t_1 , when electrons are accelerating:

$$F = qE \quad E = V/d$$

when q = Electron charge

F = Force on electron

E = Electric field strength

d = length of the neck of the C.R.T.

V = Potential difference between anode and cathode

$$\therefore F = \frac{q}{d} \cdot V$$

for acceleration

$$m \frac{d^2x}{dt^2} = \frac{qV}{d} \quad \dots\dots(1) \quad \text{since } F = m \frac{d^2x}{dt^2}$$

when m = Mass of electron.

x = Distance of the electron from the cathode.

t = Time taken for the electron to go through distance x .

integrating equation (1)

$$\frac{dx}{dt} = \frac{q}{m} \cdot \frac{V}{d} \cdot t + C_1 \quad \dots\dots\dots \text{constant of integration}$$

$$\text{when } t = 0 \quad dx/dt = 0 \quad \therefore C_1 = 0$$

integrating again

$$x = \frac{q}{m} \cdot \frac{V}{d} \cdot \frac{t^2}{2} + C_2 \quad \dots\dots\dots \text{constant of integration}$$

when $x = 0$ $t = 0$ $C_2 = 0$

therefore $t^2 = \frac{2mx d}{Vq}$ but $x = d$ at the end of the neck

$\therefore t^2 = \frac{2md^2}{qV}$ $\therefore t_1 = d \sqrt{\frac{2m}{qV}}$

for an electron $q/m = 1.759 \times 10^{11} \text{ C/Kg}$

in an average C.R.T. $V = 15.25 \text{ KV}$ $d = 10\text{mm}$

$\therefore t_1 = 2.73 \times 10^{-9} \text{ seconds}$

ii) calculation of time when electrons are at constant speed: t_2

q = electron charge

m = electron mass

V = potential difference

v = speed of electron

$\frac{1}{2}mv^2 = qV$ $v^2 = \frac{2qV}{m}$ $v = \sqrt{\frac{2qV}{m}}$

speed = $\frac{\text{distance}}{\text{time}} = \frac{d}{t} = v$

$\therefore t = \frac{d}{\sqrt{2qV/m}}$ $\therefore t_2 = d \sqrt{\frac{m}{2qV}}$

$\frac{q}{m} = 1.759 \times 10^{11} \text{ C/Kg}$

$V = 15.25 \text{ KV}$

$d = 150\text{mm}$

Where d is the average distance from the end of the neck to the screen.

$$3-\text{po.} \therefore \underline{t_2 = 2.05 \times 10^{-9} \text{ seconds}}$$

The component values of the 3-pole active filters used in sections 3.4.VIII and 6.2.VII are calculated with the aid of a normalized table from Brokaw (1970). Two filter designs were

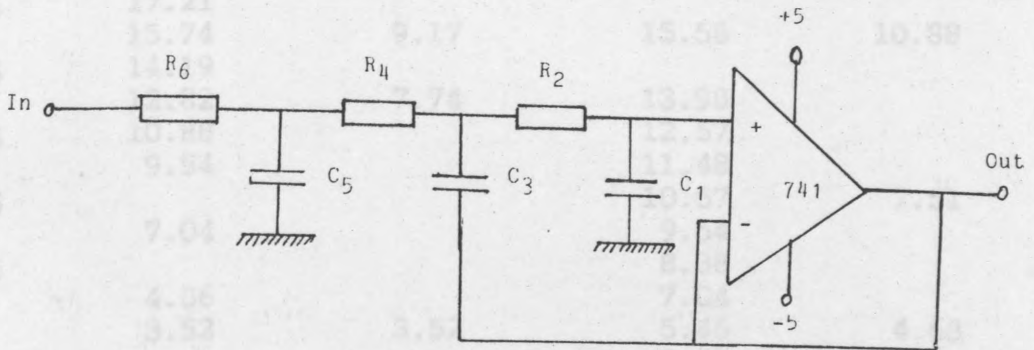
involved. 3) The time delay in the phosphor glow was about 1 to 2 μs in a long-persistence tube and about 0.2 μs in a short-persistence tube (Brimar, 1975/76).

However, the design in section 3.4.VIII was later altered to a cut-off frequency of 20Hz.



3-Pole Active Filters

The component values of the 3-pole active filters used in sections 3.4.VIII and 6.2.VII are calculated with the aid of a normalised table from Brokaw (1970). Two filter designs were investigated for two different input impedances. Chebychev 1dB ripple and Optimal 3dB ripple for 10K-ohms and 100K-ohms input resistances. They all were calculated for a cut-off frequency of 10Hz. However, the design in section 3.4.VIII was later altered to a cut-off frequency of 20Hz.



Chebyshev 1dB Chebyshev 1dB Optimal 3dB Optimal 3dB

$R_2=R_4=R_6=10K$
 $C_1=103.84nF$
 $C_3=26.15uF$
 $C_5=4.15uF$

$R_2=R_4=R_6=100K$
 $C_1=10.384nF$
 $C_3=2.615uF$
 $C_5=0.415uF$

$R_2=R_4=R_6=10K$
 $C_1=0.22uF$
 $C_3=12.5uF$
 $C_5=3.3uF$

$R_2=R_4=R_6=100K$
 $C_1=0.02uF$
 $C_3=1.22uF$
 $C_5=0.32uF$

Frequency	(1) Output/dB	(2) Output/dB	(3) Output/dB	(4) Output/dB
1	19.67	19.78	19.55	20.00
1.25	19.55	19.67	19.55	
1.50	19.44	19.67	19.55	
1.75	19.32		19.32	
2	19.20	19.44	19.20	
2.5	19.08	19.08	18.84	20.00
3	18.72	18.59	18.59	19.78
3.5		17.93	18.32	
4	18.46	17.36	17.92	19.32
4.5			17.79	18.84
5	18.52	15.92	17.64	18.46
5.5			17.50	17.79
6	18.84	14.61	17.36	17.06
6.5			17.36	
7	19.44	13.06	17.21	15.74
8	19.55	11.77	17.21	13.98
8.5	19.08			
9	18.46	10.40	16.75	12.82
9.5	17.21			
10	15.74	9.17	15.56	10.88
10.5	14.19			
11	12.82	7.74	13.98	
11.5	10.88		12.57	
12	9.54		11.48	
12.5			10.57	7.51
13	7.04		9.54	
13.5			8.38	
14	4.86		7.04	
15	3.52	3.52	5.46	4.68
16			3.52	
17	-1.16		1.02	
18			-0.56	
19			-1.80	
20	-6.02	0	-2.50	0
22			-5.00	
25	-10.10		-8.52	
30	-12.04	-7.18	-12.04	-4.08
35			-18.06	
40				-6.02

Copies of the Printed Circuit Boards

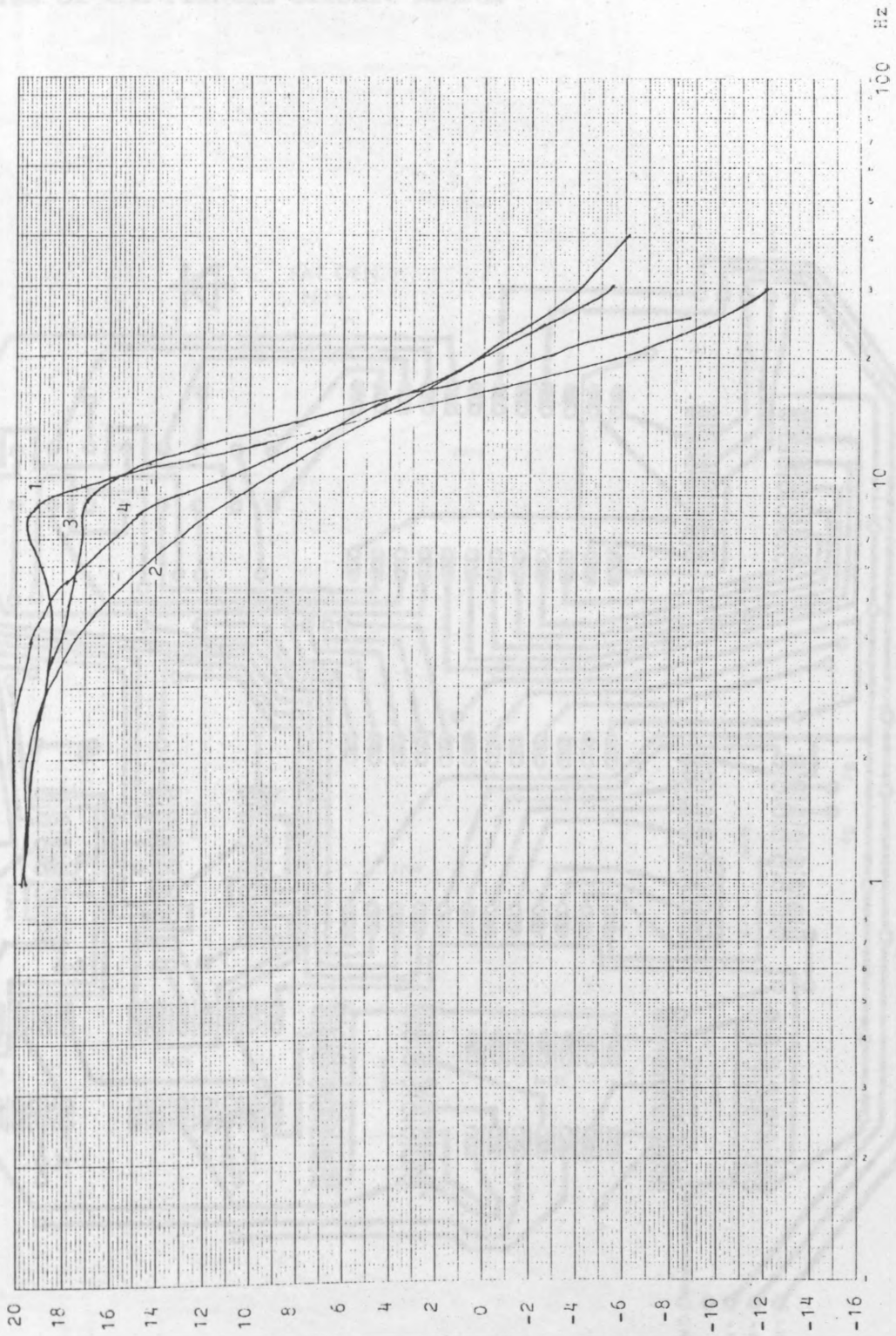


Fig. XI.2 Frequency Response

**Appendix 12 has
been removed for
copyright reasons**

**Appendices 13 and 14
have been removed for
copyright and data
protection reasons**

REFERENCES

- Bjork A. (1952), *Experientia*, vol. 8, P226-7.
- Forian L. (1970), *Clinical Refraction Duane cover test*, 3d ed. Chicago, 1970.
- American Microsystem (AMI)(1978), Video Display Generator, Data Sheet/Application Note, August 1979.
- Ross L.D.J. (1984), *The Double Magnetic Induction Method for measuring eye movements* result in Norway and Italy, *Transaction Biomedical*, Vol. 31(1), P19-27.
- Anderson J.R. (1947), Ocular Vertical Deviations, *Brit. J. Ophth.*, Supp. 12, P80.
- Bahill T.A., Brockenburgh A., Troust T. (1981), Variability and Development of a Narrative Data Base for Saccadic Eye Movement, *Investigation of Orthalmology and Visual Sciences*, P116-125.
- Boysen P.R. (1988), *The frequency responses of contact lens shall assemblies*, *Vision Research*, Vol. 2, P513-23.
- Barber H.O., Stockwell C.W. (1980), Manual of Electronystagmography, The C.V. Mosby Co., 2nd Edition.
- Barlow H.B. (1952), Eye movements during fixation, *J. Physiol.* (London), Vol.116, P290-306.
- Barlow H.B. (1963), Slippage of contact lenses and other artefacts in relation to fading and regeneration of supposedly stable retinal images, *Q.J.Exp. Psychology*, Vol.15, p36-51.
- Bechai N.R.L. (1977), Measurement of the rotation of a disk from its elliptical projection with an application to eye movements, *J. Opt. Soc. Am (USA)*, Vol 67 no.10, P1336-9.
- Benghi H., Thomas J.C. (1968), Three Electronic methods for recording ocular tremor, *Med. & Biol Eng. & Comput.* Vol.6, P171.
- Russell G. (1935), *How people look at pictures*, Chicago: Bielschowsky A. (1938), Signs & Symptoms of Heterophoria, *Am. J. Ophth.* Vol.21, P1219-29.
- Byford G.W. (1964), *The stability of contact lens eye movement*

Bjork A. (1952), *Experientia*, vol.8, P226-7.

Borish I. (1970), *Clinical Refraction Duane cover test*, 3d ed. Chicago, p818-9.

Bour L.O.J. (1984), The Double Magnetic Induction Method for measuring eye movements result in monkey and man, *IEEE transaction Biomedical*, Vol.31(5), P419-27.

Boyce P.R. (1967), *Proc. R. Soc.*, Vol.167, P293.

Boyce P.R. (1968), The frequency responses of contact lens stalk assemblies, *Vision Research*, Vol.8, P475-80.

Brimar (1975/76), *Industrial Cathode Ray Tubes*.

Brokaw P. (1970), *Simplify 3-Pole Active Filter Design*, E.D.N., DEC. P23-28.

Brown B. (1977), Clinically useful eye movement recording system, *Am. J. of Opt. Physiol. Opt.*, 54, P56-60.

Brown C.R. (1980), An improved photoelectric system for 2-D eye movement recording, *Behav. Res. Methods and Instrum.* (USA), Vol.12, No.6, P596-600.

Burian H.M. (1941), Fusional movements in permanent Strabismus; study of the role of the central and peripheral retinal regions in the act of binocular vision in squint, *Arch. Ophth.* Vol.26, P626-652.

Buswell G. (1935), *How people look at pictures*, Chicago; University of Chicago Press.

Byford G.H. (1962), The fidelity of contact lens eye movement

- recording, Opt. Acta Vol.9, P223-236.
- Byford G.H. (1963), Non-linear relations between the corneo-retinal potential and horizontal eye movements, J. Physiol. (London), Vol.168, P14-15.
- Carpenter R.H.S. (1977), Methods of measuring eye movements, Movements of the eye, Poin Ltd., Appendix I, P309-325.
- Carter R.B. (1876), Practical treatise of diseases of the eye, Philadelphia, H.C Lea, P496.
- Clayton G.B. (1979), Operational amplifiers, 2nd Ed., Newnes - Butterworths, P242.
- Collewijw H., Mark F., Jansen T.C. (1975), Precise recording of human eye movements, Research note, Vision Research, Vol.15, P447-450.
- Comet B. (1983), An eye movement recording method operating with a closed eye, Med. & Biol. Eng. & Comput., Vol.12(5), P628-31.
- Corby N. (1977), The development of a minicomputer based real time eye tracking system and applications to pattern recognition, Proceedings of the IEEE International Conference on Cybernetics and Society, P583-8.
- Cornsweet N. (1958), New technique for the measurement of small eye movement, Am. J. Opt. Soc., Vol.48, P808.
- Cornsweet T.N. (1973), Accurate 2-D eye tracker using 1st and 4th Purkinje Images, Am. J. Opt. Soc., Vol.63, P921.

- Crane H., Steele C. (1978), Accurate 3-D eye tracker, Applied Optics, Vol.17, P691-705.
- Davies W.L., Plant G.R. (1978), The recording and analysis of human ocular microtremor, Proceedings of J. Physiol, P276.
- De La Barre E.B. (1898), A method of recording eye movements, Am. J. of Psychology, Vol.9, P572.
- Ditchburn R.W. (1973), Eye-movements and visual perception, Clarendon Press, Oxford, P17.
- Dodge R. (1901), The angle velocity of eye movements, Psychol. Rev., Vol.8, P145.
- Duane A. (1896), New classification of motor anomalies of the eye based upon physiologic principles, together with their symptoms, diagnosis and treatment, Ann. Ophth. & Otol, Vol.5, P1002.
- Du Bois-Reymond (1849), Untersuchungen Uber Thierische Elektrizitat.
- Eizenman M. (1984), Precise non-contacting measurement of eye movements using the corneal reflex, Vis. Res., Vol.24(2), P167-174.
- Faraday A. (1969), Factors affecting the experimental recall of dreams, PhD. Thesis, University College, London.
- Fender D.H. (1964), Contact lens stability, Biomed. Sci. Instr. Vol.2, P43-52.
- Feuk T., McQueen D. (1971), The angular dependence of light scattered from rabbit corneas, Invest. Ophth., Vol.10, P294.

- Findlay J.M. (1974), A simple apparatus for recording microsaccades during visual fixation, Quarterly J. of Exp. Psycho., Vol.26, P167-170.
- Fisher D.G. (1982), An automated eye movement laboratory for on-line electrooculography, Behav. Res. Methods & Instrum. (USA), Vol.14(2), P113-20.
- Foulds R.A. (1981), Eye gaze system for communication input, Midcon 1981 conference 2nd, Chicago, Nov.10-12.
- Fuller D.G., Laqua H., Machemer R. (1977), Ultrasonic diagnosis of massive periretinal proliferation in eyes with opaque media (Triangular retinal detachment), Am. J. Ophth., Vol.83, P460-4.
- Geddes L.A., McCardy J.D., Hoff H.E. (1965), The impedance nystagmogram - A record of the level of anesthesia in the horse, Southwestern Veterinarian, Vol.19, P000.
- Haines J.D. (1977), Non-contacting ultrasound transducer system suitable for eye movement recording, Ultrasound Med. and Biol., Vol.3, P39-45.
- Hainline L. (1981), An automated eye movement recording system for use with human infants, Behav. Res. Method & Instrum. (USA), Vol.13(1), P20-4.
- Haith M.M. (1969), Infrared television recording and measurement of ocular behaviour in the human infant, Am. Psychologist, Vol.24, P279-83.
- Hall R.J. (1972), The measurement of eye behaviour, US Army Human Engineering Lab. Tech. Memorandum, P18-72.

Jackson E. (1970), The Hirschberg test: A re-evaluation, Am. J.

Hering E. (1879), Über Muskelgerausche des Auges, Sitzungsber.
Akad. Wiss. Wien Math. Naturwiss Kl., Abt.3(79), P137-154.

Jones R. (1977), 2-D eye movement recording using a photoelectric

Hering E. (1899), Über die Anormale Lokalisation der
Netzhautbilder bei Strabismus Alternans, Deutsches Arch.
Klin. Med., Vol.64, P23.

Wallerstein R. (1977), Kinesthetic Photography, Psychol.

Hess W.R. (1908), Eine neue untersuchungsmethode dei
doppelbildern, Arch. Augenh, Vol.62, P233-8.

Kassai E. (1977), A new eye movement measurement using CCD

Hirschberg J. (1881), On the quantitative analysis of diplopic
strabismus, Brit. M. J., Vol.1, P5-6.

P141.

Hofmann F.B., Bielschowsky A. (1900), Die verwertung der
kopfneigung zur diagnose der augenmuskellahmungen, V.
Graefe's Arch. Ophth., Vol.51, P174.

Kivier M.S. (1977)

Hugonnier R. (1969), Strabismus, Heterophoria and Ocular motor
paralysis, P335-55 & 417.

Interpretation of eye movements, Vol.2(1).

I.B.M., Interactive Graphics and Image Display, IBM Technical
Disclosure Bulletin, Vol.19, No.7.

Leuchtit E. (1977), A new eye movement measurement using CCD

Information Control Corporation, Understanding Light Pens, ICC.

P59-61.

Ishikawa S., Yamakazi A. (1971), A new technique for registering
eye movement (X-Y Tracker), Acta Soc. Ophth. (JAPAN),
Vol.75, P1110-7.

Leuchtit E. (1977), A new eye movement measurement using CCD

Jackson E. (1900), Essentials of refraction and of diseases of
the eye with a consideration of ocular injuries,
Philadelphia W.B. Saunders Co., P207-8.

- Jones R. (1970), The Hirschberg test: A re-evaluation, Am. J. Optom. & Physiol. Opt., Vol.47(2), P105-14.
- Jones R. (1973), 2-D eye movement recording using a photoelectric matrix method, Vis. Res., Vol.13, P425-31.
- Judd C.H. (1905), General introduction to a series of eye movements by means of Kinetoscope Photography, Psychol. Monogr., Vol.7, P1.
- Kasai T. (1982), Methods of eye movement measurement using CCD image sensors and their resolutions of measurement, Trans. Inst. Electron. & Commun. Eng. (JPN), Sect. E., Vol.E65(2), P141.
- Kestenbaum A. (1946), Clinical Methods of neuro-ophthalmological examination, Grune & Stratton Inc., P156.
- Kiver M.S. (1973), Television Simplified, Chapter 1 & 2.
- Lancaster W.B. (1939), Detecting, measuring, plotting and interpreting ocular deviations, Arch. Ophth., Vol.22(5), P867-880.
- Landolt E. (1879), A manual of examination of the eyes, a course of lectures delivered at the Ecole Partique, Philadelphia, P59-61.
- Lees V.T. (1949), A new method of applying the screen test for inter-ocular muscle balance, Brit. J. Ophth., Vol.33, P54-9.
- Lewellyn-Thomas E. (1960), The television eye marker as a recording and control mechanism, IRE Trans. Med. Electron, Vol.7, P196.

- Mackworth N.F., Mackworth H.H. (1958), Eye fixation recorded on changing visual scenes by the television eye-marker, J. Opt. Soc. Am., Vol.48, P439.
- Maddox E.E. (1898), Tests and studies of the ocular muscles, Bristol J., Wright & Co., London, P288-9.
- Marchant J. (1967), The oculometer, NASA, CR-805.
- Matin L. (1964), Measurement of eye movements by contact lens techniques, J. Opt. Soc. Am., Vol.54.
- Mellers S.H. (1980), An evaluation of eye position monitor system, University of California, MSc Thesis, Oct 80.
- Merchant J., Morrisette R. (1974), Remote measurement of eye direction allowing subject motion over one cubic foot of space, IEEE Transactions on Biomed. Eng., Vol.21, P309-17.
- Merton P.A. (1956), Compensatory rolling movements of the eye, J. Physiol. (London), Vol.132, 25p-27p.
- Monty R.A. (1975), An advanced eye movement measuring and recording system featuring unobtrusive monitoring and automatic data processing, Am. Psychol., Vol.30, P331-5.
- Morra B. (1982), A Microcomputer-Based Eye Movement Automatic Analysis System, conference Medcomp 82, 1st IEEE Computer Society Int. Conf. on Medical Computer Science, P248-253.
- Mowrer O.H., Ruch R.C., Miller N.E. (1936), The corneo-retinal potential difference as the basis of the Galvanometric method of recording eye movements, Am. J. Physiol., Vol.114, P423.

- Nettleship E. (1900), Diseases of the eye, Philadelphia, Lea Bros. & Co., P380.
- Nystagmus Action Group (1986), London Refraction Hospital.
- Ohm J. (1906), Zur untersuchung des doppletsehens, Centralbl. Prakt. Augenh., Vol.30, P326.
- Ohm J. (1928), Die hebelnystagmo-graphie, Albrecht Von Graefes Arch. Ophth., Vol.120, P235-52.
- Ohm J. (1939), Arch. Ohren - Nasen - U. Kehlkopfh, P146-223.
- Orschansky J. (1898), Eine methode die augenbewegungen direkt zu untersuchen (Ophthalmographie), Zentralbl-Physiol., Vol.12, P785-90.
- Park G., Park R. (1933), Am. J. Physiol. Vol.104, P545.
- Peters M.J., Dunajski Z. (1982), Measuring miniature eye movements by means of a squid magnetometer, Cryogenics, Vol.22(6), P267-70.
- Raehlmann E. (1878), Uber den nystagmus und seine 'A' tiologie, Arch. fur Ophth., Abt. III, Vol.24, P237-317.
- Rashbass C., Westheimer G. (1960), Recording rotational eye movements independently of lateral displacements, J. Opt. Soc. Am., Vol.50, P512.
- Rashbass C. (1960), New method for recording eye movements, J. Opt. Soc. Am., Vol.50, P642.
- Ratliff & Riggs (1950), Involuntary motion of the eye during monocular fixation, J. Exp. Psychol., Vol.40, P687-701.

R.C.A. (1970), Linear Integrated Circuits, Operational Amplifiers
CA3029, File Number 316.

Renleu J.P.H. (1982), The measurement of eye movement using
double magnetic induction, IEEE Trans., BME, Vol.29, P740-
744.

Restori M. (1985), Real-Time immersion B-scan & C-scan technique
in ophthalmic diagnosis, Ultrasound in Med. & Biol.,
Vol.11(1), P185-92.

Riva C.E. (1979), Laser doppler technique for measurement of eye
movement, Applied Optics, Vol.18(14), P2486-2490.

Robinson D.A. (1963), A method of measuring eye movement using a
scleral search coil in a magnetic field, IEEE Trans., BME,
Vol.10, P137-45.

Robinson D.A. (1964), The mechanics of human saccadic eye
movements, J. Physiol., Vol.174, P245-64.

Robinson D.A. (1965), The mechanics of human smooth pursuit eye
movement, J. Physiol., Vol.180, P569-91.

Roper-Hall (1978), Methods and Theories of Testing Extraocular
Movements, International Ophthalmology System & Orbit, Burde
& Karp, P7-18.

Rouse M.W. (1980), A new method of concomitancy testing, Am. J.
of Opto. & Physiol. Optics, Vol.57(1), P56-63.

Salapatek P., Kessen W. (1966), Visual scanning of triangles by
the human newborn, J. Exp. Child Psychol., Vol.3, P155-67.

- Sandeman D.C. (1968), A sensitive position measuring device for biological system, Comparative Biochem Physiol., Vol.24, P635-8.
- Sattler C.H. (1927), Uber die genaue messung und darstellung von bewegungsstorungen der augen, Klin, Monatsbl, Augenh, Vol.78(1), P161-79.
- Schlag J. (1983), Comparison of EOG and search coil techniques in long-term measurements of eye position in alert monkey and cat, Vision Res. (6B), Vol.23(10), P1025-30,
- Sheena D. (1973), Two digital techniques for eye position measurement, Medical Instrumentation conference, Association for the advancement of medical instrumentation, 8th Annual Meeting.
- Shirley A.W. (1980), Non-contact method of measuring the frequency and amplitude of the microtremor of the eye through the closed eyelid, Med. & Biol. Eng., Vol.18, P358.
- Sloane A.E. (1951), Analysis of methods for measuring diplopia fields, Arch. Ophth., Vol.46(3), P277-310.
- Solomons H. (1978), Binocular Vision, a programmed text, P211.
- Stark L., Sandberg A. (1961), A simple instrument for measuring eye movements, Quarterly Progress Report 62, Research Lab. of Elec., Massachusetts Institute of Technology, Vol.62, P268.
- Steven G.T. (1906), Motor apparatus of the eye, Philadelphia, F.A. Davis Co., 1906.

- Stuart G.C. (1984), Digital subtraction of eye movement artefact from patten ERG recording, Neuro Ophth., Vol.3(4), P281-4.
- Sullivan G., Weltman G. (1963), The impedance oculogram; a new technique, J. Appl. Physiol., Vol.18, P215-16.
- Swann L.A. (1931), The ocular muscles and the treatment of heterophoria and heterotropia, 1st Ed., The Hatton Press Ltd., P1-16.
- Takahashi M. (1984), Study of Pursuit Eye Movement by Random to-and-fro Target Movement, Acta-Oto-Laryngoleyica, S406, P224-26.
- Texas Instruments (1978), The TTL Data Book for Design Engineers, Texas Instruments, P6.6-6.7.
- Thomas J.G., Crookley D. (1977), Transducer for recording five eye movement through the closed eyelid, Med. & Biol. Comput., Vol.15. P705-6.
- Thomson W.D., Dunn G.M. (1985), Preliminary Report on an Automated System for the Measurement, Recording and Analysis of Oculomotor Motility, An Internal Report, The City University.
- Tiffany F.B. (1902), Anomalies and diseases of the eye, Kansas City, Hudson Kimberly Pub. Co., P543.
- Tokyo Shibaura Electric Co. Ltd., Chalnicon - New Camera Tubes for Colour T.V., Toshiba Review, No.76.
- Torok N., Guillemin V., Barnothy J.M. (1951) Photoelectric nystagmo-graphy, Ann. Otol., Rhinol Laryngol, Vol.60, P917.

- Von Noorden G.K., Maumence A.E. (1967), Atlas of strabismus, 2nd Ed., St. Louis, Mosby, P44-59.
- Von Noorden G.K. (1985), Binocular vision and ocular motility, 3rd Ed., P174.
- Wheless L.L. (1965), The effects of intensity on the eye movement control system, PhD. Thesis, University of Rochester.
- White J.W. (1944), Clinical application of the screen (cover) test described in details, Am. J. Ophth., Vol.27, P977-86.
- William C.H. (1901), A new instrument for testing the position of the axes of the eyes, Tr. Am. Ophth. Soc., Vol.9, P388.
- Yarbus A.L. (1967), Eye movements & vision, Plenum Press, New York.
- Yoshida O. (1972), Chalnicon; new camera tubes for colour T.V., Tokyo Shibaura Electric Co. Ltd., Toshiba Review No. 76, Dec.1972.
- Young L., Sheena D. (1975), Survey of eye movement recording methods, Behaviour Res. Methods of Instrumentation, Vol.7(5), P397-429.
- Zeevi Y.Y. (1982), Measurement of eye movement with a ferromagnetic contact ring, IEEE Trans. on BME, July 1982, P511-22.
- Ziegler S.L. (1893), A convenient prism scale, Ann. Ophth. & Otol., Vol.2, P262-72.